


1996

High density polyethylene pipe in highway applications

Brent Matthew Phares
Iowa State University

Follow this and additional works at: <https://lib.dr.iastate.edu/rtd>

 Part of the [Civil Engineering Commons](#), and the [Structural Engineering Commons](#)

Recommended Citation

Phares, Brent Matthew, "High density polyethylene pipe in highway applications" (1996). *Retrospective Theses and Dissertations*. 17278.
<https://lib.dr.iastate.edu/rtd/17278>

This Thesis is brought to you for free and open access by the Iowa State University Capstones, Theses and Dissertations at Iowa State University Digital Repository. It has been accepted for inclusion in Retrospective Theses and Dissertations by an authorized administrator of Iowa State University Digital Repository. For more information, please contact digirep@iastate.edu.

High density polyethylene pipe in highway applications

by

Brent Matthew Phares

A Thesis Submitted to the

Graduate Faculty in Partial Fulfillment of the

Requirements for the Degree of

MASTER OF SCIENCE

Department: Civil and Construction Engineering
Major: Civil Engineering (Structural Engineering)

Approved:

In Charge of Major Work

For the Major Department

For the Graduate College

Iowa State University
Ames, Iowa

1996

Copyright © Brent Matthew Phares, 1996. All rights reserved.

This paper is dedicated to all my loved ones. To my parents and grandparents for all of their love and encouragement and to Ann for putting up with me while completing this research when it seemed like the research was more important than she was.

TABLE OF CONTENTS

LIST OF TABLES	vi
LIST OF FIGURES	vii
1. THE PROBLEM AND OBJECTIVES	1
1.1 General Background	1
1.2 Objectives and Scope	4
2. LITERATURE REVIEW	5
2.1 Potential Failure Modes	6
2.2 Design Practices	9
2.3 Pipe Performance Parameters	17
2.4 Research	19
2.5 Pipe Structure General Analysis	32
2.6 Early Work of Anson Marston	34
2.7 Early Work of M.G. Spangler	35
2.8 Flammability	36
2.9 Ultraviolet Radiation	38
2.10 Longitudinal Stresses in Buried Pipes	39
2.11 State DOT's use of HDPE Pipes	39
2.12 Iowa Counties use of HDPE Pipes	42

2.13	Specifications	44
3.	TESTING PROGRAM	56
3.1	Overview	56
3.2	Parallel Plate Testing	56
3.3	Flexural Testing Program	63
3.4	Field Tests	71
4.	EXPERIMENTAL RESULTS	89
4.1	Parallel Plate Tests	89
4.2	Flexural Testing	112
4.3	In Situ Live Loading	130
4.4	Comparison of Strain for Failure Tests	191
5.	SUMMARY AND CONCLUSIONS	195
6.	RECOMMENDED RESEARCH	200
	REFERENCES	201
	ACKNOWLEDGEMENTS	205
	APPENDIX A--EI FACTORS FOR FLEXURAL SPECIMENS AT ALL LOAD INCREMENTS FOR ONE SERVICE TEST	207
	APPENDIX B--QUESTIONNAIRES	211
	APPENDIX C--STATE RESPONSES TO HDPE PIPE SURVEY	219
	APPENDIX D--DERIVATION OF STRAIN RESPONSE TO PARALLEL PLATE TESTING	227

APPENDIX E--APPROXIMATION OF SECTION PROPERTIES FOR PARALLEL
PLATE TEST ANALYSIS

LIST OF TABLES

Table 2.1.	Use of HDPE pipe by state DOT's.	41
Table 3.1.	Manufacturer A specimens tested at Iowa DOT.	58
Table 3.2.	Manufacturer B specimens tested at Iowa DOT.	59
Table 3.3.	Manufacturer C specimens tested at Iowa DOT.	59
Table 3.4.	Manufacturer A specimens tested at ISU.	62
Table 3.5.	Manufacturer C specimens tested at ISU.	63
Table 3.6.	Length parameters of flexural specimens.	69
Table 4.1.	Average stiffness values by ASTM D2412.	90
Table 4.2.	Comparison of average stiffness values.	91
Table 4.3.	Average stiffness factors.	92
Table 4.4.	Average EI factors for all specimens during service level loading.	116
Table 4.5.	Ultimate loads for all field tests.	190
Table 4.6.	Comparison of failure strain during failure tests.	193
Table A.1	Flexural EI factors for service test #1 for specimen A36.	208
Table A.2	Flexural EI factors for service test #1 for specimen A48.	208
Table A.3	Flexural EI factors for service test #1 for specimen C36.	209
Table A.4	Flexural EI factors for service test #1 for specimen C48.	210

LIST OF FIGURES

Fig. 2.1.	Excessive ring deflection as a failure mode.	6
Fig. 2.2.	Localized wall buckling as a failure mode.	7
Fig. 2.3.	Wall crushing as a failure mode.	7
Fig. 2.4.	Iowa DOT bedding specifications.	45
Fig. 2.5.	Hancor recommended backfill envelope.	49
Fig. 2.6.	'Best' backfill according to Amster Howard.	50
Fig. 2.7.	'Better' backfill envelope according to Amster Howard.	51
Fig. 3.1.	Schematic of parallel plate test.	57
Fig. 3.2.	Iowa DOT test machine.	60
Fig. 3.3.	Instrumentation for measuring change in diameters.	60
Fig. 3.4.	Testing orientations used in parallel plate tests.	62
Fig. 3.5.	Plan view of flexural test load frame.	64
Fig. 3.6.	Elevation view of flexural test frame.	65
Fig. 3.7.	Side view of beam support.	67
Fig. 3.8.	End view of pipe connection to plywood.	67
Fig. 3.9.	View of neoprene pads used in HDPE pipe corrugation valleys.	68
Fig. 3.10.	Schematic of test setup used in flexural tests.	69
Fig. 3.11.	Instrumentation of end supports.	72
Fig. 3.12.	Location of strain gages used in field tests.	74

Fig. 3.13.	Deflection monitoring setup.	75
Fig. 3.14.	In situ load test frame.	77-78
Fig. 3.15.	Trench geometry for ISU1.	79
Fig. 3.16.	Trench geometry for ISU2, ISU3, and ISU4.	80
Fig. 3.17.	Schematic of backfilling process.	82
Fig. 3.18.	Cross section of embankment.	82
Fig. 3.19.	Endview of backfill used on ISU1.	82
Fig. 3.20.	Dry density at each lift for ISU1.	83
Fig. 3.21.	Endview of backfill used on ISU2 and ISU4.	84
Fig. 3.22.	Dry density at each lift for ISU2.	85
Fig. 3.23.	Endview of ISU3 trench.	86
Fig. 3.24.	Dry density at each lift for ISU3.	87
Fig. 3.25.	Dry density at each lift for ISU4.	88
Fig. 4.1	Strain locations for parallel plate tests.	93
Fig. 4.2.	Manufacturer A, circumferential strain to 5% deflection.	94-96
Fig. 4.3.	Manufacturer B, circumferential strain to 5% deflection.	97-99
Fig. 4.4.	Manufacturer C, circumferential strain to 5% deflection.	100-102
Fig. 4.5.	HDPE 24 in. diameter pipes: load/ft versus circumferential strain to failure.	104
Fig. 4.6.	HDPE 30 in. diameter pipes: Load/ft versus circumferential strain to failure.	105

Fig. 4.7.	HDPE 36 in. diameter pipes: Load/ft versus circumferential strain to failure.	106
Fig. 4.8.	HDPE 48 in. diameter pipes: Load/ft versus circumferential strain to failure.	107
Fig. 4.9.	Load/ft vs. change in vertical inside diameter.	110
Fig. 4.10.	Load/ft vs. change in horizontal inside diameter.	111
Fig. 4.11	Theoretical vs. experimental strain for parallel plate specimen C24 at 130 plf.	113
Fig. 4.12	Theoretical vs. experimental strain for parallel plate specimen C36 at 113 plf.	114
Fig. 4.13.	Moment vs. midspan deflection for failure tests.	118
Fig. 4.14.	Moment vs. quarter point deflection for failure tests.	119
Fig. 4.15.	Moment vs. change in inside diameter at midspan.	120
Fig. 4.16.	Moment vs. change in inside diameter at quarter points.	121
Fig. 4.17.	Strain gage locations and identification in flexural specimens.	122
Fig. 4.18.	Moment vs. longitudinal strain for specimen A48 under service loads.	123
Fig. 4.19	Moment vs. longitudinal strain and deflected shape for specimen C48 under service loads.	125-127
Fig. 4.20.	Moment vs. longitudinal strain for failure tests.	129
Fig. 4.21.	Backfilling circumferential strain at Section 2.	132
Fig. 4.22.	Backfilling circumferential strain at Section 4.	133
Fig. 4.23.	Backfilling circumferential strain at Section 6.	134

Fig. 4.24.	Changes in inside diameter during backfilling at Section 2.	137
Fig. 4.25.	Changes in inside diameter during backfilling at Section 4.	138
Fig. 4.26.	Changes in inside diameter during backfilling at Section 6.	139
Fig. 4.27.	Backfilling longitudinal strain at Section 2.	140
Fig. 4.28.	Backfilling longitudinal strain at Section 4.	141
Fig. 4.29.	Backfilling longitudinal strain at Section 6.	142
Fig. 4.30.	Hydraulic cylinder and load cell used during in situ pipe tests.	145
Fig. 4.31.	Longitudinal strains at Section 1: service load test; load at center.	146
Fig. 4.32.	Longitudinal strains at Section 2: service load test; load at center.	147
Fig. 4.33.	Longitudinal strains at Section 3: service load test; load at center.	148
Fig. 4.34.	Longitudinal strains at Section 4: service load test; load at center.	149
Fig. 4.35.	Longitudinal strains at Section 5: service load test; load at center.	150
Fig. 4.36.	Longitudinal strains at Section 6: service load test; load at center.	151
Fig. 4.37.	Longitudinal strains at Section 7: service load test; load at center.	152
Fig. 4.38.	Comparison of theoretical vertical stress distribution and experimental strain at the crown.	155
Fig. 4.39.	Theoretical horizontal stress distribution with varying Poisson's ratio.	156
Fig. 4.40.	Longitudinal strain modulus at the crown versus distance from load.	157
Fig. 4.41.	Longitudinal strain modulus at the springline versus distance from load.	158
Fig. 4.42.	Longitudinal strain modulus at the invert versus distance from load.	159
Fig. 4.43.	Circumferential strains at Section 2: service load test; load at center.	161

Fig. 4.44.	Circumferential strains at Section 4: service load test; load at center.	162
Fig. 4.45.	Circumferential strains at Section 6: service load test; load at center.	163
Fig. 4.46.	Circumferential strain modulus at the crown versus distance from load.	165
Fig. 4.47.	Circumferential strain modulus at the springline versus distance from load.	166
Fig. 4.48.	Circumferential strain modulus at the invert versus distance from load.	167
Fig. 4.49.	Longitudinal strain at Section 1: service load test; load at Section 2.	169
Fig. 4.50.	Longitudinal strain at Section 2: service load test; load at Section 2.	170
Fig. 4.51.	Longitudinal strain at Section 3: service load test; load at Section 2.	171
Fig. 4.52.	Longitudinal strain at Section 4: service load test; load at Section 2.	172
Fig. 4.53.	Longitudinal strain at Section 5: service load test; load at Section 2.	173
Fig. 4.54.	Longitudinal strain at Section 6: service load test; load at Section 2.	174
Fig. 4.55.	Longitudinal strain at Section 7: service load test; load at Section 2.	175
Fig. 4.56.	Circumferential strain at Section 2: service load test; load at Section 2.	177
Fig. 4.57.	Circumferential strain at Section 4: service load test; load at Section 2.	178
Fig. 4.58.	Circumferential strain at Section 6: service load test; load at Section 2.	179
Fig. 4.59.	Longitudinal strain at Section 1: service load test; load at Section 6.	180
Fig. 4.60.	Longitudinal strain at Section 2: service load test; load at Section 6.	181
Fig. 4.61.	Longitudinal strain at Section 3: service load test; load at Section 6.	182
Fig. 4.62.	Longitudinal strain at Section 4: service load test; load at Section 6.	183
Fig. 4.63.	Longitudinal strain at Section 5: service load test; load at Section 6.	184

Fig. 4.64.	Longitudinal strain at Section 6: service load test; load at Section 6.	185
Fig. 4.65.	Longitudinal strain at Section 7: service load test; load at Section 6.	186
Fig. 4.66.	Circumferential strain at Section 2: service load test; load at Section 6.	187
Fig. 4.67.	Circumferential strain at Section 4: service load test; load at Section 6.	188
Fig. 4.68.	Circumferential strain at Section 6: service load test; load at Section 6.	189
Fig. 4.69.	Longitudinal strain at 2000 lb of applied load versus vertical soil pressure.	192

ABSTRACT

In the past, culvert pipes were made only of corrugated metal or reinforced concrete. In recent years, several manufacturers have made pipe of lightweight plastic for example high density polyethylene (HDPE) - which is considered to be viscoelastic in its structural behavior. It appears that there are several highway applications in which HDPE pipe would be an economically favorable alternative. However, the newness of plastic pipe requires the evaluation of its performance, integrity, and durability. A review of the Iowa Department of Transportation Standard Specifications for Highway and Bridge Construction reveals limited information on the use of plastic pipe for state projects. The objective of this study was to review and evaluate the use of HDPE pipe in roadway applications. Structural performance, soil-structure interaction, and the sensitivity of the pipe to installation was investigated. Comprehensive computerized literature searches were undertaken to define the state-of-the-art in the design and use of HDPE pipe in highway applications.

A questionnaire was developed and sent to all Iowa county engineers to learn of their use of HDPE pipe. Responses indicated that the majority of county engineers were aware of the product but were not confident in its ability to perform as well as conventional materials. Counties currently using HDPE pipe in general only use it in driveway crossings. Originally, we intended to survey states as to their usage of HDPE pipe. However, a few weeks after initiation of the project, it was learned that the Tennessee

DOT was in the process of making a similar survey of state DOT's. Results of the Tennessee survey of states have been obtained and included in this report.

In an effort to develop more confidence in the pipe's performance parameters, this research included laboratory tests to determine the ring and flexural stiffness of HDPE pipe provided by various manufacturers. Parallel plate tests verified all specimens were in compliance with ASTM specifications. Flexural testing revealed that pipe profile had a significant effect on the longitudinal stiffness and that strength could not be accurately predicted on the basis of diameter alone.

Realizing that the soil around a buried HDPE pipe contributes to the pipe stiffness, the research team completed a limited series of tests on buried 3 ft-diameter HDPE pipe. The tests simulated the effects of truck wheel loads above the pipe and were conducted with two feet of cover. These tests indicated that the type and quality of backfill significantly influences the performance of HDPE pipe. The tests revealed that the soil envelope does significantly affect the performance of HDPE pipe in situ, and after a certain point, no additional strength is realized by increasing the quality of the backfill.

1. THE PROBLEM AND OBJECTIVES

1.1 General Background

Corrugated high-density polyethylene (HDPE) piping is a lightweight, flexible product manufactured by using a high-density polyethylene resin with a corrugating process. The fact that the pipe is corrugated provides a highly durable and strong matrix. Since the pipe is lightweight, it is easier to handle and requires less time and manpower to install than other conventional culvert materials.

A review of the Iowa Department of Transportation Standard Specifications for Highway and Bridge Construction reveals limited information on the use of HDPE pipe for state projects. Section 4146.01 states that "approval and acceptance will be based on sampling and testing or on the producer's certification subject to monitor testing as provided in Materials IM 443 and Materials IM 446." Corrugated polyethylene pipe (4146.02) is limited to a maximum diameter of 36 in., while acrylonitril-butadiene-styrene sewer pipe is limited to 12 in. in diameter. It is permitted, however, to use polyethylene sewer pipe (4146.03) and polyvinyl chloride sewer pipe (4146.04) up to a maximum of 48 in. in diameter.

It appears that there are several applications in which using HDPE pipe would be a favorable economic alternative. Reinforced concrete pipe and corrugated metal pipe have been the standard products of choice. Familiarity with these products and standardization of acceptance testing and installation procedures have made their use widespread. On the

other hand, the newness of HDPE pipe in the market requires the evaluation of its performance, integrity and durability. AASHTO (1992) designation M294-90 type "S" (smooth walled, corrugated polyethylene pipe) provides a specification for this type of pipe. This specification provides two cautions:

- This pipe is intended for applications where soil provides support to its flexible walls.
- When the ends are exposed, consideration should be given to protection of the exposed ends due to the combustibility and deterioration caused by ultraviolet radiation.

Use of HDPE pipe is not universally accepted among states. In a 1990 North Carolina investigation, a survey was made of the other 49 states to determine if they were using AASHTO M294 type "S" polyethylene pipe (PE pipe) and what restrictions they may have on its use. Of the 40 states that responded: 7 had not approved its use, approval was pending in one state, and 32 had approved its use to some extent. Of the 32 approving its use, there were restrictions of some type in 30 states. In the other two states, restrictions were implied. Eleven states approved its use for cross drainage, while 9 states prohibited this application. Nine states use HDPE pipe in sideline applications, 3 use it in slope drainage applications and 5 use it in sewer applications.

Current AASHTO Specifications (Section 18, AASHTO 1992) clearly indicate that flexible culverts are dependent on soil-structure interaction and soil stiffness. In particular, the type and anticipated behavior of the foundation material must be considered; the type, compacted density, and strength properties of the envelope immediately adjacent to the

pipe must be established, and the density of the embankment material above the pipe must be determined. Handling and installation rigidity is measured by a flexibility factor, FF (see Sec. 18.2.3).

$$FF = \frac{D^2}{EI} \quad (1)$$

where

D = Effective diameter.

E = Modulus of elasticity of pipe material.

I = Average moment of inertia per unit length of the pipe.

This same flexibility factor (FF) is in the proposed AASHTO LRFD Bridge Design Specifications and Commentary (AASHTO 1994). For HDPE pipe, FF is limited to 0.095 in./kip in both AASHTO specifications.

Moser (1990) disagrees with using D^2/EI as a measure of a pipes resistance to deflection. In his text, he correctly says that the bending strain for a given soil pressure is directly proportional to D^2/EI while ring deflection is a function of D^3/EI .

The suitability of using HDPE pipe for roadway application should be evaluated. In this research, only HDPE pipe was investigated; the decision to limit the study to only HDPE pipe was reached after consulting with W. Lundquist, Bridge Engineer, and B. Barrett, Chairman of the task force reviewing underroad drainage for the Iowa DOT.

1.2 Objectives and Scope

The primary objective of this research was to review and evaluate the use of HDPE pipe in roadway applications. Structural performance, soil-structure interaction, and the sensitivity of HDPE pipe to installation procedures were investigated. At the initiation of the project, a comprehensive literature review was made. Information also was obtained on HDPE pipe usage by Iowa County Engineers and other state DOT's.

In the laboratory portion of the investigation, parallel plate tests and flexural beam tests of HDPE pipe were completed. The variables investigated in these tests were pipe diameter and pipe manufacturer. Four HDPE pipes were tested in the field portion of the investigation. In these tests, pipe diameter and manufacturer were held constant and quality of bedding and type of backfill material used were varied. In all field tests, cover was kept constant (2 ft) and specimens were subjected to concentrated loads which simulated highway wheel loads.

The results of the investigation are summarized in this report. The literature review and results of the surveys are present in Chapter 2. Descriptions of the laboratory and field tests employed as well as the instrumentation used are presented in Chapter 3. Results of the various tests are summarized in Chapter 4. The summary and conclusions of the investigation are presented in Chapter 5.

2. LITERATURE REVIEW

A literature search was conducted to gather available information on the use of HDPE pipe in highway applications. Several methods of searching were used. Initially, the Transportation Research Information Service through the Iowa DOT Library was checked. Following this search, the Geodex System-Structural Information Service in the ISU Bridge Engineering Center Library as well as several computerized searches through the university library were made.

The literature on behavior of plastic pipe is extensive with many excellent articles based on both experimental and analytical studies at numerous universities such as Utah State University, University of Massachusetts, and the University of Western Ontario. In addition, the industry has sponsored and conducted numerous proprietary studies. The literature review is not intended to be all inclusive but focuses on issues that are pertinent to this phase of the investigation.

Although several manufacturers of HDPE pipe provided various reports on the subject, a significant portion of research they have funded or completed themselves is proprietary and thus not available in the open literature.

In the following sections, a large variety of HDPE pipe topics are reviewed, for example: failure modes, current design practices, parameters that affect soil-structure interaction, current research , flammability, etc.

2.1 Potential Failure Modes

The possible failure modes of PE pipes are discussed by Goddard (1992) and Nazar (1988). Their findings may be summarized as follows:

1. Ring deflection is the most common failure mode (see Fig. 2.1). Ring deflection is limited to avoid reversal of curvature, limit bending stress and strain, and to avoid pipe flattening. In addition to affecting structural aspects, excessive deflection may reduce the flow capacity of the pipe and may cause joint leakage.

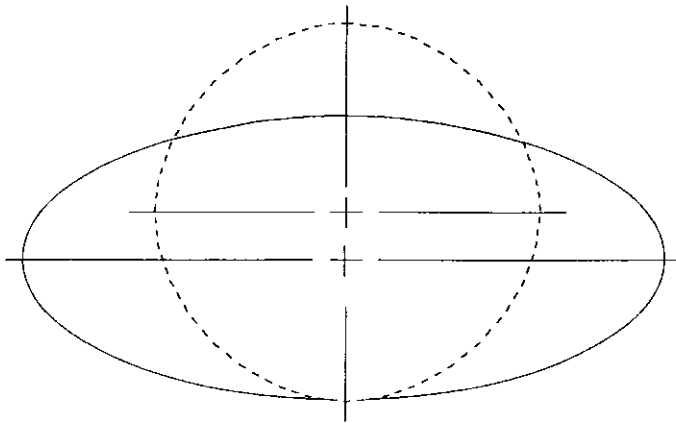


Figure 2.1. Excessive ring deflection as a failure mode.

2. Localized wall buckling is the most common failure mode when flexible pipes are exposed to high soil pressures, external hydrostatic pressure, or an internal vacuum. As expected, the more flexible the pipe the lower the resistance to buckling. An example of wall buckling is illustrated in Fig. 2.2.

3. Compressive wall stresses can theoretically lead to wall crushing if excessive in magnitude (see Fig. 2.3). The viscoelastic properties of thermoplastic material make this mode of failure very unlikely; field and laboratory tests tend to confirm this view.

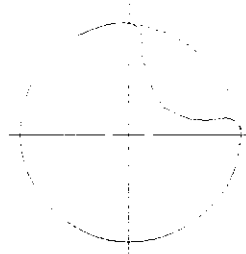


Figure 2.2. Localized wall buckling as a failure mode.

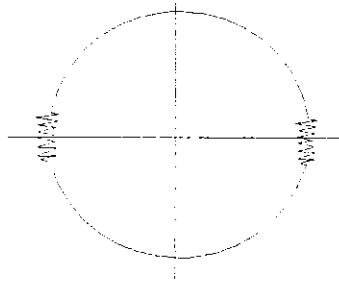


Figure 2.3. Wall crushing as a failure mode.

4. Pipe wall strain is mostly a post-construction concern. However, excessive wall strain can cause the pipe to fail. This problem can be eliminated by employing proper installation techniques. Allowable wall strain for thermoplastic polyethylene ranges from 4% to 8%.

Nazar (1988) describes potential material failures in more basic terms:

1. Tensile Failure. If the material is loaded very quickly and continuously, it resists with a force that is largely elastic. As the elongation continues, the deformation will become predominantly inelastic. The force required to continue the deformation may decrease (due to a decrease in cross-sectional area) and the material may yield and eventually fracture at its ultimate strength.
2. Compressive Failure. Likewise, if compressed, the plastic will undergo a similar elastic to inelastic alteration. A quality HDPE pipe will unlikely fracture, but will most likely fail because of its inability to hold its shape.
3. Flexural Failure. Flexural deformations of pipe grade HDPE rarely lead to fracture. However, the pipe may be rendered unusable by collapse or excessive deformation.
4. Creep Rupture Failure. This mode of failure is a slow and brittle-appearing failure in which the HDPE breaks at a relatively low deformation. The sustained deformation failure occurs when the material changes from a ductile material to a brittle one and thus the failure mechanism of fracture changes.
5. Environmental Stress Cracking (ESC). This mode of failure is nearly the same as creep rupture failure except that ESC refers to creep rupture in the presence of plasticizer or detergents. These agents greatly accelerate the rate of cracking for susceptible materials.

2.2 Design Practices

Current design practices are to prevent the aforementioned modes of failure.

Goddard (1992) gives the following design parameters.

Deflection

The most commonly used formula in pipe design is Spangler's Iowa Deflection Formula. Moser (1990) refers to this equation as well (Eqn. 2). One alternate equation for determining deflection due to applied loads is suggested by Greenwood and Lang (1990). Their equation is based on the following parameters that may affect pipe deflection: pipe stiffness, soil stiffness, applied loads, trench configuration, haunch support, non-elliptical deformation, initial ovalization, time, and variability. This equation for deflection can be written in its most basic form as shown in Eqn.3.

$$\Delta_x = \frac{D_L(kWr^3)}{EI + 0.061E'r} \quad (2)$$

where

Δ_x = Horizontal deflection of the pipe.

D_L = Deflection lag factor (usually 1.5).

k = Bedding constant.

W = Load per unit length of pipe.

r = Pipe radius.

E = Modulus of elasticity of pipe material.

I = Moment of inertia of the pipe wall.

E' = Modulus of soil reactions.

$$\delta_{VL} = \frac{W}{S_p + S_s} \quad (3)$$

where

- W = Total external load.
- S_p = Pipe stiffness.
- S_s = Soil stiffness.
- δ_{VL} = Vertical deflection.

Substituting expressions for W, S_p , and, S_s the following equation for deflection results in:

$$\delta_{VL} = \frac{k_x \left(\frac{\Delta V}{\Delta H} \right) (C_L \gamma H + W_L)}{\frac{8C_{TP}EI}{D^3} + 0.061(0.6\zeta)E_s} \times 100 \quad (4)$$

where

- δ_{VL} = Vertical deflection due to imposed loads.
- k_x = A factor related to the likelihood of achieving uniform bottom support.
- $\Delta V/\Delta H$ = Typical ratio of vertical to horizontal deflection.
- C_L = 1 for long term deflections.
- γ = Unit weight of the overburden soil.
- H = Depth of cover.
- W_L = Live loads.
- C_{TP} = Pipe stiffness retention factor.
- E = Modulus of elasticity of the pipe material.
- I = Moment of inertia of the pipe wall.
- D = Pipe diameter.
- ζ = Leonhardt factor.
- E_s = Embedment soil modulus.

One additional design consideration intended to limit installation deflections is the so-called flexibility factor (FF). Moser (1990) discounts this as an indicator of deflection resistance and suggests that it not be used to classify a pipe's stiffness characteristics for deflection control. However, the AASHTO Load and Resistance Bridge Design Specifications and Commentary specifies a limiting value for the flexibility factor as a handling and installation requirement. The flexibility factor is defined in Eqn. 1. This parameter is limited by a minimum of 0.095 in./kip in both the current AASHTO and proposed AASHTO LRFD bridge specifications.

Wall Buckling

Goddard (1992) cites Moser (1990) as giving the following equation for wall-buckling design:

$$P_{cr} = 2 \sqrt{\frac{E'}{(1-\nu^2)} \left(\frac{EI}{R^3} \right)} \quad (5)$$

where

- P_{cr} = Critical Buckling Pressure.
- E' = Modulus of soil reaction.
- E = Modulus of elasticity of pipe material.
- R = Pipe radius.
- ν = Poisson's ratio.

Wall Crushing

The potential for wall crushing is checked by the AASHTO design procedure.

Using service load design procedures, the equation is:

$$T = P \left(\frac{D}{2} \right) \quad (6)$$

where

T = Thrust.

P = Design load.

D = Pipe diameter.

The design load is assumed to be the weight of the soil load above the pipe calculated by multiplying the soil density times the height of cover. Any anticipated live load must be added to this dead load. With the wall thrust determined, the required pipe wall area can then be calculated by the following:

$$A = \frac{T}{f_a} \quad (7)$$

where

A = Required wall area.

T = Thrust.

f_a = Allowable minimum tensile strength divided by a safety factor of 2.

Pipe Wall Strain

Pipe wall strain is primarily a post-construction concern. Within the normally specified deflection limits, outer tensile strains are not a concern. If poor installation techniques leave large localized deformations, wall strains will need to be checked.

Allowable strains for thermoplastic pipe are 4% to 8%. To check bending strains, the following equation should be used:

$$E_b = 6 \left(\frac{t}{D} \right) \left(\frac{\Delta Y}{D} \right) \quad (8)$$

where

E_b = Bending strain.

t = Wall thickness.

D = Diameter.

ΔY = Vertical Deflection.

Moser (1995, pp. 1) indicates that the current design procedure leads to a design that is fundamentally incorrect. In an attempt to refine the design of HDPE pipes, he has developed a problem statement to address this.

The objective of this work will be to provide a clear, concise design procedure for HDPE pipes that will permit the cost-effective application of HDPE pipes in transportation industry applications with utmost safety. The design procedure will predict the limiting height of cover based on deflection, buckling, and ring

compression. The design procedure so developed would be proposed to replace the current AASHTO procedure. The development of the standard will involve a thorough review of existing research, a review of other related standards, a review of current state practice, and some original research, testing, and test development.

Schrock (1990) notes that the most difficult problem confronting the designer of flexible pipelines is the selection of realistic values for the soil modulus and external load parameters required for design. This difficulty arises from the large potential variation in native and pipe embedment soil characteristics. Also, he notes that the modulus of soil reaction varies with soil types and depths.

Zicaro (1990, pp 3) adds that the flexible pipe design procedures proposed by some manufacturers ignore the long established recommendations by Spangler (1941), and continue to use his equation in their attempt to show the adequacy of their proposed product. Also, he feels that another factor not currently considered in the design of flexible pipes, the relationship of the backfill modulus to the in situ soil modulus, is of extreme importance.

Many designers only use the soil modulus of the backfill material independent of softness or firmness of the adjacent material, or width of the placed backfill. This relationship addressed by Leonhardt (1978) recognizes that a narrow band of firm material adjacent to a soft material does not provide the same restraint as a wide

band of firm material and vice versa. He refers to this as the combined soil modulus which considers the affect of the width of the side fill soil placed, as well as the stiffness of both the backfill and in situ materials.

Also, typically overlooked "is the strain that results when deformations (flattening of the crown or invert) occur; this strain increases as a function of the decrease in the pipe to soil stiffness ratio."

A study was completed by Katona (1988) on the allowable fill height for various sized corrugated polyethylene pipe. To determine the values of allowable fill height, the computer program CANDE was used. The study satisfied all criteria of AASHTO for service load design. The values from CANDE were verified by comparison with experimental laboratory data from Utah State University. The result of the study is a set of design tables for various manufacturer's pipe for various diameters which give the allowable fill heights that satisfy AASHTO requirements. The analyses were developed based on structural consideration of the pipe size, corrugation geometry, backfill soil quality, and design life. It was determined that the allowable fill height for 24 in. HDPE pipes with "good" quality soil ranged from 43.7 to 55.6 ft for short term design and 26.7 to 31.3 ft for long term design. However, for a "fair" quality soil the allowable fill heights were reduced to 30.2 to 40.2 ft for the short term and 12.2 to 15.4 ft for long term design. Obviously, the design life and quality of soil envelope had a significant affect on the allowable fill height.

A report prepared by the AASHTO Special Liaison Committee for Flexible Culverts (1995) examines the influences of installation variations on the in situ performance of both flexible and rigid pipes. It was determined that the traditional assumption that flexible pipes are more dependent upon proper installation techniques than rigid pipes is unjustified. The change in philosophy has resulted from new refinements in the design of concrete pipes. From the investigation, it was suggested that consideration should be given to increasing the safety factors for concrete pipes. At the same time, it was advised that the safety factors for flexible pipes be reduced in view of the lesser degree of sensitivity to soil envelope conditions.

A publication by the Corrugated Polyethylene Pipe Association (1995, pp 2-3) describes why the design and application of flexible pipes is superior to rigid pipe.

Both flexible and rigid pipe require proper backfill, although the pipe/backfill interaction differs. When flexible pipe deflects against the backfill, the load is transferred to and carried by the backfill. When loads are applied to rigid pipe, on the other hand, the load is transferred through the pipe wall into the bedding.

Flexible pipe offers significant structural benefits to the project designer. In many situations, a properly installed flexible pipe can be buried much deeper than a similarly installed rigid pipe, because of the flexible pipe/backfill interaction. A rigid pipe is often stronger than the backfill material surrounding it, thus it must support earth loads well in excess of the prism load above the pipe. Conversely, a

flexible pipe is not as strong as the surrounding backfill; this mobilizes the backfill envelope to carry the earth load. The flexible/backfill interaction is so effective at maximizing the structural characteristics of the pipe that it allows the pipe to be installed in very deep installations, many time exceeding allowable cover for rigid pipe when identically installed.

2.3 Pipe Performance Parameters

The primary method for determining the acceptability of a particular HDPE pipe is by using the ring stiffness of the pipe. The wall stiffness of pipes is a function of the material type as well as the geometry of the pipe wall; this is often expressed in terms of EI, the stiffness factor, where E is the material's flexural modulus of elasticity and I is the moment of inertia. The test method described in ASTM D2412 is generally the accepted procedure for determining the pipe stiffness at 5% deflection. The following formula is used to calculate the stiffness factor from the results of the parallel plate test:

$$EI = 0.0186 \frac{F}{\Delta_y} D^3 \quad (9)$$

where

E = Flexural modulus of elasticity.

I = Moment of inertia.

D = Mean diameter.

F = Load applied to the pipe ring.

y = Measured change in inside diameter in the direction of load application.

The extent of deformation that a pipe undergoes may be limited by the material's ductility. The ductility is often expressed as a material strain limit. The principle formula utilized for determining strain from deflection on parallel plates is:

$$\varepsilon_f = 4.28 \left(\frac{\Delta_y}{D} \right) \left(\frac{t}{D} \right) \quad (10)$$

where

- ε_f = Strain.
- t = Wall thickness.
- D = Mean diameter.
- Δ_y = Measured change in deflection in the direction of load application.

A phenomena that is somewhat unique to polyethylene pipes is that they undergo stress relaxation when the strain in the pipe wall is constant. This is generally not considered a design constraint. This phenomena, and its affect on the ring stiffness measured in the parallel plate test, was the subject of a study completed by Janson (1990). In the study, pipe specimens (by ASTM D2412) were held at constant deformation in the 0.8% to 3.7% strain region for 10,000 hours. The force needed to hold the specimens in the constant state of deformation was monitored throughout. Extrapolation of the 10,000 hour data gave the long-term creep modulus. As expected, over the 10,000 hour test, significant decrease was noted in the modulus. The effect of this decrease in modulus is not entirely understood and as a result it is suggested that the ring stiffness value by ASTM

D2412 be based upon a short-term modulus measured after 3 minutes with the pipe deflected to a constant value of 5%.

A study performed by McGrath, Selig, and DiFrancesco (1994) indicates that the long-term decrease in load, or stress relaxation, is unaffected by short-term load increases if followed by immediate unloading. The tests also indicate that any new loads imposed on the pipe (i.e., short pulse loads) may be treated as controlled by the short-term modulus even though the remainder of the loads on the pipe may be governed by the long-term modulus. Of particular interest is the fact that this phenomena held true even after the deflection levels had exceeded the linear viscoelastic limit.

2.4 Research

The following section summarizes some of the experimental HDPE pipe related research completed to date not discussed previously. The research includes laboratory tests, field tests, and the monitoring of numerous installations. Most testing has focused on the effects of deep fill on the performance of HDPE pipe. Monitoring of field installed pipes in most instances has focused on visual inspection of installations over a number of years.

2.4.1 Laboratory Tests

Watkins, Reeve, and Goddard (1983) completed a testing program to determine the relation of buried polyethylene pipe deflection to height of soil cover under large wheel loads at various backfill densities. In their study, three diameters of corrugated polyethylene pipe were tested: 15 in., 18 in., and 24 in. Seven pipes (one 15 in. dia., one 18 in. dia., and five 24 in. dia.) were buried so that cover varied from one end to the other (i.e., pipe 1: 5 in. cover at end 1, 20 in. cover at end 2; pipe 4: 6 in. cover at end 1, 30 in. cover at end 2, etc.) Pipes were subjected to H-20 load as well as "super-loads" simulated by 27 kips/wheel. In all but one case, native soil was used. It was determined for pipes in typical native soil compacted to 80% standard density, less than 1 ft of soil cover was adequate protection against H-20 loads and up to 54 kips/axle "super-loads". Constraining influence of the sidefill material was determined by removing the cover and applying the 16 kip wheel load directly on the pipe. Removing the cover did not substantially affect the pipe deflection.

A considerable amount of HDPE related research has been completed at Utah State University (USU) which was summarized by Goddard (1992). Much of the work has involved the large soil cell at USU which simulates very large soil pressures on buried pipe (Watkins and Reeve 1982). On the basis of the work done in 1982 on corrugated polyethylene pipe, the measured deflections were found to be 50% to 67% of those predicted by the Modified Iowa Formula. The testing gave wall thrust values that

exceeded the AASHTO equations by factors ranging from 2 to 10 without wall failure occurring. Results in these tests also exceeded the predicted wall buckling pressures by approximately 50%. With deflections less than 5% in these tests, wall strain was well under the 1% strain limit for HDPE.

In 1993, Moser and Kellogg (1993) tested four 48 in. diameter smooth-lined corrugated HDPE pipes for Hancor, Inc. to determine structural performance characteristics as a function of depth of cover. Variables investigated included type of soil, compaction of soil, and vertical soil loading (simulating depth of cover). In this investigation it was concluded that structurally, there are no reasons why HDPE pipes cannot perform well. Clearly, pipes deflect more in loose soil than in dense soil because loose soil compresses more. If the pipe is buried under high soil cover, or large surface loads, the backfill around the pipe should be granular and carefully compacted.

Moser (1994) tested three 48 in. diameter high density profile-wall (Honeycomb Wall Design) polyethylene pipes for Advance Drainage Systems, Inc. to determine the structural characteristics as a function of depth of cover. The variables investigated were the same as those in the 1993 tests. From the structural point of view, it was concluded there are no reasons why HDPE pipes cannot perform well. In the three tests, the Proctor Density was 75%, 85%, and over 96.5%. In the same order, the load at the performance limit in these three tests was found to be 34 ft of cover, 60 ft of cover, and 180 ft of cover.

Selig, DiFrancesco, and McGrath (1994, pp 1) describe a new test for use in the

evaluation of buried pipe. The new test has been developed to study the behavior of buried pipe under circumferential compression loading. The setup consists of a cylindrical steel vessel and an inflatable bladder. A pipe section is placed at the center of the vessel and the annulus is filled with tamped sand. This test is conducted by slowly increasing the internal bladder pressure while monitoring the pipe performance. "The test has demonstrated that significant circumferential shortening can occur in plastic pipe section with corrugating cross-sections. This produces beneficial positive arching when the pipe is in service. The test also provides a basis for determining plastic pipe wall design limits in compression."

2.4.2 Field Tests

In 1987, a 24 in. corrugated polyethylene pipe was installed in a 100 ft highway fill under I-279 north of Pittsburgh, PA., (Adams, Muindi, and Selig 1988). Pipe shape and circumference were monitored along with soil pressure at the crown and the springline, free field soil strains, and trench strain measurements. The pipe's vertical diameter shortened 4.3%. This deflection represents only 35% of that predicted by the Iowa Formula. This study demonstrated that soil arching and the circumferential shortening, which are not taken into consideration in traditional calculations, add a degree of conservatism to the design.

R.W. Culley (1982) of the Saskatchewan Department of Highways and Transportation conducted a test in which 600 mm (23.62 in.) diameter corrugated

polyethylene pipe was subjected to 25,000 passes of a 4100 kg (9040 lb) dual-wheel load moving at 16 km/h (10 mph). The pipe had a cover of slightly over 400 mm (15.75 in.) Vertical (approximately 1 mm) and horizontal deflections (approximately 1/3 mm) remained essentially constant during the test.

2.4.3 Monitoring of Installations

The adequacy or inadequacy of plastic pipe designs is best exemplified by their performance in real world installations. The following are just a few of the many installations that have been investigated.

In 1985, a study was completed of nearly 200 cross drain installations of corrugated polyethylene pipe by Hurd (1986). The results of this study yielded the conclusion that deflection was more the result of construction than from service loads. Additionally, the problems were mainly in pipes of smaller diameter (i.e., 12 in. and 15 in.).

Fleckenstein and Allen (1993) reported on the field performance of corrugated smooth lined polyethylene pipe in Kentucky. The report focused on the installation and performance of the pipe after placement in eleven different project sites. The installations were either for storm sewers, cross drains, or entrance pipes. The inspection techniques at each site were similar and included observations for pipe coupling separation, siltation, rips or tears, sagging and vertical and horizontal deflection. Pipes of 15 in., 18 in., and 36 in. diameter were inspected.

At three of the projects, rips or tears were discovered in the pipe wall. It appeared as if most of the rips were related to improper backfill and/or improper handling of the pipes. On several of the projects, slight to significant offsets were observed. Large longitudinal separations at the pipe ends appeared to have been caused by improper construction. Only one project had signs of vertical offsets. However, several of the projects had pipes that showed signs of significant vertical sagging. In those cases, it appeared as if the pipes had been improperly bedded. The largest pipe deflections occurred in the entrance pipes. However, four entrance pipes under shallow crushed stone fill did not show any deflection. Another observation noted was that pipe deflection was dependent on the backfill. Long term deflections did not appear to be a problem when the pipes were properly installed.

In summary, the observations indicated that the pipes performed satisfactorily as crossdrains and entrance pipes when properly bedded and backfilled using a material with high shear strength. The following are some of the recommendations made: (1) polyethylene pipe should be installed according to ASTM 2321, with the addition of granular backfill. Granular backfill should be used to a minimum height of one ft above the pipe crown. (2) An ASTM Class I or Class II type backfill should be used for all polyethylene pipe. (3) Entrance pipes should have a minimum cover of one ft. (4) Further research should be conducted to determine the minimum shear strength needed to provide adequate side support.

In 1980, the Missouri Highway and Transportation Department began installing corrugated polyethylene pipe (CPE) (McDaniel 1991) on an experimental basis to evaluate the performance and applicability of the pipe. There were 41 installations--24 under bituminous roadways and 17 under field entrances to secondary highways. Single wall pipe was used at all locations except at one crossroad installation in which double wall pipe with smooth wall interior was used. In this report, only the crossroad installations (23 single wall CPE primarily installed in 1987 and one double wall CPE installed in 1989) are documented. The CPE at these sites ranged from 15 in. to 30 in. in diameter.

At 20 installations, the pipe was backfilled with crushed stone while at the other four sites the native material was used for backfill. At 12 of the 24 locations, there was less than 12 in. of backfill over the pipe.

Where properly installed, the maximum vertical deflection (based on nominal pipe diameter) was determined to be 5.47%; average vertical deflection was found to be 3.47%. At the four sites where native backfill material and poor compaction was achieved, maximum vertical deflections ranged between 7.5% and 10.8%. In 1990, there was no evidence of damage from chemical attacks, abrasive material, or ultra-violet radiation. Numerous single wall inlets and outlets, however, were damaged by mowing equipment and vehicular traffic. The double wall CPE pipe with smooth wall interior provided significant advantages over the single wall CPE pipe.

A 1986 review of 16 culvert installations (3 years after installation) in western

Pennsylvania by Casner, Cochrane, and Bryan (1986), where soil and water pH tends to be low, led to the recommendation that corrugated polyethylene pipe be used in maintenance operations and be included on new design projects. At these sites, pipe diameter was either 15 in. or 18 in. Cover at the sites varied from a maximum of 3 ft at one site to a minimum of 2 in to 9 in. at another site. At one particular site, due to acidic water conditions, corrugated steel pipe had to be replaced approximately every 6 months due to corrosion. All polyethylene culverts performed well; there was no evidence of attack by the acidic waters in the area.

An 18 month evaluation of large diameter corrugated polyethylene pipe meeting (AASHTO designation M294 type "S") by The North Carolina Department of Transportation (1991) has lead to the conclusion that if corrugated polyethylene pipe is placed utilizing controlled installation procedures, it will perform acceptably. However, the reality is that most installations by state crews or by contractors are not placed utilizing ideal procedures. Because of this, the usage was limited to:

1. Temporary installations, such as detours.
2. Permanent slope drain installations.

When used, a minimum of 18 inches of cover is required.

During the fall of 1990 and the spring of 1990, smooth walled corrugated PE pipe was heavily marketed to the Materials and Tests Unit of the North Carolina Department of Transportation (1991, pp 4-5). The product was used on a "trial use" status with HDPE

pipes evaluated in four counties. Deflection testing equipment was used to determine the effects of live loading and soil loading on the performance of the pipe in place. This equipment could be adjusted to be 5% and 7.5% less than the inside diameter of the pipe being evaluated. The deflection equipment was then pulled through the pipe until it was stopped by the deformed shape of the pipe (5% or 7.5% less than the inside pipe diameter). The distance of travel was then noted. The results of the deflection tests are as follows.

Ten of the 11 cross drains had deflections greater than 7.5%; the other one exhibited little or no deflection. In many of the cross drain applications, deflections were notably greater than 7.5%, however equipment was not available to determine to what extent they exceeded this amount. All four slope drains experienced minor or no deflections. The 7.5% deflection gage failed to pass through one of them, but this was due to poor joint alignment instead of deflection. The storm drain tested had deflections between 5% and 7.5%. At two of the test sites, the majority of the pipe used in cross drains application was under recently constructed secondary roads. Although nearly every cross drain pipe showed deflections greater than 7.5%, the pavements exhibited no noticeable signs of stress due to settlement of the backfill. This would indicate that the majority of the deflection probably occurred during installation and not necessarily due to live loading.

Todres and McClinton (1985, pp 428-437) summarized work on the stress and

strain responses of a soil-pipe system (a 16-in. natural gas pipeline near Racine, Wisconsin) to vehicular traffic. "It was found that the use of the Boussineq solution greatly overestimated the soil response, whereas the use of the elastic-layer theory provided satisfactory estimates. The good correspondence between theory and field measurements suggests that the presence of the pipe did not significantly affect the stress field in the pavement-subgrade system." Determining the effects of the soil pressure on circumferential stress was determined to be very complex, but "a simple approach was used that appears to offer reasonable estimates in the absence of a definitive solution". In addition to the field study, a laboratory simulation experiment in which a pipe buried in a large sand box was subjected to loads. Axial bending effects were observed, and it was found that these could be predicted reasonably well by beam-on-elastic foundation theory.

An inspection of a 36-in. diameter HDPE pipe was performed by Drake (1991, pp 1-2) in the Leestown Industrial Park in Fayette County, Kentucky. "The backfill over the pipe was 3 ft at the entrance and appeared to be from 2.5 ft to 3.5 ft throughout the length of the drain. A bituminous surfaced parking lot is constructed over the pipe." Vertical deformation of the pipe (pipe flattening) was observed; the shortening of the pipes vertical diameter was in the range of 15% to 25%.

This deformation had apparently occurred prior to the paving of the parking area above the pipe because there was no noticeable settlement of the bituminous surface. Major problems with the joints and couplings were observed; the

couplings were not performing their function of holding the pipe ends together. Some of the upstream pipe sections had separated and had moved downward approximately 4 to 5 in. allowing water to flow out of the pipe and under the downstream pipe sections. It appears that the coupling band was unable to resist the shear and moment forces normally occurring at a joint.

Over a nine year period Goddard (1990) monitored the first 24" diameter HDPE cross-drain installed by a state highway department. The site had previously been identified as a highly volatile one because of the known high acidity and elevated abrasion levels. The pipes deflection was measured 4 times over the nine years and compared with theoretical values from CANDE.

In the nine year period there was no increase in deflection from the first inspection in 1982 or signs of UV degradation. The pipe showed no affects of degradation from the acidic water or the high levels of abrasives. From the theoretical investigation, it was found that field data was in range and fit well with controlled test values. Of particular interest was the fact that the pipe deformation was more than 3 times greater at the pipe joint indicating that the joint was weaker than the remainder of the pipe.

In 1988, an installation of 2,000 ft of 18 in. to 36 in. diameter pipes were installed in the highly alkaline environment of western Colorado. In a report by Hunt (1991), a review of the installation was documented. The site is in the central western slope area of Colorado where there are large amounts of spring run-off. Immediately after

construction, there appeared to be little if any deformation. Additionally, three years after construction the deformation had not increased noticeably. Despite the high flow of alkaline water, no visible damage was observed. Additionally, the exposed ends showed no UV deterioration. There had been a fire in one of the pipes due to a large amount of sawdust in the pipe from a nearby sawmill. The fire burned about 10 ft into the culvert and exposed some of the surrounding soil. However, this soil did not collapse. The results of the monitoring resulted in the pipe being recommended as an alternative to steel or concrete when corrosion, weight, ease of installation, or aesthetics is a concern. The conclusions of the paper advised the designing engineer to ensure that the contractor maintains at least 95% maximum density in lifts no greater than 6 in. with extra care given to the areas underneath the haunches.

Fleckenstein and Allen (1988) performed an evaluation of ADS HDPE N-12 pipe in Lexington, Kentucky. The pipe was installed at two locations. The first was a 15 in pipe with 1 ft of cover and the second was a 15 in pipe with 6 ft of cover. It should be noted that during installation of the pipes vibratory compaction was not being completed on the backfill material. The pipes were performing well. However, it is noted that this may not have been the best test section to monitor pipe performance because the roadway above the pipe was used infrequently and is very rarely under heavy loads. The biggest problem with these installations was clogging of the pipe from large amounts of organic material.

Consistent throughout all reports reviewed was the importance placed on the

installation technique. The reports recommended a strict adherence to "proper" installation techniques.

To illustrate the importance of the soil restraint at the springline, Gabriel (1990) offers a simple comparison of a pipe without horizontal restraint (curved beam with a roller) and a pipe with horizontal restraint (arch with pinned ends). Each system is subjected to a point load, P , at the crown. From the simple calculations it is seen that the maximum moment in the curved beam is $0.5 \cdot P \cdot \text{radius}$. On the other hand, the maximum moment in the arch is seen to be $0.5 \cdot P \cdot \text{radius} - H \cdot \text{radius}$; where H is the horizontal force at each of the pinned ends. It is obvious then that the additional restraint lowers, as is the case in many indeterminate structures, the maximum moment. This simple analogy clearly illustrates the importance of proper horizontal restraint.

Goddard (1992) presents a summary of his findings based on laboratory testing and field installations:

1. The current traditional design procedures, although intended for flexible (elastic) pipes, appear to offer a conservative design approach for currently manufactured thermoplastic pipe, at least within the 48 in. and smaller size range.
2. Existing state reports on thermoplastic pipe in actual service indicate good performance, particularly when installed with reasonable care.
3. Performance of thermoplastic pipe when poorly installed, is comparable with

more traditional products when poorly installed.

4. Design procedures will continue to evolve as additional research is completed.

2.5 Pipe Structure General Analysis

Gabriel (1993) offers this simplified structural analysis of flexible pipes, he considers the pipe as acting as a combination of a beam and a column.

A column, barring a buckling response, would shorten according to the following relationship:

$$s = \frac{PL}{EA} \quad (11)$$

where

- s = Shortening of the column.
- E = Young's modulus for the material.
- A = Cross-sectional area of the column.
- P = Load.
- L = Column length.

or simplified as

$$s = \frac{P}{K_c} \quad (12)$$

where

- s = Shortening of the column.
- P = Load.
- K_c = Material stiffness + geometric stiffness.

This analysis considers the ring compression to act in a column-like manner.

In the following relationships, changes in diameter due to bending of the ring are examined. For the analysis, consider a beam in bending with deflection defined as

$$a = \frac{PL^3}{48EI} \quad (13)$$

where

- I = Moment of inertia resisting bending.
- P = Load.
- L = Length of beam.
- E = Modulus of elasticity
- a = Deflection of beam.

Or simply,

$$a = \frac{P}{K_b} \quad (14)$$

where

- a = Deflection of beam.
- P = Load.
- K_b = Material stiffness + geometric stiffness.

Therefore the entire deflection of the pipe ring is

$$D_v = \frac{P}{K_c} + \frac{P}{K_b} \quad (15)$$

or after rearranging and simplifying,

$$D_v = \frac{P}{K_p} \quad (16)$$

with

$$K_p = \frac{K_b K_c}{K_c + K_b} \quad (17)$$

The familiar Iowa type formulas neglect the resistance to deflection contributed by the ring compression in this simplified analysis. Gabriel (1993) cites this and an inappropriate coupling of the effective pipe stiffness and effective soil stiffness as the sources of error in current design practices. He recommends the development of new deflection equations that more accurately predict the deflection in HDPE pipes.

2.6 Early Work of Anson Marston

Anson Marston investigated the problem of determining loads on buried conduits. In 1913, he published his original paper entitled "The Theory of Loads on Pipes in Ditches and Test of Cement and Clay Drain Tile and Sewer Pipe." This was the beginning of calculating earth loads on buried pipes. The Marston load equation for flexible pipes is

$$W_c = C_d \gamma B_c B_d \quad (18)$$

where

W_c = Load.

C_d = Load coefficient.

γ = Unit weight of soil.

B_c = Outside diameter of culvert.

B_d = Horizontal width of ditch at top of conduit.

It should be noted that the Marston load represents an upper limit loading and that real loads are somewhat lower than those predicted by Marston. The load on a rigid conduit is assumed to have a B_c^2 term in place of the $B_c B_d$ term since the trench is, theoretically, not involved (Moser, 1990).

2.7 Early Work of M.G. Spangler

Spangler (1941), a student of Anson Marston, observed that the Marston theory for calculating loads on buried pipe was not adequate for flexible pipes. This prompted Spangler to study flexible pipe behavior to determine an adequate design procedure. His research and testing led to the derivation of the Iowa formula which he published in 1941. He incorporated the effects of the surrounding soil on the pipe's deflection. He also assumed a uniform pressure over part of the bottom while he assumed the horizontal pressure on each side would be proportional to the deflection of the pipe into the soil.

This equation can be used to predict deflections if the three empirical constants K ,

D_L , and e are known. In 1958, R. K. Watkins, a graduate student of Spangler, investigated the modulus of passive resistance through models and examined the Iowa formula dimensionally. The analysis determined that e could not possibly be a true property of the soil because its dimensions are not those of a true modulus. As a result, another soil parameter was defined, the modulus of soil reaction, $E' = er$ (e and r as defined above). Consequently, a new formula called the modified Iowa formula was proposed with this substitution. The modified Iowa equation is the currently used deflection equation (see Eqn 2).

2.8 Flammability

A study completed by the Phillips Chemical Company (1983, pp 13) concluded the following about polyethylene's flammability.

Testing according to ASTM D635 and MVSS 302 classify polyethylene as burning with a rate of 1 in. per minute. Flash temperature was found to be 645° F with a self-ignition temperature of 660° F. In addition, the minimum concentration of oxygen which will just support combustion is 17.4%.

From a study performed by the Florida Department of Transportation (Kessler and Power 1994, pp 2-3), it was concluded that FDOT's present policies concerning the use of HDPE pipe were adequate concerning fire safety. The study included field burn tests, a survey of the usage and experience of state DOT's with HDPE pipes, and standard

laboratory burn tests on polyethylene coupons. Also included was a burn test on a mitered end section with concrete apron. The evaluation focused on evaluating the fire risk from grass fires and does not consider other sources of fire such as vandalism or fuel spills.

During the field burn tests, it was noted that the fire spread rapidly to the point where soil completely encased the pipe. At that point, the fire slowed to a steady circumferential flame. Typical in field burn specimens was a reduction in pipe wall thickness which lead to soil falling into the pipe which helped to slow spread of the fire. The reduction in pipe wall thickness is obviously a major point of concern since the loss of material reduces the pipes ability to carry load. Out of the 41 states responding to the study, only four reported incidents of fire and the total number of fires was reported as eight.

With the number of fires reported and the total number of years of service of the HDPE pipes, the rate of fires is one fire per state every 48 years. Based on the results of this study, the overall risk of damage to HDPE pipes from fire is considered minimal.

However, it was noted that mitered end sections of HDPE pipes are subject to fire damage and possible destruction when exposed to grass fires.

A performance evaluation of HDPE pipes by the Materials and Tests Unit of the North Carolina Department of Transportation (1991) indicated that during a flammability test the double layer design of the pipe caused the fire to be constantly fueled throughout the length of the pipe. As the inner layer burned, the corrugations would melt and droop

over the edge of the pipe, like a sheet, thus providing more burnable surface area. The flames would burn up the drooping sheet of plastic and eventually ignite the smooth wall interior. As the interior wall burned, it would melt the corrugation above it causing it to droop down into the pipe thus repeating the process across each corrugation. The pipe burned at an approximate rate of 1 ft per 20 minutes. The relative ease at which it caught fire and burned raised questions about its potential applications. Any application where the ends are exposed makes it susceptible to fire damage. Consequently, proper end protection is advised.

2.9 Ultraviolet Radiation

Also addressed by the North Carolina Department of Transportation (1991) is the concern about the long term effects of ultraviolet (UV) degradation on HDPE pipe stored in direct sunlight for extended periods of time, and its effect on the exposed ends after installation. Unprotected plastics will lose impact strength over time when exposed to UV radiation. To help counter this, manufacturers have incorporated carbon black, which is UV absorbent, into the material. According to manufacturers, the UV absorbent will prevent any substantial loss of strength in the pipe by limiting the effects of UV degradation to a small fraction of the pipe wall thickness. The damaged outer layer then provides protection to the remaining wall thickness.

2.10 Longitudinal Stresses in Buried Pipes

According to Watkins (1985, pp408-416), most of the analyses for design of buried pipe are directed toward ring performance, (i.e., radial and circumferential stresses, strains and deflections of a two-dimensional transverse cross-section).

Adequate longitudinal strength is assumed so long as the specifications include uniform bedding and compacted pipe zone backfill. Pipe manufacturers are expected to provide adequate longitudinal pipe strength for ordinary buried pipe conditions. The pipeline designer only considers longitudinal stresses under extraordinary conditions such as supporting a buried pipeline on piles. However, significant longitudinal bending may be caused by (1) soil movement and (2) non-uniform bedding. Soil movement is caused by heavy surface loads, differential subgrade soil settlement, landslides, etc. Some soil movements can be predicted. Non-uniform bedding is inevitable. Despite specifications calling for uniform bedding, high/hard spots and low/soft spots occur. With soil loads on top, the pipe tends to bend down over the hard spots and longitudinal stress is generated.

2.11 State DOT's use of HDPE Pipes

Originally it was intended that a survey of states would be made to learn of their current practice and limitations or restrictions on the use of HDPE pipe. A few weeks after this investigation was initiated, it was learned from the Iowa DOT Office of Bridges

and Structures that the Tennessee DOT was making a similar survey. Realizing that state bridge engineers would not be receptive to receiving a second survey on the same subject, the Tennessee DOT was contacted to see if the research team could obtain the results from their survey. The Tennessee DOT was very helpful and provided the results of their survey which are summarized in the following paragraphs.

Based on the results of the Tennessee DOT survey, the primary concerns of state DOT's is the combustibility and the required construction techniques of the pipe. There is great concern on the flammability of HDPE under normal brush fires. Many DOT's have read conflicting reports on the actual fire risk and are unwilling to commit to using HDPE pipes in larger quantities until the risk is more completely investigated. It is widely known that the quality of construction (i.e., compaction techniques, quality of backfill material, etc.) are directly related with the effectiveness of HDPE under load. However, states have very little information concerning what must be done to ensure a successful installation; many times what one agency determines is best is regarded by others as incorrect. Table 2.1 summarizes the use of HDPE pipe by state DOT's. As may be observed (based on the 42 states that responded) only one state permits use of HDPE pipe 48 in. in diameter. The majority of states (76%) permit use of HDPE pipe up to 36 in. in diameter while 17% of the states permit use of HDPE pipe up to 24 in. in diameter. The majority of states (83%) permit use of HDPE pipe in storm drains and driveways, however only 48% of the states permit use of HDPE pipe in cross drains. Over 80% of the states (42 out of 50) states

allow HDPE pipe to be bid in drainage applications when pressure ratings are not required.

All 42 states that are using HDPE pipe commented that the pipe's performance was satisfactory. An example of the questionnaire used by the Tennessee DOT to obtain information from other states is provided as Exhibit B-2 in Appendix B. A brief summary of the responses of the various states is presented in Appendix C.

Table 2.1. Use of HDPE pipe by state DOT's.

Diameter of pipes used	Number of years used	Number of states	Number of states using for each application		
			Cross drains	Storm drains	Driveways
≤15 in.	4	1	0	1	0
≤24 in.	2	1	0	0	1
	3	1	0	1	1
	4	2	0	2	1
	5	1	0	0	0
	6	1	1	1	1
	8	1	0	1	1
≤30 in.	8	1	1	1	1
≤36 in.	1	5	1	4	4
	3	5	2	4	3
	4	5	2	4	5
	5	7	6	6	6
	7	3	2	2	3
	8	5	3	5	5
	10	1	1	1	1
11	1	0	1	1	
≤48 in.	11	1	1	1	1

2.12 Iowa Counties use of HDPE Pipes

In order to gain an understanding about the current use of HDPE pipes as well as the problems with installing them and any long-term problems with currently installed pipes, a survey was sent to the 99 Iowa counties requesting input on their use of the pipes. An example of the questionnaire used is included as Exhibit B-1 in Appendix B. Eighty-seven (88%) of 99 counties responded to the questionnaire. Of those responding, 17 reported using HDPE pipe. Five counties use HDPE pipe exclusively in new construction and ten counties use HDPE pipe in the rehabilitation of sites where other types of pipe were originally used. Two counties have used HDPE pipe in both applications.

Three counties using HDPE pipe in new construction indicated that it had been used in one or two installations. One county had used it in three to four projects and three counties have used HDPE pipe in six or more projects. These seven counties reported no unusual installation techniques; however, one county described an uplift failure of a new installation. Specifically, uplift seemed to be a problem in low-slope installations when the inlet ends were exposed to high water levels.

Of those counties using HDPE pipe in rehabilitation projects, eight counties reported the use of the pipe in one or two projects. One county responded that HDPE pipe had been used in three to four rehabilitation projects and two counties noted it had been used in more than six projects. One common problem in installing HDPE pipe in remediation projects is in the pressure grouting phase. One agency reported leaking joints

while another indicated that the flowable mortar may not have been sufficiently fluid and may have resulted in voids in the cured grout between the original structure and the HDPE pipe. However, another county reported no problems pressure grouting between the existing pipe and the new HDPE pipe. Other problems include collapse, clogging, and uplift of single-walled pipes. One county reported that during the installation of HDPE pipe, braces placed to resist uplift from the flowable mortar caused deformation of the pipe and led to a less than satisfactory installation. One county indicated that the relative newness of the pipe resulted in the agency fabricating a large "oil-filter-type" wrench to tighten the couplers between pipe segments.

Counties not currently using HDPE pipe expressed concerns with: chemical deterioration, clogging, uplift when exposed to high hydrostatic pressures, problems from exposure to ultraviolet light, burning, crushing under high fill, crushing of unsupported ends, and excessive deformation. One county currently using HDPE pipe indicated that it assumes no responsibility after five years in driveway installations.

Currently, there is minimal use of HDPE pipe by Iowa counties; with only 17% of the counties reporting some use of the product. Some counties currently not using HDPE pipe have explored the possibility of using it, but are reluctant because of concerns of performance and installation problems. Counties that do have a few installations are reluctant to significantly increase the use of the pipe, even though nearly all pipes used in new construction have been reported to be performing satisfactorily to date. Currently, no

county has employed any tie down systems to resist potential uplift problems. However, only 24-in. diameter pipes have been used in most installations, and very few of the 36-in. and 48-in. pipes have been installed. Larger diameter pipes of other types have consistently shown more susceptibility to uplift. The large range of uses and problems noted in the responses to the questionnaire verifies the need for the experimental work undertaken in this investigation so that engineers feel comfortable using larger diameter HDPE pipe at various sites.

2.13 Specifications

There are a variety of different specifications and recommended installation techniques for HDPE pipes. They vary from the very non-specific to a very precise methodology. Summarized in the following sections are the Iowa DOT and AASHTO specifications and some recommended practice from industry that are related to the bedding requirements for HDPE pipe.

2.13.1 Iowa DOT

The current specification for the burial of HDPE pipe is given in Section 2416.04 of the Standard Specifications for Highway and Bridge Construction (1992, pp 354-355, 267). The specification is primarily concerned with the bedding of the pipe. Currently, there are two classes of bedding in the specification, Class B bedding and Class C bedding. However, only the Class B bedding has been used by the Iowa DOT. The specification

reads as follows are shown in Fig. 2.4.

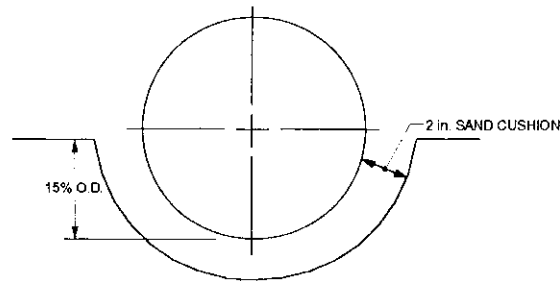
The surface upon which pipe sections are to rest shall be brought to a suitable elevation to fit the desired grade and camber, and the base shall be prepared as shown in the contract documents. When specified, the base shall be Class B bedding. When not specified, the base shall be Class C bedding.

1. Class B Bedding

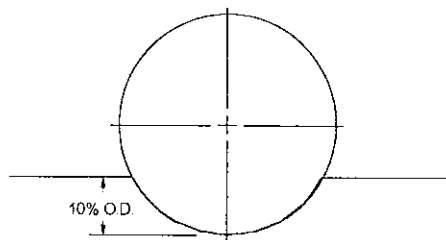
Class B bedding shall consist of a 2 inch cushion of sand shaped with a template to a concave saddle in compacted or natural earth to such a depth that 15 percent of the height of the pipe rests on the sand cushion below the adjacent ground line.

2. Class C Bedding

Class C bedding shall consist of a concave saddle shaped with a template, or shaped by other means and checked with a template, in compacted or natural Earth to such depth that 10 percent of the height of the pipe rests below the adjacent ground line.



a. Class B bedding



b. Class C bedding

Figure 2.4. Iowa DOT bedding specifications.

The material to be used in backfilling around the pipe shall be as follows:

When pipes are laid wholly or partly in a trench, granular backfill may be required for backfill as provided in Article 2402.09. The remainder of the fill, to at least one-foot above the top of the pipe, shall be compacted earth with slopes as outlined.

Article 2402.09 is as follows:

When granular backfill material is specified, backfill material shall meet requirements of Section 4133... Granular backfill shall be constructed in layers of not more than 8 inches. Each layer shall be thoroughly tamped or vibrated to insure compaction.

As per Section 4133, the granular material, if required, shall have the following composition:

20%-100% passing No. 30 sieve

100% passing the 3 in. sieve

0%-10% passing No. 200 sieve

2.13.2 Hancor Recommendations

In published literature, Hancor (1991, pp 7, 7-8) recommends the following for backfill and bedding material:

Hancor recommends achieving a backfill modulus of at least 100 psi around the pipe. Higher E' values provide additional stability. In most installations, however, when anticipated traffic loads are standard H-20 and soil covers limited to about twenty feet, the minimum E' value is sufficient.

It is the combination of soil quality, or class, and compaction that results in the

backfill modulus. Class I, representing angular aggregates, and Class II are the most highly recommended backfill classes for material surrounding the pipe. Class I soils can achieve the minimum E' value by simply dumping the material around the pipe. Class II soils require some compaction, although only around 85%, to achieve the E' value. Class III materials are permitted in the backfill envelope but require closer supervision during compaction to achieve the minimum backfill modulus. The three classes of backfill are described as follows:

Class I:

Graded stone, crushed stone, crushed gravel, coral, slag, crushed shells, cinders.

Dumped in place.

Lift Placement Depth = 18 in.

ASTM D2487 -- Notation not applicable.

Class II:

Coarse sands and gravels; variously graded granular, non-cohesive sands and gravels; small amounts of fines permitted.

ASTM D2487 -- GW, GP, SW, SP

Minimum Standard Proctor Density = 85%.

Lift Placement Depth = 12 in.

Class III:

Fine sand and clayey gravels, fine sands, sand/clay mixtures, gravel/clay mixtures.

ASTM D2487 -- GM, GC, SM, SC

Minimum Standard Proctor Density = 90%.

Lift Placement Depth = 9 in.

Backfill Placement is described as follows:

Perform a subsurface exploration to determine if zones of soft material are present. If soft materials are found, excavate and replace with granular fill. If no undesirable foundation material is found, a few inches of bedding should be placed and compacted on the foundation. The bedding can be shaped, but it is more common to tamp the fill under the haunches. The next layer, the haunching, is the most critical in that it provides the support and strength of the pipe. Lifts should be completed as outlined to the springline. The initial backfill extends from the spring line to a minimum of 12 in. above the crown of the pipe. This area of backfill sets the pipe in place. Compaction of this area should be done with care so as not to damage the pipe. The final backfill, which extends from the initial backfill to the ground surface, does not provide any structural characteristics to the pipe. Proper compaction in this area is not as critical for the pipes performance as in the other layers. A cross section of this is shown in Fig. 2.5.

It should be noted that this is very similar to the ASTM D2321 standard practice for underground installation of thermoplastic pipe for sewers and other gravity-flow applications.

2.13.3 Amster Howard's Recommended Installation Procedure

Amster Howard (1995), a consulting geo-technical engineer and noted researcher in the area of buried pipes, recommends a series of installations that range from 'good' to 'better' to 'best'. The best installation procedure utilizes a cement slurry (see Fig. 2.6). It is used to fill the gap between the pipe and the trench to ensure complete contact. The strength of the slurry can be quite low, 100-200 psi at 7 days, and is not meant to be a structural mix. The pipe is laid on soil pads (or sand bags) to a height of 3 in. above the foundation soil and leveled to the proper grade. The slurry is added on one side of the

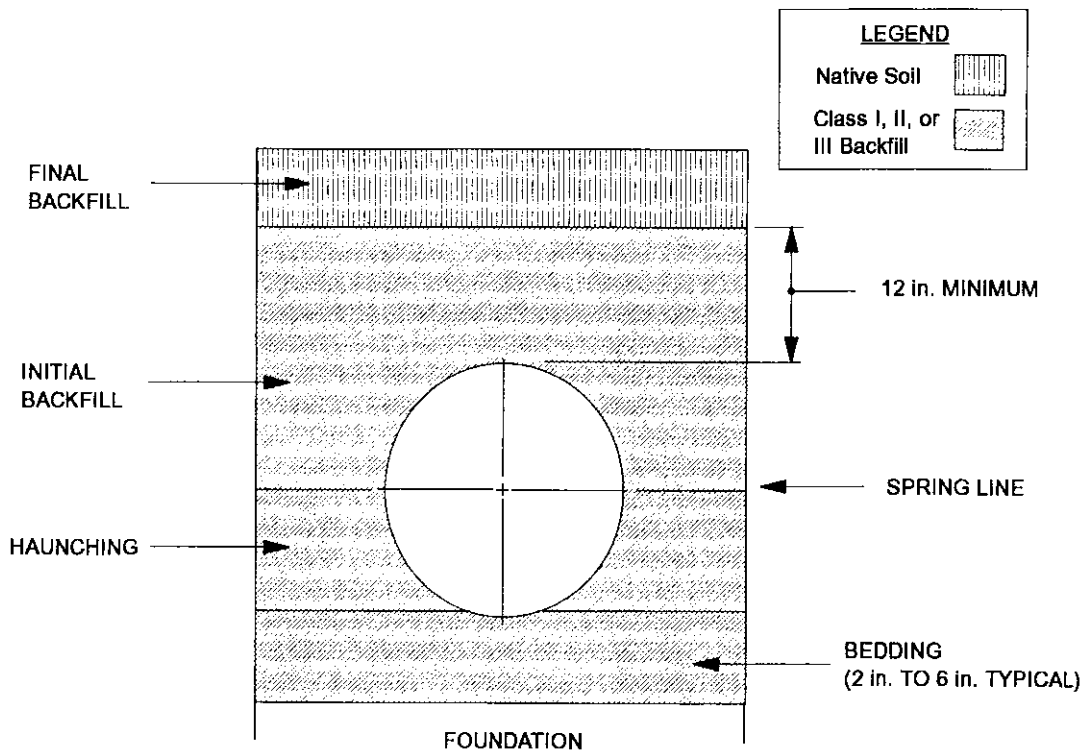


Figure 2.5. Hancor recommended backfill envelope.

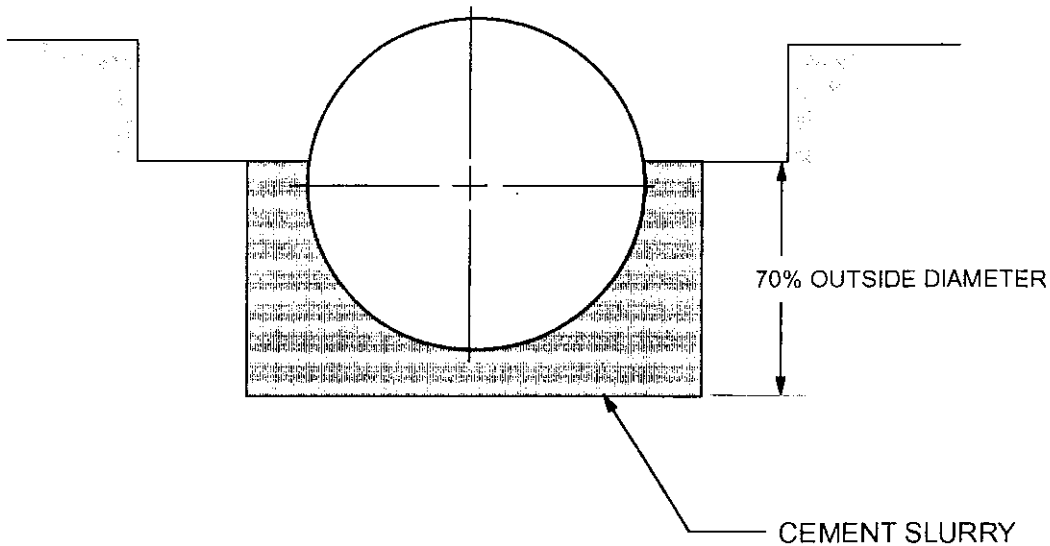


Figure 2.6. 'Best' backfill according to Amster Howard.

pipe until it appears on the other side. The slurry is poured to a height of 70% of the outside diameter of the pipe. The trench is excavated so that a minimum of 3 in. is clear on all sides.

The 'better' installation consists of using a select granular material as the embedment material as well as the bedding material (see Fig. 2.7). This select granular material is a cohesionless, free-draining material. Specifically, 5% fines or less with the maximum size not to exceed 3/4-in., and not more than 25% passing the No. 50 sieve. The bedding is placed uncompacted to a 4-in. depth and the pipe is placed on this pad. The backfill is compacted to a height of 70% of the outside diameter in 6-in. lifts with tampers or rollers providing the compactive effort. The backfill material above 70% can be any

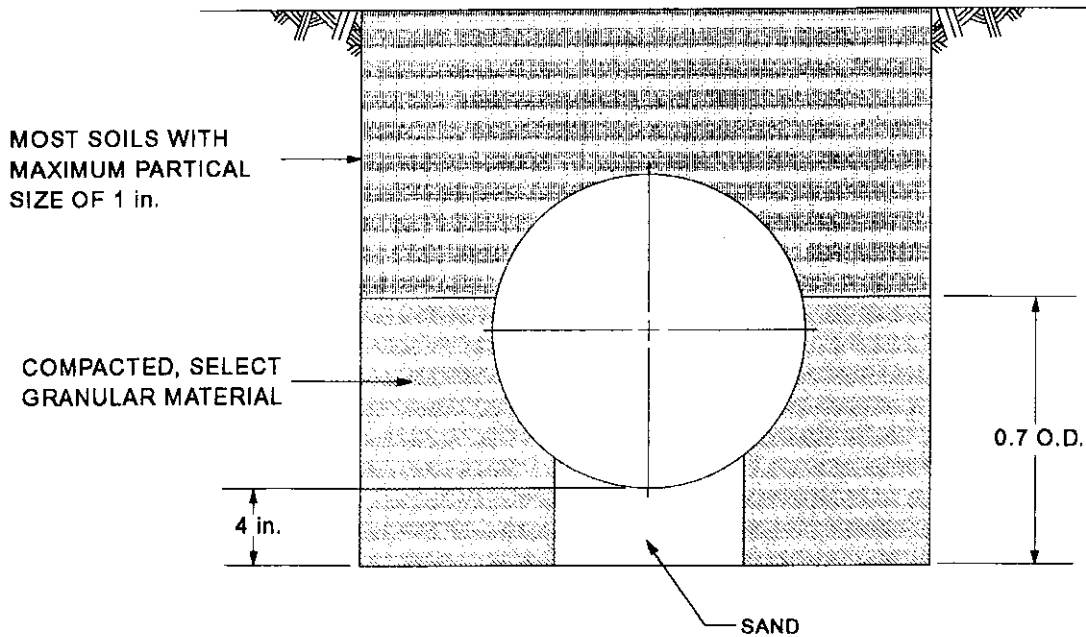


Figure 2.7. 'Better' backfill envelope according to Amster Howard.

soil with a maximum particle size of 1-in. Soil is placed to a minimum of 30-in. above the invert of the pipe before any compaction equipment is used and the soil is left uncompacted to achieve full soil arching to distribute loading away from the pipe.

The 'good' installation employs the use of the same backfill material as the 'better' installation; however, the material is simply dumped in and little to no compactive effort is applied. Similar to the 'better' installation, the 'good' installation has an uncompacted sand bedding upon which the pipe is laid.

2.13.4 Advanced Drainage Systems (ADS) Recommended Backfill Envelope

ADS (Goddard, 1992) recommends following the provisions of ASTM D2312. Additionally, ADS gives recommendations for the minimum trench width as the outside diameter plus 16 in. or the outside diameter times 1.25 plus 12 in. whichever is greater. Poor in situ soil conditions will require substantially wider backfill as well as deeper foundation and bedding. Trench width and foundation should be based on a thorough site investigation.

Additionally, ADS offers suggested means of trench control through the use of wrapping the backfill and bedding material with a geotextile. Particularly severe conditions may require a geonet or geogrid, often in combination with a geotextile.

They note that recent development of flowable, low strength cement or fly ash backfill provides the ability to reduce trench width and still get adequate backfill support. This can be particularly helpful in municipal street installations.

ADS warns that flexible pipe should never be installed in a concrete cradle as is done for rigid pipe in a Class A installation. This type of installation could create concentrated forces at the ends of the cradle when the pipe deforms.

2.13.5 ASTM Recommendation for Underground Installation of Thermoplastic Pipe

ASTM D2321 provides recommendations for the installation of thermoplastic pipes in gravity flow applications as shown in Fig. 2.5. The specification gives

recommendations for the types of soils that can be used in each section of the backfill envelope. Additionally, the minimum compaction required is also outlined and tabulated.

The excavation of the trench is also covered in the specification. "Trench walls shall be excavated to ensure that sides will be stable under all working conditions. Slope trench walls should be sloped or supports provided in conformance with all safety practices. Pipes should never be laid in standing or running water and at all times runoff and surface water should be prevented from entering the trench."

In the absence of an engineering evaluation, 24 in. of cover or one pipe diameter shall be provided for Class IA and IB, and a cover of at least 36 in. or one pipe diameter for Class II, III, and IV embedment.

2.13.6 The "Greenbook" Specifications

The latest edition of the "Greenbook", Standard Specification for Public Works Construction, (scheduled for publication in early 1996) officially approves the use of HDPE drainage pipe in public construction. This new specification which is modeled after the California DOT specification for corrugated HDPE pipe approves the use of 12 in. through 36 in. annular corrugated smooth interior HDPE with bell-and-spigot joints for storm drains, culverts, and subsurface drains. The "Greenbook" specification includes requirements regarding backfill materials and deflection testing and is the official specification, bedding and contract document for nearly all cities and counties in Southern

California.

2.13.7 1992 AASHTO Standard Specifications for Highway Bridges

Section 18 of the AASHTO Standard Specifications for Highway Bridges (1992) gives a design methodology for buried plastic pipes. AASHTO recognizes that a buried flexible pipe must be treated as a composite structure of the pipe ring and the soil envelope, and that both materials are vital in the structural design of the plastic pipe.

Service load design, which is traditionally used in culvert design, gives three design equations. The equations deal with the required wall area due to thrust, wall area to resist buckling, and the so-called flexibility factor. Minimum cover for the design loads shall be the greater of the inside diameter divided by 8 or 12 in. whichever is greater and shall be measured from the top of a rigid pavement or the bottom of a flexible pavement.

AASHTO also gives a standard specification for 12 to 36-in. diameter Corrugated Polyethylene Pipe in M 294. The specifications covers the requirements and methods of testing for corrugated polyethylene pipe, couplings, and fittings. Test methods are described or referenced for pipe stiffness, pipe flattening, brittleness, and environmental stress cracking. Minimum requirements are given for each type of test.

2.13.8 LRFD AASHTO Bridge Design Specifications

Thermoplastic pipe design is also included in the LRFD AASHTO Bridge Design Specifications (1994). The specification again provides equations for checking the wall resistance to thrust, buckling, and the handling and installation requirements. Minimum cover is specified as the inside diameter divided by 8 or 12 in., whichever is greater. The so-called flexibility factor is still included in the LRFD AASHTO Bridge Design Specifications.

3. TESTING PROGRAM

3.1 Overview

Since HDPE pipe is a relatively new construction material and the behavior of the material is not well documented or known, a testing program was initiated to gain some basic understanding of the nature of HDPE as a structural material as well as a buried structure. The testing program consisted of a series of parallel plate tests on pipe ranging from 2-ft to 4-ft in diameter following the provisions of the American Society of Testing and Materials (ASTM) D2412, a sequence of flexural tests for determining flexural stiffness of 3-ft and 4-ft diameter pipe, and field tests of buried 3-ft diameter pipe for determining the contribution of the backfill and bedding soil on the performance of the pipe. The HDPE pipe specimens used in the various tests were provided by three different manufacturers which are identified in the acknowledgments. In this report, specimens will only be identified as Manufacturer A, Manufacturer B, or Manufacturer C and by pipe diameter in inches (i.e., 24 = 24-in. pipe diameter, 36 = 36-in. pipe diameter, etc.).

3.2 Parallel Plate Testing

Since it was easier to control the rate of loading using the Satec testing machine at the Iowa DOT Material Testing Facilities (Ames, Iowa) all specimens 36-in. in diameter or less, were tested at the Iowa DOT. Specimens with 48-in. diameters were tested in the ISU Structures Laboratory since they were too large for the Iowa DOT testing machine.

Parallel plate tests consisted of placing specimens between two rigid plates and applying a line load to the pipe (see Fig. 3.1). The rate of head travel was controlled and the desired stiffness values were calculated at 5 % deflection. Additionally, stiffness at 10 and 30 % deflection were also calculated. Ultimate loads of pipe specimens were also obtained and the behavior noted.

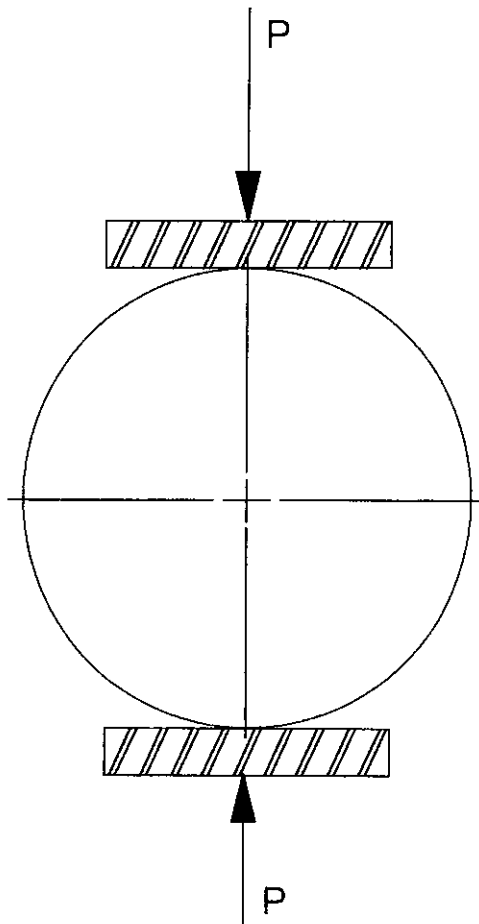


Figure 3.1. Schematic of parallel plate test.

The provisions of ASTM D2412 require the length of the specimen to be the same as the inside diameter of the specimen; however, the size of the testing machine loading table limited the length of the specimen to 30-in. This limit resulted in all 36 in. diameter specimens being shorter than the length specified in ASTM D2412. The 14 specimens tested at Iowa DOT are listed in Tables 3.1, 3.2, and 3.3 by manufacturer. Parameters of the specimens (actual diameter, wall thickness, etc.) were measured at 8 different locations and averaged as specified by ASTM. The wall thickness range is defined as the difference between the largest and the smallest thickness measurements divided by the largest thickness expressed as a percent. The number of gages is in reference to the number of strain gages used on each specimen. Gages were oriented along perpendicular axis. When the number of gages indicated is 8, both the circumferential and longitudinal strain was measured; however, specimens with 4 gages had gages in the circumferential direction only.

Table 3.1. Manufacturer A specimens tested at Iowa DOT.

Nominal Diameter (in.)	Actual Diameter (in.)	Wall Thickness (in.)	Wall Thickness Range (%)	Length (in.)	Number of Gages
24	24.07	0.254	29.95	23.44	8
24	24.03	0.270	20.00	23.00	4
30	29.95	0.133	46.06	31.88	8
30	30.02	0.145	33.24	31.63	4
36	35.56	0.305	33.30	28.50	8
36	35.38	0.297	27.33	27.62	4

Table 3.2. Manufacturer B specimens tested at Iowa DOT.

Nominal Diameter (in.)	Actual Diameter (in.)	Wall Thickness (in.)	Wall Thickness Range (%)	Length (in.)	Number of Gages
24 ^a	23.95	0.277	30.00	22.95	8
24 ^a	24.09	0.227	39.94	22.66	4
24 ^b	24.45	0.273	30.00	24.27	8
24 ^b	24.28	0.258	39.94	23.21	4

^aSingle Wall Profile^bDouble Wall Profile

Table 3.3. Manufacturer C specimens tested at Iowa DOT.

Nominal Diameter (in.)	Actual Diameter (in.)	Wall Thickness (in.)	Wall Thickness Range (%)	Length (in.)	Number of Gages
24	24.09	0.203	25.00	25.20	8
24	24.11	0.156	33.24	24.77	4
36	36.36	0.195	42.86	29.65	8
36	36.45	0.209	31.45	29.89	4

The Iowa DOT testing machine consists of an electronically controlled loading table (Fig. 3.2) and a basic computer controlled data acquisition system (DAS) that collects load and table deflection data. Data were collected via this system in addition to the strain and deflection data recorded using an ISU DAS. Each pipe section was instrumented with four Celesco transducers for measuring change in diameters along perpendicular axes. Changes in diameter were monitored in two planes close to the ends of the specimen (see Fig 3.3) to observe any type of non-uniform loading and/or deformation. Additionally,

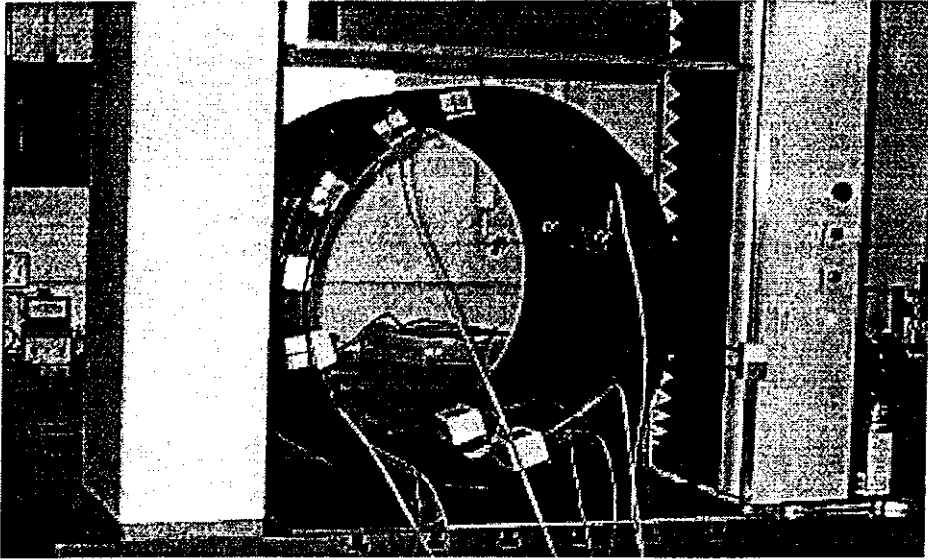


Figure 3.2. Iowa DOT test machine.

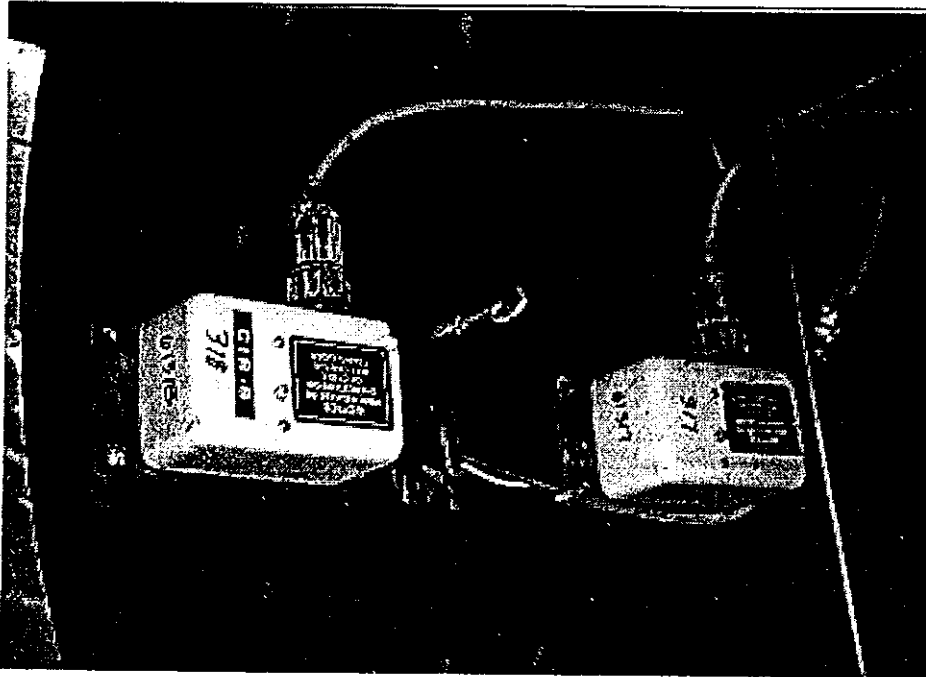


Figure 3.3. Instrumentation for measuring change in diameters.

electrical resistance strain gages were installed along the same perpendicular axes. Two pipes of the same manufacturer and size were tested. The first specimen had four bi-axial strain gages measuring circumferential and longitudinal strains, while the second specimen had four uniaxial strain gages for measuring circumferential strains only.

Testing consisted of a series of five tests on each specimen. Tests were run to 5% deflection with the pipe in a 0-degree rotation position (Fig. 3.4a), 22.5-degree rotation (Fig 3.4b), 45-degree rotation (Fig 3.4c), and 67.5-degree rotation (Fig 3.4d). The specimens were then returned to the 0-degree point and tested to failure. Specimens were rotated so that the strain and deflection response could be monitored in 16 different orientations. In all tests, data were recorded by the two DAS's on set time intervals based on the estimated length of each test.

Similar to the Iowa DOT testing machine, the size of the loading platen in the ISU testing machine limited the length of the specimens. Pipe segments were limited to 21 in. in length and therefore were not in complete compliance with ASTM D2412. Any diameter of pipe could be tested in the machine however rate of loading had to be controlled "by-hand". Specimens tested at ISU are described in Table 3.4 and Table 3.5 following the same measurement procedures previously defined.

Four 48 in. diameter specimens were tested using the ISU test machine. All specimens were instrumented similarly to the smaller specimens that were tested at the Iowa DOT. Testing procedures employed (4 tests to 5% deflection plus an ultimate load

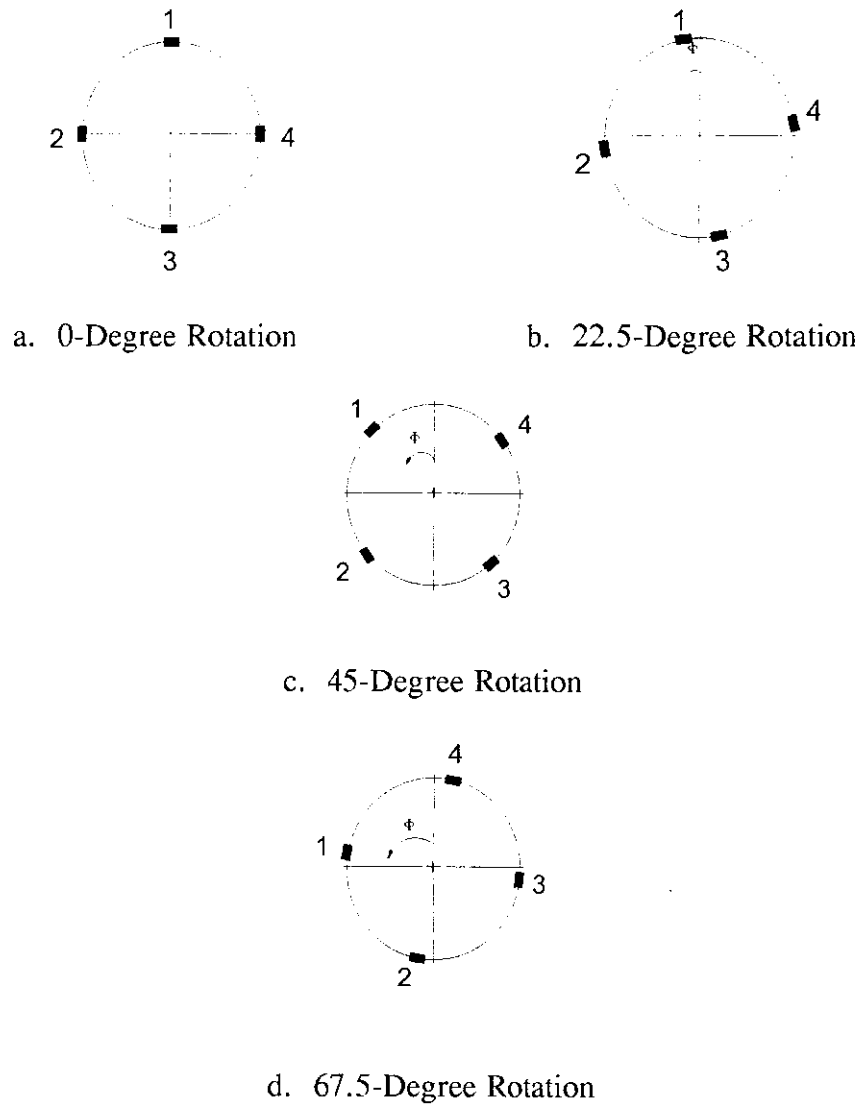


Figure 3.4. Testing orientations used in parallel plate tests.

Table 3.4. Manufacturer A specimens tested at ISU.

Nominal Diameter (in.)	Actual Diameter (in.)	Wall Thickness (in.)	Wall Thickness Range (%)	Length (in.)	Number of Gages
48	48.06	0.173	30.00	20.36	8
48	48.20	0.145	35.43	20.20	4

Table 3.5. Manufacturer C specimens tested at ISU.

Nominal Diameter (in.)	Actual Diameter (in.)	Wall Thickness (in.)	Wall Thickness Range (%)	Length (in.)	Number of Gages
48	47.38	0.176	42.86	21.38	8
48	47.64	0.164	33.33	20.61	4

test), and rate of loading ("hand" controlled) were the same as those used at the Iowa DOT. Data (applied load, resulting strains, changes in diameter, etc.) were recorded using laboratory DAS's.

3.3 Flexural Testing

Since no bending stiffness data for large diameter HDPE pipes were available in the literature, a limited series of flexural testing on the larger diameter HDPE pipe was initiated. Two sizes, 3-ft and 4-ft diameter, and two manufacturers, A and C, were selected for testing.

3.3.1 Test Frame

In order to test each HDPE pipe in flexure, specimens were simply supported and third point loading were applied. A plan view and side view of the load frame are shown in Figs. 3.5 and 3.6, respectively. The frame was set up to resist the loads associated with the testing of the largest test specimens and to allow movement of the loading cylinder to

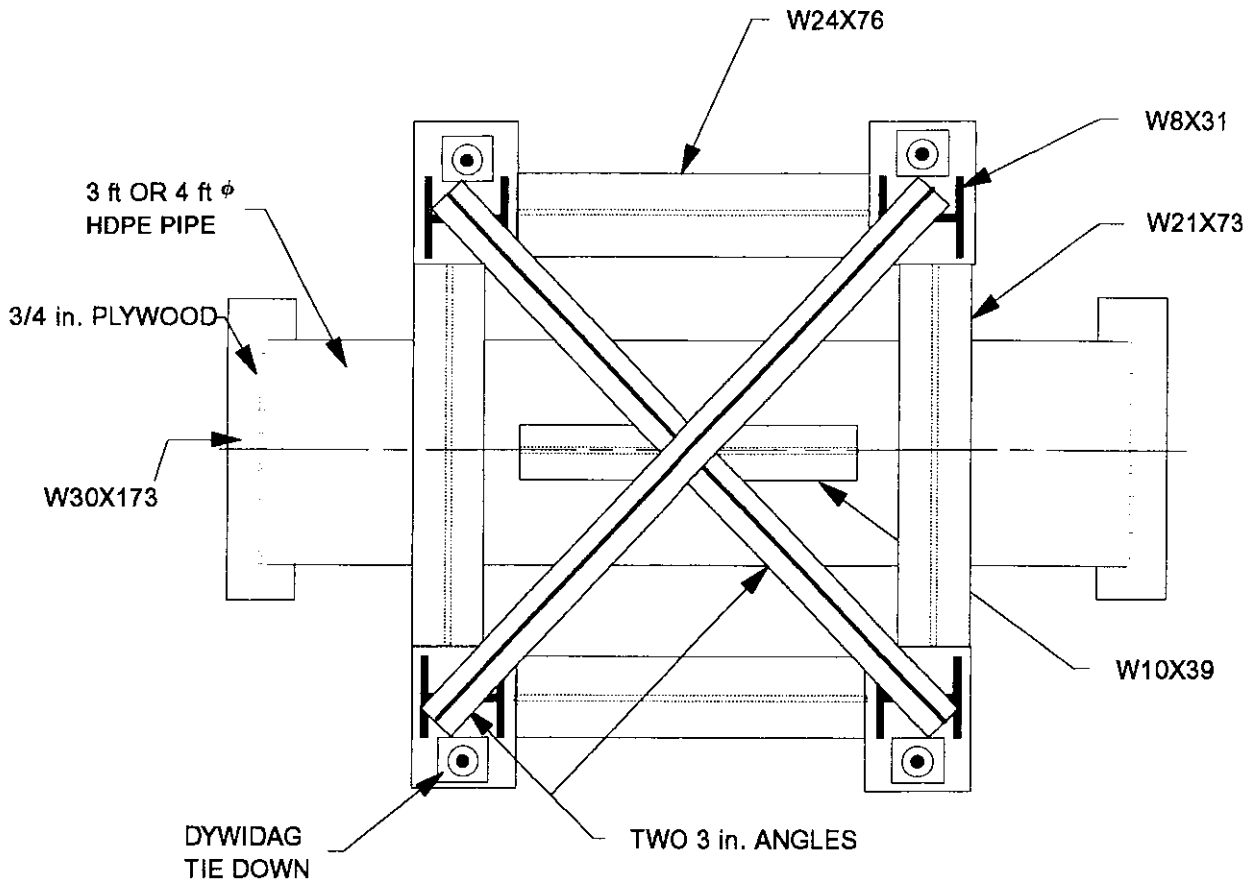


Figure 3.5. Plan view of flexural test load frame.

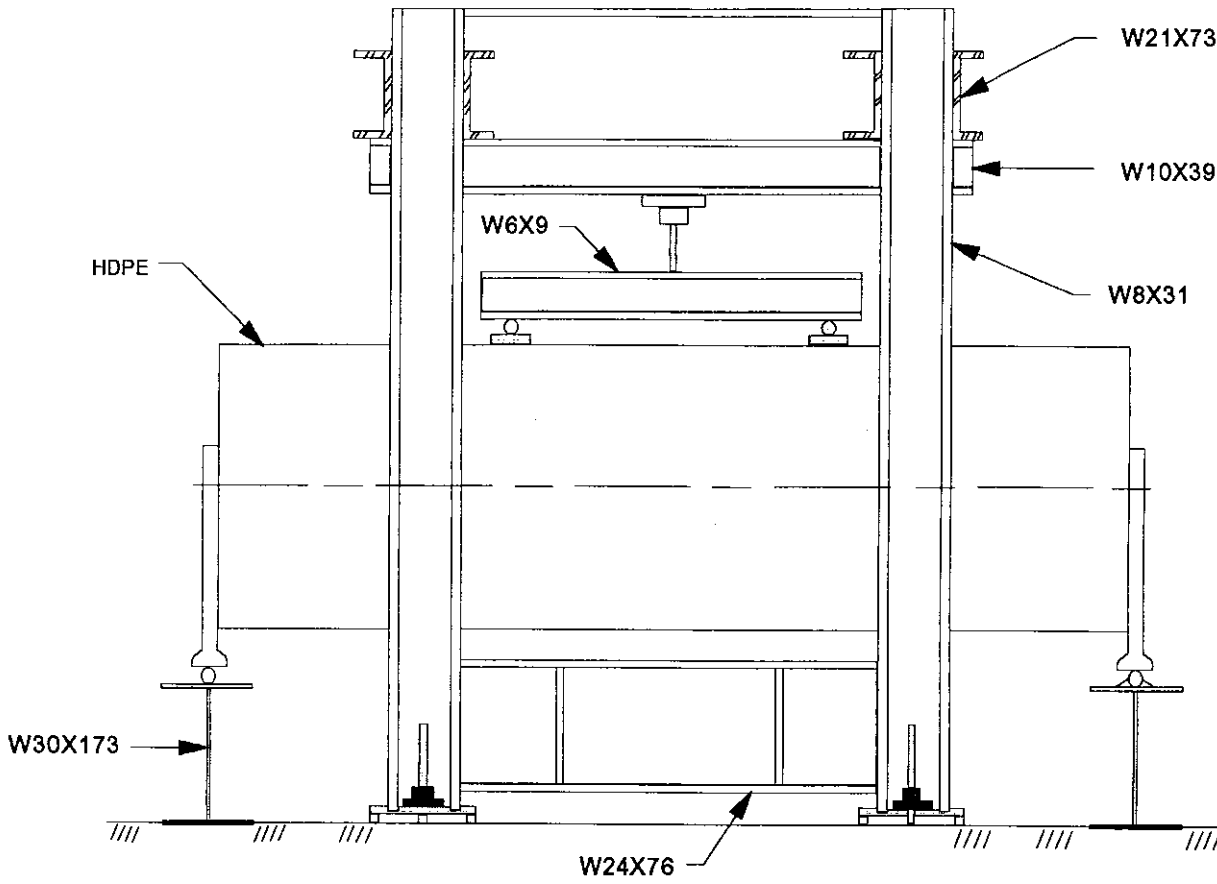


Figure 3.6. Elevation view of flexural test frame.

desired locations.

Support for the pipe ends were simple supports; pin and roller ends were constructed from 3/4-in. plywood and 3-in. steel angle. The pipe specimens were connected to the 3/4-in. plywood end diaphragms using 1/2-in. diameter bolts and 3-in. steel angles as shown Fig. 3.7 (side view) and Fig. 3.8 (cross-section). The use of the plywood supports provided a rigid restraint that limited deformation of the cross section at the ends of the pipe specimens. Bolted connections were designed to resist the largest anticipated loads. The combination of the 3-in. angles and plates along the bottom of the plywood plus the 1-in. diameter steel rods (see Figs. 3.7 and 3.8) made it possible to simulate pin and roller supports at the ends of the specimen.

These supports permitted rotation of the pipe at both ends and allowed free longitudinal movement on the roller end. During testing, the plywood was reinforced by structural steel sections along the axis of loading to prevent buckling of the plywood (not shown above).

3.3.2 Testing Procedure

Hydraulic cylinders provided the load on the pipes. One hydraulic cylinder used with a spreader beam achieved the desired two-point loading configuration. Each end of the spreader beam (W6x9) was supported by a roller support to limit restraint on the top of the pipe. Load was transmitted to the top of the pipe through a 12-in. x 12-in. x 1-1/16-in.

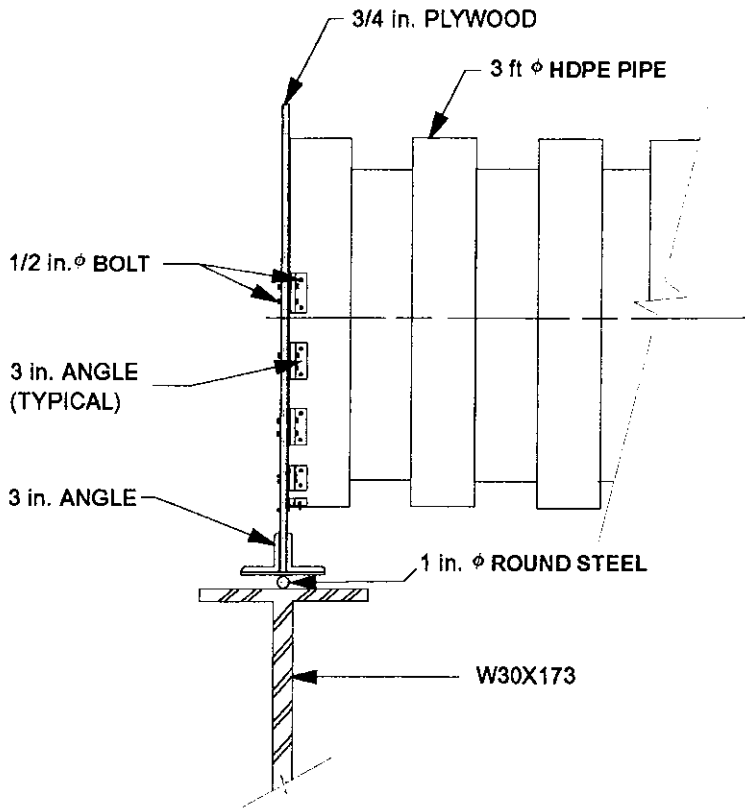


Figure 3.7. Side view of beam support.

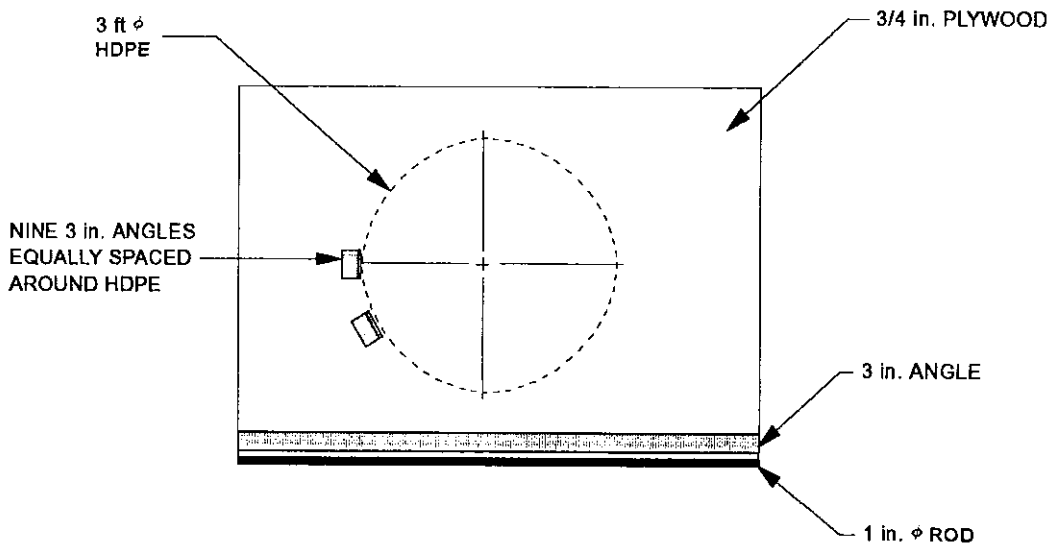


Figure 3.8. End view of pipe connection to plywood.

steel plate. In testing Specimen A36 (i.e., manufacturer A, diameter 36-in.) the plate was placed directly on the pipe; this resulted in a premature failure of the specimen by "folding over" of the corrugations under the load plates. Subsequent tests utilized neoprene pads in the valley of corrugations as shown in Fig. 3.9 which eliminated the folding over problem.

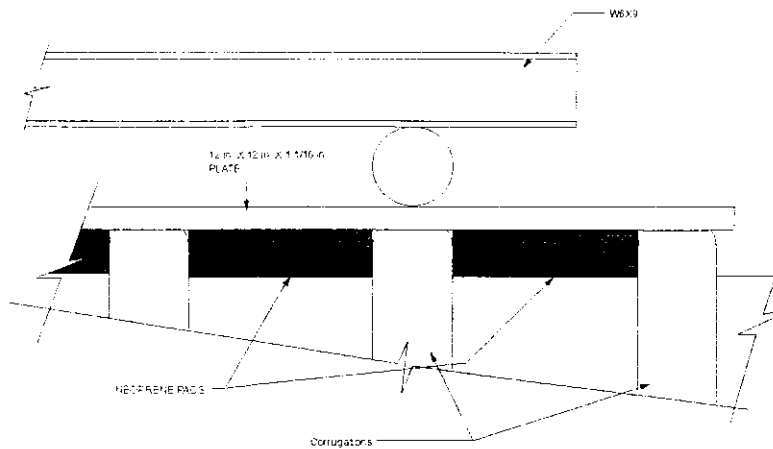


Figure 3.9. View of neoprene pads used in HDPE pipe corrugation valleys.

All specimens were a nominal 20-ft in length; the location of the load points used in each specimen was based on third point loading and the actual length of the specimen. A total of six specimens were tested with a total of four combinations of manufacturer and pipe diameter. The set up of each is presented in Fig. 3.10 with the length parameters given in Table 3.6. Note, in this table A36.1 indicates the first 36-in. diameter specimen from Manufacturer A, A36.2 indicates the second 36-in. diameter specimen from manufacturer A, etc.

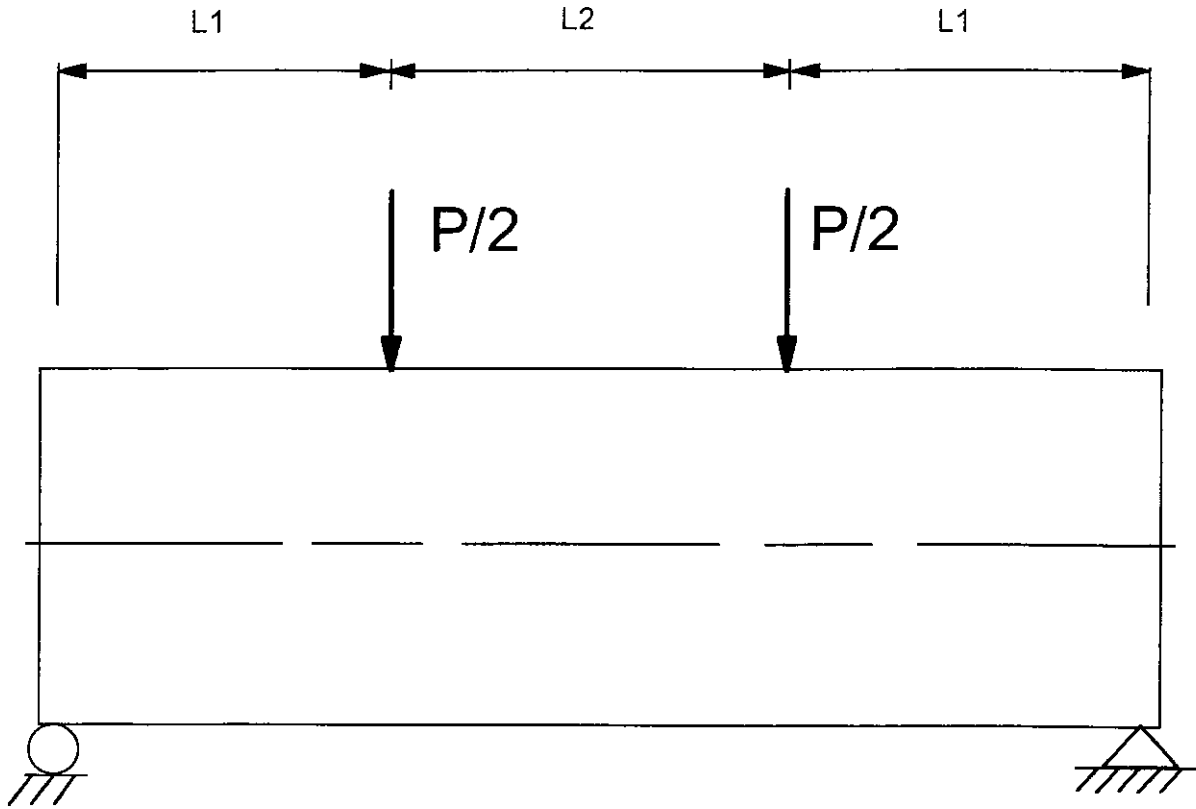


Figure 3.10. Schematic of test setup used in flexural tests.

Table 3.6. Length parameters of flexural specimens.

Specimen	L1	L2	Total Length
A36.1	6 ft - 8 in	6 ft - 5 in	19 ft - 9 in
A36.2	6 ft - 5 in	6 ft - 4 in	19 ft - 2 in
C36	6 ft - 8 in	6 ft - 5 in	19 ft - 9 in
A48	6 ft - 7 in	6 ft - 8 in	19 ft - 10 in
C48.1	6 ft - 6 in	6 ft - 6 in	19 ft - 6 in
C48.2	6 ft - 7 in	6 ft - 4 in	19 ft - 6 in

The testing program included four service load tests and a failure load test of each specimen. The magnitude of loading in the service load tests was limited so that only elastic deformations occurred in the HDPE specimens. After each service load test, all loads were removed and specimens were permitted to "recover" for a period of at least 60 minutes. In the failure load tests, the HDPE pipe was loaded until the load on the pipe ceased to increase and/or deformations became excessive.

3.3.3 Instrumentation

Test specimens were instrumented with electrical resistance strain gages, vertical deflection transducers, horizontal and vertical diameter change transducers, and end rotation transducers. Strain gages were attached to the HDPE pipe surface and coated with an appropriate protective covering. These 350-ohm gages were connected to the DAS using three-wire leads to minimize lead wire effects. Typically, strain gages were located at the quarter points and at the centerline of the specimens. Gages at the quarter points were located at the top and bottom of the inside of the pipe for measuring longitudinal strains. The six gages at the center of the specimens were mounted on the inside at the top, bottom, and at midheight for determining both longitudinal and circumferential strains. On one of the two 48-in.-diameter specimens from Manufacturer C, additional gages were monitored on the outside of the pipe at the same locations as the gages on the inside of the pipe specimen.

Vertical deflections were determined at the quarter points and at the centerlines of the pipes using Celesco transducers attached to the bottoms of the pipes. Deflections as large as 14-in. could be read with accuracy of ± 0.001 in. Vertical deflections were used to calculate the flexural stiffness factor of the HDPE pipes and to quantify the deflected shape of the pipe.

Celesco string transducers were also used to determine the end rotation and movement of end supports as shown in Fig. 3.11, and to monitor changes in vertical and horizontal diameters during loading. Diameter changes were monitored at the same locations as the strain measurements (with a slight offset to avoid inducing stress concentrations). Changes in the specimen diameters at the various locations along the specimens provided supplemental data to strain readings and were used in determining the deflected shape of the top surfaces of the pipe specimens. Data from the load cell, strain gages, and deflection transducers were monitored and recorded with the laboratory DAS at intervals of applied load.

3.4 Field Tests

In the first two phases of laboratory work, the strength of the HDPE pipe itself was investigated. Obviously, in a typical field situation, the pipe behavior is influenced not only by its own strength characteristics but also by its interaction with the surrounding soil. Investigation of this soil-structure interaction was the primary objective of this third testing

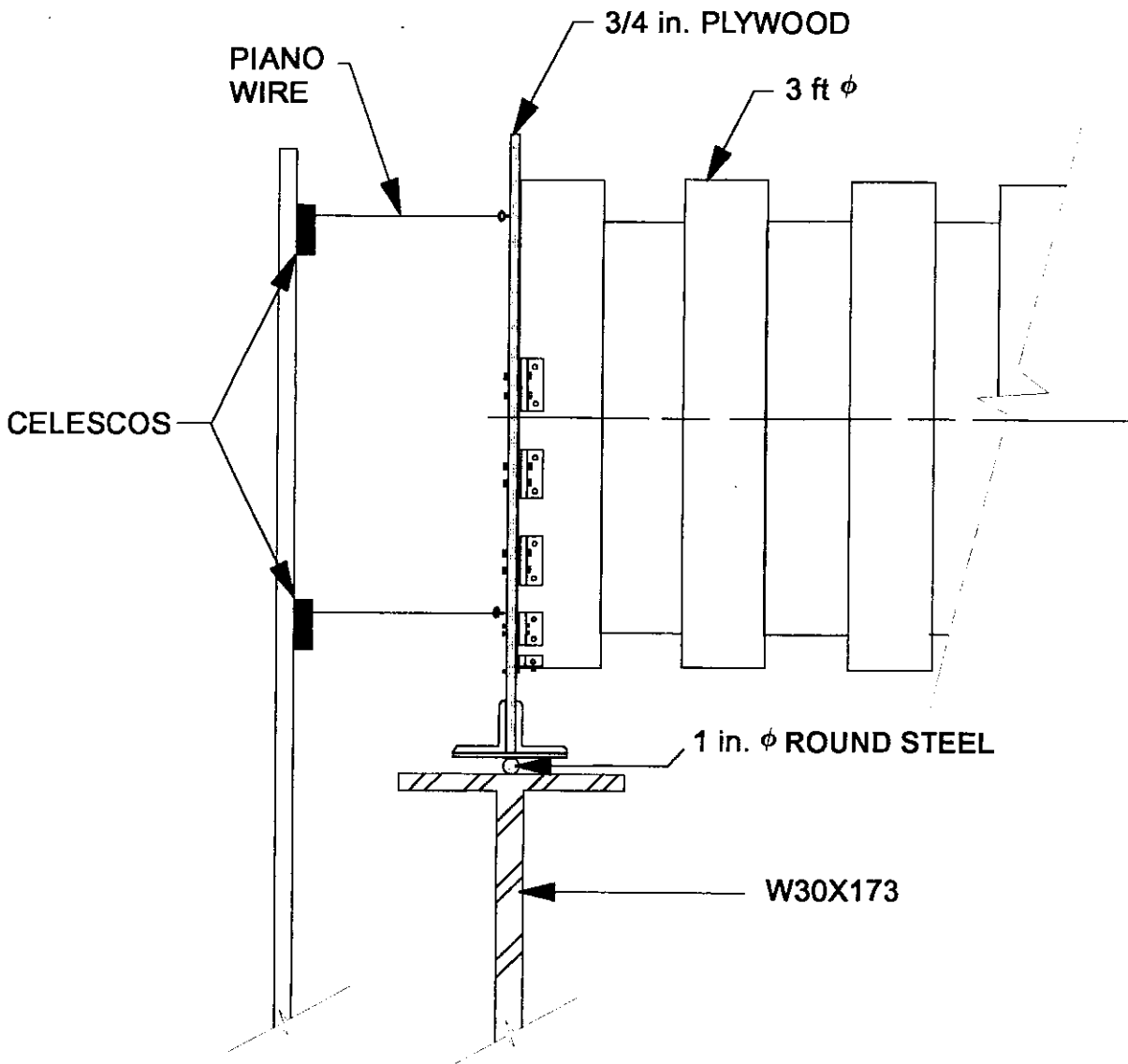


Figure 3.11. Instrumentation of end supports.

phase. Four full-scale field tests were conducted to obtain insight into this soil-structure interaction.

3.4.1 Description of Test Specimens

The manufacturer and size of HDPE pipes tested in this phase of the project were kept as a constant. Specimens were 36-in. diameter pipes from Manufacturer C. Specimens were a nominal 20-ft in length.

3.4.2 Instrumentation

Data collected in the field tests included strains on the inner surface of the pipes, change in diameter of the pipe cross section, and movement of the top surface of the pipe. Strains and change in diameter were read and recorded using a computer controlled DAS located in the ISU Structures Laboratory. Data were obtained during the actual test as well as during backfilling operations. Movement of the upper pipe wall was read manually with surveying transits during load tests.

Seven longitudinal sections were instrumented with strain gages as shown in Fig. 3.12. Gages to measure circumferential and longitudinal strains were placed at the centerlines and quarter points of the specimens (Sections B in Fig. 3.12). Additionally, uni-axial strain gages were placed on the crown, invert, and at one springline (Sections A in Fig. 3.12)

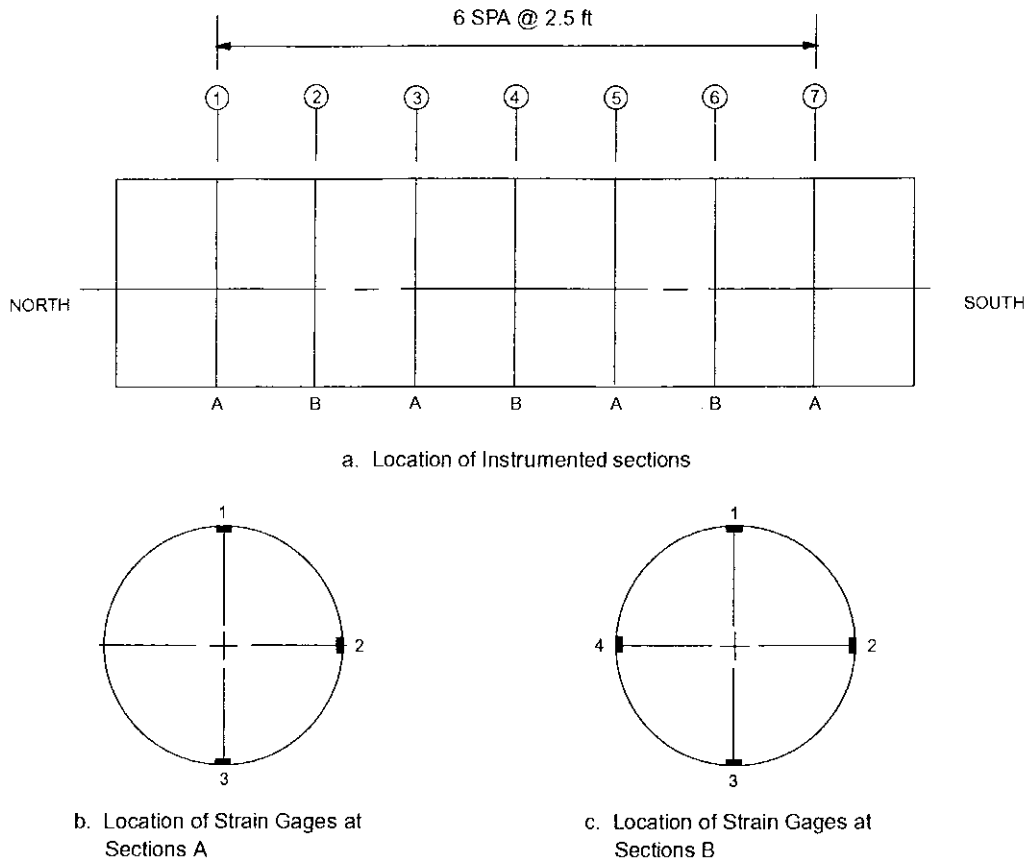


Figure 3.12. Location of strain gages used in field tests.

Celesco transducers with piano wire attached were connected to the inside walls of the HDPE pipe near the sections that were instrumented with bi-axial strain gages (Sections 2, 4, and 6 in Fig. 3.12). It was necessary to slightly offset the deflection instrumentation (4 in. south of the strain gaged sections) to avoid inducing stress concentrations. For the remainder of this report, the deformations will be referenced

according to their magnetic orientation (i.e., Celescopes near Section 2 designated north, Celescopes near Section 4 designated center, Celescopes near Section 6 designated south).

Vertical deflection of the upper surface of the specimens was measured using vertical steel rods attached to the HDPE pipe near Sections 1, 3, 5, and 7 (shown in Fig 3.12) as illustrated in Fig. 3.13.

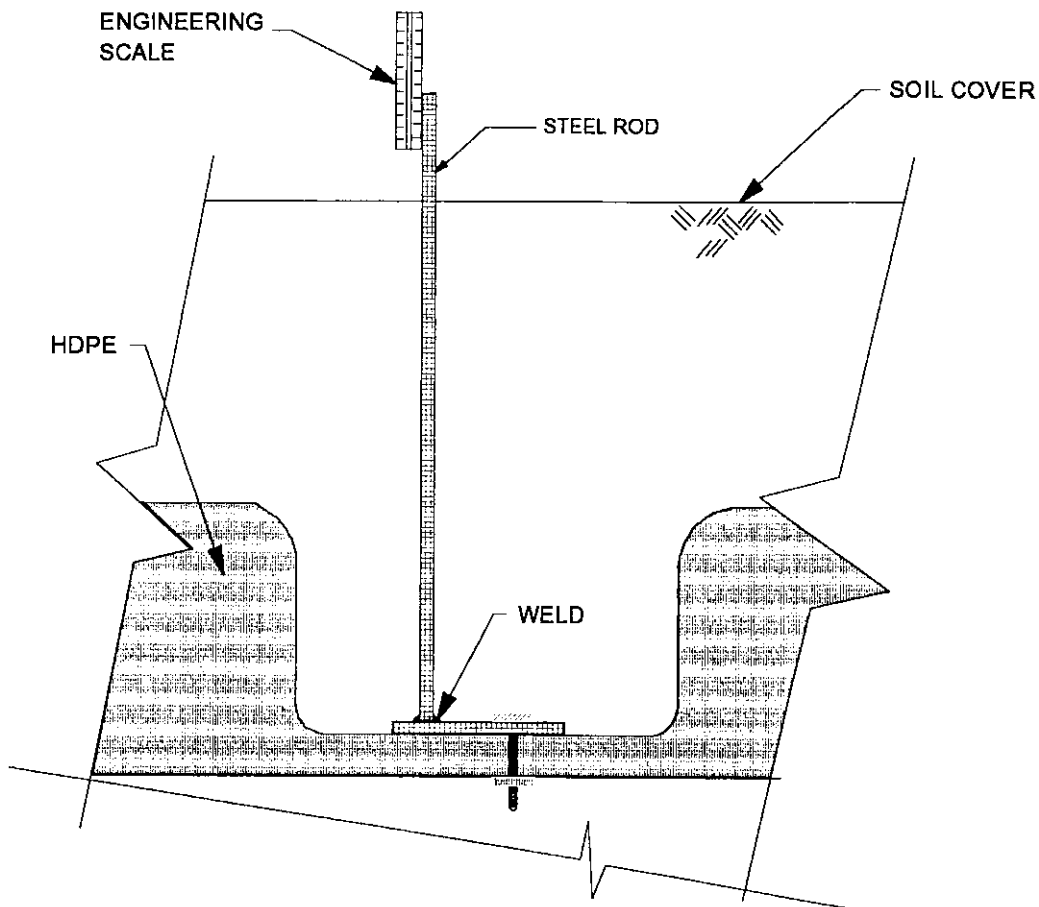


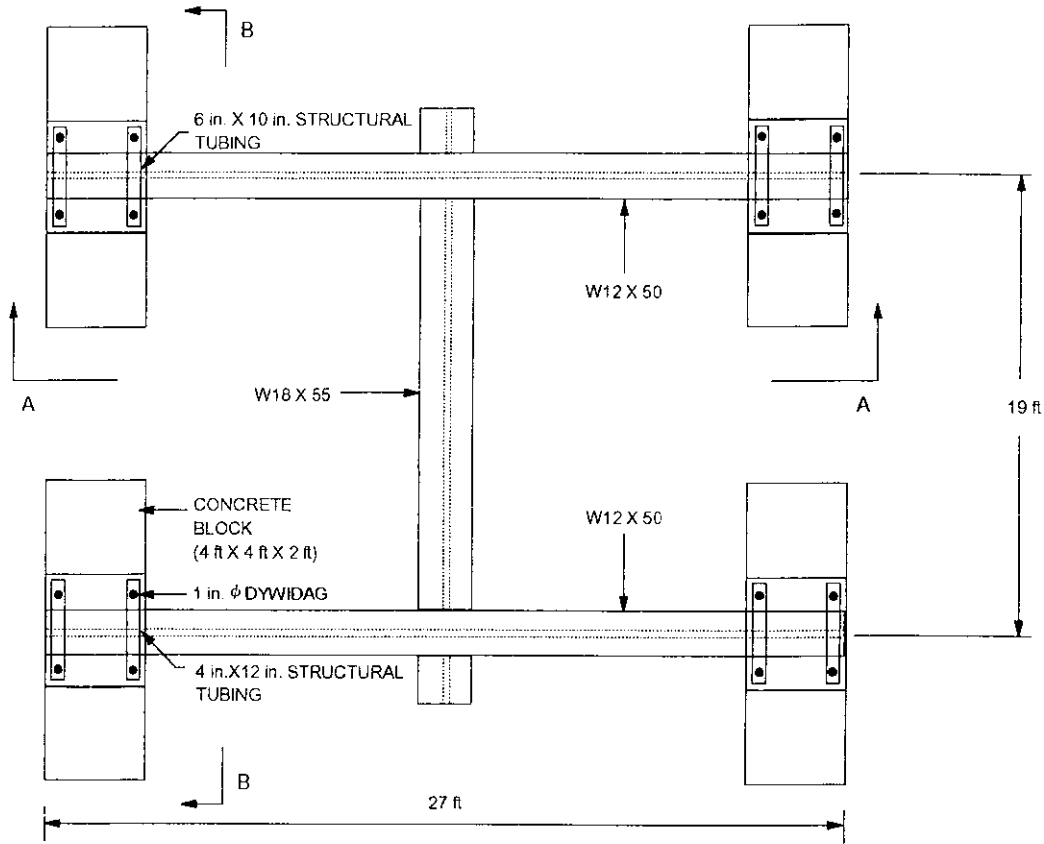
Figure 3.13. Deflection monitoring setup.

3.4.3 Description of Load Frame

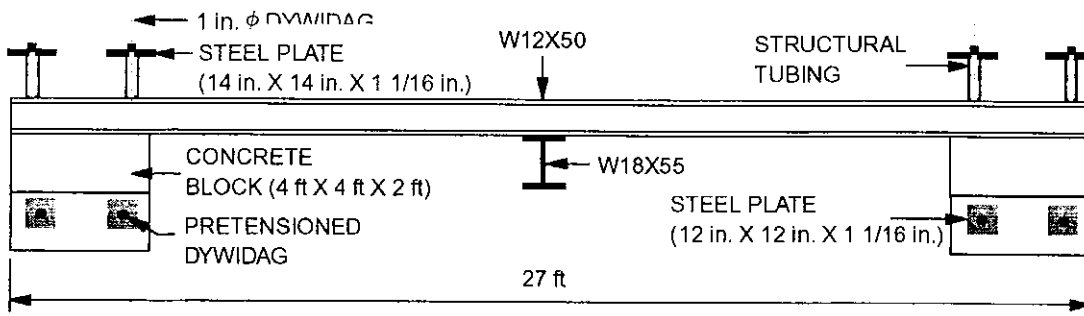
Live loads passing over the pipe were simulated with the use of a single load point one sq-ft in area. Load was applied at three different points on each test specimen. Loads were provided by hydraulic cylinders reacting against an overhead frame which was connected to a set of concrete blocks. The sixteen blocks (4-ft x 4-ft x 2-ft) weighed approximately 4800-lbs each, thus nominally 78,000-lbs could be resisted by the loading system. Actually, the loading system has a slightly greater capacity as the previous value does not include the weight of the steel framework. As shown in Fig 3.14, the concrete block and steel framework are connected by post-tensioning tendons through holes precast at the appropriate locations in the blocks. The loading system allows different loading configurations to be constructed for future tests if desired.

3.4.4 Trench Excavation and Bedding Preparation

An area directly west of the ISU Structures Laboratory was the location of the in situ tests. The test trench was excavated using a combination of a large backhoe and a smaller tractor hoe. The bottom of the trench was approximately 6-ft wide and the sides of the trench were sloped at approximately 1:1. Excavated soil was kept on site and mounded in an attempt to keep the soil dry. After the trench was excavated, the bottom of the hole was leveled by hand with shovels. Density tests were then performed on the foundation soil to obtain base data.

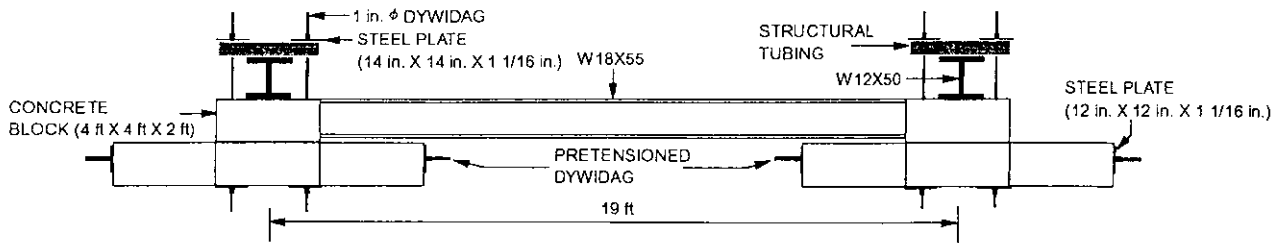


a. Plan view of load frame



b. Section A-A

Figure 3.14. In situ load test frame.



c. Section B-B



d. Photograph of in situ test frame

Figure 3.14. Continued.

The bedding was then prepared according to the type of test to be run. In the following descriptions specimens are designated as ISU1, ISU2, ISU3, and ISU4. As previously noted, all specimens were 3-ft in diameter from Manufacturer C. For ISU1, the pipe was placed on the bottom of the trench with no further foundation preparation (Fig. 3.15).

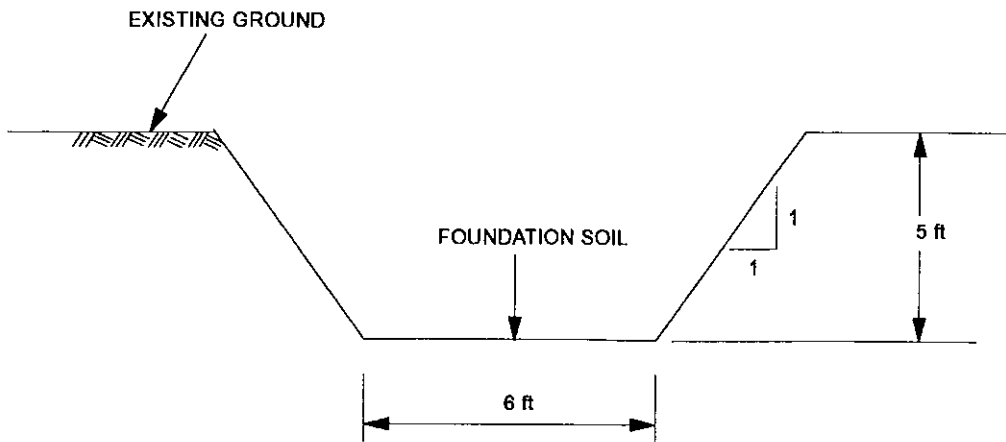


Figure 3.15. Trench geometry for ISU1.

The foundation preparations for ISU2, ISU3, and ISU4 followed the provisions of Class B bedding as per the Iowa DOT specifications. This specification requires that 15% of the total pipe height rest in a saddle cut from compacted or natural ground. Templates were prepared and used to check the concave saddle cut from the natural ground. A 2-in. cushion of sand was then placed in the entire saddle and smoothed by hand (see Fig. 3.16).

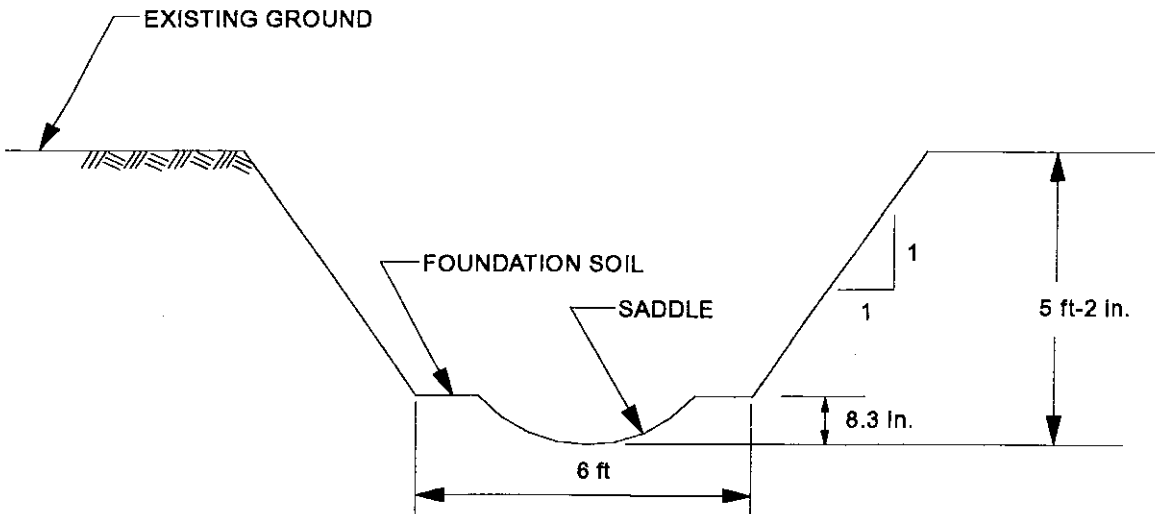


Figure 3.16. Trench geometry for ISU2, ISU3, and ISU4.

3.4.5 Placing Pipe Specimens

Each section of pipe which had been previously instrumented was carefully placed in the trench on the foundation or in the saddle by 5 laboratory personnel. Test specimens were then rotated so that the previously attached strain gages were in a vertical and horizontal orientation.

3.4.6 Backfilling

Proper backfilling techniques require a knowledge of the inherent properties of the material used as backfill. Compaction of the native glacial till at the test site required an impact-type tamper, whereas the granular backfill used in some of the tests required the use

of a vibratory tamper. Density measurements were taken on each side of the pipe at the quarter points and centerline after completion of each lift. Soil lifts were placed at 25%, 50%, and 75% of the pipe diameter (9-in. lifts), as well at the crown of the pipe. The three lifts above the crown of the pipe were 12-in., 6-in., and 6-in. depths. A typical cross section detailing the backfill process as well as the 2-ft of cover above the pipe is shown in Fig 3.17. Backfilling alternated from side to side of the pipe so that the two fills were kept at approximately the same height at all times. As is shown in Fig 3.18, an embankment with a slope of 2:1 was formed at each end during backfilling.

ISU1 was backfilled entirely with native material that was simply "dumped" in as shown in Fig. 3.19. The native material used is a glacial till with a maximum standard proctor density of 118.1-pcf . No compactive effort was applied to the backfill and a very loose fill resulted. The densities of the "dumped" backfill are presented in Fig. 3.20. As may be seen, the dry density at the crown of the pipe ranges between 38-pcf and 53-pcf whereas the density at 9-in. from the invert of the pipe vary from 42-pcf to 77-pcf. Dry densities shown at the bottom of the pipe are for the undisturbed native soil.

As is shown in Fig. 3.21, ISU2 was backfilled with granular backfill to 70% of the pipe diameter and met the requirements of the Iowa DOT bedding and material specifications presented earlier. Backfill densities are shown in Fig 3.22. As indicated in this figure a relatively constant dry density of approximately 125-pcf was achieved in the granular backfill and approximately 115-pcf achieved in the compacted native glacial till.

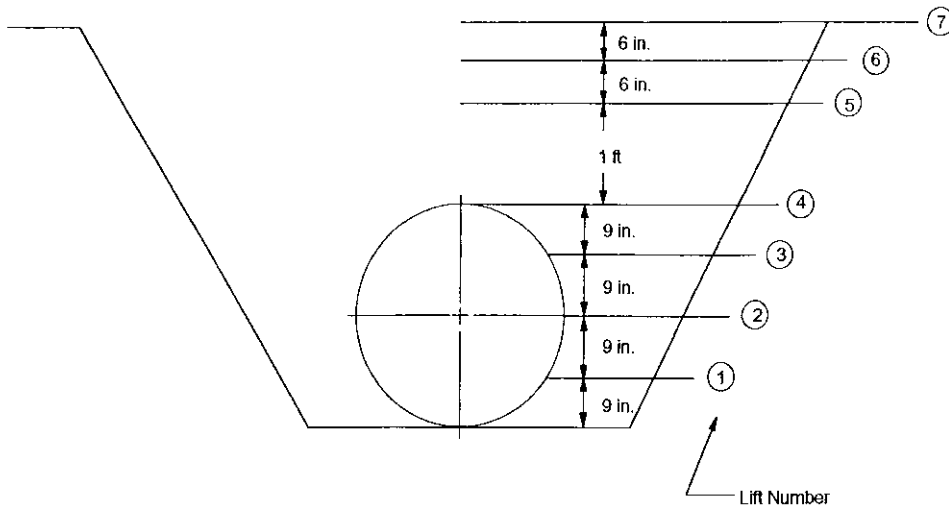


Figure 3.17. Schematic of backfilling process.

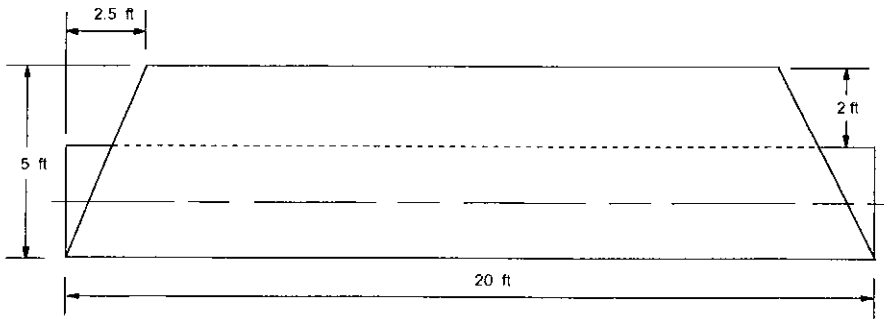


Figure 3.18. Cross section of embankment.

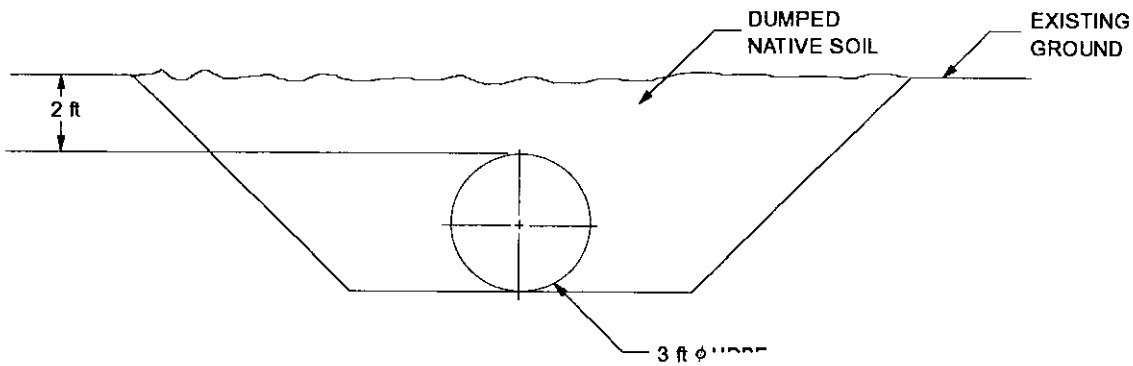
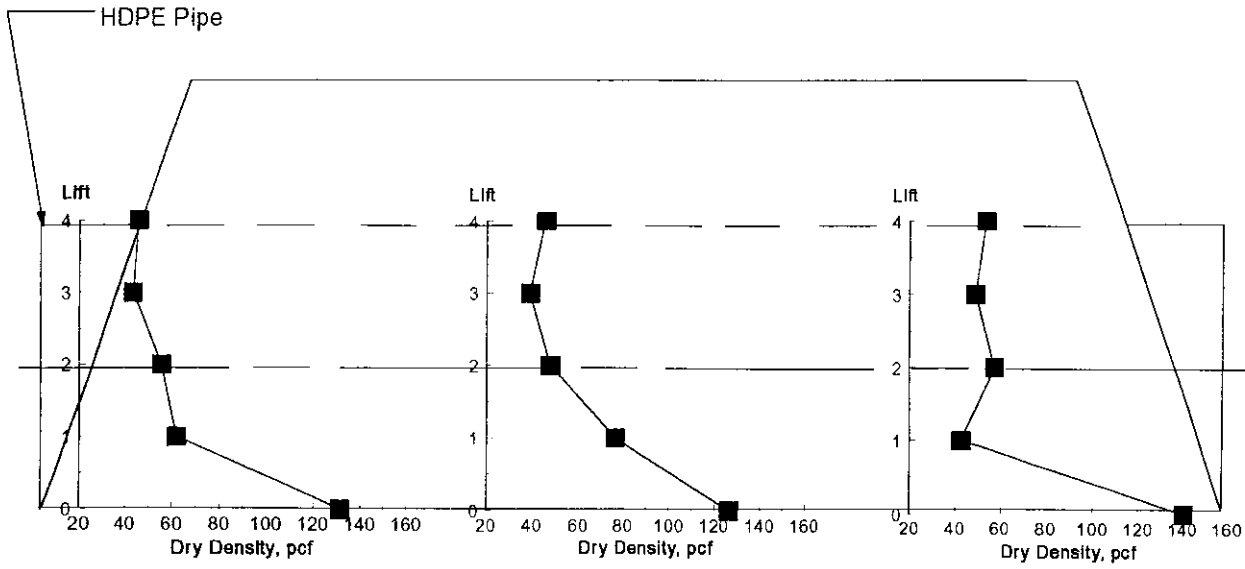
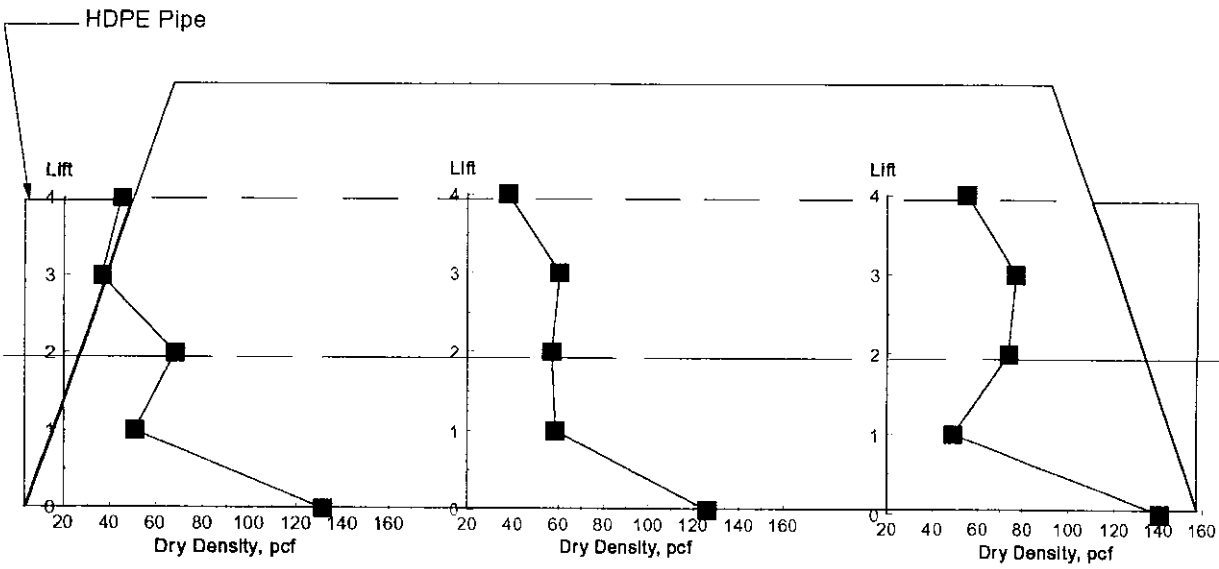


Figure 3.19. Endview of backfill used on ISU1.



a. East Side



b. West Side

Figure 3.20. Dry density at each lift for ISU1.

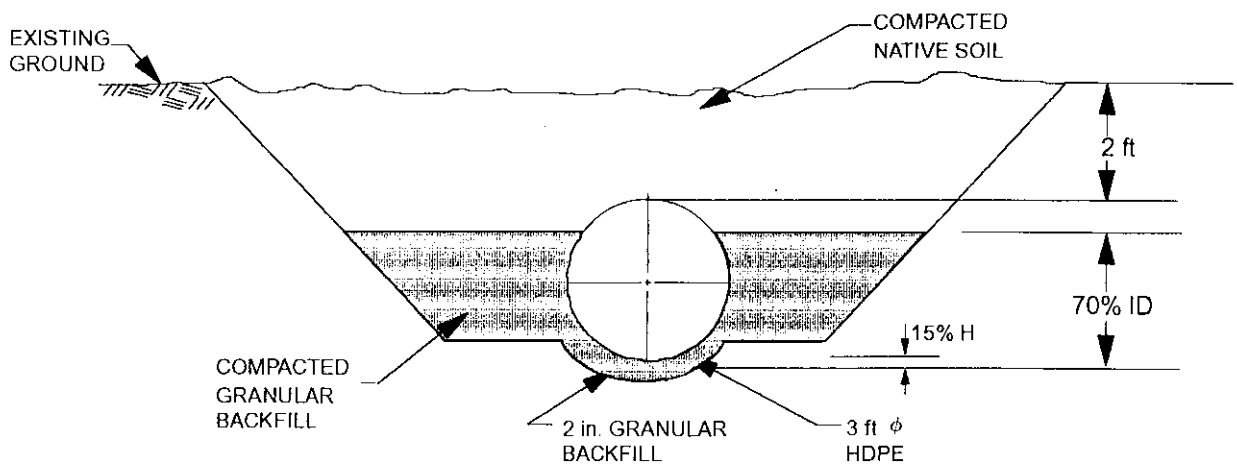
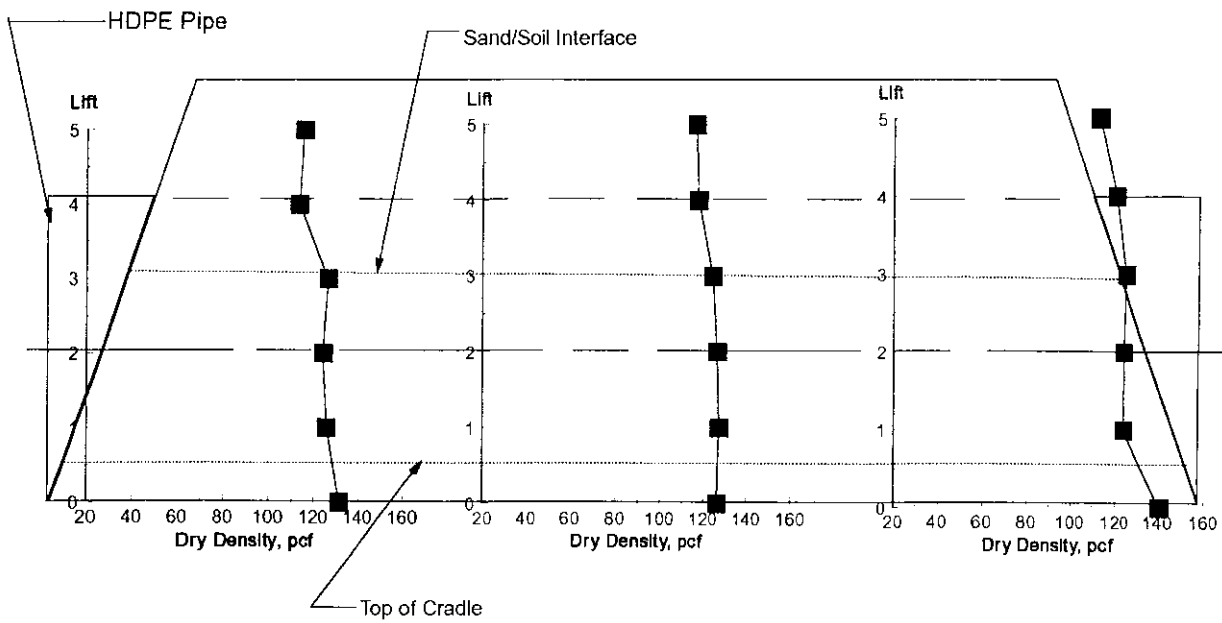
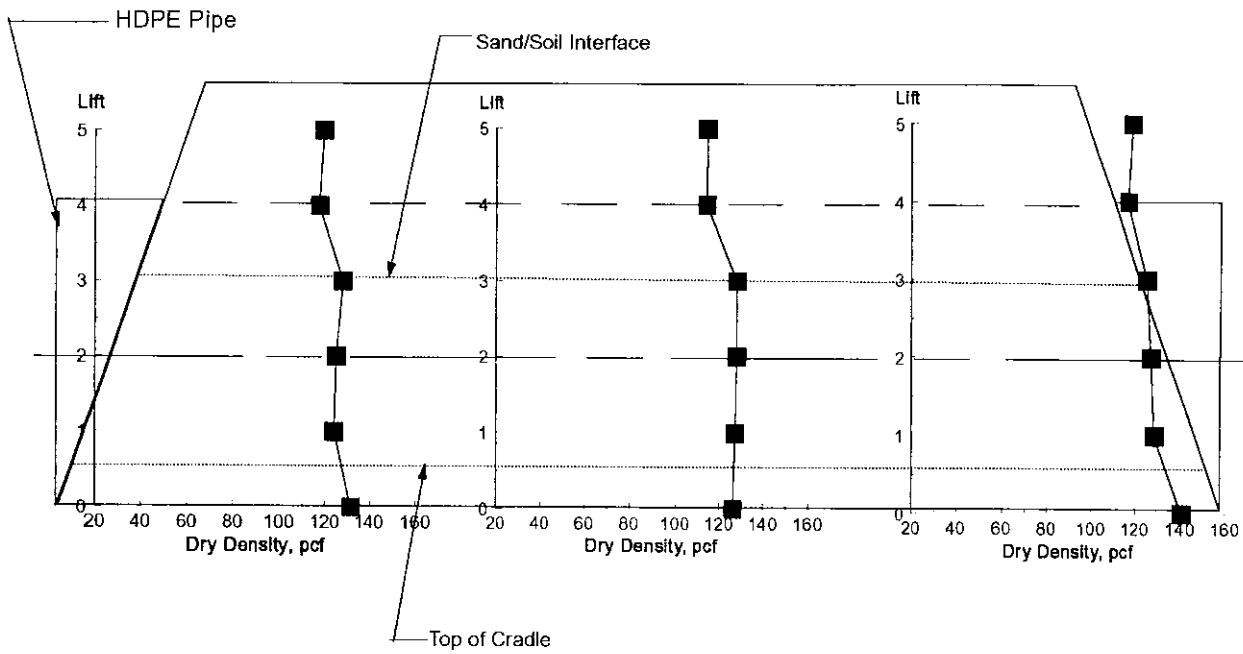


Figure 3.21. Endview of backfill used on ISU2 and ISU4.



a. East Side



b. West Side

Figure 3.22. Dry density at each lift for ISU2.

ISU3 was backfilled with compacted granular backfill to 1-ft above the crown of the pipe. The remaining backfill again was compacted native glacial till, as shown in Fig. 3.23. Densities for ISU3 are shown in Fig. 3.24. As may be seen, similar to that obtained in ISU2, the dry density obtained in the compacted granular backfill and the compacted native glacial till were both approximately 125-pcf.

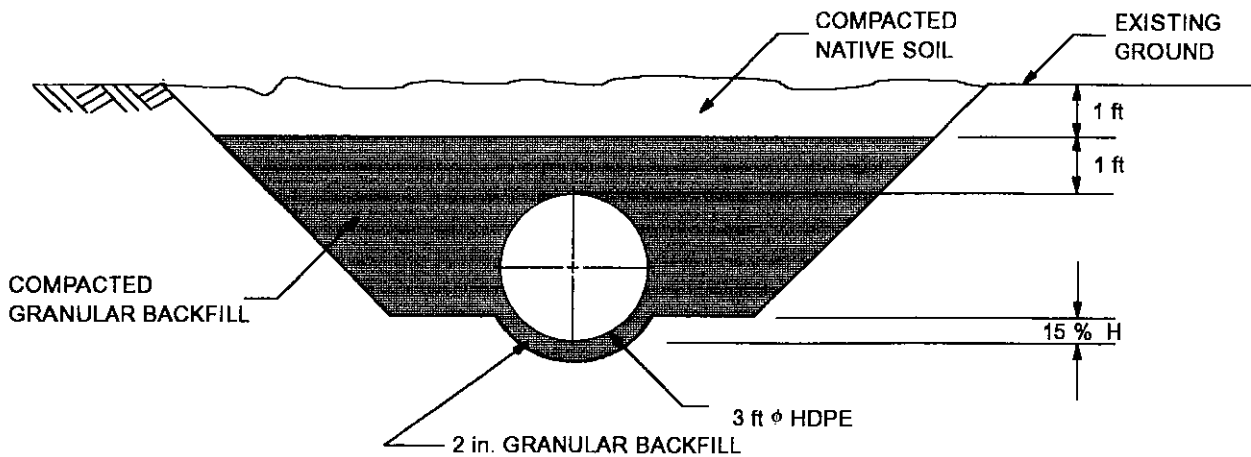
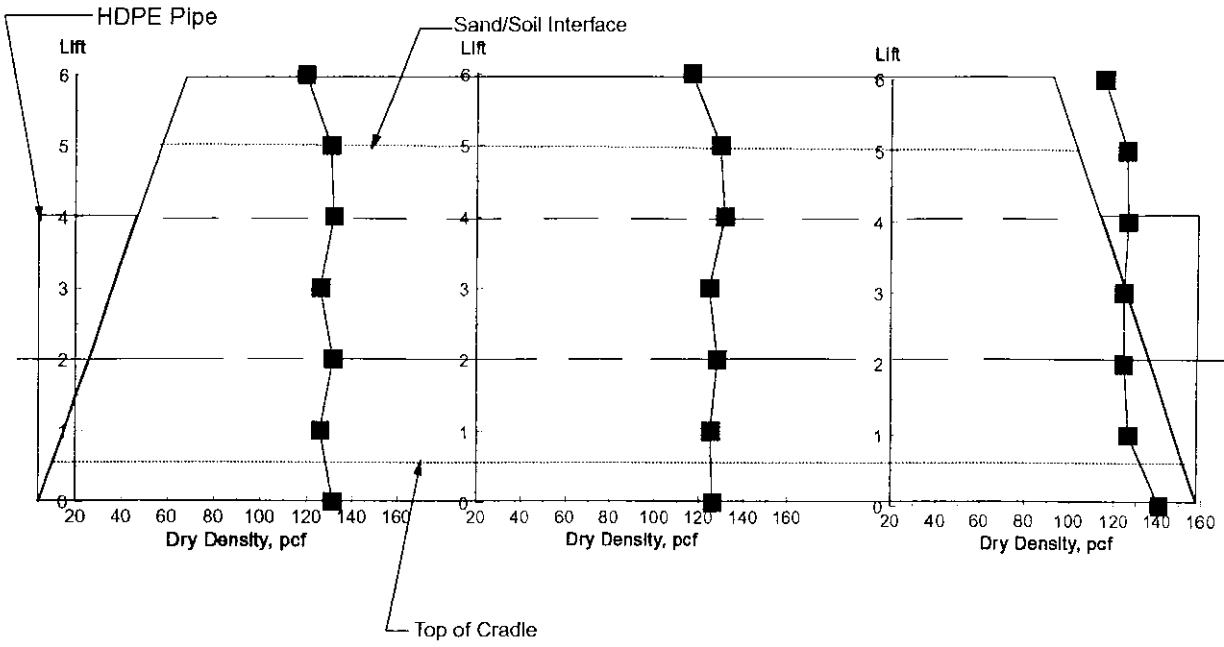
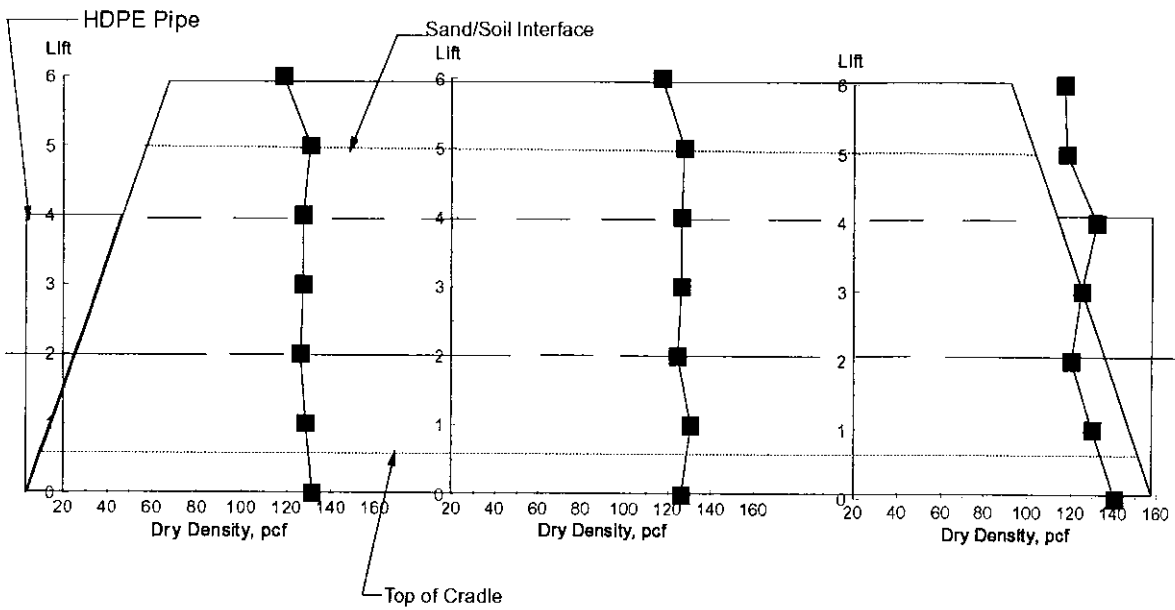


Figure 3.23. Endview of ISU3 trench.

ISU4 was backfilled in the same manner as ISU2 to check the repeatability of the results. Average dry densities obtained in the ISU4 test (see Fig. 3.25) were 125-pcf and 122-pcf in the compacted granular backfill and compacted native glacial till, respectively. These are essentially the same as the values obtained in the ISU2 test.

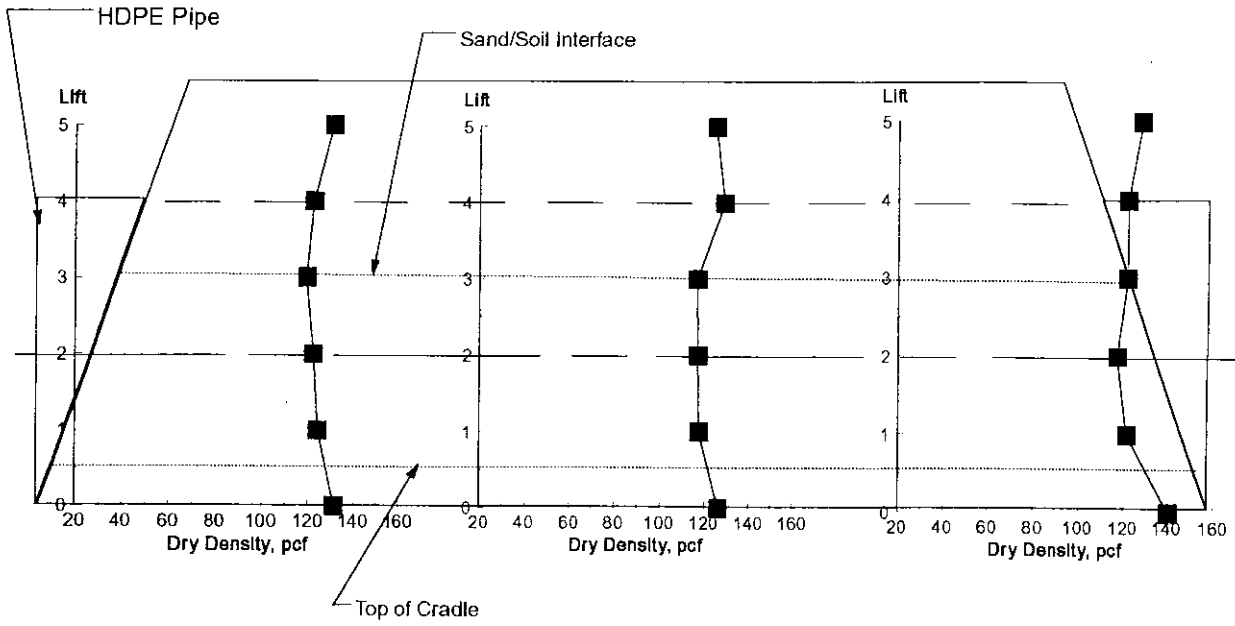


a. East Side

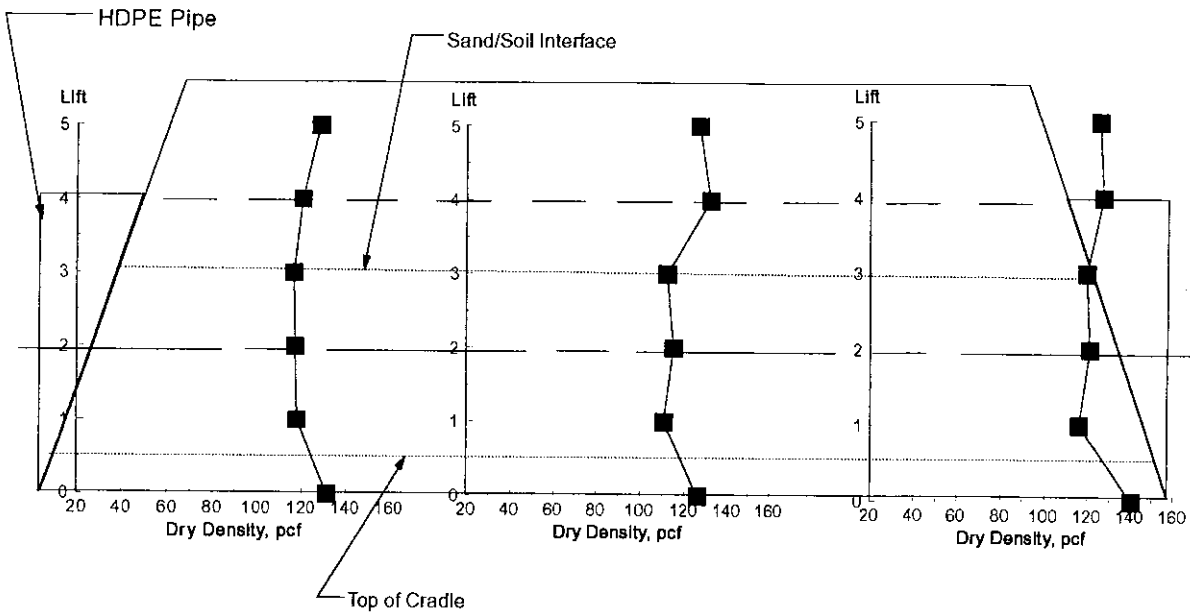


b. West Side

Figure 3.24 Dry density at each lift for ISU3.



a. East Side



b. West Side

Figure 3.25. Dry density at each lift for ISU4.

4. EXPERIMENTAL RESULTS

4.1 Parallel Plate Tests

Parallel plate tests consisted of testing short pipe specimens in ring compression to: (1) show specification compliance of pipe stiffness, (2) investigate the load/strain characteristics, and (3) observe the failure modes HDPE pipes experience when loaded in compression along a pipe diameter.

Testing was based on ASTM testing specification D2412; however, for the 36-in. and 48-in. diameter pipes, space limitations in the testing equipment required that the specimen lengths be shorter than the required ASTM length which is equal to the inside diameter of the pipe. Each specimen was tested four times to the 5% deflection limit and once to a failure load. Failure loads are defined as those loads that cause the behavior of the specimen to change significantly (i.e., when the specimen continued to deflect without an increase in load or local buckling was observed in the pipe wall). Failure tests were run until such a change in behavior was noted. Pipes were instrumented as described in Chapter 3. Data from the five tests per specimen included applied loads, longitudinal and circumferential strains, and two sets of diameter changes. Pipe stiffnesses were also calculated for each specimen from load table deflection data and equations given in ASTM D2412. Changes in the vertical and horizontal diameters were essentially the same at each end of the specimens indicating that no non-planar deformations occurred.

4.1.1 Experimental Stiffness Values by ASTM D2412

Stiffness is calculated, as per ASTM D2412, as the load per unit specimen length divided by the load platen deflection. Stiffness values were calculated for a number of different percent deflections. Table 4.1 shows average stiffness values obtained from these tests and Table 4.2 shows a comparison to Iowa DOT and manufacturer average values for stiffness at 5% deflection. A review of data in Table 4.1 reveals a decrease in stiffness of approximately 25% in most cases when the deflection is increased from 5% to 10%. As is indicated in Table 4.2 the results obtained by ISU, the Iowa DOT, and the manufacturers do not vary significantly. Minimum AASHTO requirements for pipe stiffness based on the

Table 4.1. Average stiffness values by ASTM D2412.

Manufacturer	Diameter, (in.)	5%, (psi)	10%, (psi)	30%, (psi)
A	24	37.91	30.04	13.75
B, single wall	24	40.22	28.5	8.23
B, double wall	24	47.26	38.46	9.84
C	24	38.83	29.27	15.38
A	30	36.89	28.97	12.86
A ^a	36	36.62	26.89	11.65
C ^a	36	24.56	18.18	9.4
A ^a	48	23.10	17.09	-----
C ^a	48	22.03	15.98	-----

^a Specimen length less than that required by ASTM D2412

Table 4.2. Comparison of average stiffness values.

Manufacturer	Diameter, (in.)	ISU (psi)	Iowa DOT (psi)	Manufacturer (psi)
A	24	37.91	38.00	N/A
B, Single Wall	24	40.22	N/A	N/A
B, Double Wall	24	47.26	43.33	46.57
C	24	38.83	39.67	46.57
A	30	36.89	N/A	N/A
A	36	36.62	32.00	N/A
C	36	24.56	24.67	24.47
A	48	23.10	N/A	N/A
C	48	22.03	N/A	20.76

N/A - not available

parallel plate tests are provided to specify minimum pipe strengths. The minimum requirements for pipe stiffness are based on 5% deflection and are as follows:

34 psi for 24-in. diameter pipe

28 psi for 30-in. diameter pipe

22 psi for 36-in. diameter pipe

18 psi for 48-in. diameter pipe

Therefore, all specimens tested by ISU satisfied ASTM requirements.

In addition to the stiffnesses presented above, a stiffness factor, or EI value, was determined. The general equation for calculating the stiffness factor by parallel plate test data was given in Chapter 2 as Eqn 9. Table 4.3 shows the average stiffness factors.

Table 4.3. Average stiffness factors.

Manufacturer	Diameter, (in.)	Average Stiffness Factor, (lb-in. ² /in.)
A	24	9,660
B, single walled	24	10,480
B, double walled	24	12,120
C	24	9,990
A	30	18,530
A	36	31,950
C	36	21,310
A	48	47,460
C	48	45,310

4.1.2 Load versus Circumferential Strain

Figure 4.1 shows the strain gage orientation and designation used in the parallel plate tests. Illustrated in Fig. 4.2 through 4.4 are the results of the parallel plate tests on the pipe specimens from each manufacturer during tests to the 5% deflection limit. In some figures (i.e., Fig. 4.2c, Fig. 4.3d, etc.) the ordinate axis shows tensile strains while in the other figures (i.e., Fig. 4.3g, 4.4b, etc.) the ordinate axis shows compressive strains. As has been previously noted, due to testing machine limitations, several of the larger diameter specimens had to be shorter than the ASTM required length. To take this variation into account, in Figs. 4.2 through 4.4, load/length (lb/ft) has been plotted vs circumferential strain. Each graph represents a location around the pipe circumference. The graph in each figure at the top right of the page (Fig 4.2a, 4.3a, and 4.4a) is the location directly under the upper load platen.

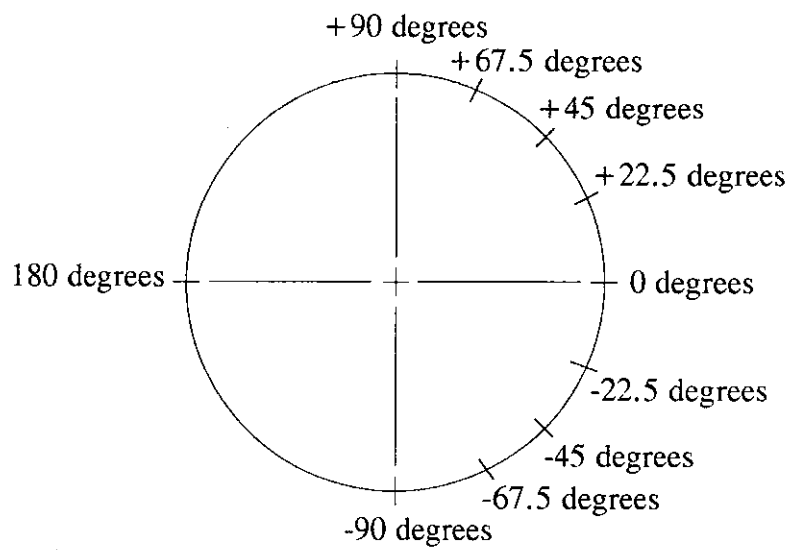
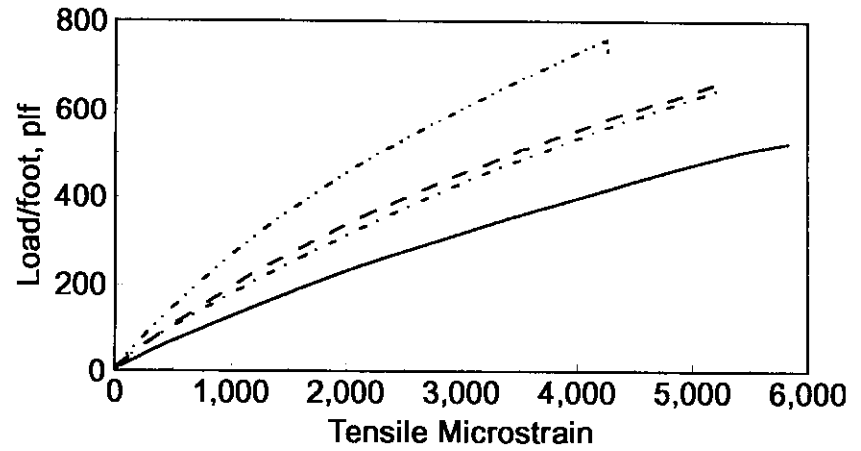


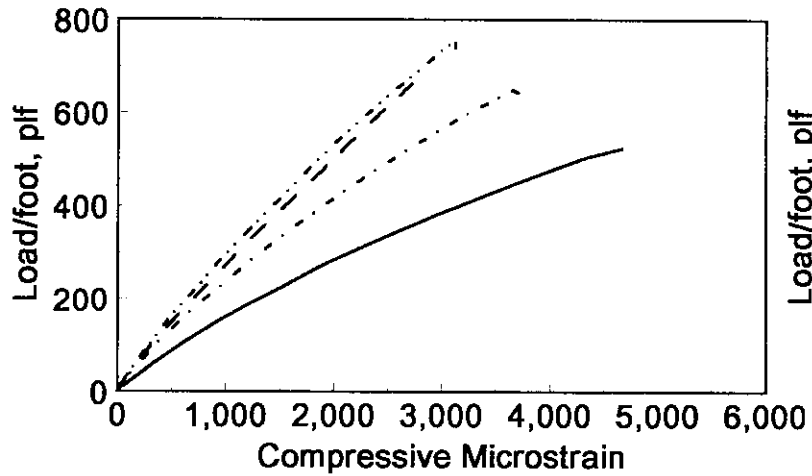
Figure 4.1. Strain locations for parallel plate tests.

Pipe Diameter Legend

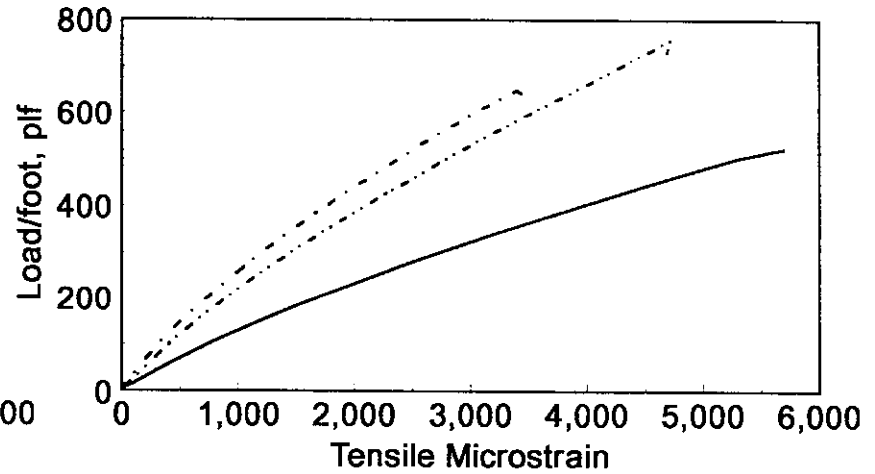
- 24 in. ———
- 30 in. - - - -
- 36 in. - - - -
- 48 in. - - - -



a. Strain at +90 degrees

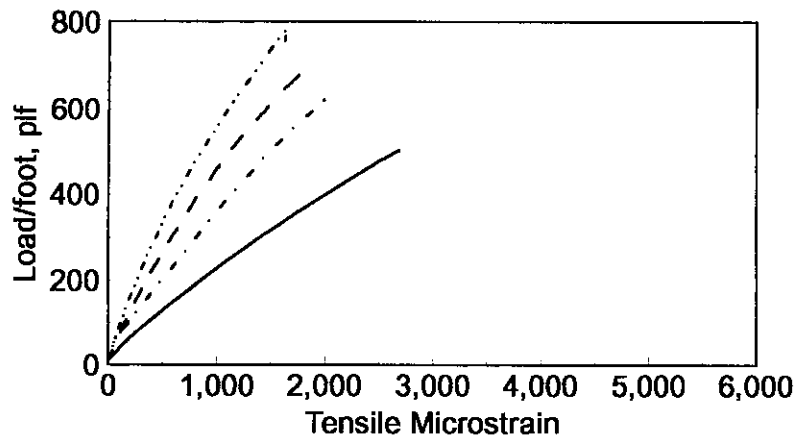


b. Strain at 0 degrees

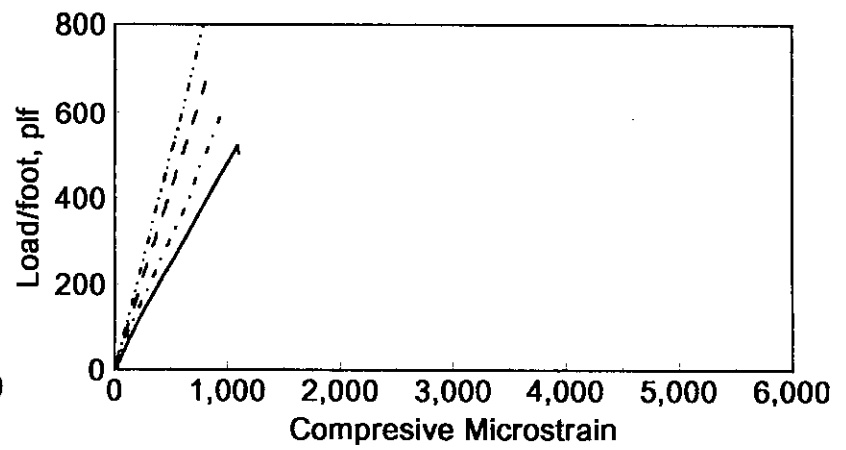


c. Strain at -90 degrees

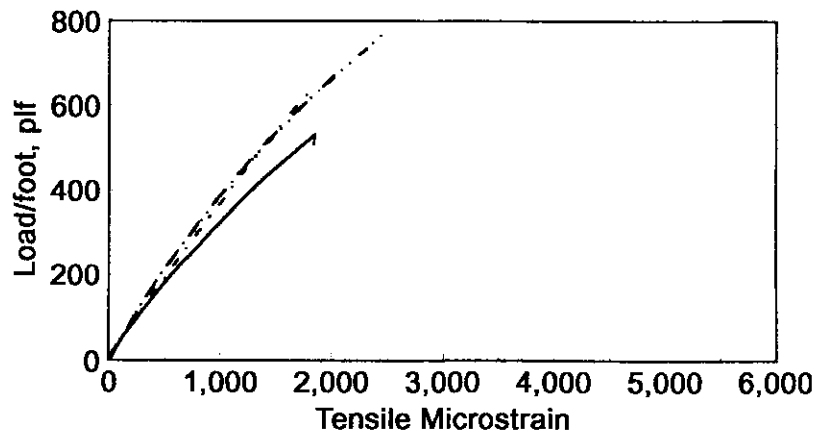
Figure 4.2. Manufacturer A, circumferential strain to 5% deflection.



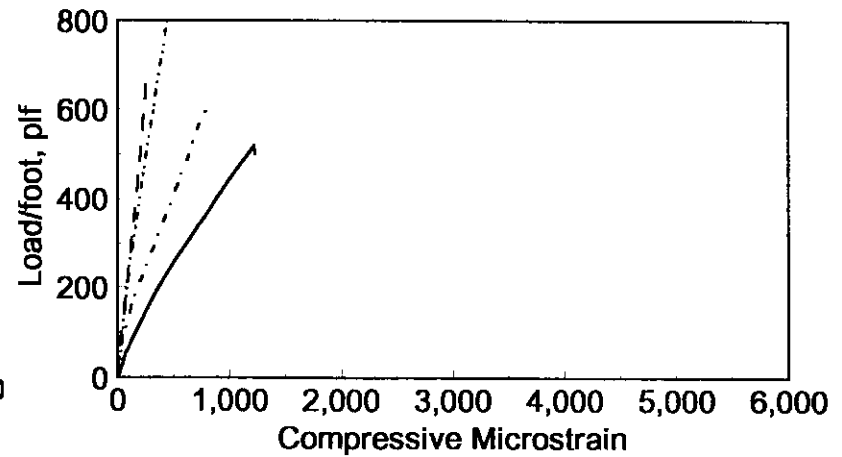
d. Strain at +67.5 degrees



e. Strain at +45 degrees

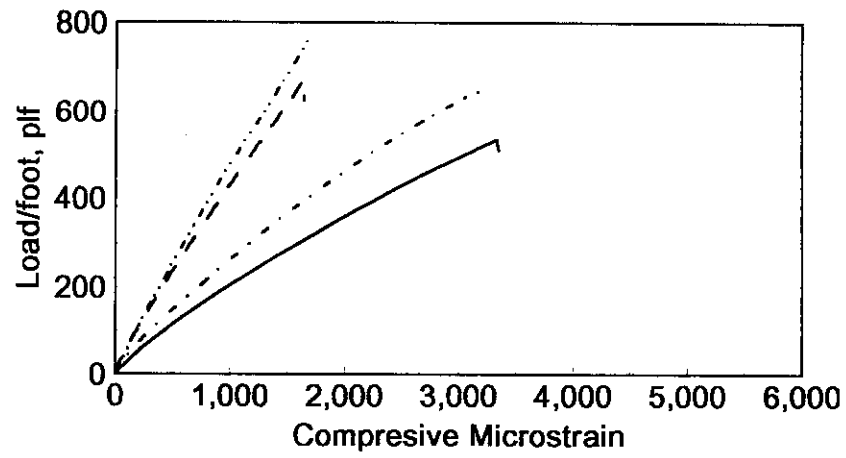


f. Strain at -67.5 degrees

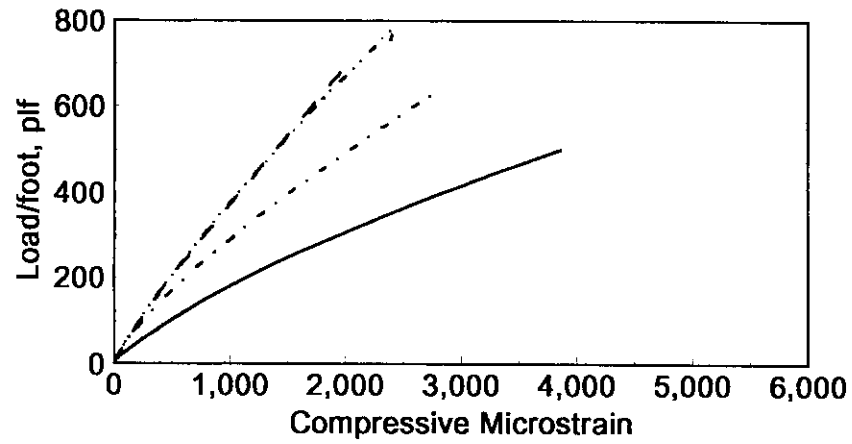


g. Strain at -45 degrees

Figure 4.2. Continued.



h. Strain at +22.5 degrees

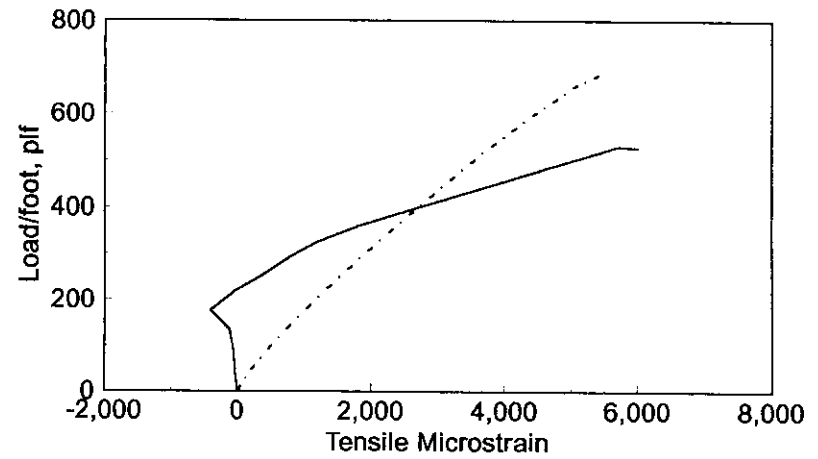


i. Strain at -22.5 degrees

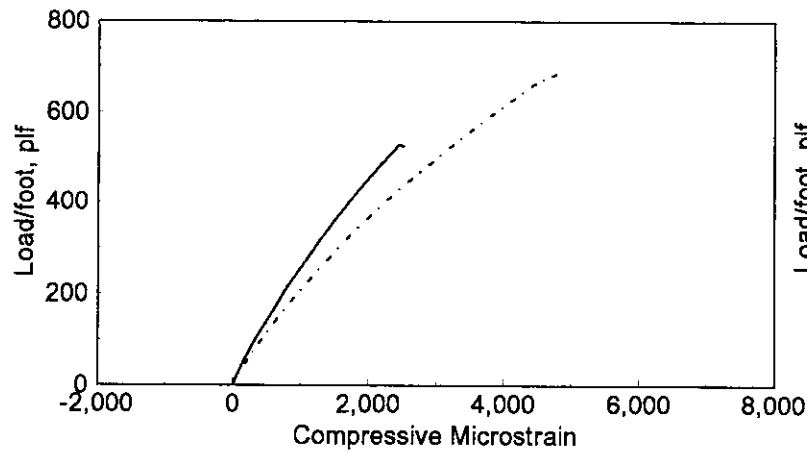
Figure 4.2. Continued.

Pipe Diameter Legend

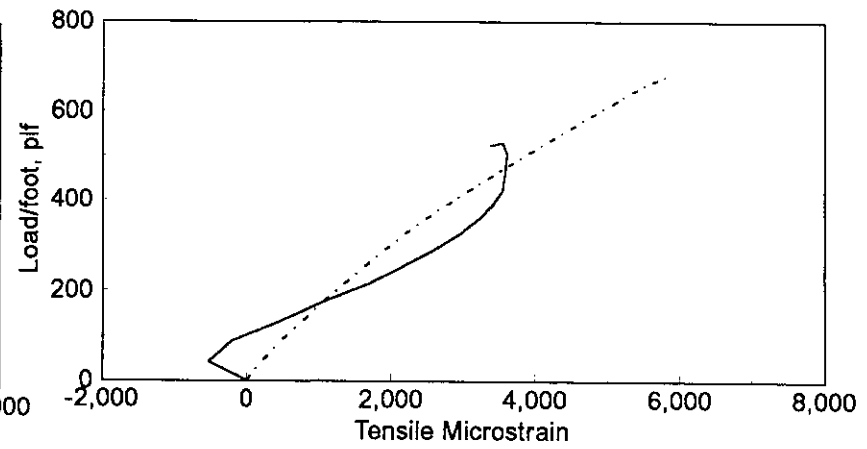
24 in. Single Wall ———
24 in. Double Wall - - - - -



a. Strain at +90 degrees

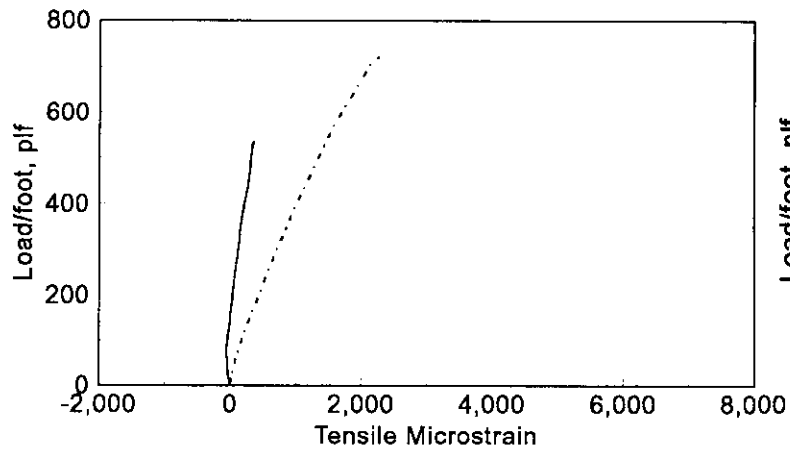


b. Strain at 0 degrees

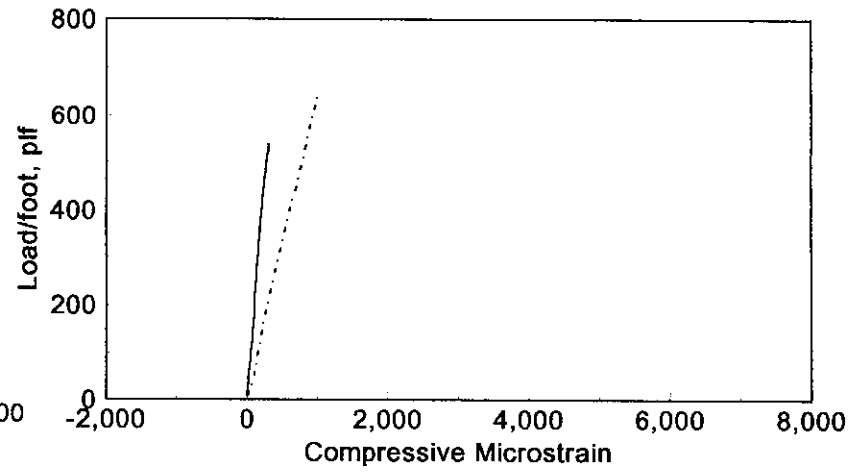


c. Strain at -90 degrees

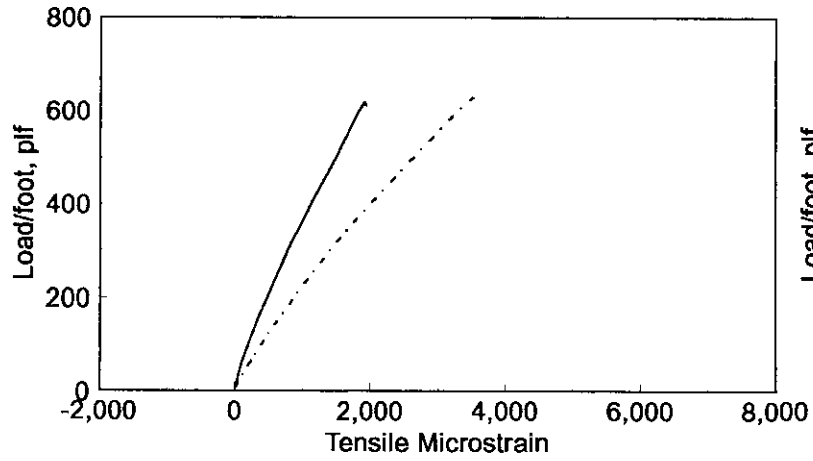
Figure 4.3. Manufacturer B, circumferential strain to 5% deflection.



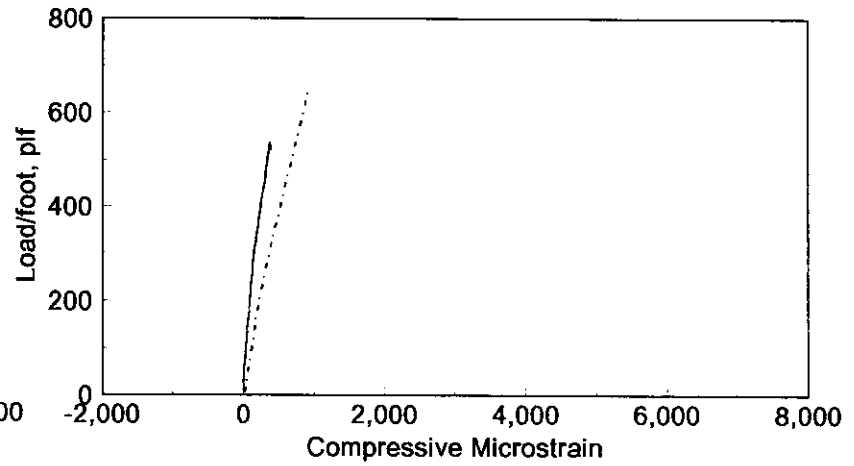
d. Strain at +67.5 degrees



e. Strain at +45 degrees

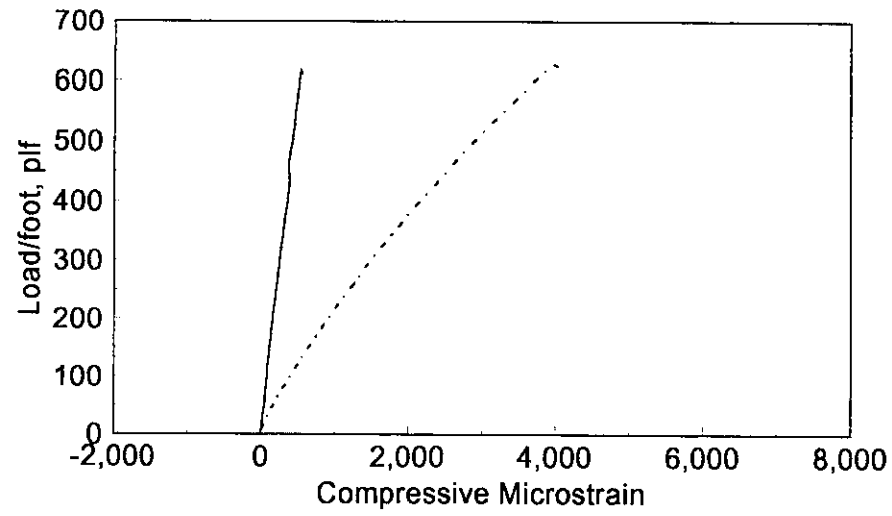


f. Strain at -67.5 degrees

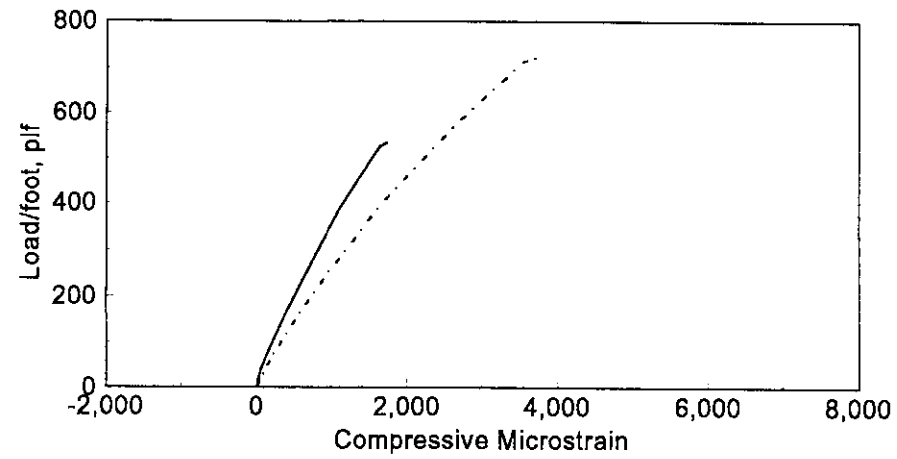


g. Strain at -45 degrees

Figure 4.3. Continued.



h. Strain at +22.5 degrees

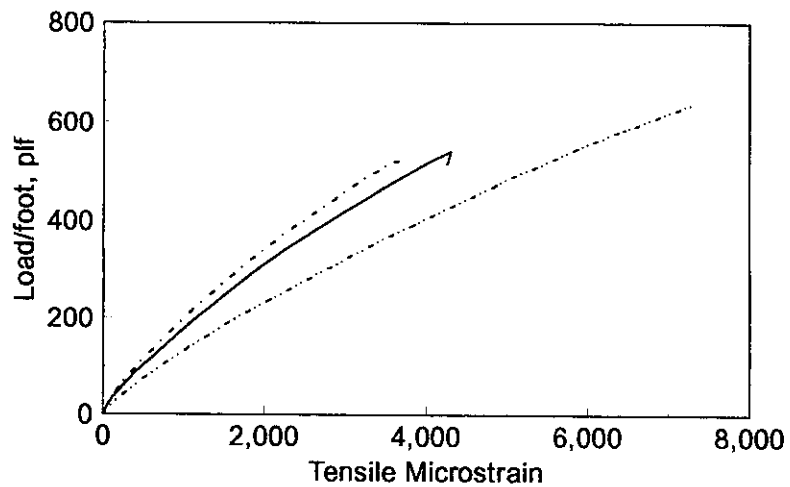


i. Strain at -22.5 degrees

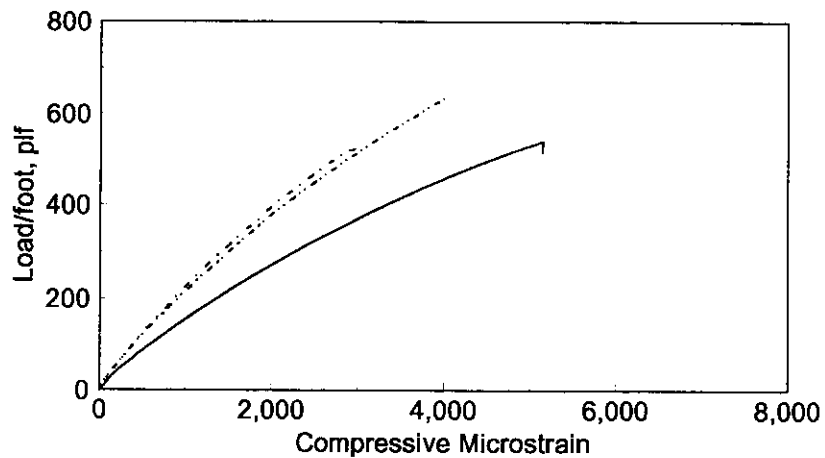
Figure 4.3. Continued.

Pipe Diameter Legend

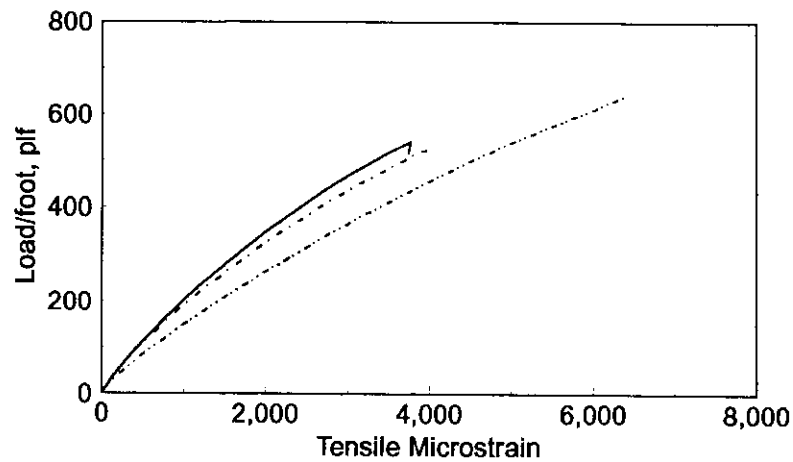
24 in. ———
 36 in. - - - -
 48 in. ·····



a. Strain at +90 degrees

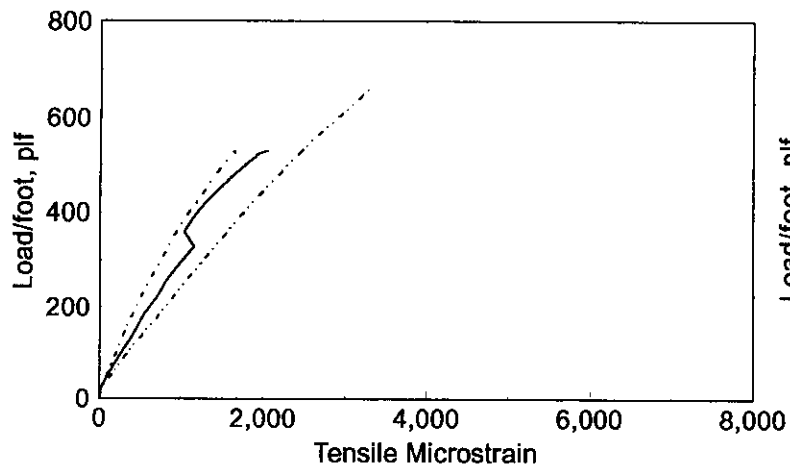


b. Strain at 0 degrees

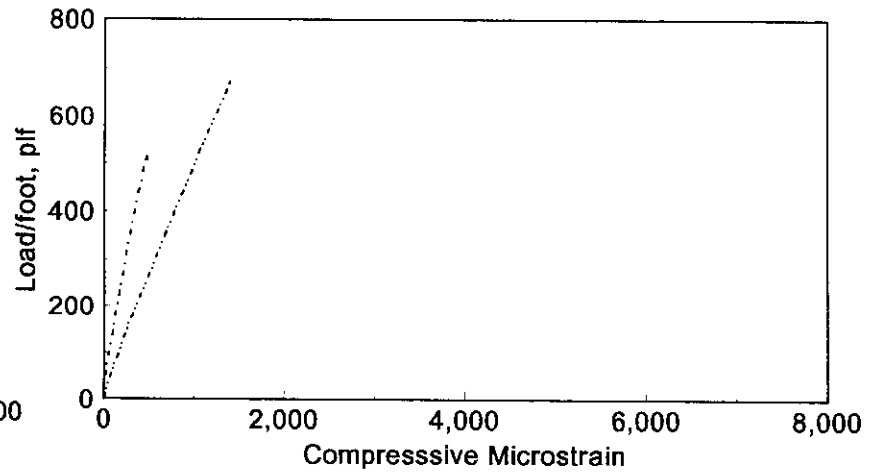


c. Strain at -90 degrees

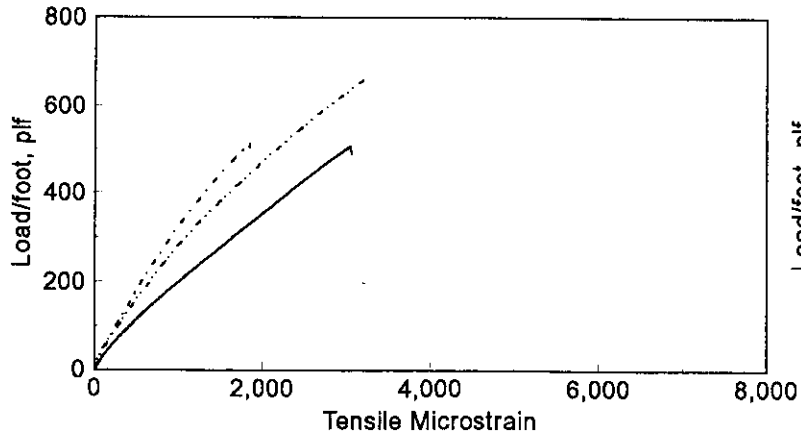
Figure 4.4. Manufacturer C, circumferential strain to 5% deflection.



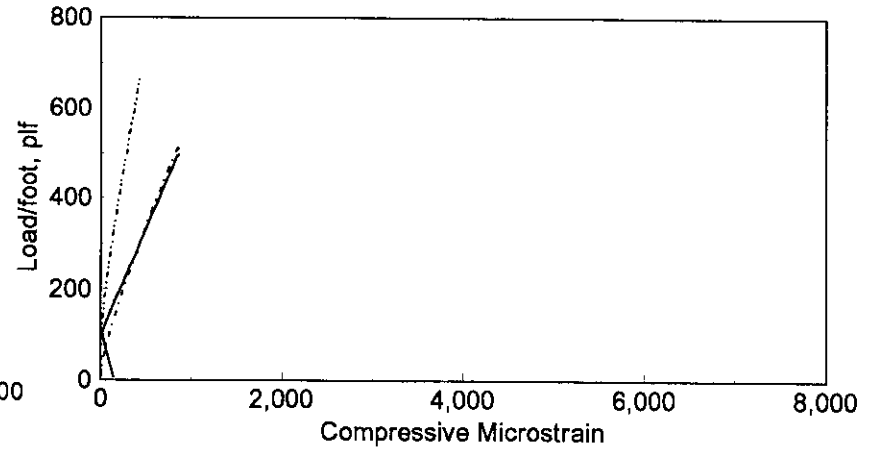
d. Strain at +67.5 degrees



e. Strain at +45 degrees

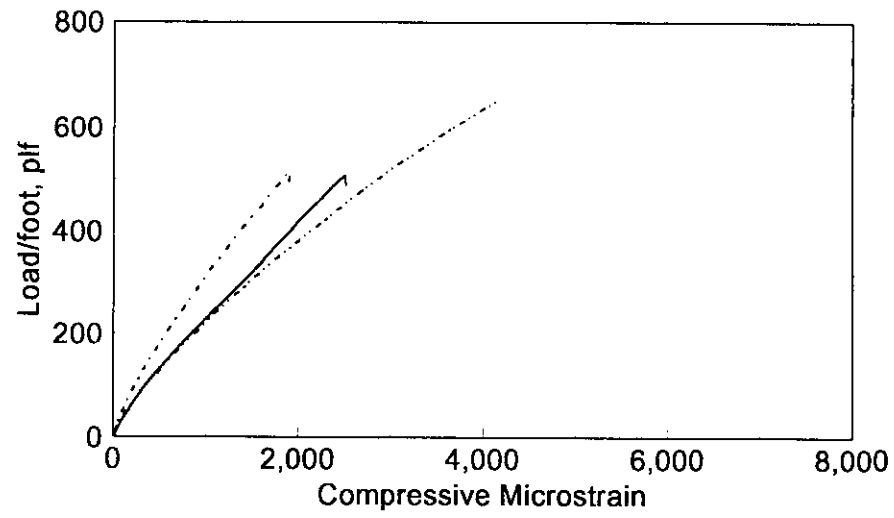


f. Strain at -67.5 degrees

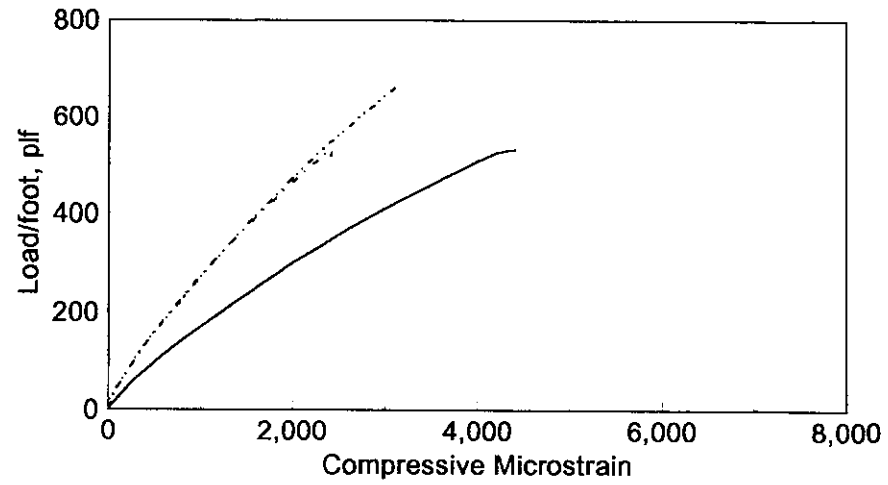


g. Strain at -45 degrees

Figure 4.4. Continued.



h. Strain at +22.5 degrees



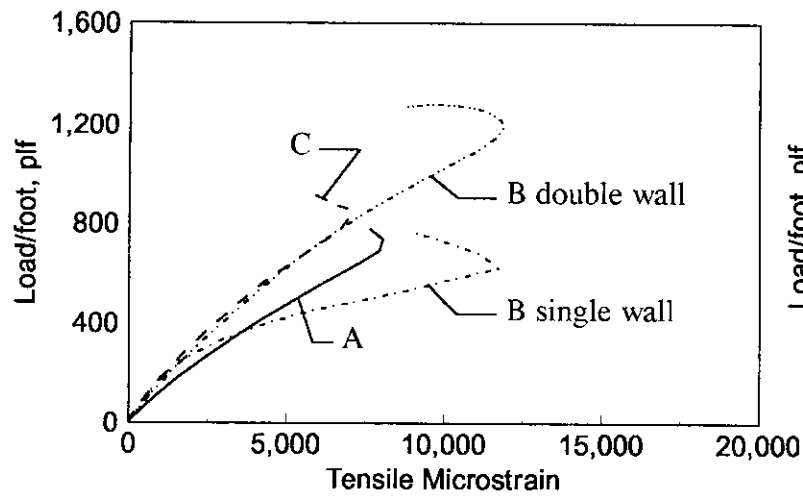
i. Strain at -22.5 degrees

Figure 4.4. Continued.

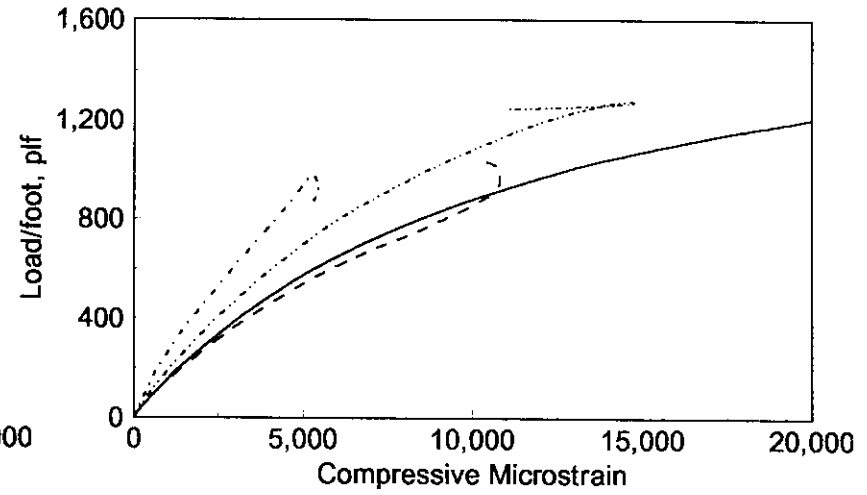
Going clockwise around the pipe circumference, each graph represents a location around the circumference at increments of 22.5 degrees. Each line on a particular graph represents a single specimen test

Figures 4.2 through 4.4 indicate that the maximum strains are at the crown and invert of each specimen. Note that strains vary from a maximum at the crown (Fig. 4.2a, 4.3a, and 4.4a) to a minimum at ± 45 degrees (Fig. 4.2e and g, 4.3e and g, and 4.4e and g) where the strains become compressive. The strains then increase in the vicinity of the springline to tension strain at the invert (Fig. 4.2c, 4.3c, and 4.4c). In most cases the curves represent expected behavior considering the stiffness of the specimens given in Table 4.1.

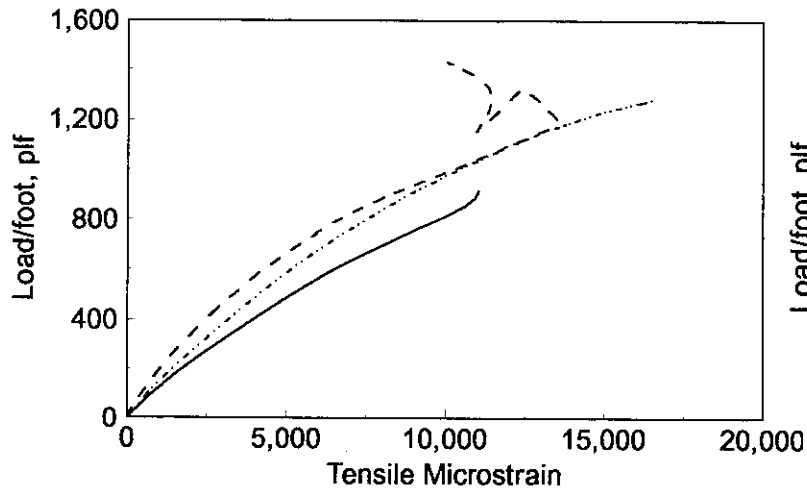
Comparisons of the circumferential strains for all manufacturers for each size pipe are shown in Figs. 4.5 through 4.8. For the 24-in. specimens (Fig. 4.5), Manufacturer C's profile reached the highest ultimate load. Note, the highest ultimate load may not be shown in the figures if the strain gages on a given specimen had failed prior to reading the ultimate load; ultimate load was recorded from the test machine. Manufacturer B's two different profiles performed substantially different from one another. No clear trends are observed for the various 24-in. diameter specimens; however in general, specimens from Manufacturer A had the highest strains. This is not observed at the crown where the single-walled specimen from Manufacturer B had higher strains and at one springline where the strains are slightly lower than those for Manufacturer C.



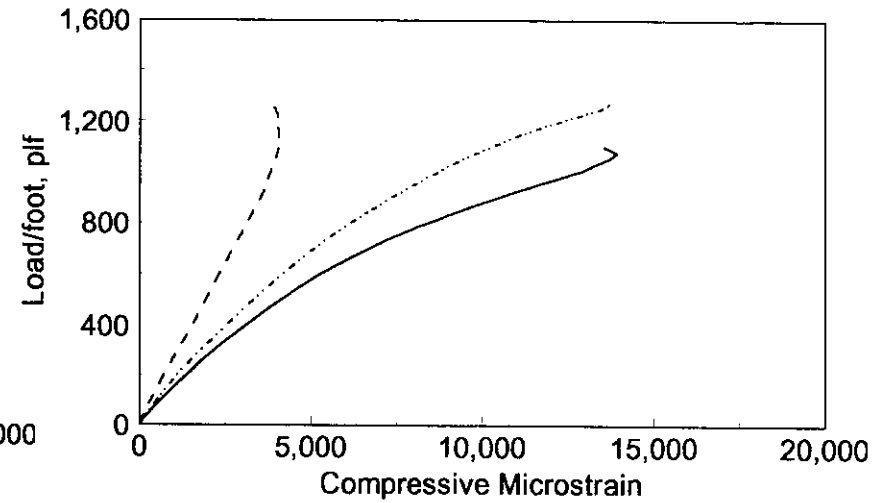
a. Strain at +90 degrees



b. Strain at 0 degrees

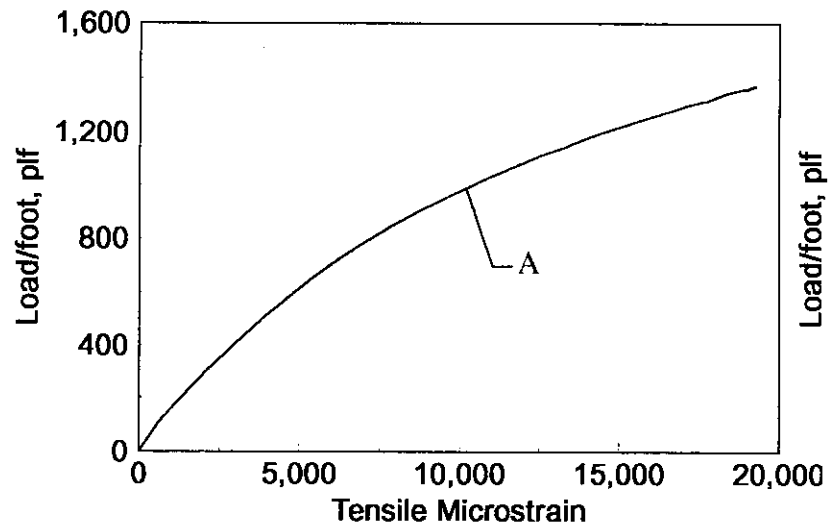


c. Strain at -90 degrees

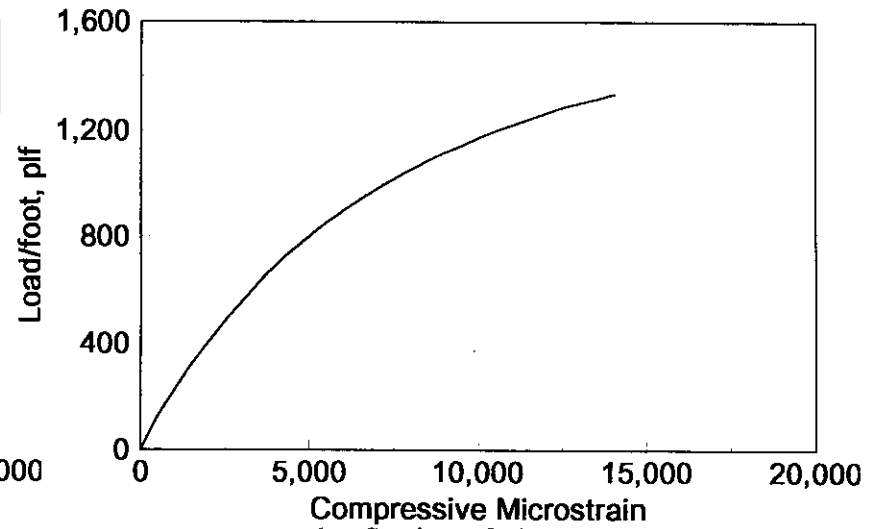


d. Strain at 180 degrees

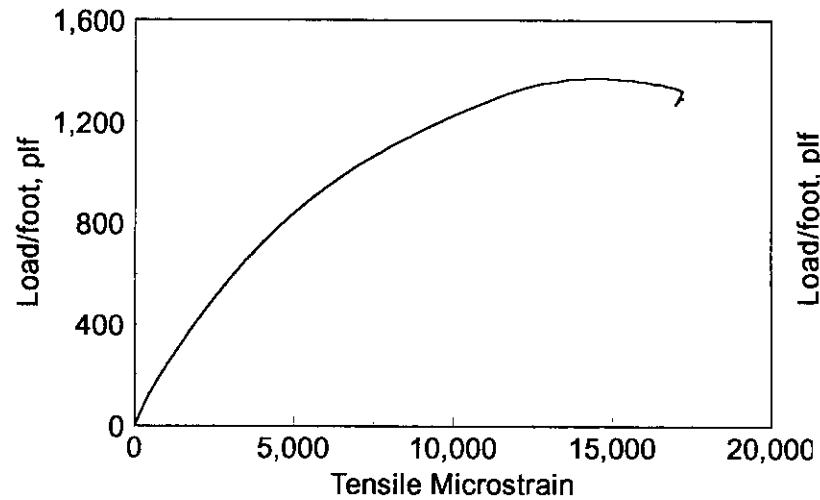
Figure 4.5. HDPE 24 in. diameter pipes: load/ft versus circumferential strain to failure.



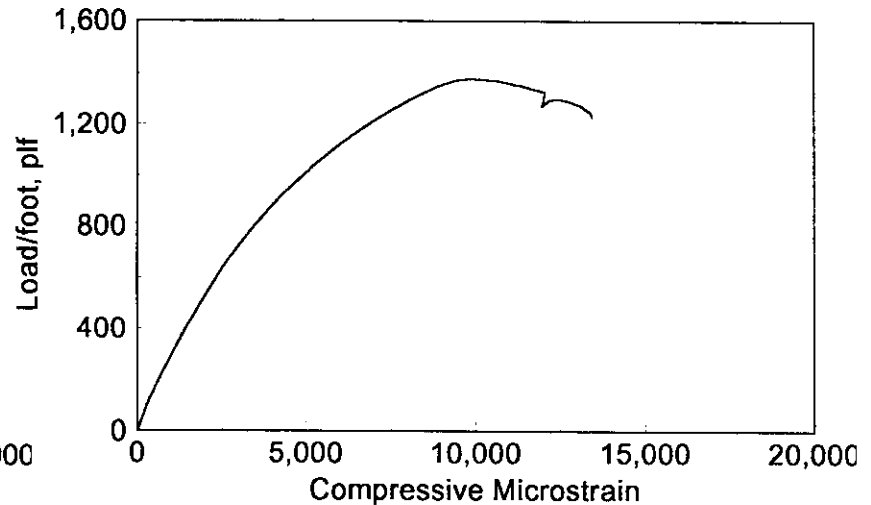
a. Strain at +90 degrees



b. Strain at 0 degrees

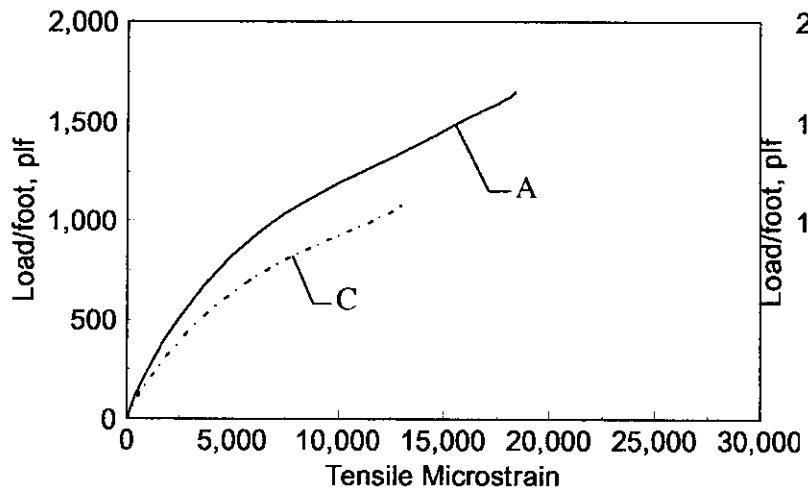


c. Strain at -90 degrees

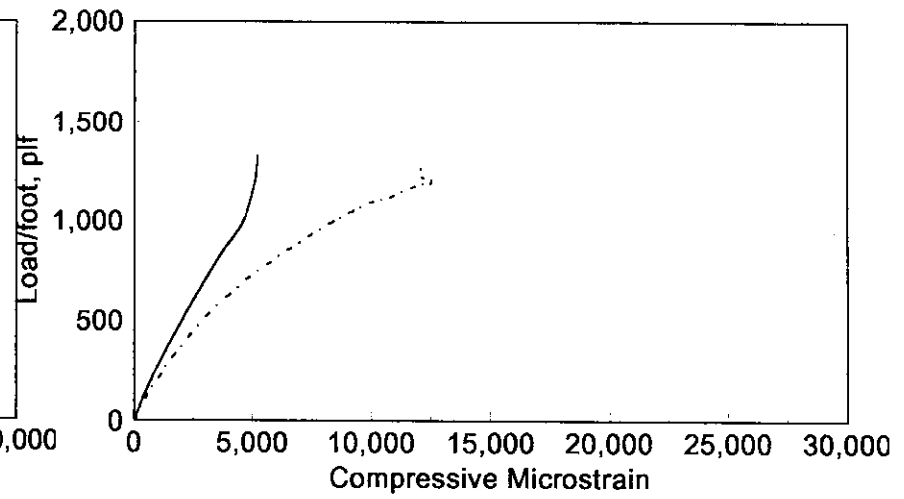


d. Strain at 180 degrees

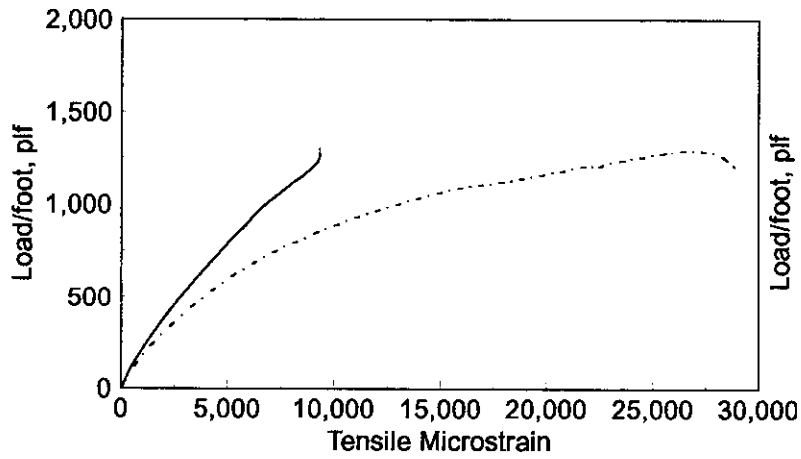
Figure 4.6. HDPE 30 in. diameter pipes: load/ft versus circumferential strain to failure.



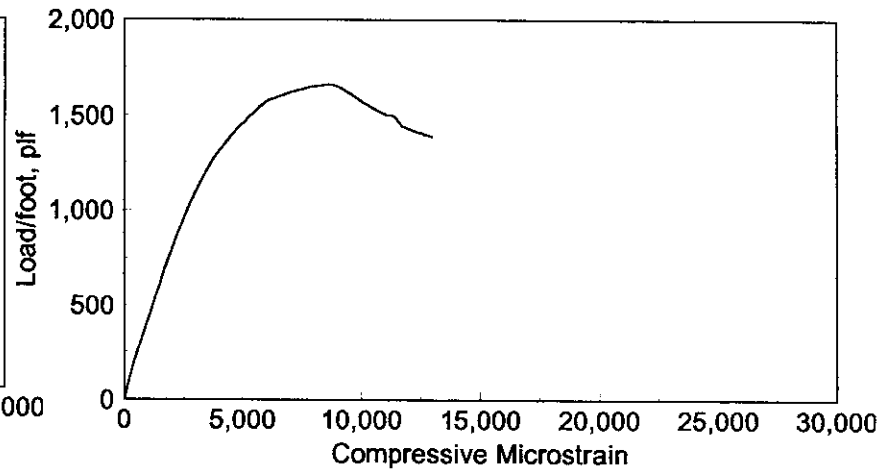
a. Strain at +90 degrees



b. Strain at 0 degrees

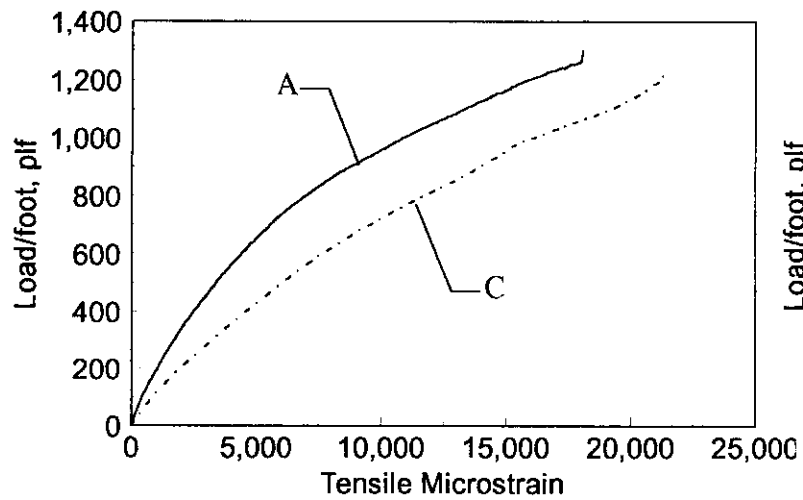


c. Strain at -90 degrees

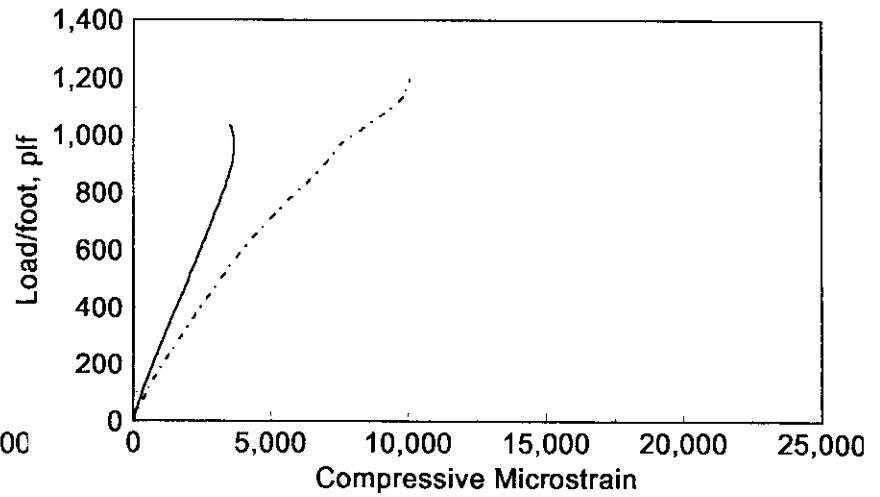


d. Strain at 180 degrees

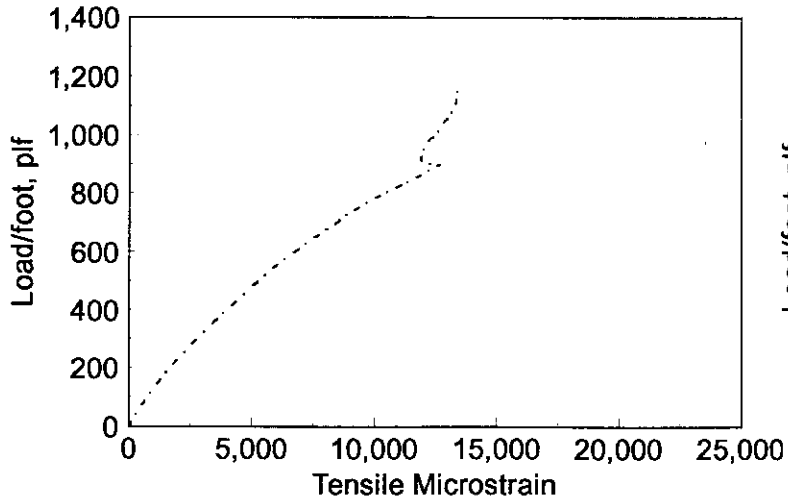
Figure 4.7. HDPE 36 in. diameter pipes: load/ft versus circumferential strain to failure.



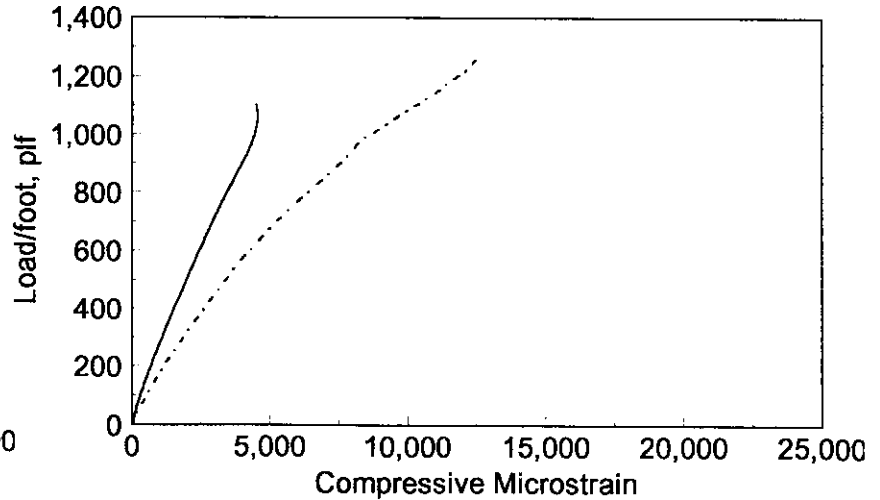
a. Strain at +90 degrees



b. Strain at 0 degrees



c. Strain at -90 degrees



d. Strain at 180 degrees

Figure 4.8. HDPE 48 in. diameter pipes: load/ft versus circumferential strain to failure.

The behavior of a 30-in. diameter specimen from Manufacturer A is shown in Fig. 4.6. Ultimate strains at all locations were generally between 12,500-microstrain and 17,500-microstrain, indicating that significant deformation occurred at all locations monitored. The shape of the curves indicate that one springline location and the invert failed at about 1400-plf. Manufacturer A was the only one that provided a 30-in. diameter specimen for testing.

Data in Fig. 4.7 indicate that the highest ultimate load was reached by Manufacturer A's 36-in diameter specimens, however strains were consistently higher in the Manufacturer C specimen.

For the 48-in. diameter specimens, the strains in the Manufacturer C specimen exceeded those in the Manufacturer A specimen (See Fig. 4.8). Strains at each of the springline locations are very similar in magnitude as are the shapes of the load/strain curves. However, symmetry is not observed from the invert to the crown.

From the data presented, it is clear that the response of "short" pipes in terms of circumferential strain in ring compression can not be accurately predicted based on diameter alone. Obviously differences in pipe geometry create large differences in pipe behavior and generalizations from a given profile cannot be extended to all pipes of the same diameter. For example, the differences in the responses of the two 24-in. diameter specimens from Manufacturer B is very clear. The pipes are the same diameter, but obviously have a very different response which can be attributed to the difference in pipe

wall geometry.

4.1.3 Load versus Change in Diameter

The load/ft versus the change in inside diameter for the failure tests are shown in Figs. 4.9 and 4.10. The ratio of change in horizontal and vertical diameter is very nearly one in all cases. Manufacturer A's 36-in. diameter pipe (labeled A36 in these curves) reached the highest load but then began to rapidly deform without an increase in load indicating a sudden failure. In contrast, manufacturer C's 36-in. diameter specimen reached the largest deflection before failure. A comparison of the 48-in. diameter specimens shows there is little difference in the deflection response. Manufacturer B's two 24-in. profiles again show pronounced differences in behavior.

4.1.4 Theoretical Strain Distribution versus Experimental Strain Distribution

As a check on the behavior of the strain results from the parallel plate tests, an analysis of the strain response for the parallel plate specimens was completed. The derivation of the equation for strain is outlined in Appendix D and the equation for the stress is shown in Equation 19.

$$\sigma = - \frac{w * \cos(90 - \theta)}{2 * \text{area}} + \frac{\left[\frac{w * r}{\pi} - \frac{w * r * \sin(\theta)}{2} \right] * y}{I} \quad (19)$$

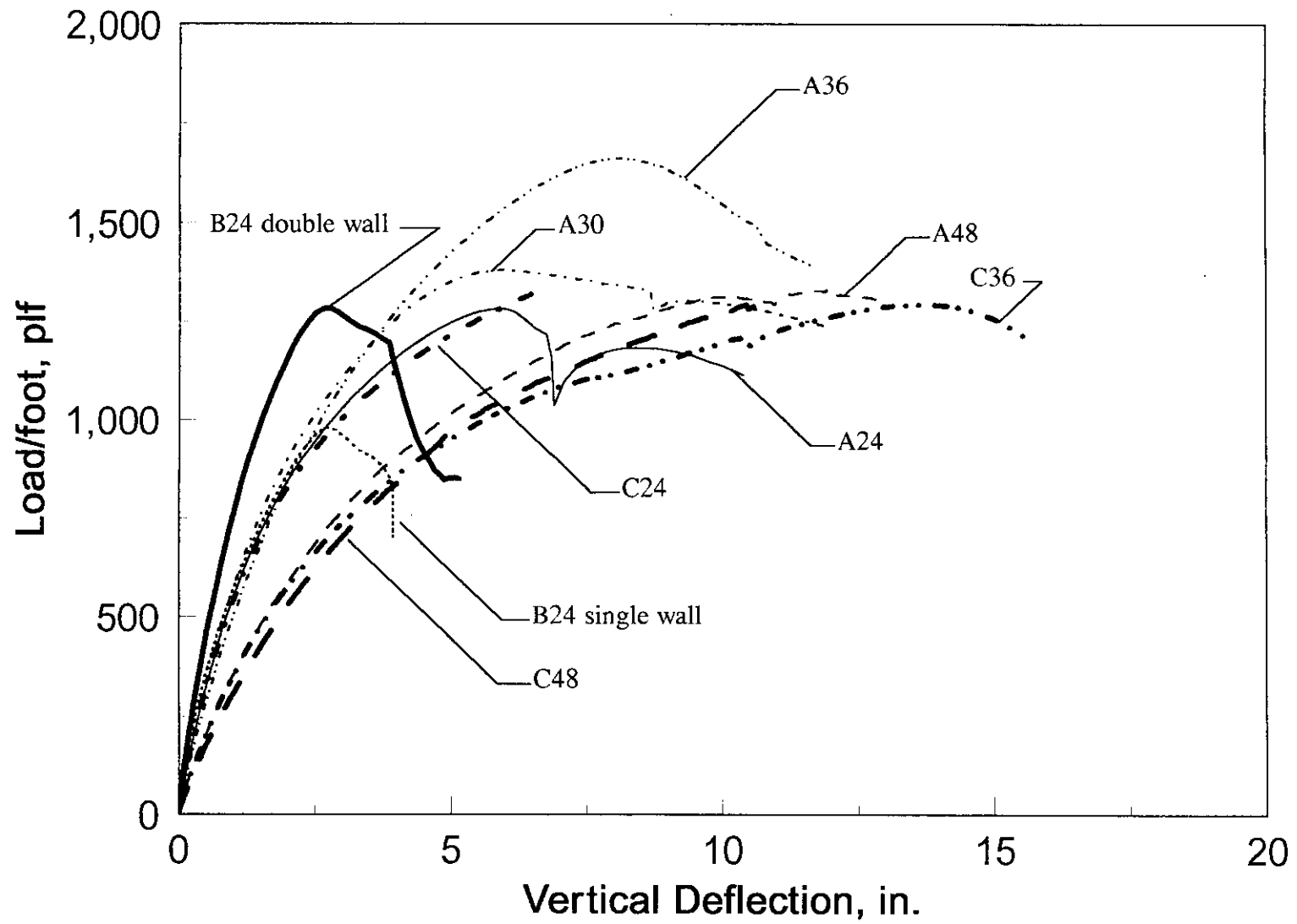


Figure 4.9. Load/ft vs. change in vertical inside diameter.

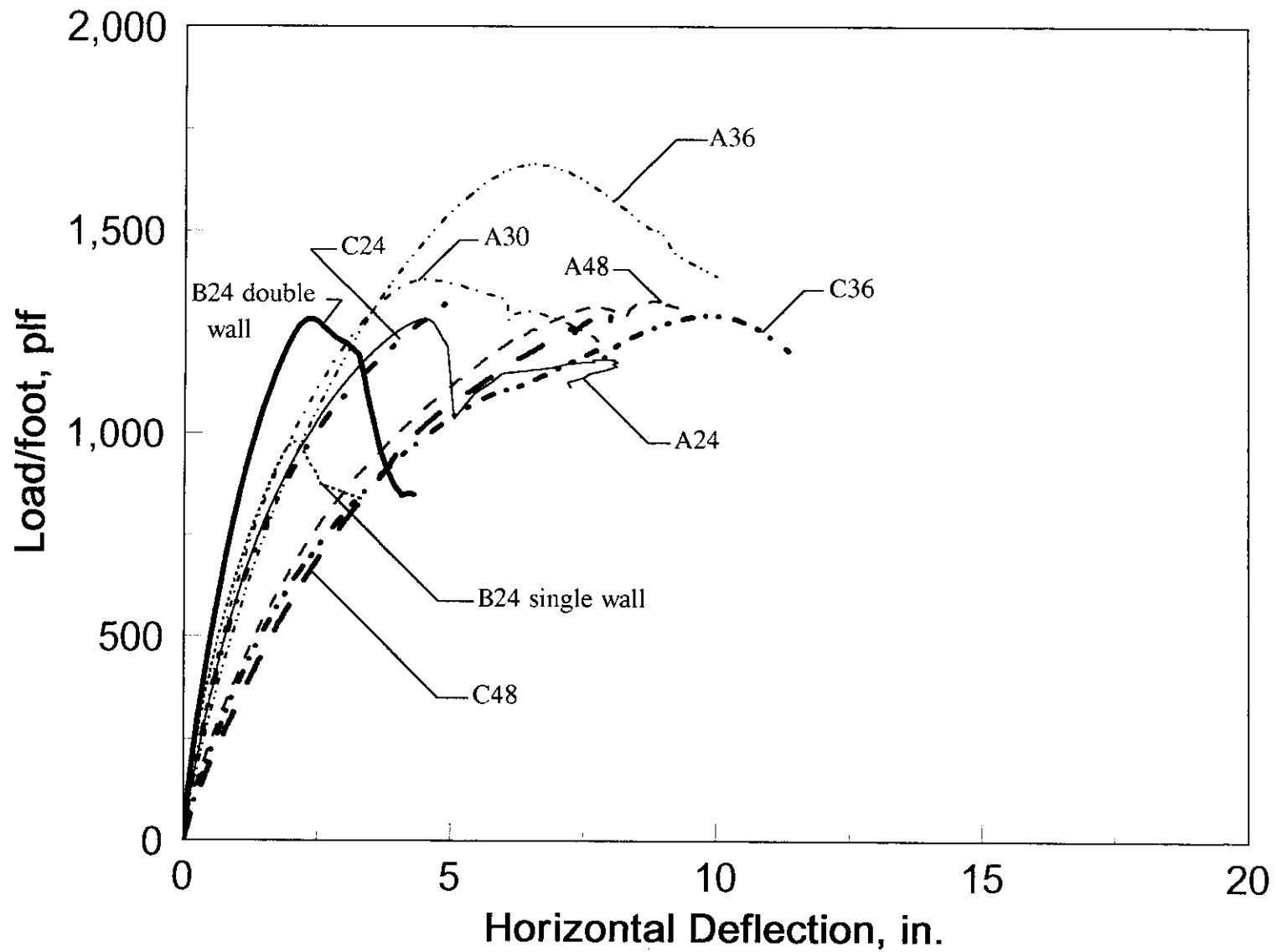


Figure 4.10. Load/ft vs. change in horizontal inside diameter.

The derivation is based on known values of moment at the crown of the pipe specimens based on the theory of elasticity. The internal forces at any point in the cross section are then determined from equilibrium. To determine the stresses at each section, the section properties were approximated from pipe manufacturer data as shown in Appendix E.

Shown in Figs. 4.11 and 4.12 are the theoretical and actual strain distribution for specimens C24 and C36 at 130 and 130 plf respectively. On each figure, are a number of lines representing $\pm 10\%$ of the section properties since they were approximations. Clearly, the theoretical and experimental data show significant agreement. This indicates that the behavior is predictable from the section properties. This relatively simple analysis of the ring system verifies the strain data obtained from the parallel plate tests.

4.2 Flexural Testing

Flexural testing consisted of testing 20-ft long pipe specimens; see Chapter 3 for details on the test setup and instrumentation. As previously noted, this type of testing was performed to determine: (1) the longitudinal stiffness of pipes, (2) the failure modes of HDPE pipes under flexural loadings, and (3) the differences in pipe strengths.

Specimens were proportioned with a span-to-depth ratio of at least five to limit shear deformations and were subjected to third-point loading. Each specimen was service load tested four times, once to a failure load, and subsequently loaded into a post-failure region. Failure was defined as those loads that cause the specimen to continue to deflect

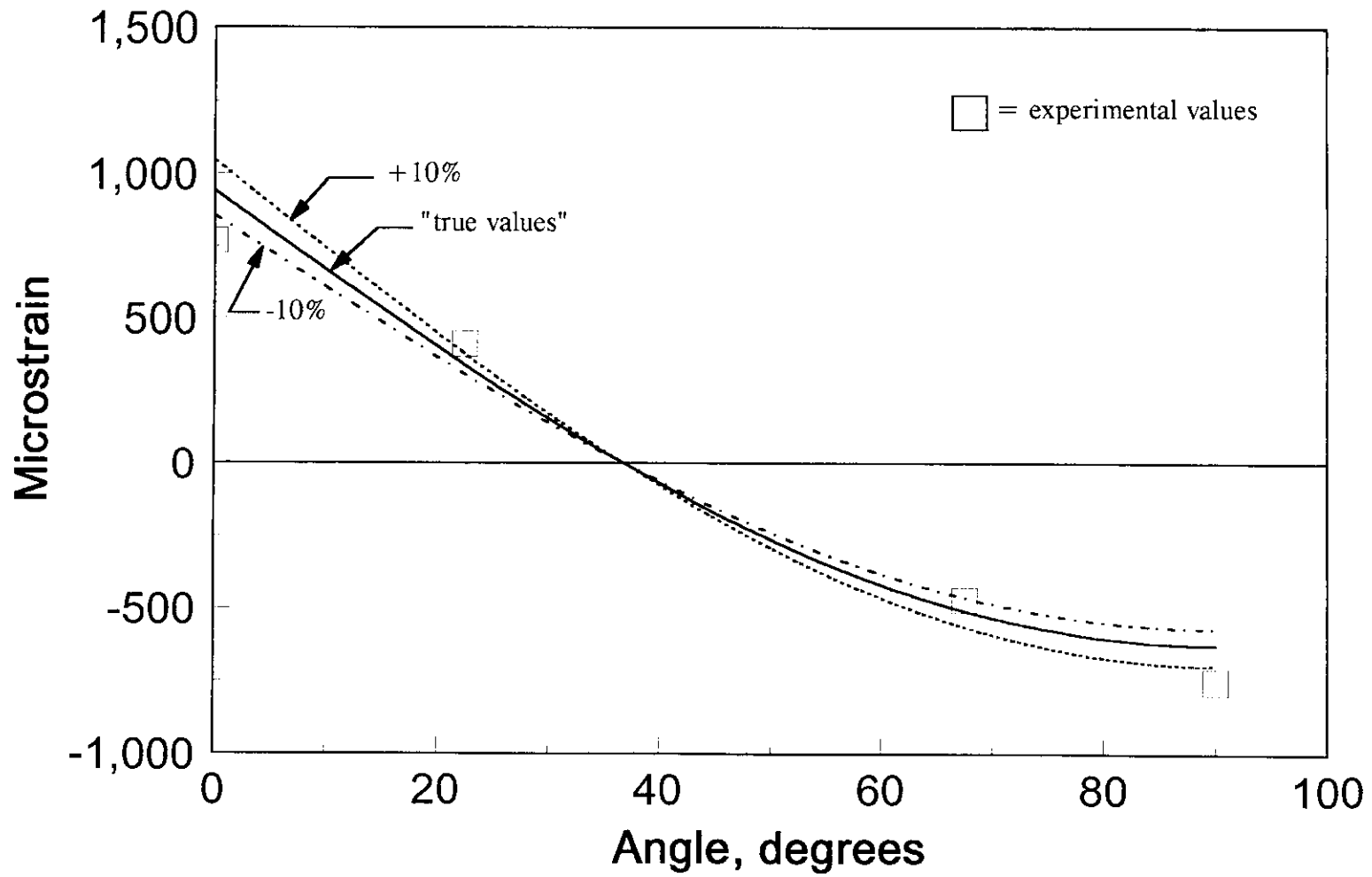


Figure 4.11. Theoretical vs. experimental strain for parallel plast specimen C24 at 130 plf.

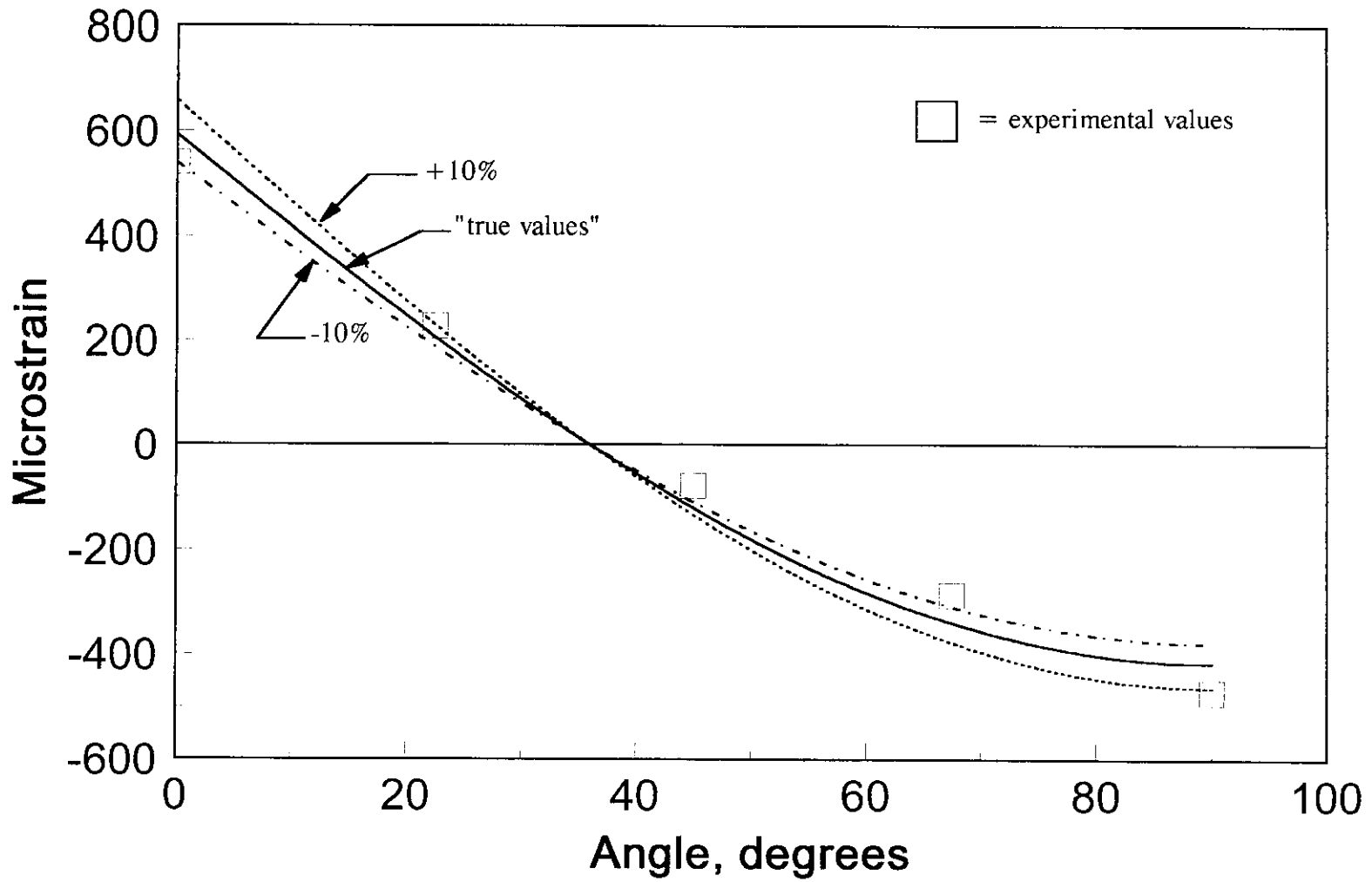


Figure 4.12. Theoretical vs. experimental strain for parallel plate specimen C36 at 113 pif.

without an increase in applied load (i.e., buckling of pipe wall, buckling of external corrugation, or development of plastic hinge). Results reported herein include maximum applied moments, longitudinal strains, deflections of the specimens, changes in inside diameter, and flexural stiffness; data from the post-failure tests are not included.

Strain measurements were made at locations on the inside of the pipe wall on all specimens. Only the data from the crown and invert sections are presented, as they are significantly higher than those at the springline (near the neutral axis).

4.2.1 Flexural EI Factor

Flexural EI factor values were calculated for all specimens from service load tests ignoring the effects of shear deformations. The factors were calculated based on the deflection at the center and at each quarter point using the principles from Castigliano's Theorem.

The average EI factors for each specimen are shown in Table 4.4. Shown are the average values based on the deflections that were of sufficient magnitude to eliminate significant digit errors. Tables in Appendix A present the actual values of the stiffness factor for a single service test at each load increment for each pipe specimen.

Since little was known about the expected loads the specimens would carry, service loads were limited to loads that caused a deflection of 0.75 in. at midspan.

As may be seen from the data in Table 4.4, there is a significant difference in the

flexural stiffness factors of pipe specimens of the same diameter. Manufacturer C has the highest EI factor for both sizes of pipes tested. The difference in flexural stiffness factor is most notable for the 48-in. specimens. As was the case with the parallel plate tests, differences in pipe geometry create very pronounced differences in pipe behavior as well as different values in Table 4.4. Average EI factors for all specimens during service level loading. the EI factor. For example, Manufacturer C's 48-in. specimen had EI factor values that were 4 times greater than those of Manufacturer A. This difference can be attributed to the difference in pipe wall geometry.

Table 4.4. Average EI factors for all specimens during service level loading.

Specimen	Service Load Test Number	EI (center) (kip-in ² *10 ⁴)	EI (west quarter pt.) (kip-in ² *10 ⁴)	EI (east quarter pt.) (kip-in ² *10 ⁴)
A36	1	5.91	5.96	5.85
	2	6.49	6.45	6.33
	3	6.67	6.73	6.05
	4	6.68	6.73	6.58
A48	1	23.63	23.90	21.82
	2	26.27	27.67	24.14
	3	27.83	31.04	25.86
	4	26.67	30.01	25.02
C36	1	45.68	48.19	46.51
	2	38.46	45.86	43.68
	3	36.06	43.70	39.71
	4	26.93	47.22	41.62
C48	1	341.87	109.96	119.81
	2	253.68	102.96	94.46
	3	117.80	102.03	117.15
	4	112.75	114.09	120.57

4.2.2 Midspan Moment versus Deflections and Changes in Inside Diameters

Deflections and changes in diameter were measured at the midspan of each specimen and at both quarter points. Changes in inside diameter were measured in both the vertical and horizontal directions.

Figures 4.13 and 4.14 show the deflections of the bottom of the pipe specimens during the failure tests. Clearly, Specimen C48 has the greatest stiffness and Specimen A36 has the least stiffness.

Specimens C36 and C48 have initially linear moment/deflection curves that show an apparent yield point. However, Specimens A36 and A48 shown more curvature in the moment/deflection curves indicating no well defined yield point.

The changes in inside diameter versus midspan moment are shown in Figs. 4.15 and 4.16. Little to no change in inside diameter was noted for all specimens except C48 in which the horizontal diameter increased and the vertical diameter decreased. The reason for this behavior will be explained in Section 4.2.3. Specimens generally failed due to the development of a plastic hinge under a load point.

4.2.3 Midspan Moment versus Longitudinal Strain

Figure 4.17 shows the location and designation of strain gages used during flexural testing; as previously noted these longitudinal gages were on the inside surface of the pipe specimens. Illustrated in Fig 4.18 are representative service load test data for Specimen

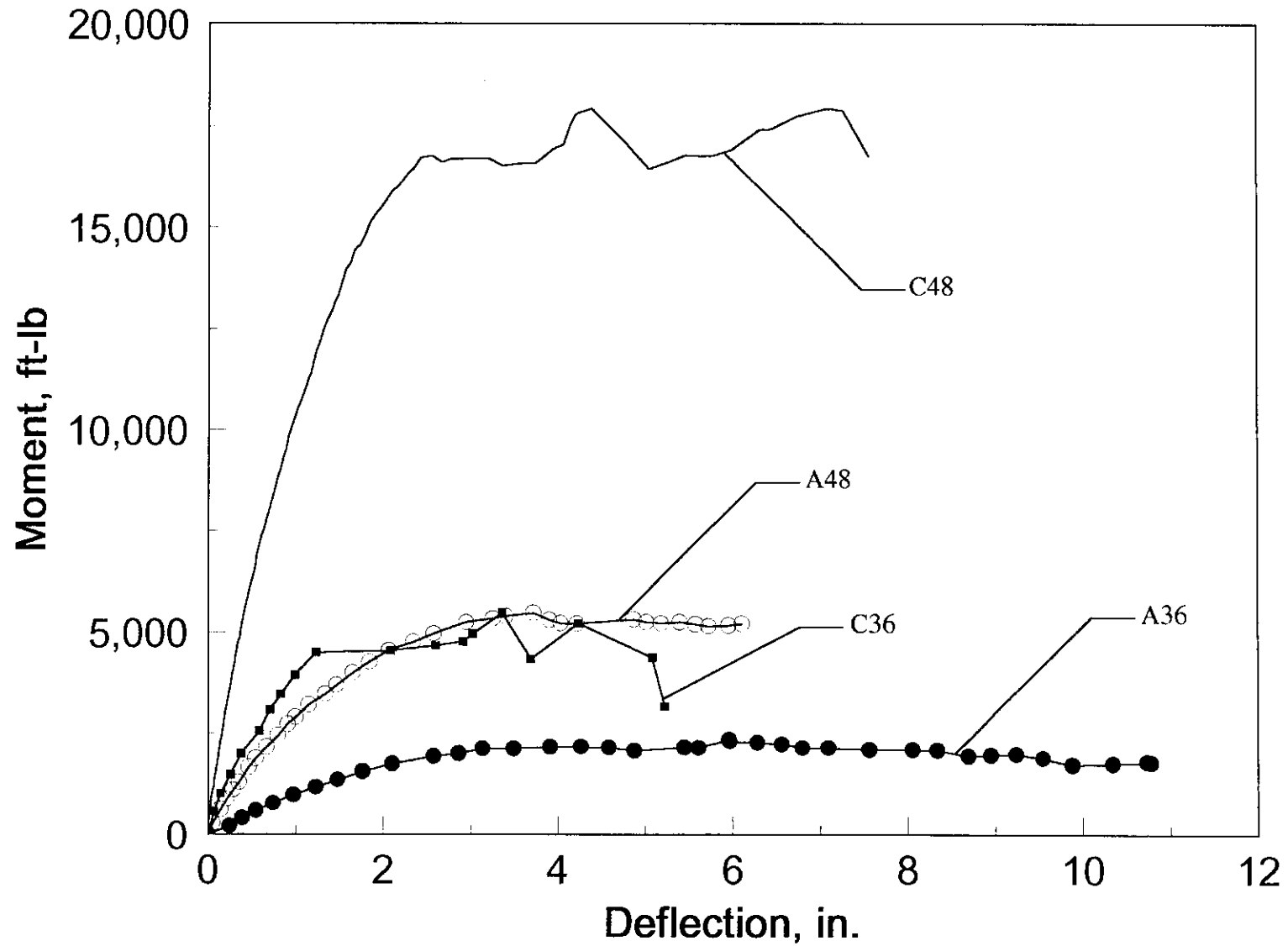
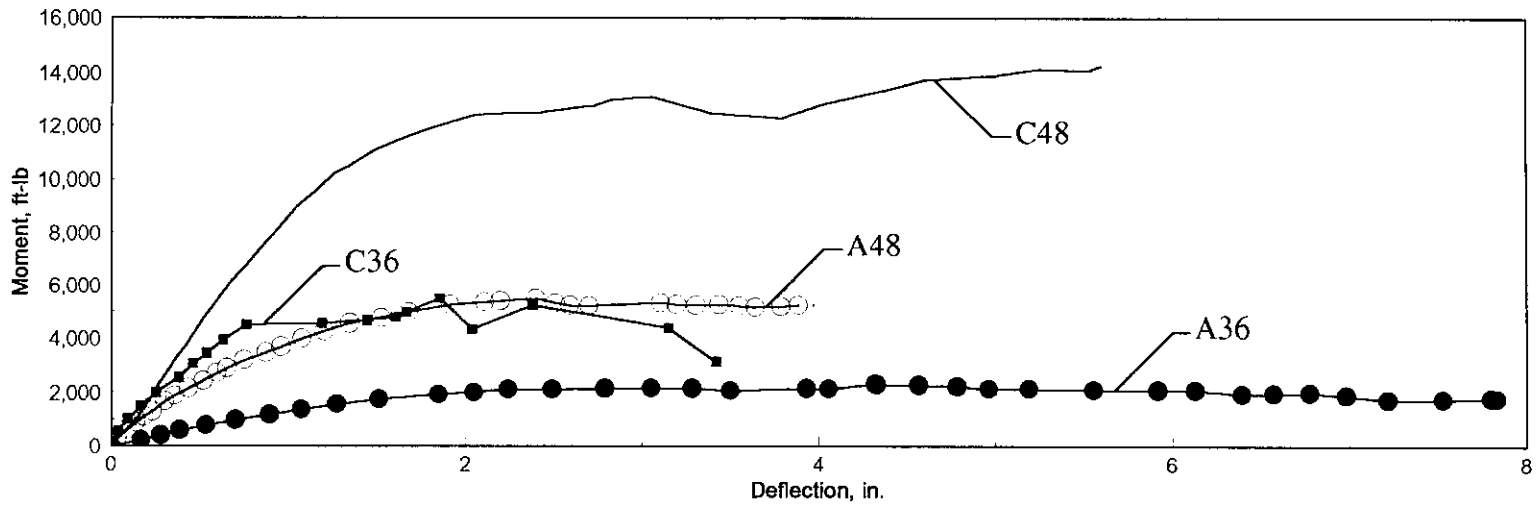
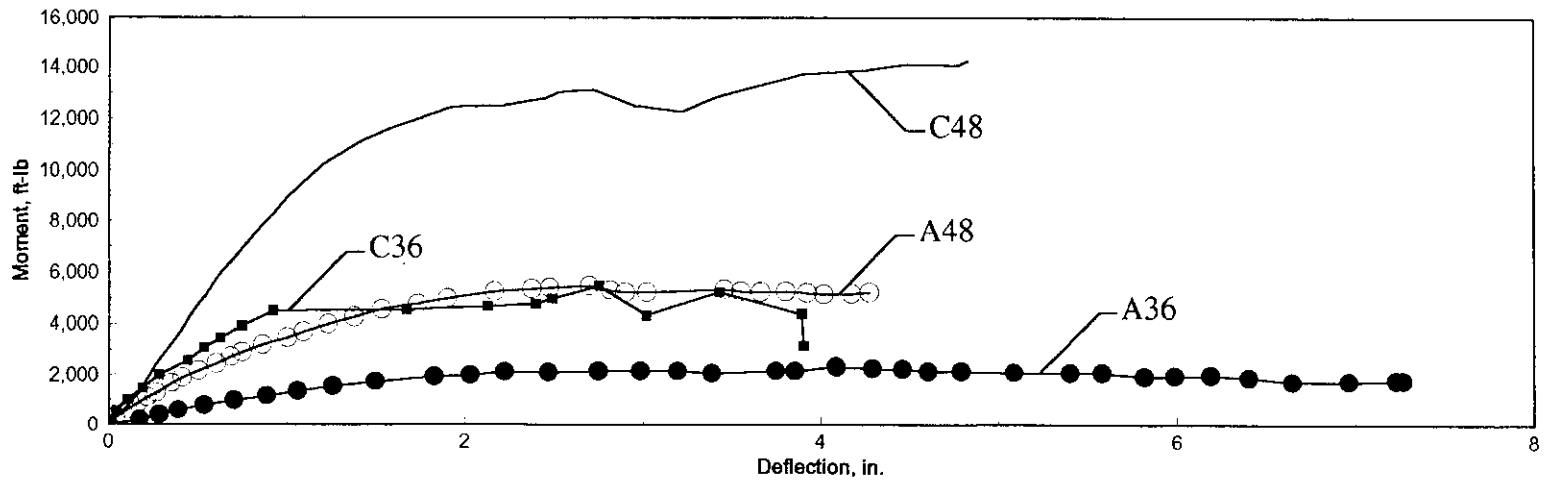


Figure 4.13. Moment vs. midspan deflection for failure tests.



a. West quarter point



b. East quarter point.

Figure 4.14. Moment vs quarter point deflection for failure tests.

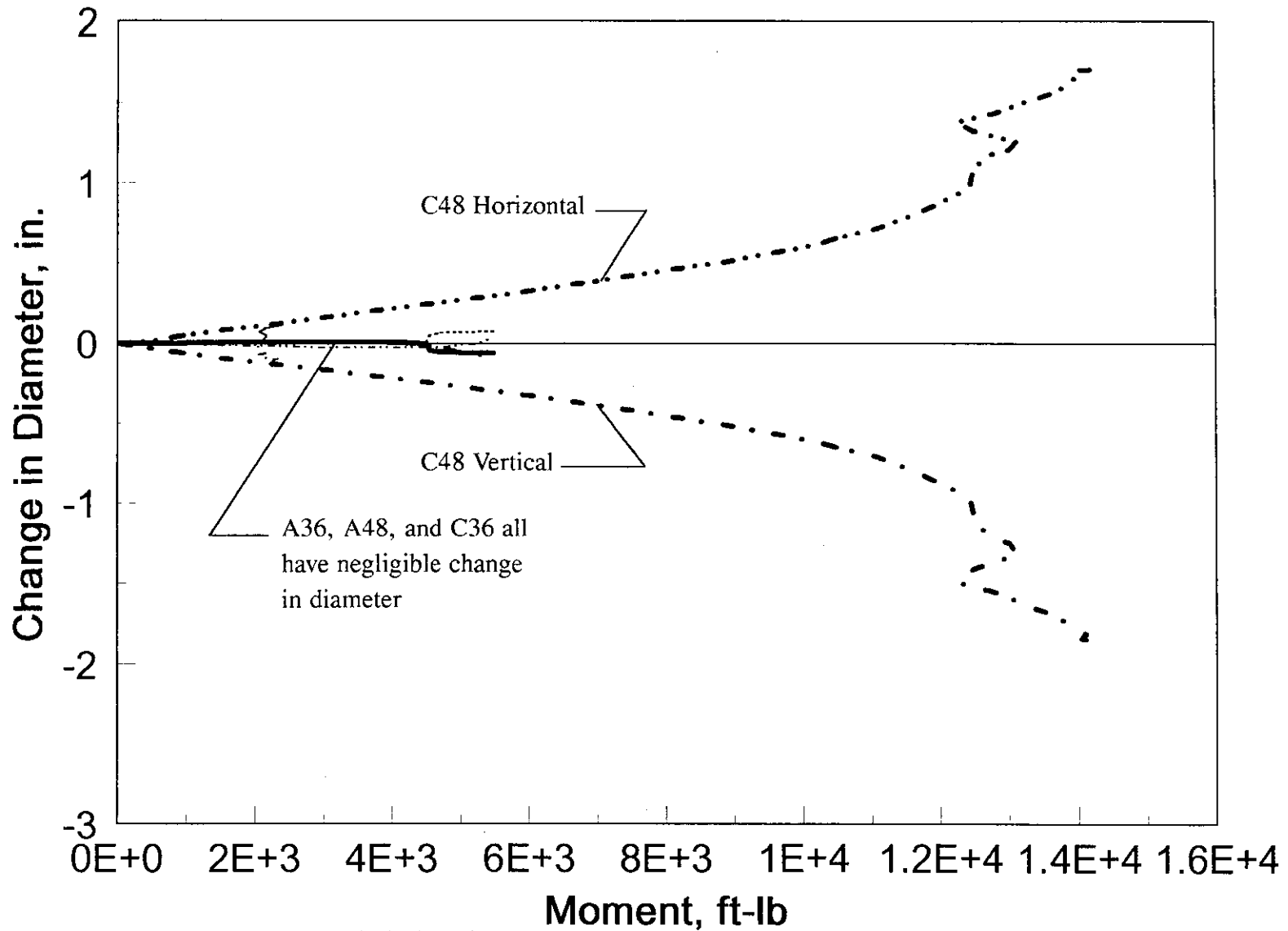
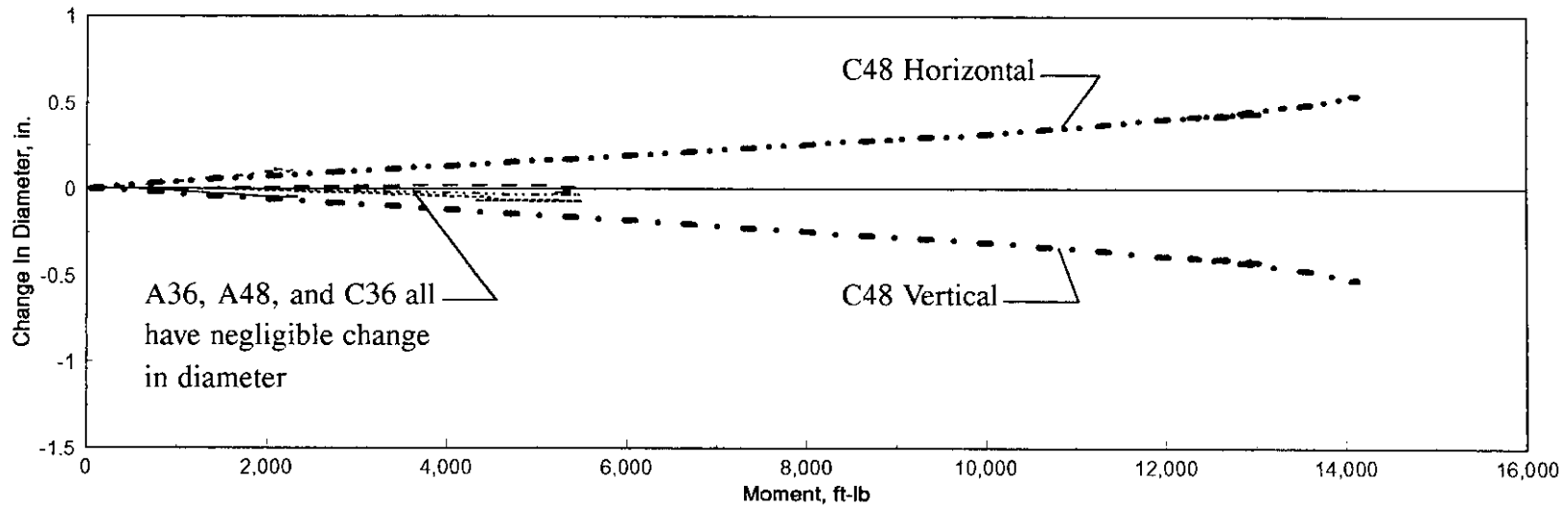
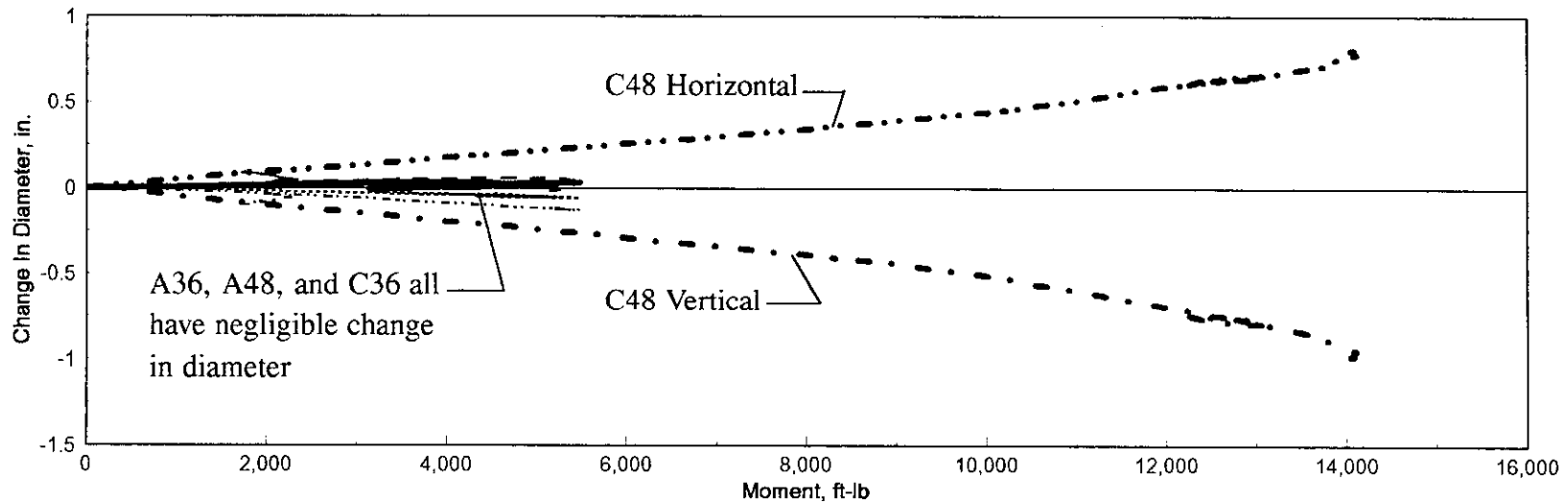


Figure 4.15. Moment vs. change in inside diameter at midspan.



a. East quarter point



a. West quarter point

Figure 4.16. Moment vs. change in inside diameter at quarter points.

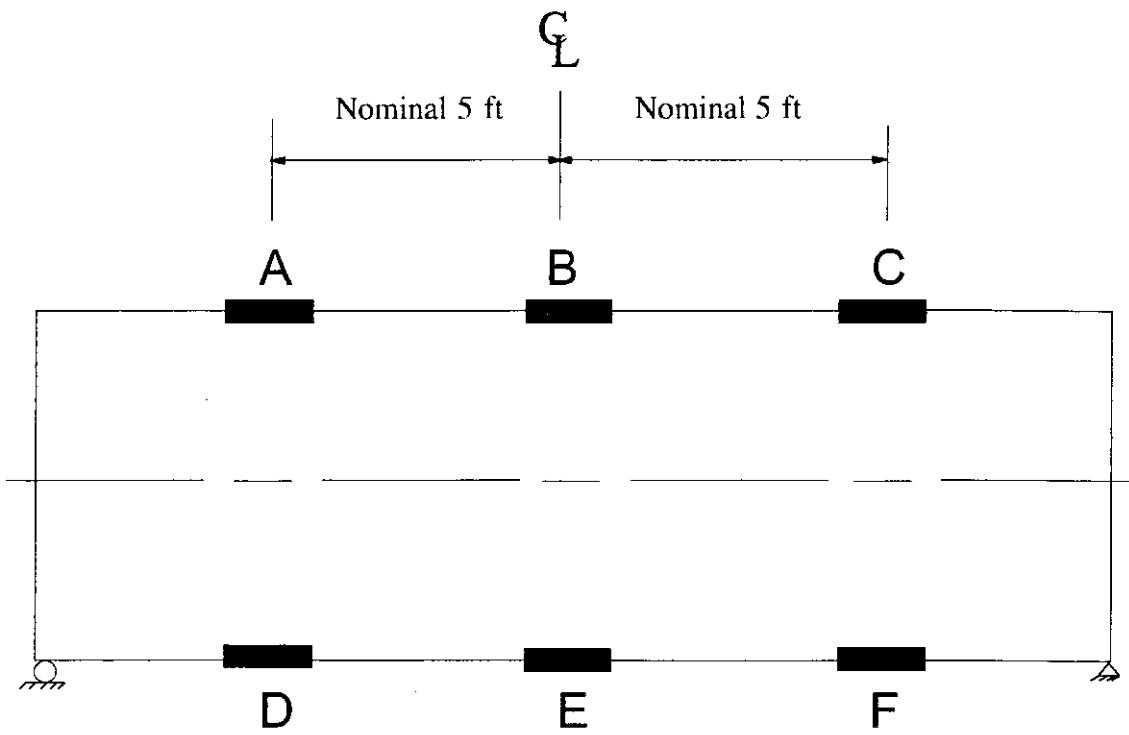
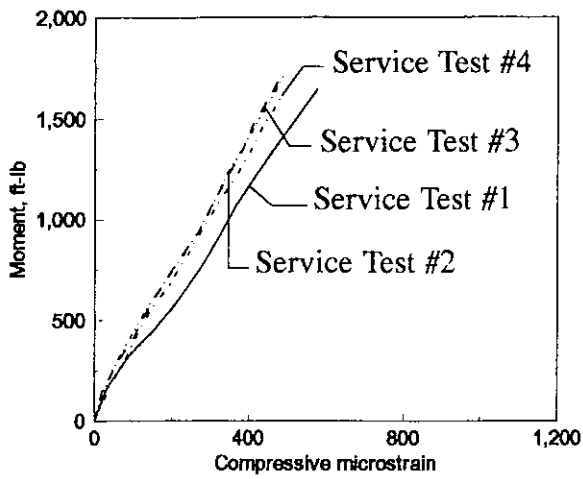
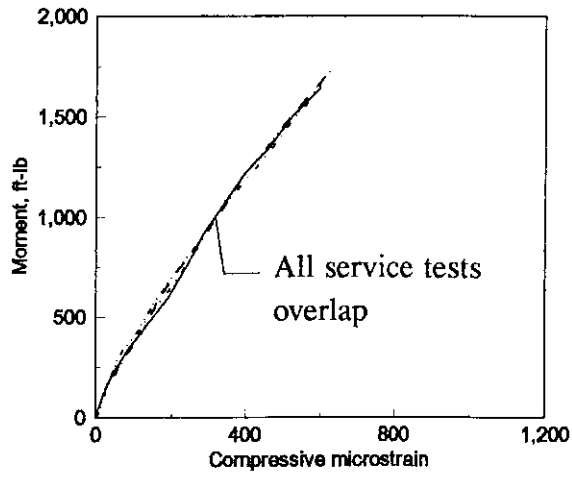


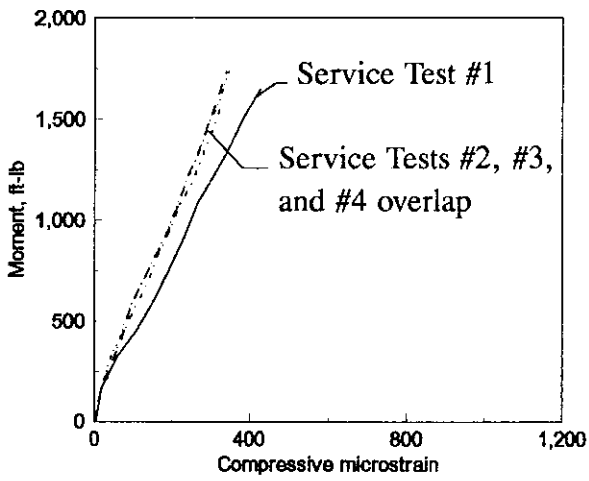
Figure 4.17. Strain gage locations and designation in flexural specimens.



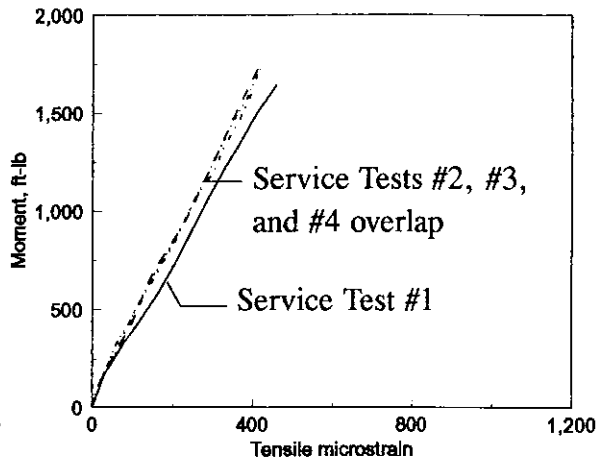
a. Position A



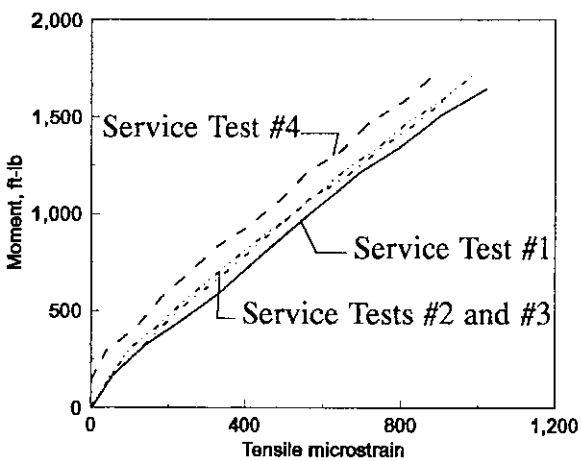
b. Position B



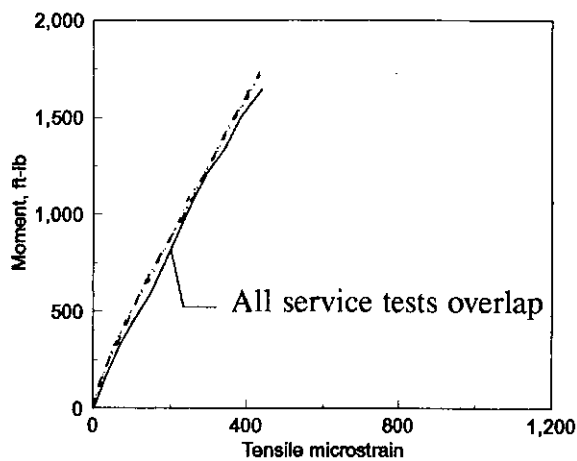
c. Position C



d. Position D



e. Position E



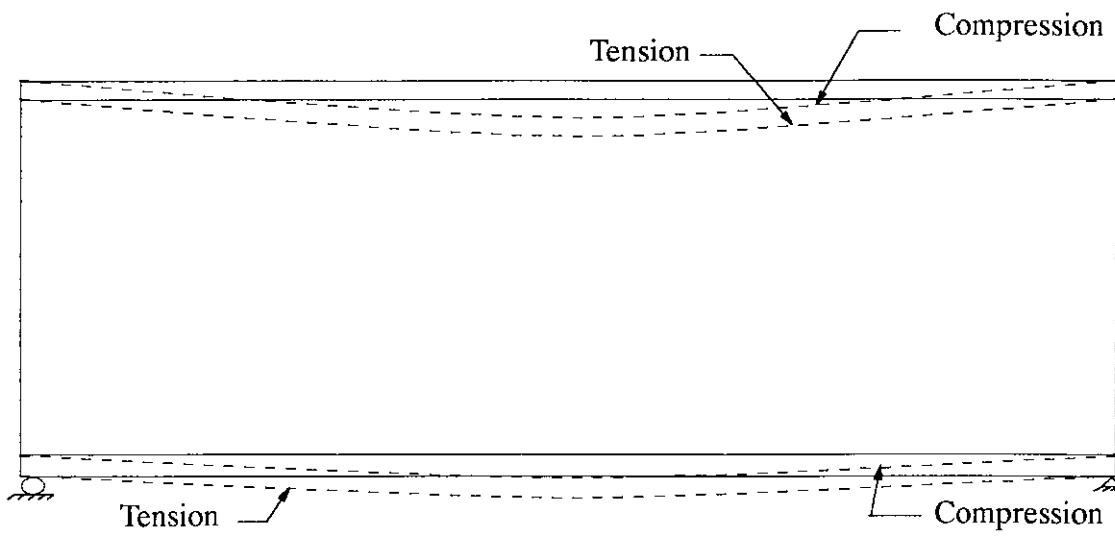
f. Position F

Figure 4.18. Moment vs. longitudinal strain for specimen A48 under service loads.

A48. Each graph represents the longitudinal strain at a given location. A review of these curves verifies the reproducibility of the data obtained in the four service load tests.

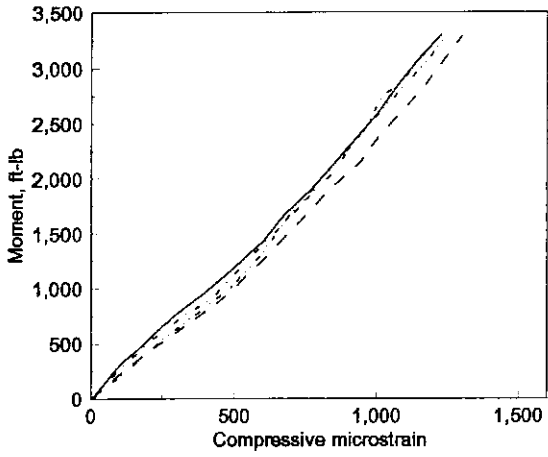
Compressive strain was recorded along the top of the specimen and tensile strain was recorded along the bottom of the specimen; this has been noted on the horizontal axis in these graphs. Typically, the strains at the bottom of the section near the roller support (Position F) are greater than those at the bottom of the section near the pinned support (Position D). The strains on the top of the sections near both pinned and roller supports (Positions A and C) were very nearly the same, indicating that the type of support has a lesser effect on the top of the pipe than on the bottom. The strain at the centerline at the top (Position B) was higher than those at the quarter points (Positions A and C). Similarly, the strains at the bottom showed a greater magnitude of strain at the centerline (Position E) than at the quarter points (Positions D and F).

Illustrated in Figure 4.19 is the behavior of Specimen C48. The wall profile of Specimen C48 is very different from other specimens and therefore this specimen exhibited significantly different behavior. Strains for the specimen are given at the quarter and center points on the inside as before with the addition of strain from additional gages on the outside of the specimen wall at the quarter points and at the centerline. The strains on the inside wall of the pipe at all locations are opposite in sign to those of other specimens. Different strain behavior might be expected based on the change in inside diameter data presented earlier. The fact that Specimen C48 was the only one that had any significant



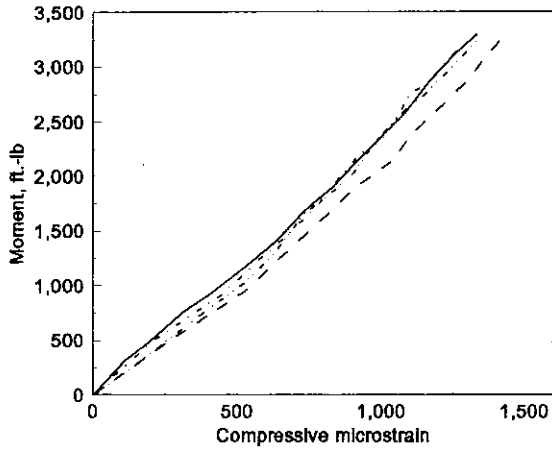
a. Sketch of deflected shape

Figure 4.19. Moment vs. longitudinal strain and deflected shape for specimen C48 under service loads.

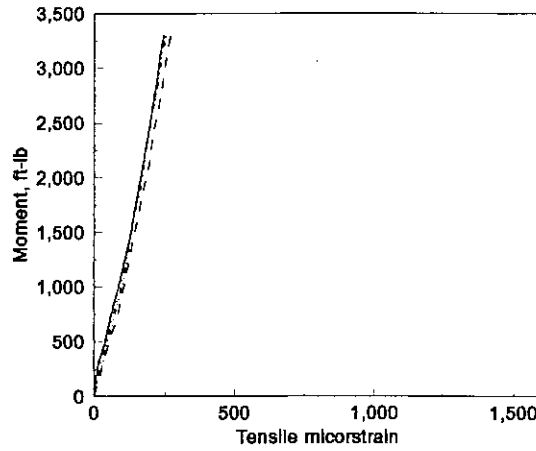


b. Position A, outside

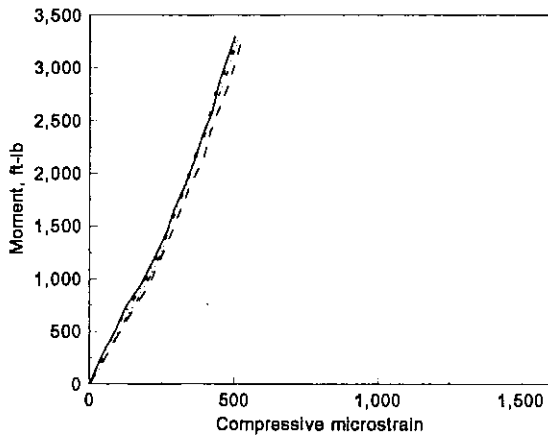
Note: No distinction is made between each service test because the lines overlap.



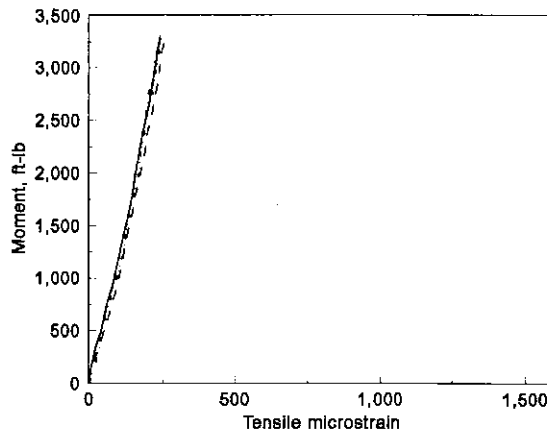
e. Position B, outside



d. Position B, inside

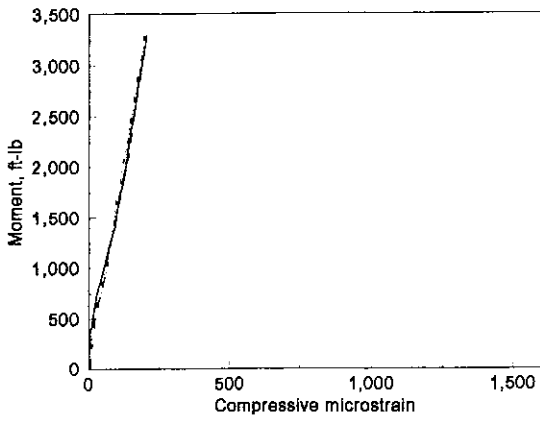


e. Position C, outside

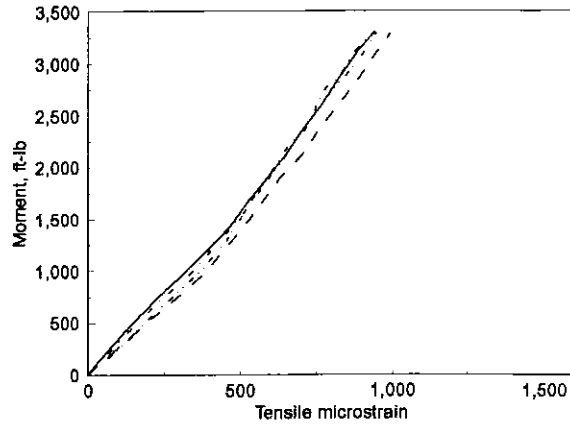


f. Position C, inside

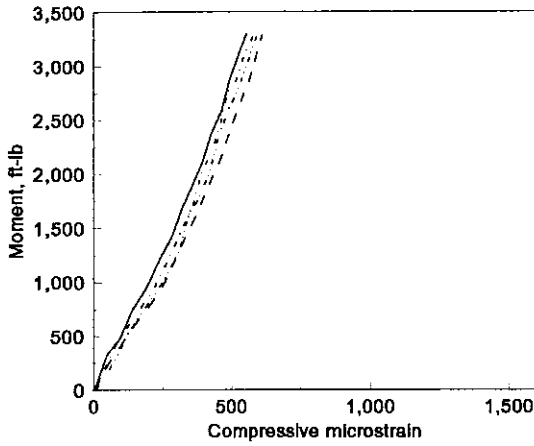
Figure 4.19. Continued.



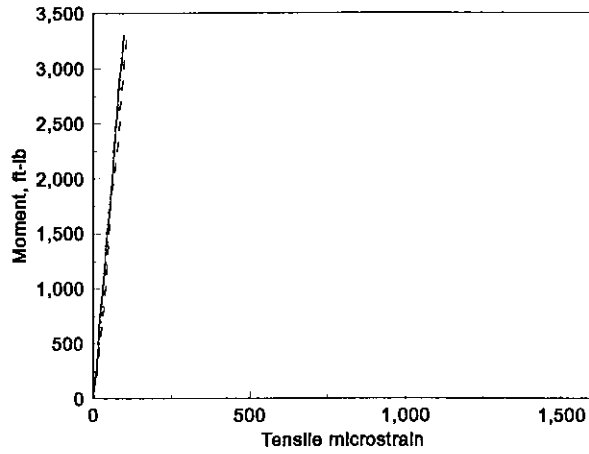
g. Position D, inside



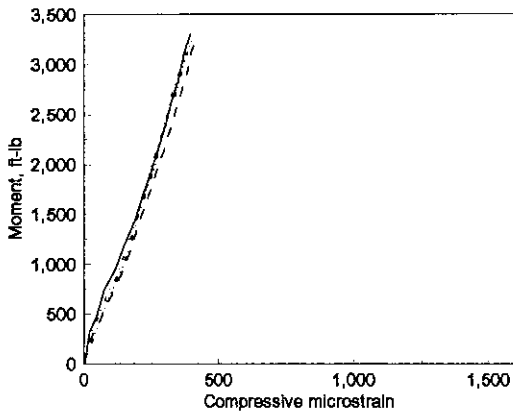
h. Position D, outside



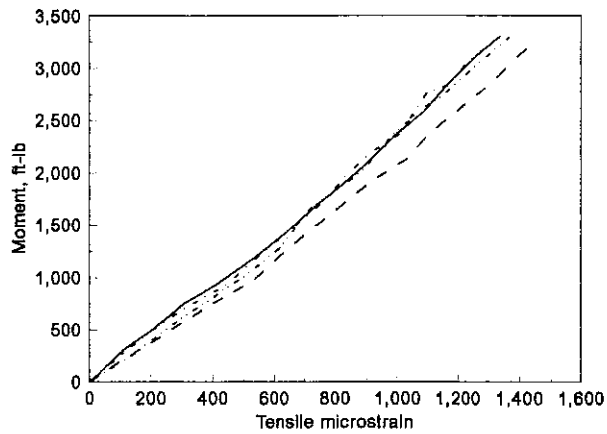
i. Position E, inside



j. Position E, outside



k. Position F, inside

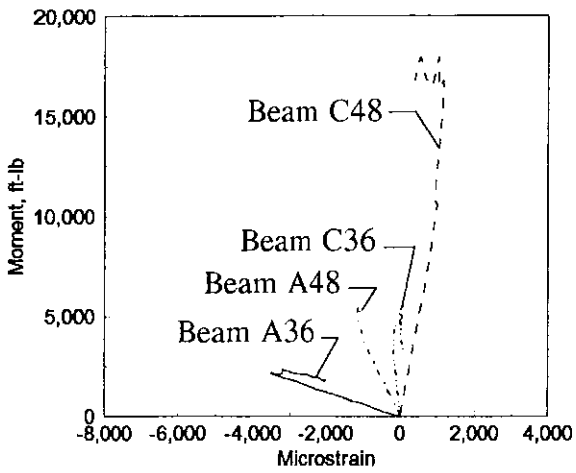


l. Position F, outside

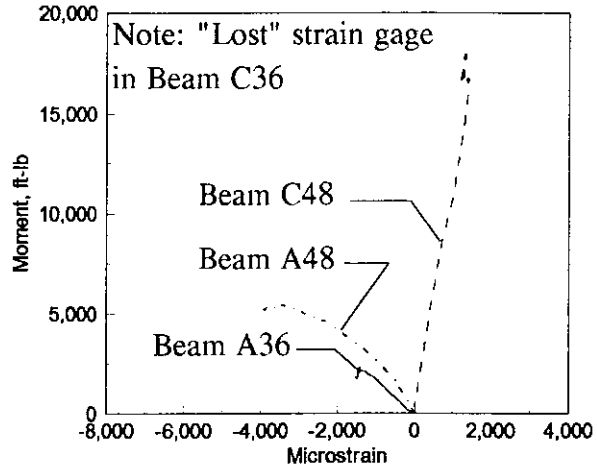
Figure 4.19. Continued.

change in inside diameter indicates that the top and bottom walls were acting independently and therefore each surface had an independent deflected shape. Thus, compression along the top surface and tension along the bottom of each wall cross-section could occur. This behavior is clearly shown by the sign of the measured strains shown in Fig 4.19. One might also expect higher strains on the top fibers because of the greater deflection when compared to that of the bottom fibers. This is the case for all locations except the tensile strain at locations C and F. A sketch of the deflected shape is also shown in Figure 4.19a indicating the tensile and compressive fibers and the difference in deflection amounts. Also note that the deflection is larger for the upper wall than the lower wall thereby creating the larger strains discussed previously.

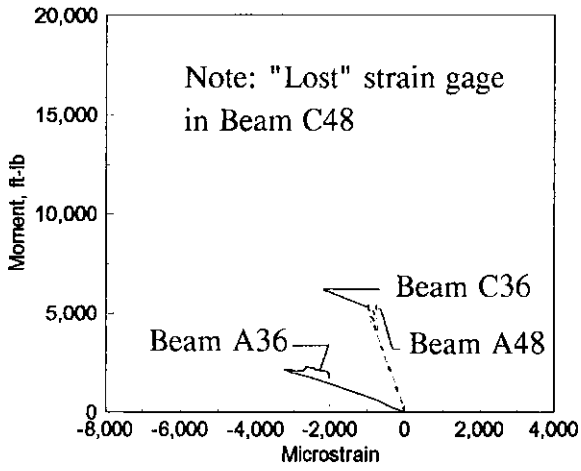
Figure 4.20 shows the comparisons of the longitudinal strains (+ strain = tension; - strain = compression) of each of the specimens during their failure tests. This shows that the least stiff specimen (A36) has higher magnitudes of longitudinal strain than the other specimens except at Position B. It also illustrates the difference in signs of longitudinal strains between specimen C48 and the remaining specimens. Clearly, as previously noted, flexural stiffness is not only a function of pipe diameter but is heavily dependent on the wall profile geometry.



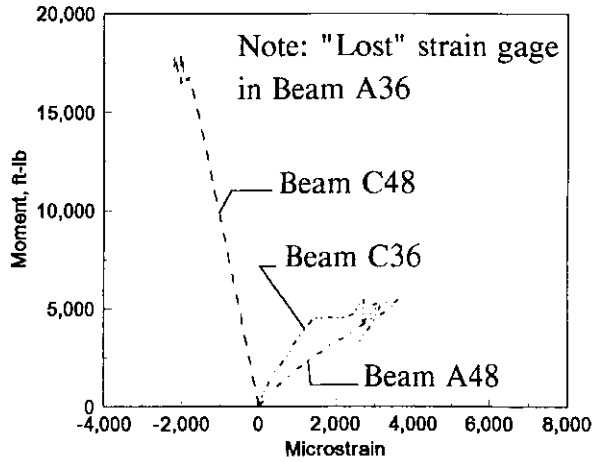
b. Position A, inside



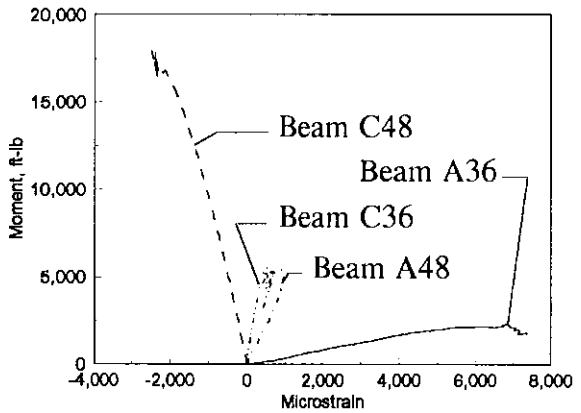
c. Position B, inside



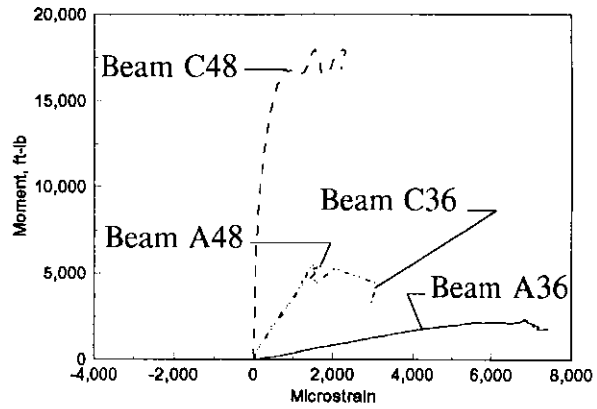
d. Position C, inside



e. Position D, inside



f. Position E, inside



g. Position F, inside

Figure 4.20. Moment vs. longitudinal strain for failure tests.

4.3 In Situ Live Loading

In situ live load tests consisted of the testing of 20-ft long pipe specimens under vertical loads. This type of testing was completed for several reasons: (1) to determine the effect of the soil on the soil/structure interaction, (2) to determine the effect of varying qualities of backfill envelopes on the pipes' performance, and (3) to determine the failure modes of HDPE pipes under concentrated live loads.

In all tests, there was minimum cover conditions of 2-ft of cover over the pipe crown. In each service load test, each specimen was initially loaded at the centerline, then the north quarter point, and finally at the south quarter point. After the service load tests had been completed, loads were applied to failure at each location. Failure was defined by the condition at which the specimen continued to deform without an increase in load. Data from the north and south load points are presented but briefly discussed because boundary effects were observed in reviewing the field data that resulted in loads near the pipe ends. Further testing needs to be completed to fully understand pipe behavior under loads near the end.

Instrumentation employed was presented in Chapter 3. Results reported herein include longitudinal and circumferential strains during backfilling, longitudinal and circumferential strains during loading, and changes in inside diameter during loading and backfilling. Movement of the pipe crown was measured and recorded as described in Chapter 3; deflections were found to be very small and thus have not been included.

4.3.1 Backfilling

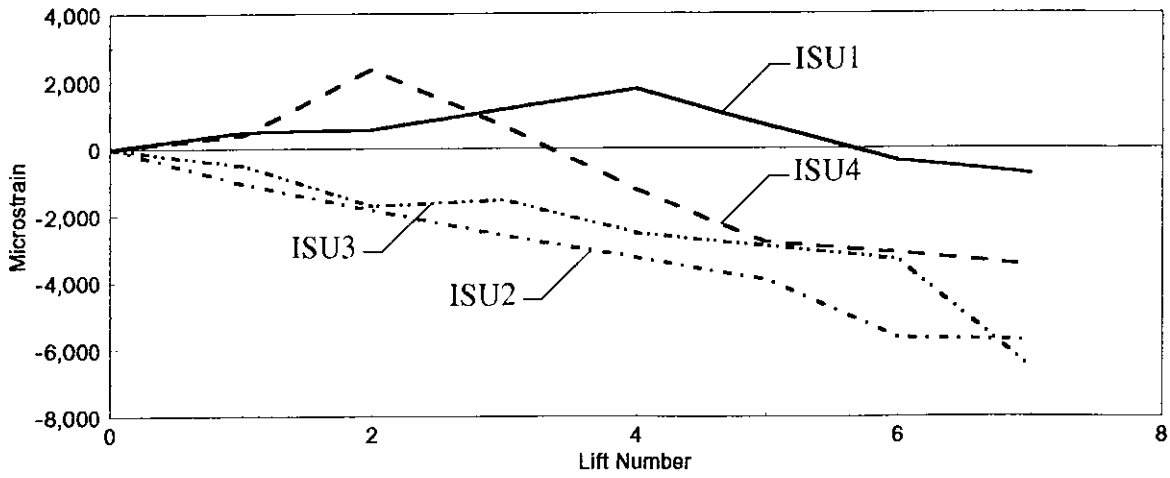
As previously described, backfills used in the four field tests utilized both native glacial till and a local granular soil. Lifts were placed in approximately 9-in. depths and leveled before compaction. After compaction, moisture and density readings were taken to confirm compaction; the desired level of 95% to 105% standard proctor was consistently achieved. Backfilling alternated from side to side of the pipe to maintain approximately the same level of fill on each side. An embankment with a slope of 2:1 was formed at each end of the pipe specimens during backfilling to allow access to the buried specimen.

4.3.2 Backfill Data

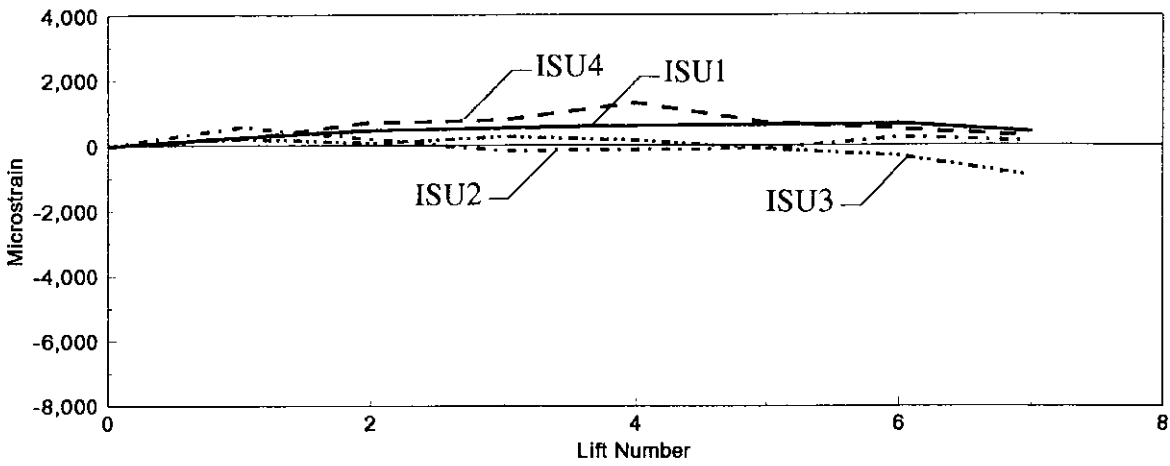
Data were recorded at the completion of most lifts during the backfilling process. Data presented herein includes circumferential strains, longitudinal strains, and changes in diameters for each lift.

The circumferential strains recorded during the backfilling process for Sections 2, 4, and 6 (see Fig.3.12) are shown in Figs. 4.21 through 4.23. Each figure contains three graphs that represent the circumferential strains at three locations: crown, springline, and invert. Strain data were taken at the springline on both sides of the pipe but did not vary significantly when compared to the variation of strains at the crown and invert. Thus, only average strains at the springline are presented.

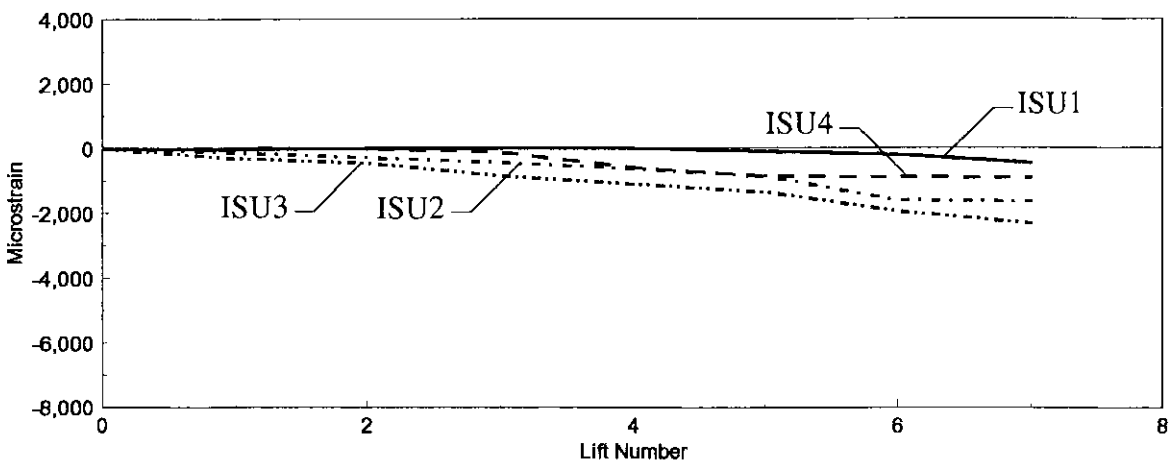
Immediately after backfilling began, the invert of the pipe experienced compressive



a. Crown

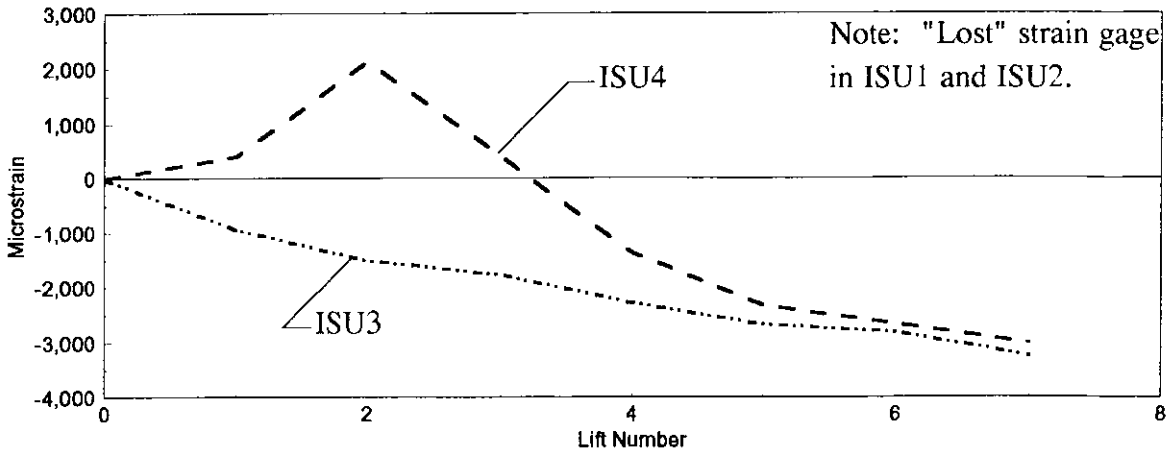


b. Springline

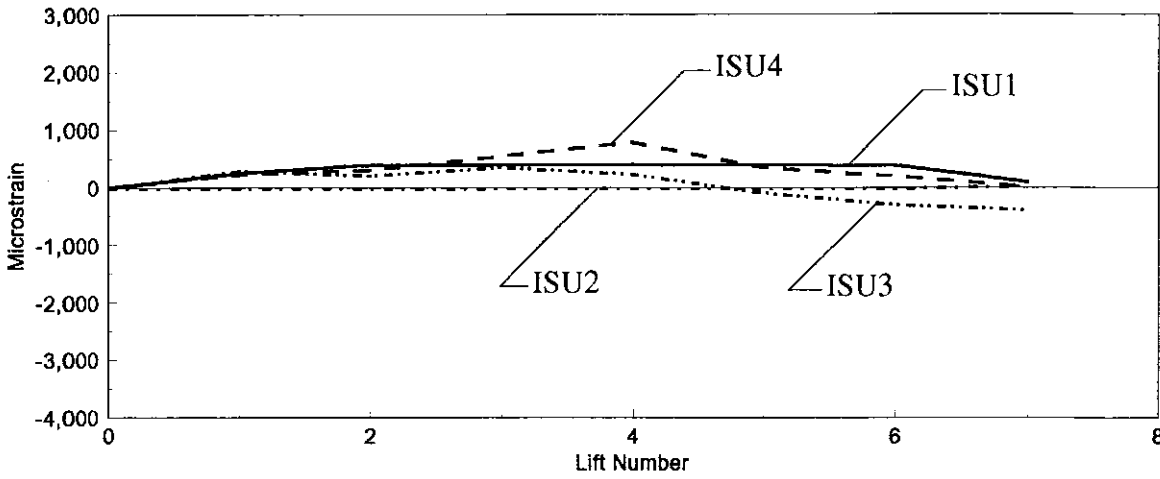


c. Invert

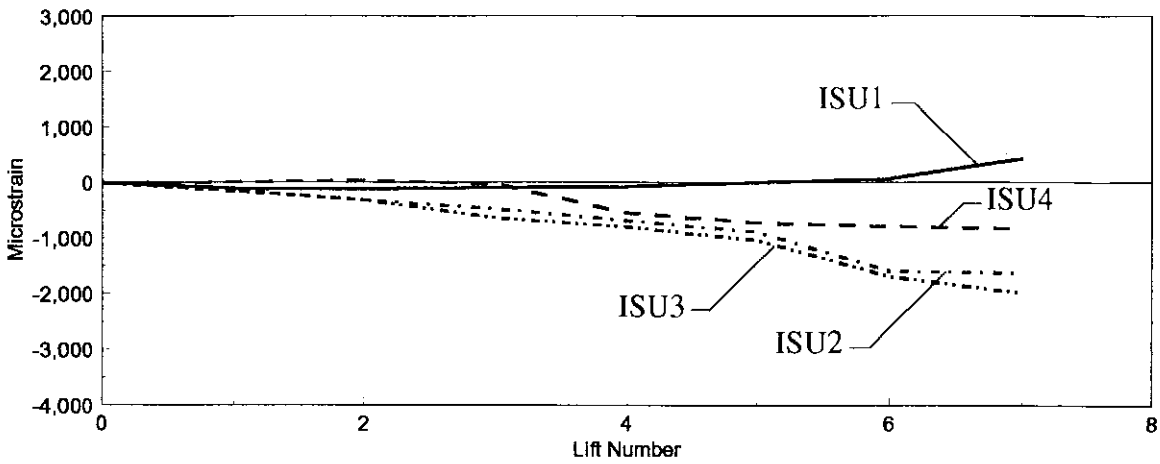
Figure 4.21. Backfilling circumferential strain at Section 2.



a. Crown

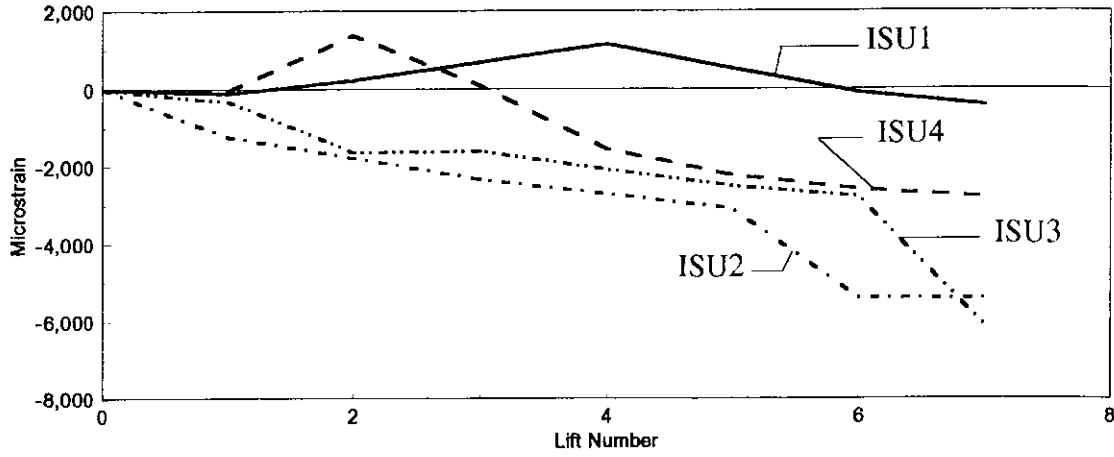


b. Springline

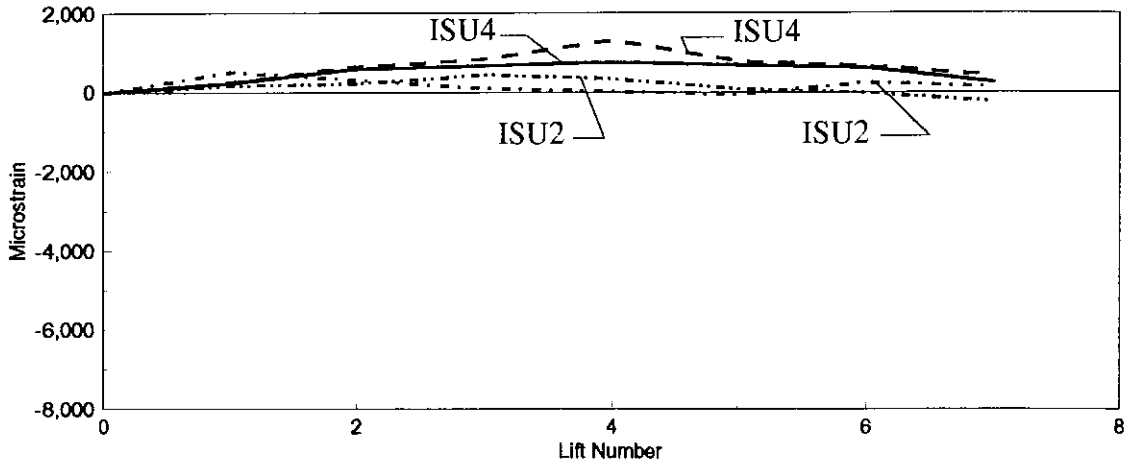


c. Invert

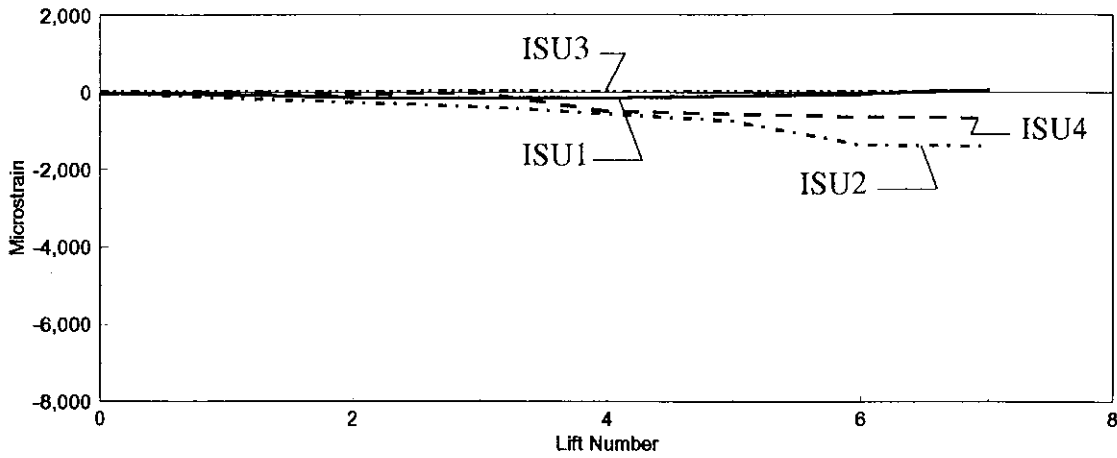
Figure 4.22. Backfilling circumferential strain at Section 4.



a. Crown



b. Springline



c. Invert

Figure 4.23. Backfilling circumferential strain at Section 6.

circumferential strains. These compressive strains continued to increase throughout the backfilling process. This compression is due to the increase in restraint imposed on the pipe by the addition of the soil envelope as well as the increase in vertical load imposed on the pipe walls. The increase of compressive strains tended to be nearly linear and varied almost directly with the lift. Circumferential tension strains occurred at the springline of the pipe during the backfilling. This is due to the deformation of the pipe cross section from the horizontal confinement of the backfill soil. As the backfill depth increased, the force on the pipe imposed by the overburden had a decreasing horizontal effect and an increasing vertical effect causing a decrease in the springline tensile circumferential strains. In other words, the pipe was first deformed so that the vertical diameter increased and then as the crown of the pipe was buried, the pipe was subjected to loads which deformed the pipe in the opposite direction. In the case of ISU3, which had the largest vertical overburden pressure (because of a higher average unit weight of the compacted fill), the increase in vertical load caused compressive circumferential strains at the springline.

The largest backfill strains recorded occurred at the pipe crown because the crown of the pipe was unrestrained for more of the backfilling process and thus was able to deform freely for a longer duration of the backfill process. In general, comparison of the strains at the three sections reveals that significantly higher strains occurred near the ends of the pipe. It was also noted that the circumferential strains are fairly symmetrical about the transverse centerline of the pipe length.

Figures 4.24 through 4.26 show the change in inside diameter versus lift. It is apparent that the vertical diameter increased and the horizontal diameter decreased at all locations. As shown, ISU3 had the greatest change. These figures indicate that ISU3 had the highest final backfilling deformation, which explains the higher final backfill strains. It can be observed that after lift four, which corresponds to the lift at the top of the pipe, essentially no additional deformation occurred. The changes in inside diameter was symmetrical about the centerline (compare data in Figs. 4.24 and 4.26). However, there was a smaller difference between the diameter changes in the center sections and the end sections than there was in the circumferential strain occurring at the same sections.

Figures 4.27 through 4.29 show the longitudinal strains which occurred during backfilling at three locations: crown, springline, and invert. There is no clear trend in the strains for a given specimen or at a given section. The random variation of the longitudinal strain data for a given specimen can be attributed to longitudinal differences in tamping sequence, actual mechanical effort applied, and differences in the type and quantities of backfill materials used. The differences between ISU2 and ISU4, which have the same backfill condition, can be explained by the fact that the trench in ISU2 was narrower than that of ISU4. The dimensions of the top and cradle of the trench were essentially the same, however the total width of the bottom of the trench in ISU4 was significantly larger. ISU4 had nearly vertical slopes whereas ISU2 had slopes more nearly equal to 1:1. This difference resulted in different backfill restraint and horizontal loads.

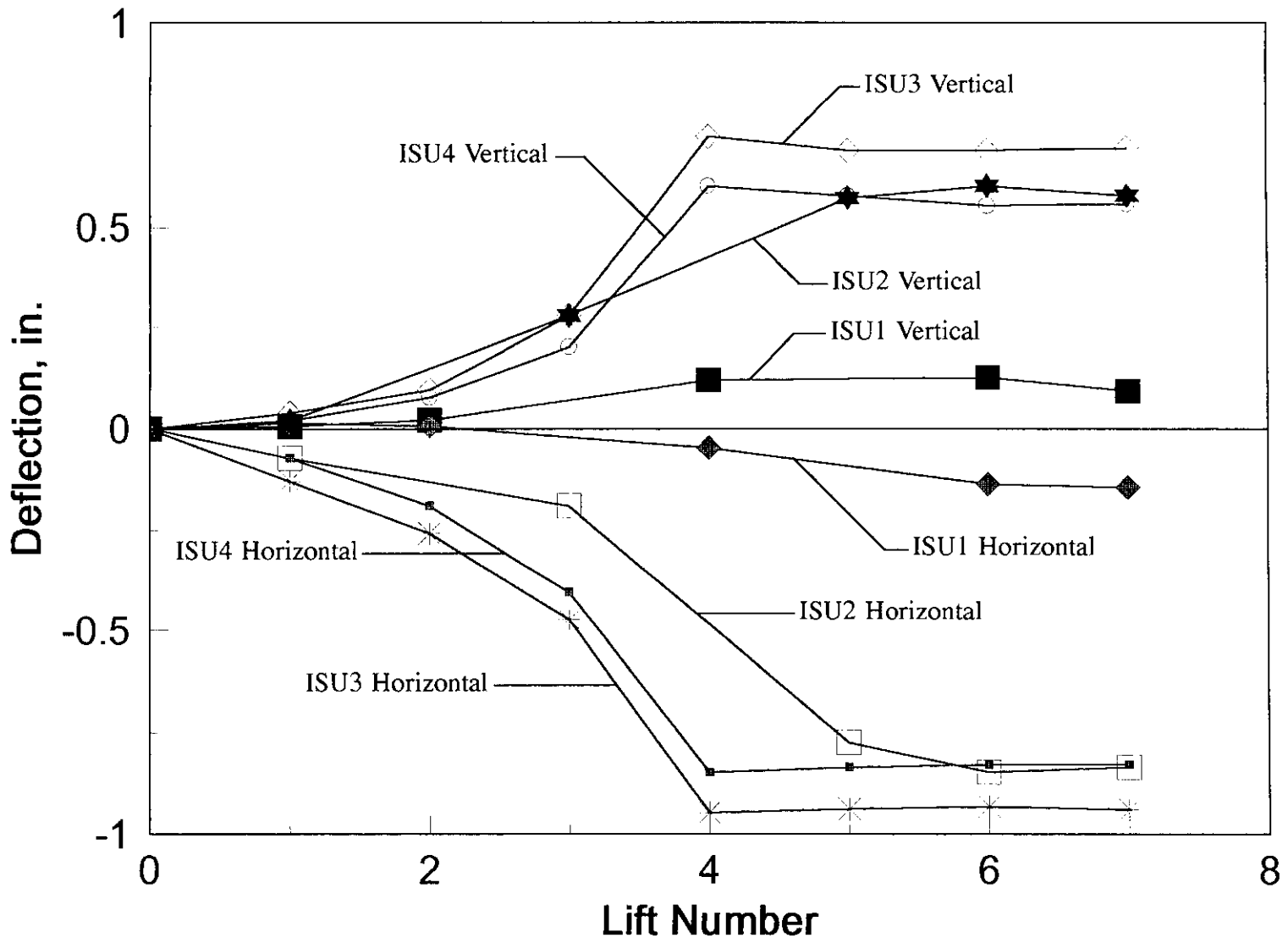


Figure 4.24. Changes in inside diameter at Section 2 during backfilling.

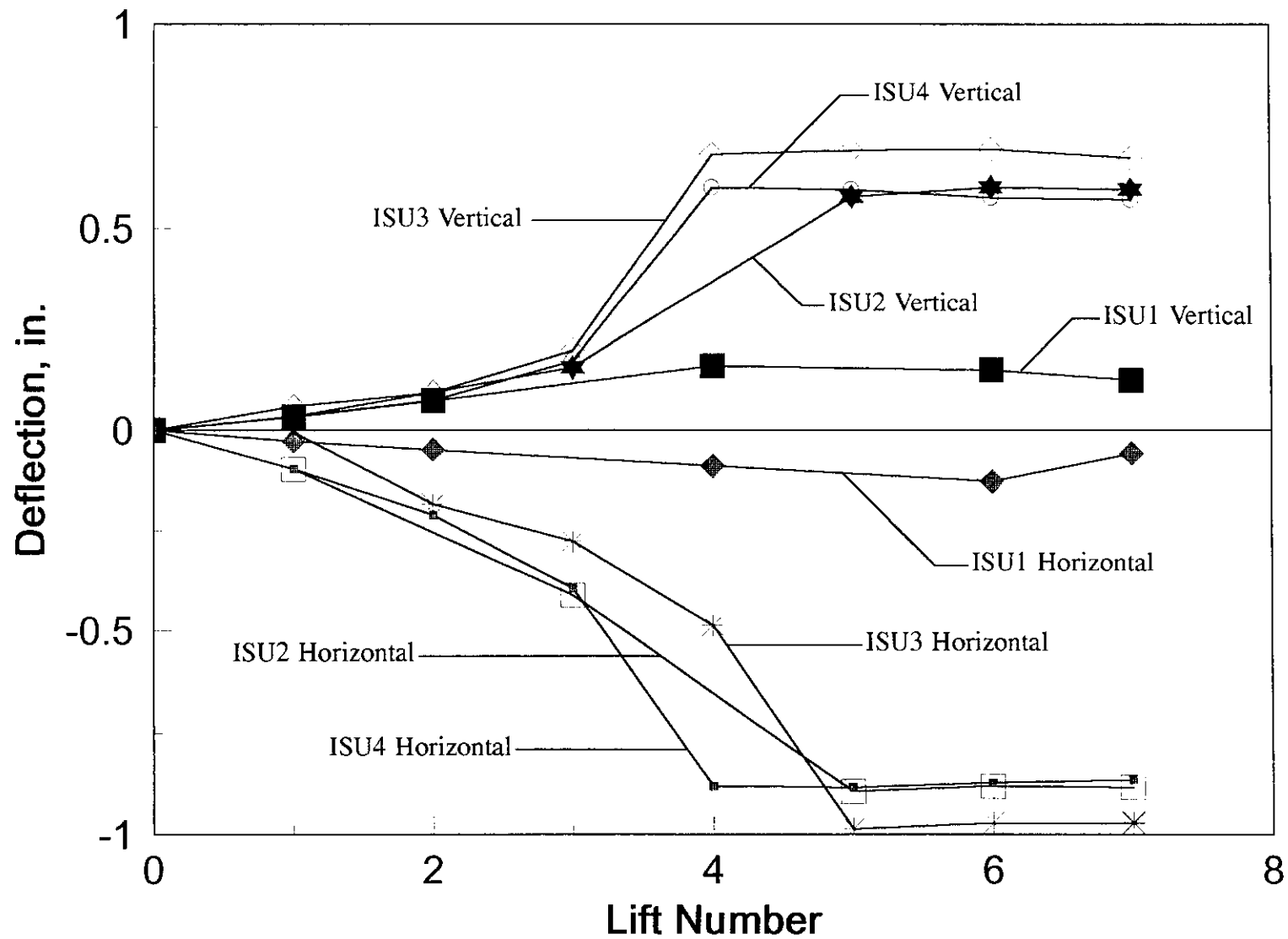


Figure 4.25. Changes in inside diameter at Section 4 during backfilling.

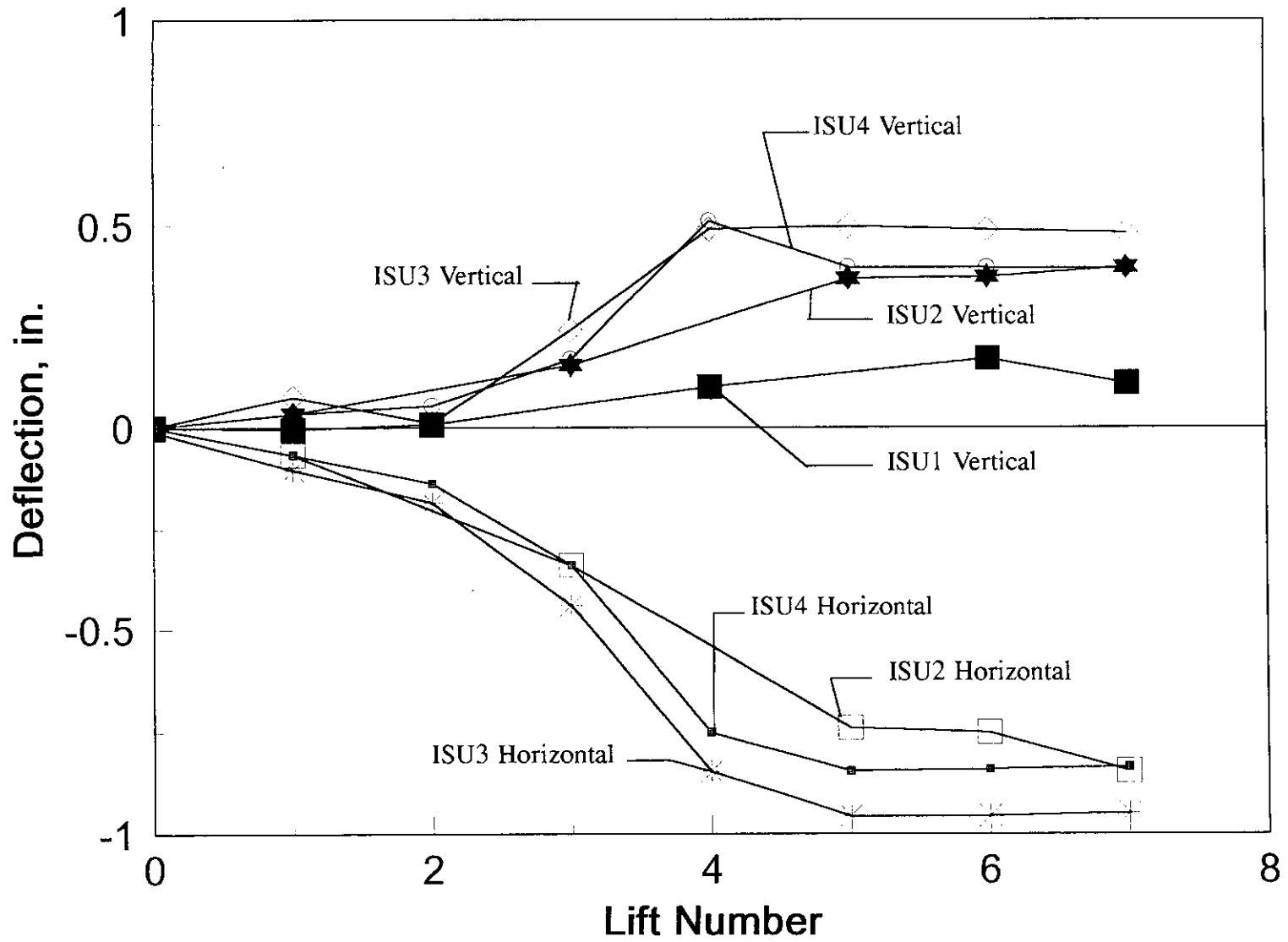
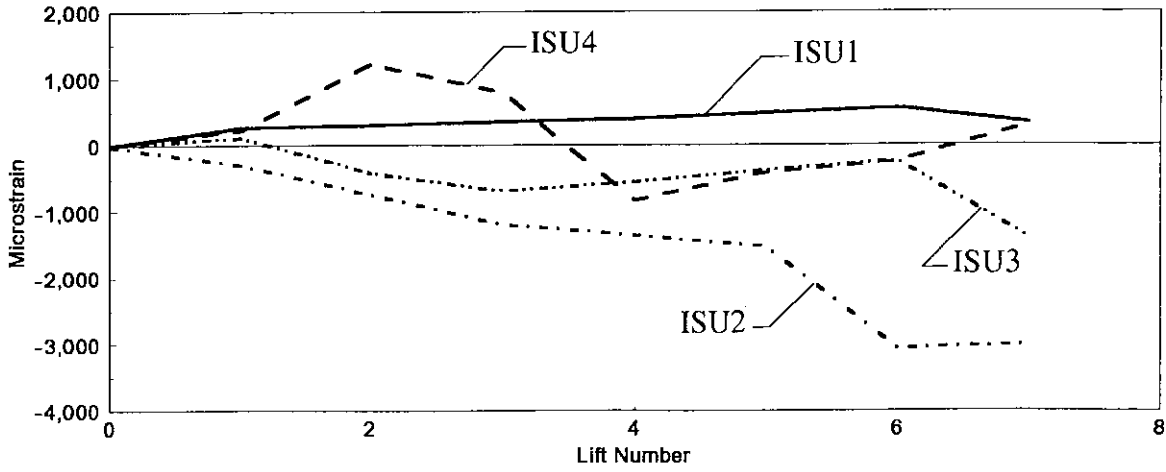
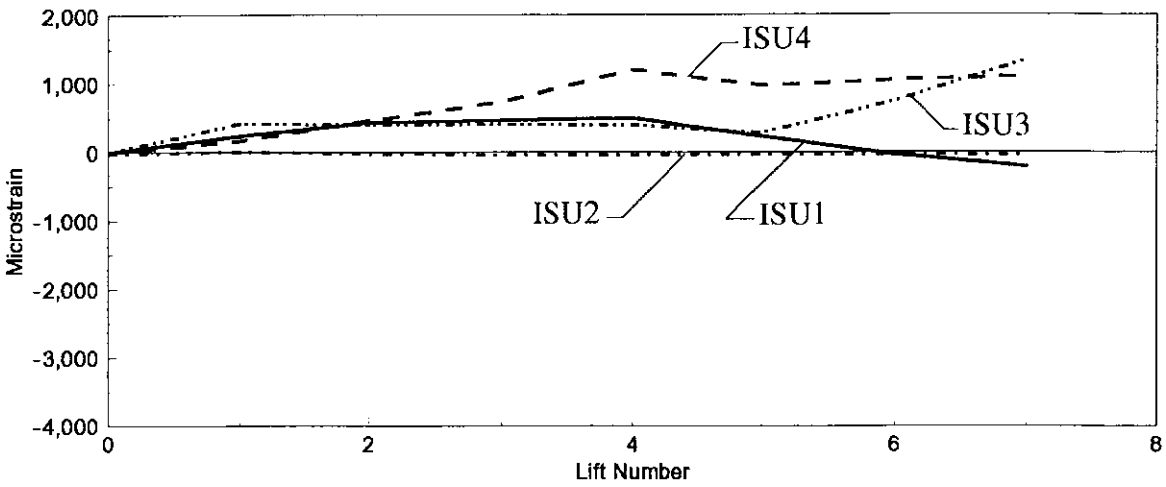


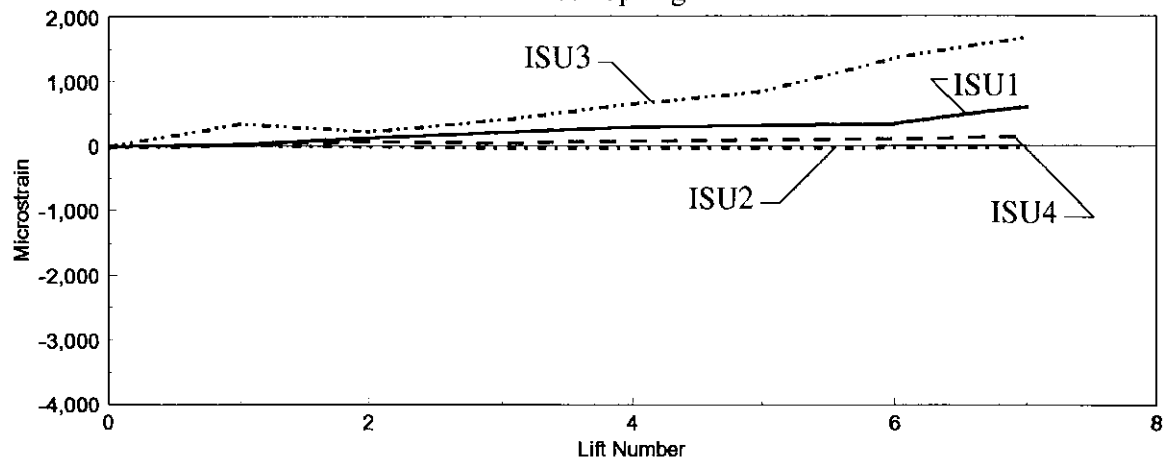
Figure 4.26. Changes in inside diameter at Section 6 during backfilling.



a. Crown

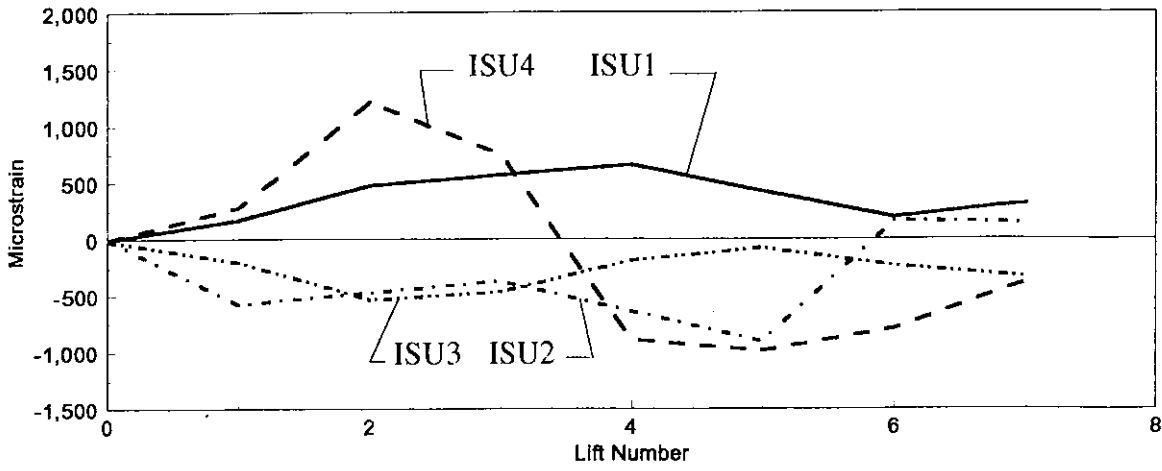


b. Springline

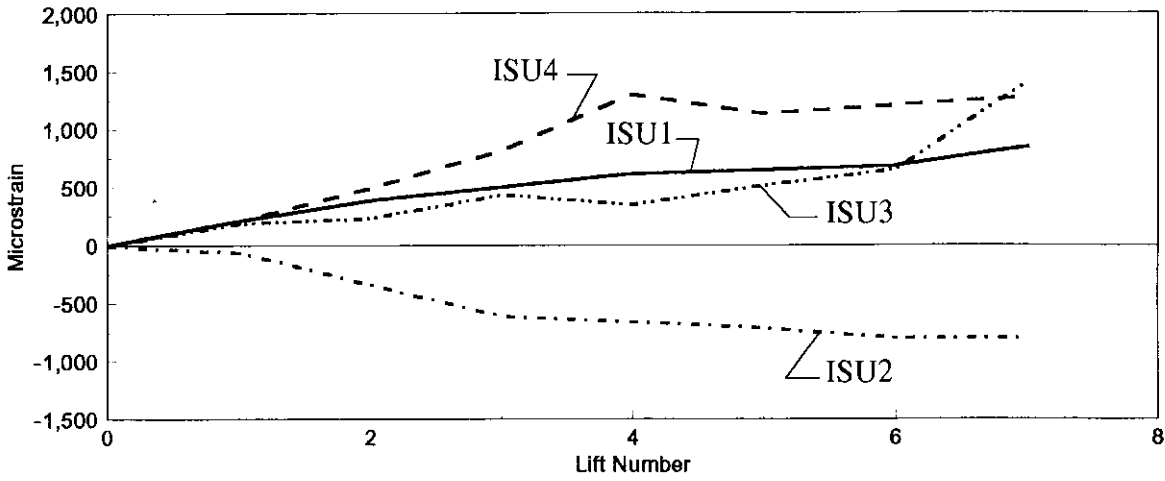


c. Invert

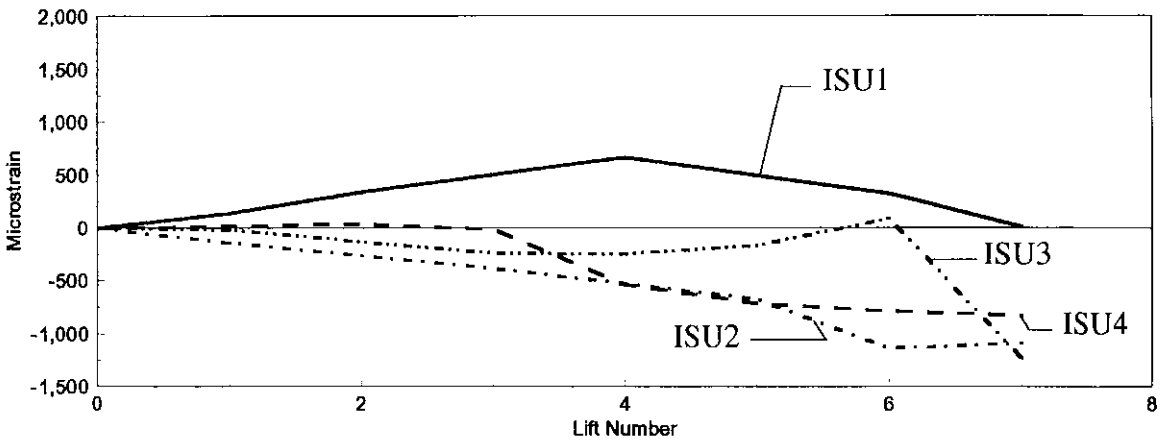
Figure 4.27. Backfilling longitudinal strain at Section 2.



a. Crown

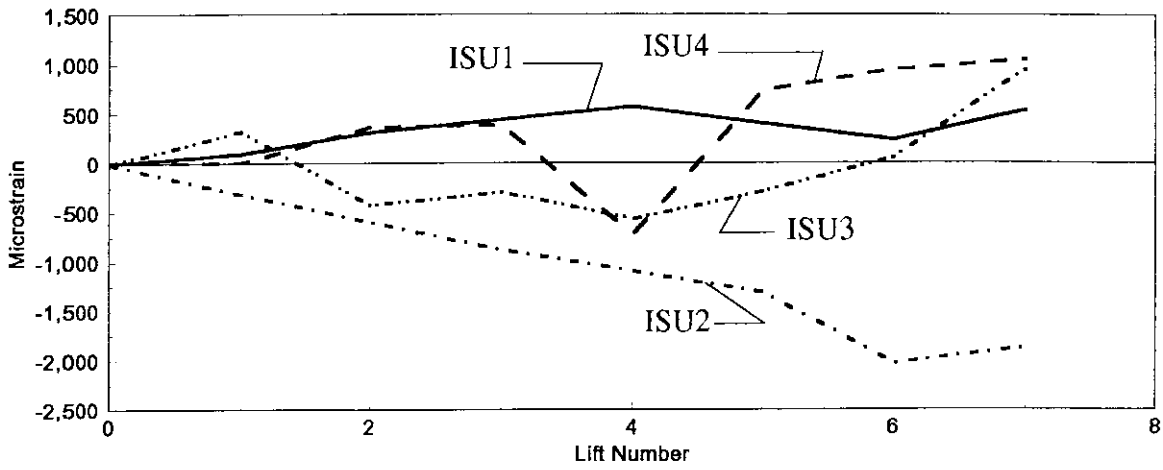


b. Springline

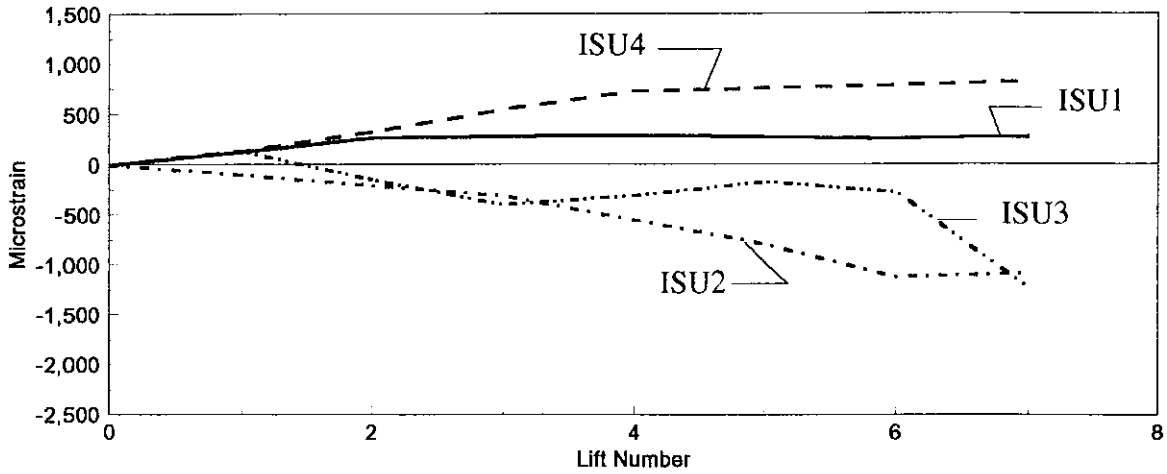


c. Invert

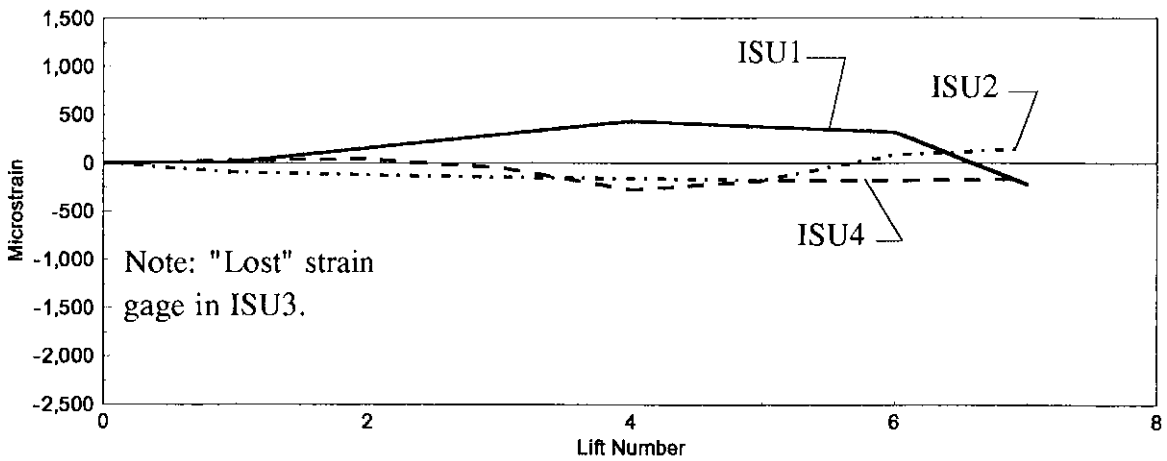
Figure 4.28. Backfilling longitudinal strain at Section 4.



a. Crown



b. Springline



c. Invert

Figure 4.29. Backfilling longitudinal strain at Section 6.

The effects of temperature on the deformation of HDPE pipes during installation is not widely known. Obviously, the crown of the pipe is considerably hotter than the remaining portions of the pipe due to radiation from the sun. At elevated temperatures, there is a reduction in strength of HDPE pipe, thus if the temperature varies around the circumference of a given HDPE pipe, the strength also varies. These effects are believed to have an influence on the circumferential strains (and to a lesser degree on the longitudinal strains) that occur in HDPE pipe during installation (i.e., the backfilling operations). Further investigation (determination of circumferential temperature-magnitude and distribution in HDPE pipe in sunlight, behavior of HDPE pipe to loading when certain portions of the pipe are at elevated temperatures, etc.) need to be undertaken to determine the significance of the previously described temperature-installation phenomena. Once the HDPE is installed, there should be minimal temperature variation in the pipe as the surrounding soil will act as insulation.

In general the circumferential strains during backfilling are larger than the longitudinal strains during backfilling. This indicates that circumferential strength is of primary importance during backfilling.

4.3.3 Applied Load Data

The loads applied during the loading portion of the field tests simulated the loads imposed by highway vehicles. Load was applied to a 1-sq ft area to simulate the size of

the tire contact area from tandem wheels. Load was applied with a hydraulic cylinder; a photograph of the hydraulic cylinder and load cell used to measure the applied load are shown in Fig.4.30.

Six load tests were performed on each of the four buried HDPE pipe specimens two at sections 5-ft from each end and two at the center of each pipe length. At each section there was a service load test (i.e. loading was limited so that only 1% deflection occurred) and an ultimate load test. Only service level strains and deflections resulting from load applied at the center of each specimen are presented in this report because of possible boundary effects when load is applied at the sections 5-ft from the pipe ends. However, ultimate loads are presented for all load points to show ultimate strengths.

4.3.4 Applied Load Results

4.3.4.1 Load at Section 4

Data from the applied load tests with the load section 4 (see Fig. 3.12) are presented in this section. Figures 4.31 through 4.37 are graphs of the longitudinal strain versus load for service tests for the specimens. Recall that Section 1 is at the north end, Section 7 is at the south end, and Section 4 is directly under the load point (see Fig. 3.12).

Each graph shows the strains at three locations on the pipe cross section (crown, springline, and invert) similar to the data shown in the previous section. The strains directly under the load point are largest at the crown. The smaller strains at the invert can

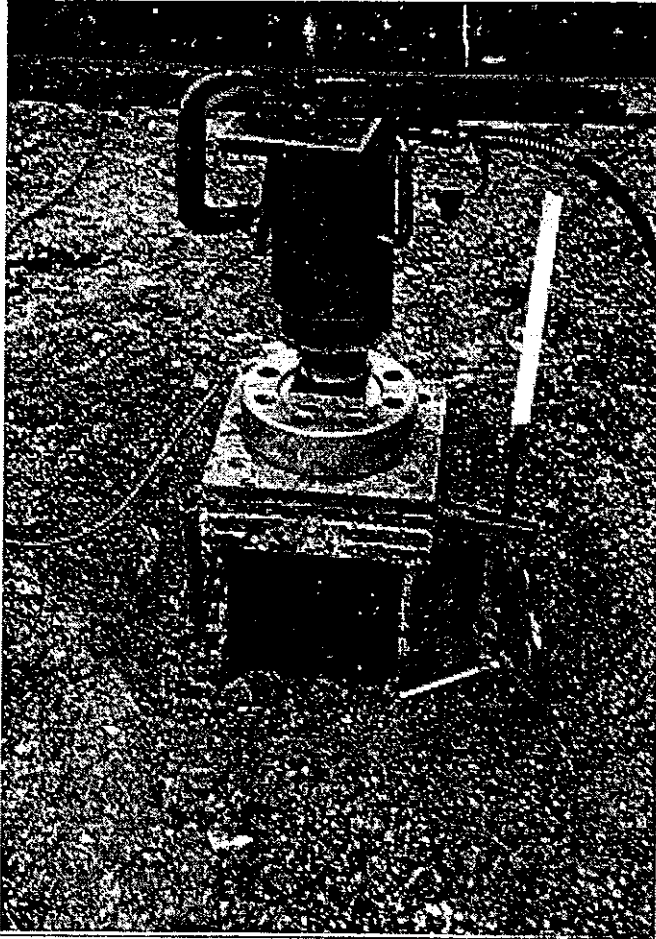
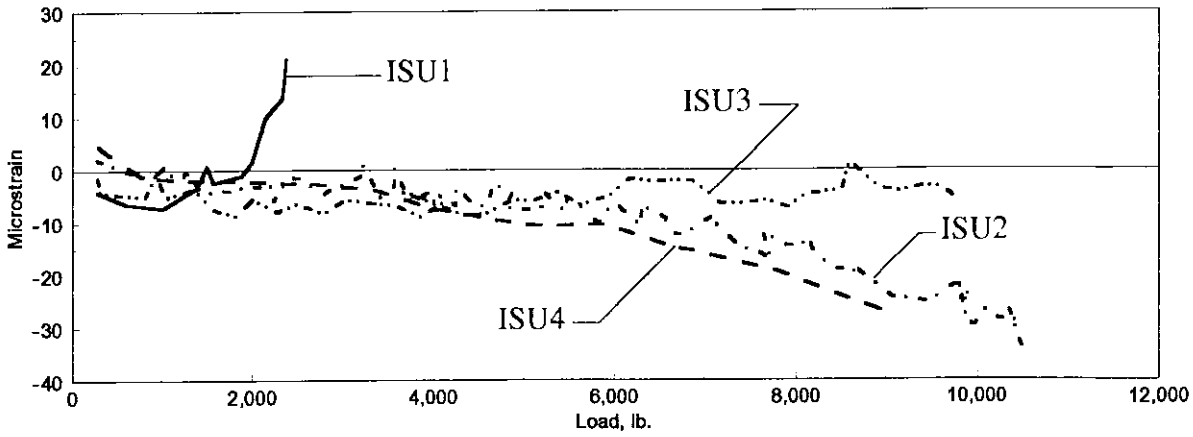
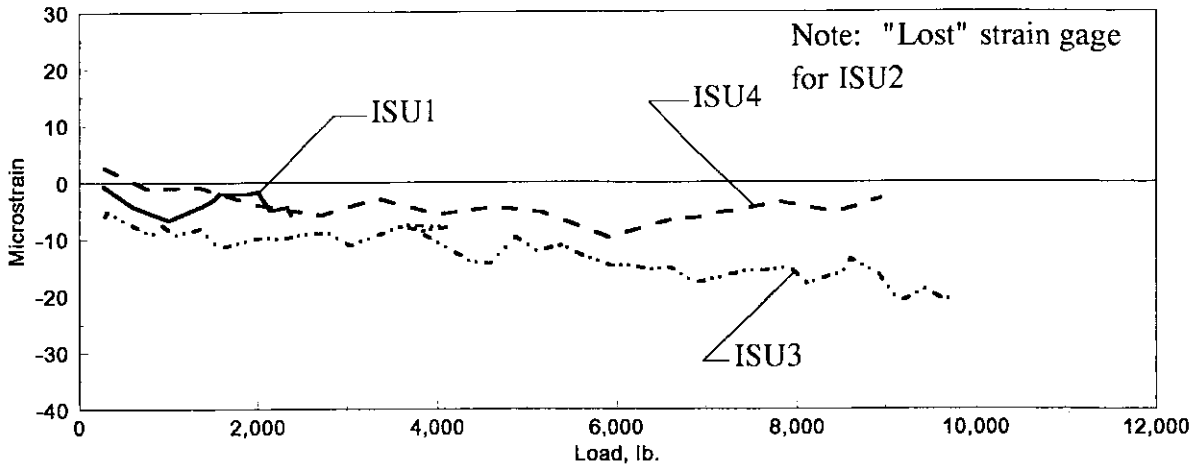


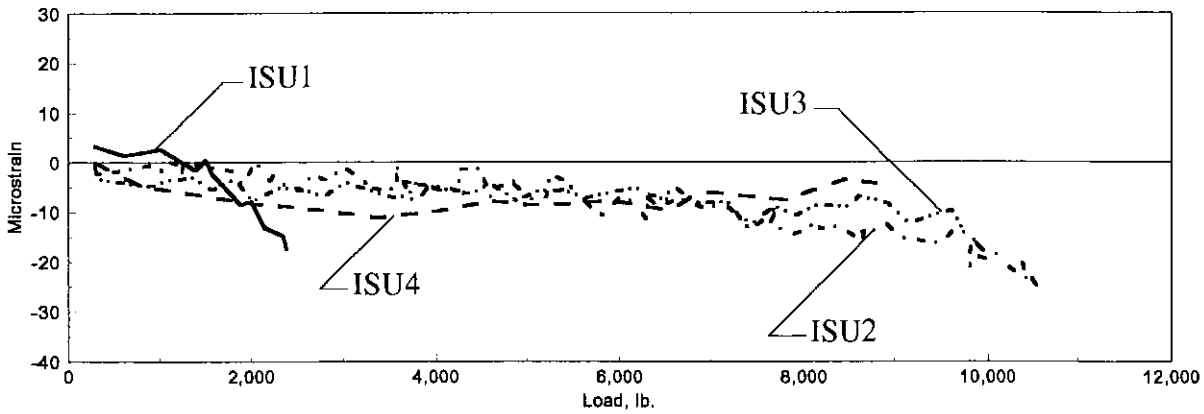
Figure 4.30. Hydraulic cylinder and load cell used during in situ pipe tests.



a. Crown

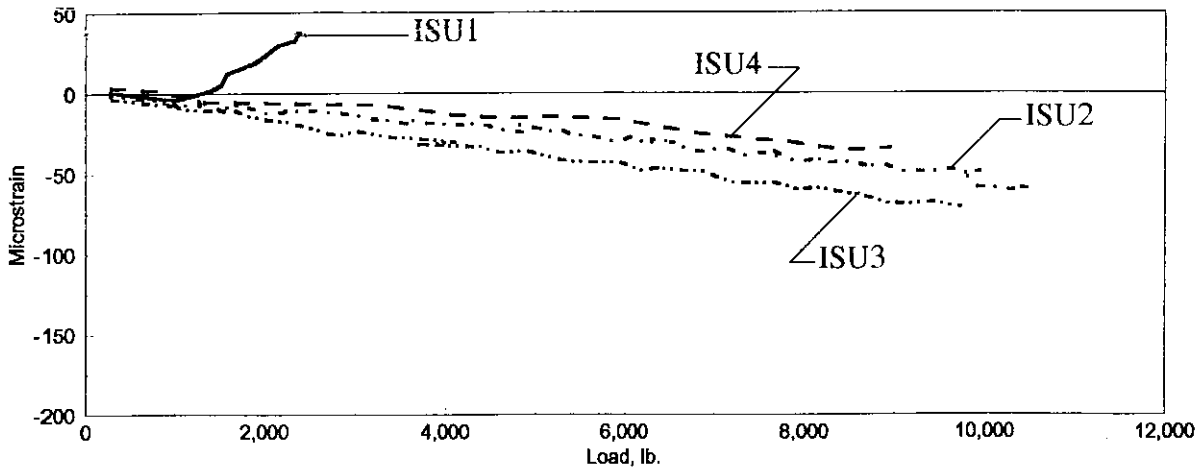


b. Springline

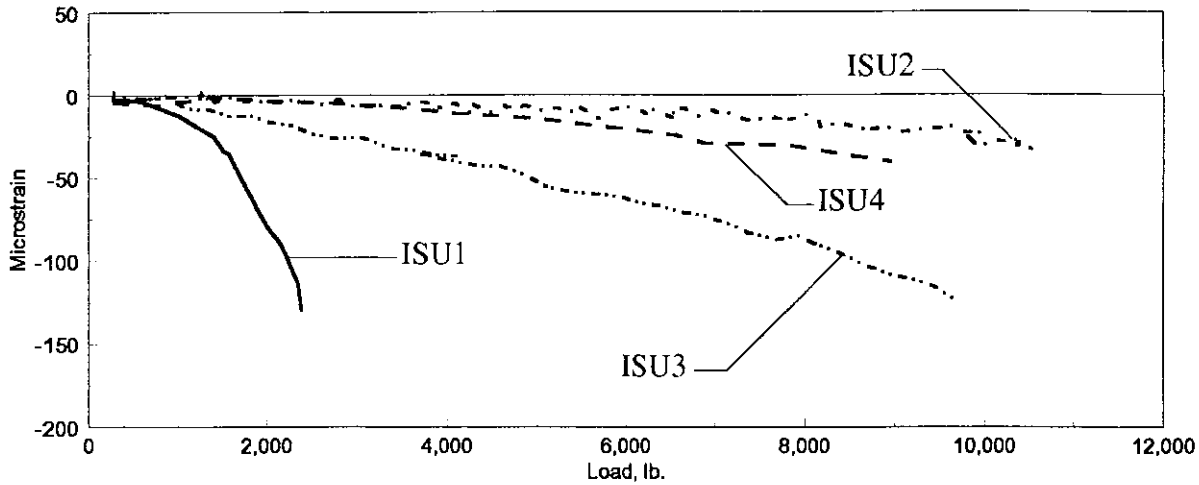


c. Invert

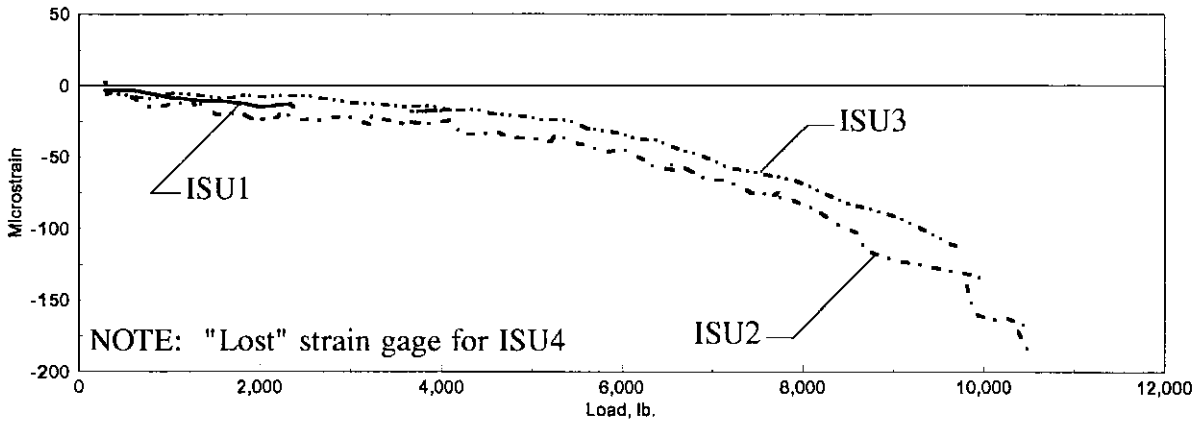
Figure 4.31. Longitudinal strain at Section 1: service load test; load at center.



a. Crown

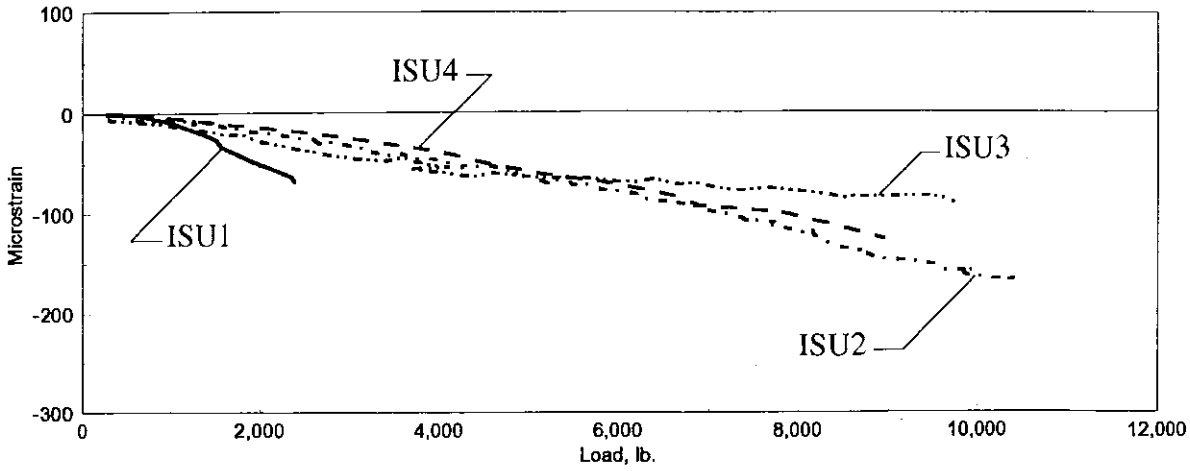


b. Springline

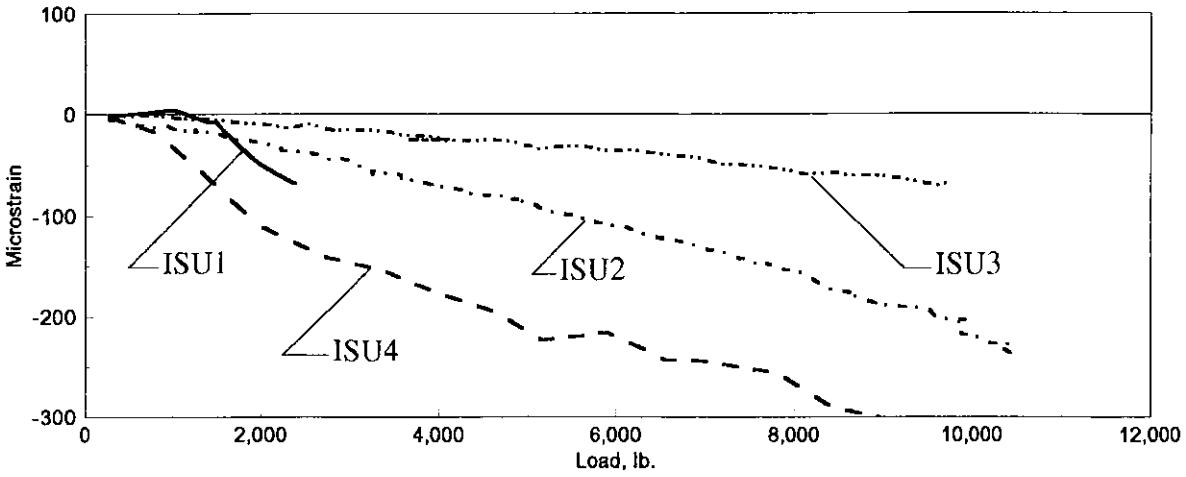


c. Invert

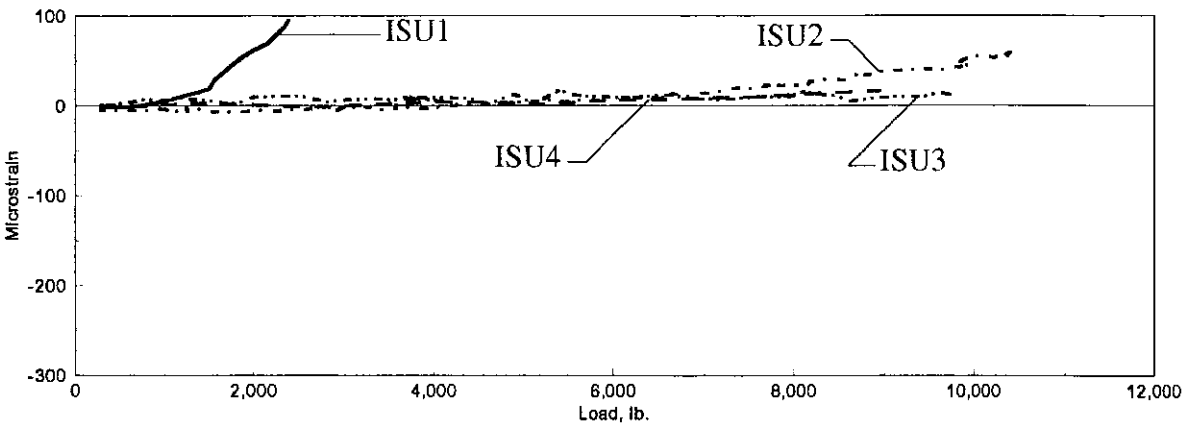
Figure 4.32. Longitudinal strain at Section 2: service load test; load at center.



a. Crown

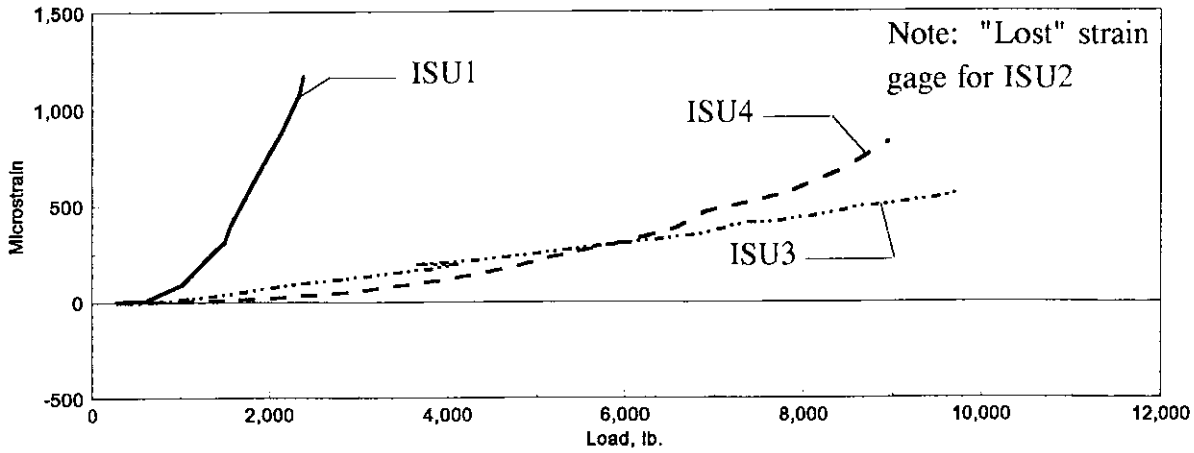


b. Springline

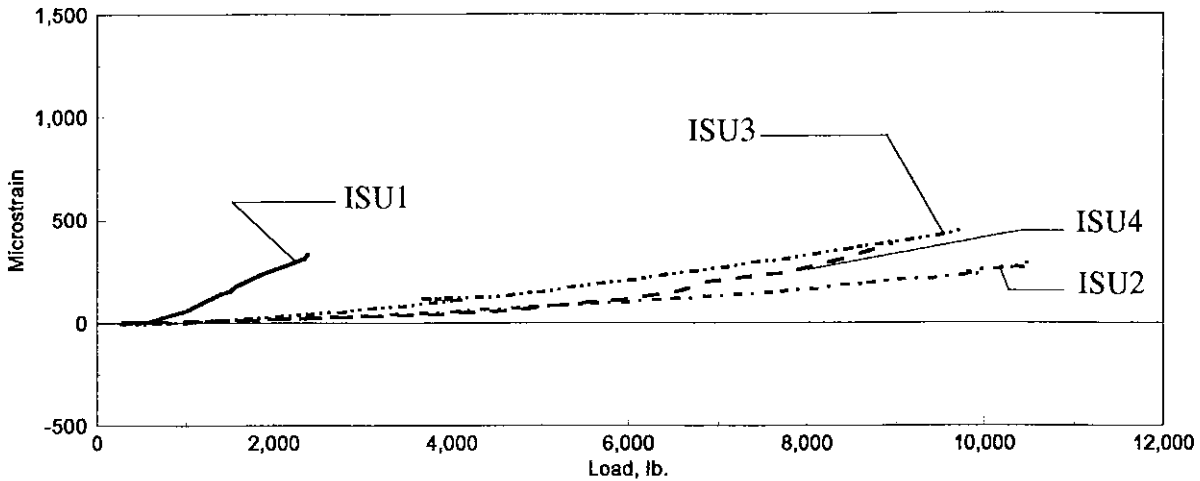


c. Invert

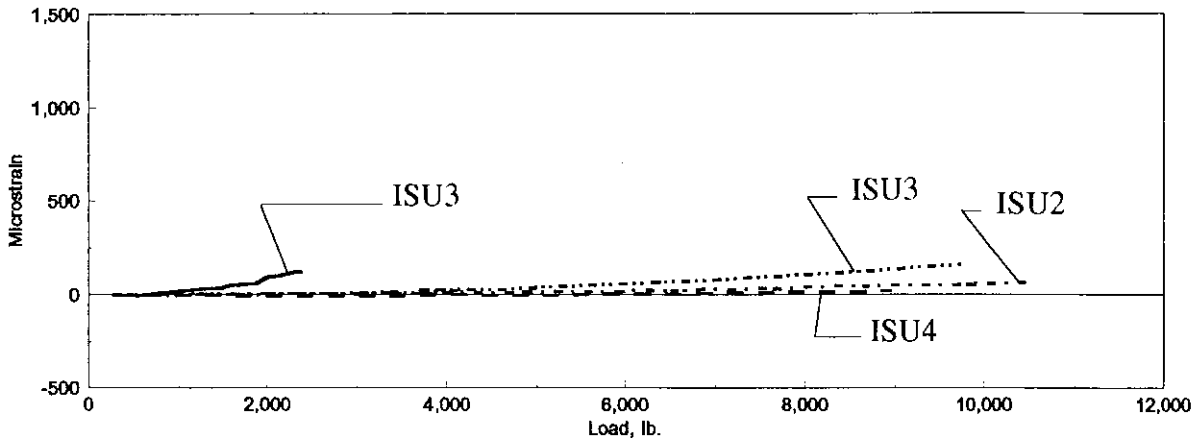
Figure 4.33. Longitudinal strain at Section 3: service load test; load at center.



a. Crown

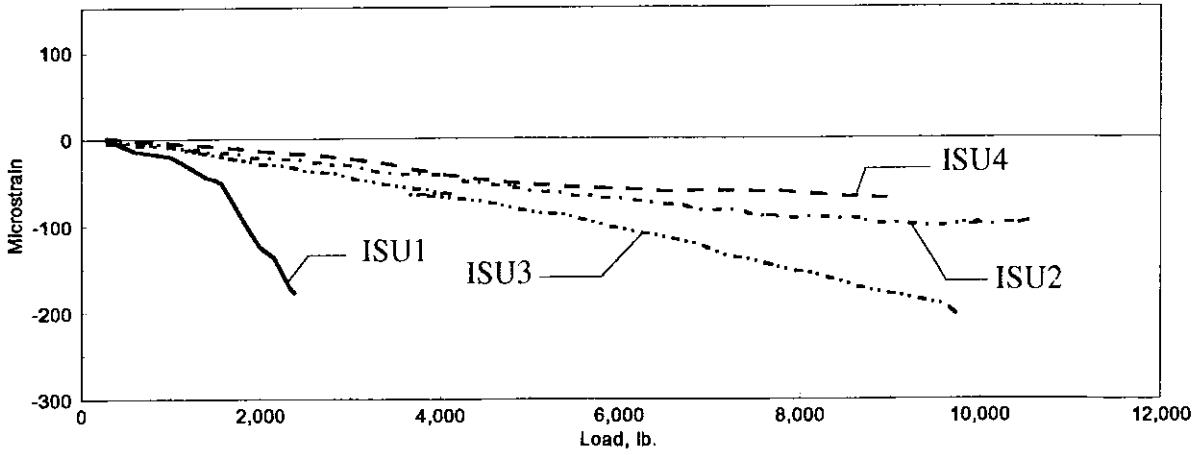


b. Sprineline

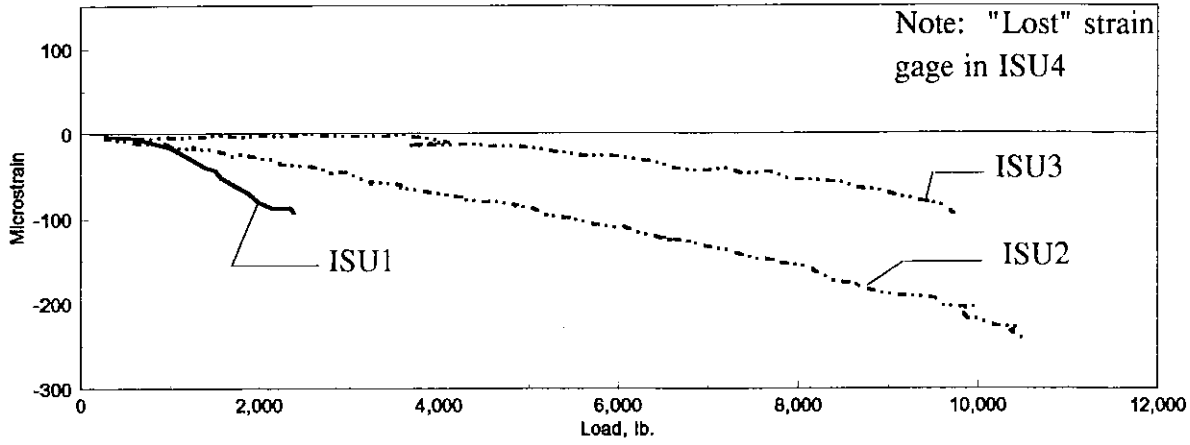


c. Invert

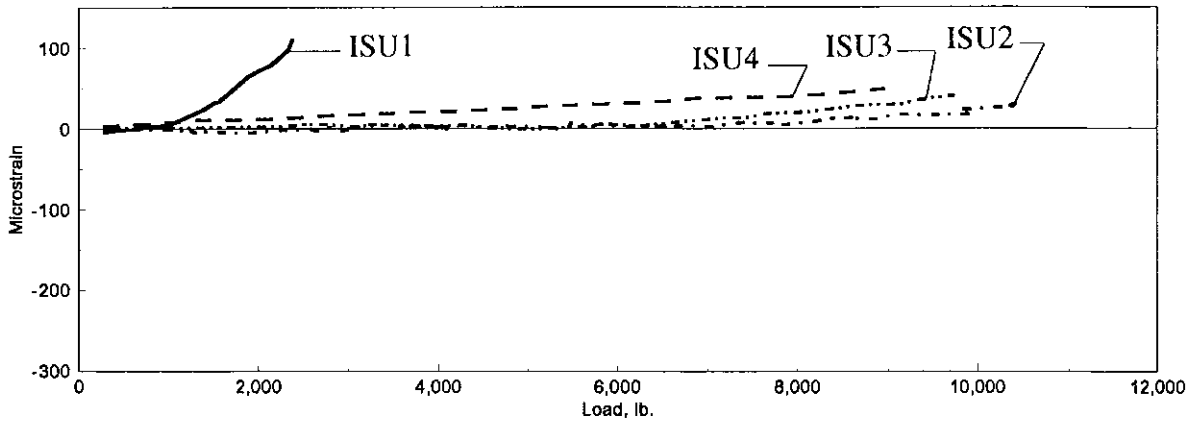
Figure 4.34. Longitudinal strain at Section 4: service load test; load at center.



a. Crown

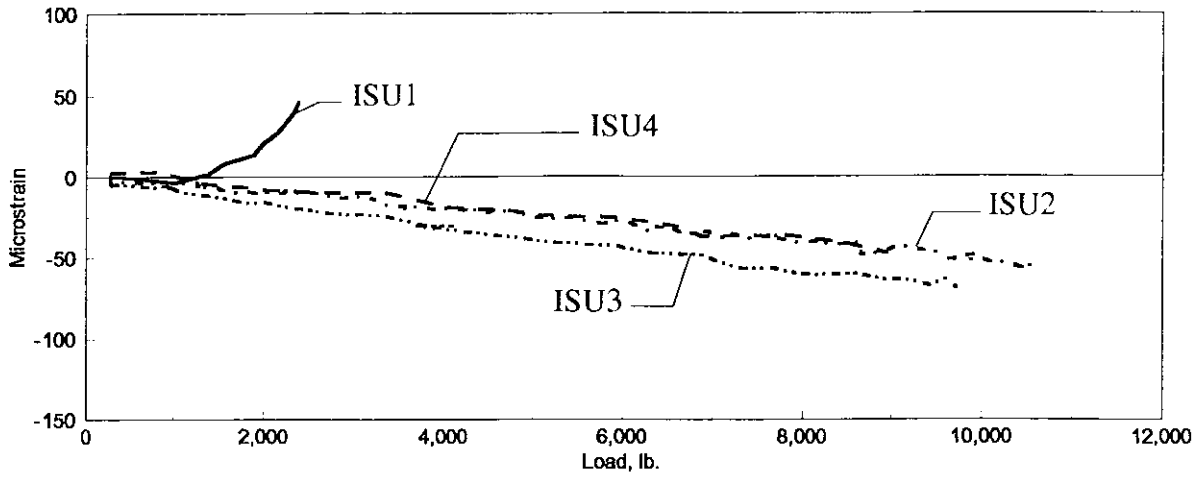


b. Sprineline

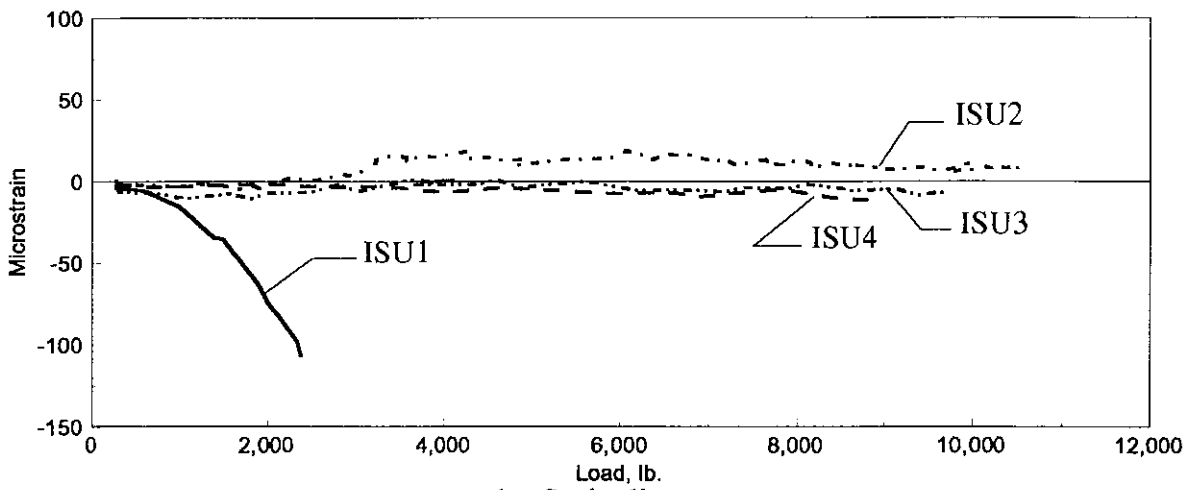


c. Invert

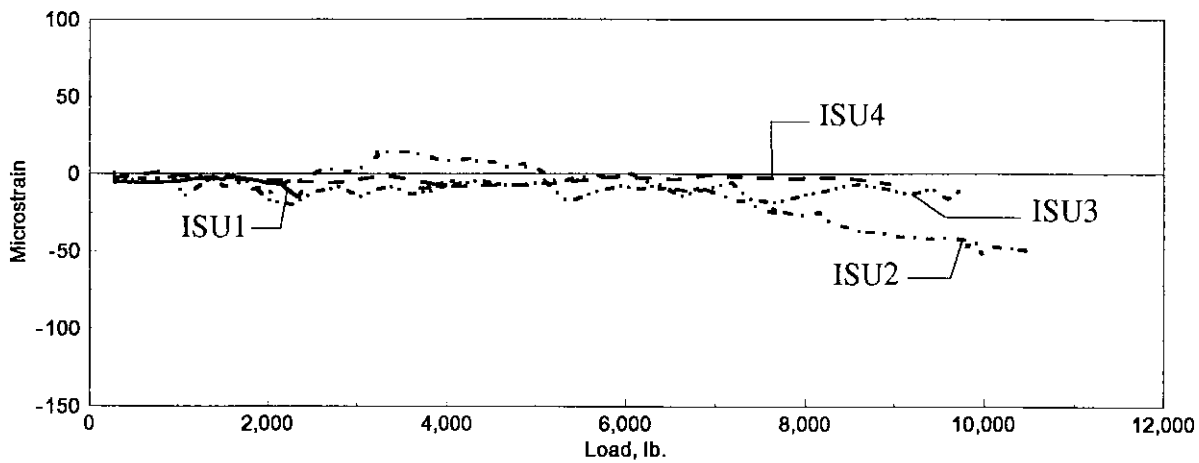
Figure 4.35. Longitudinal strain at Section 5: service load test; load at center.



a. Crown

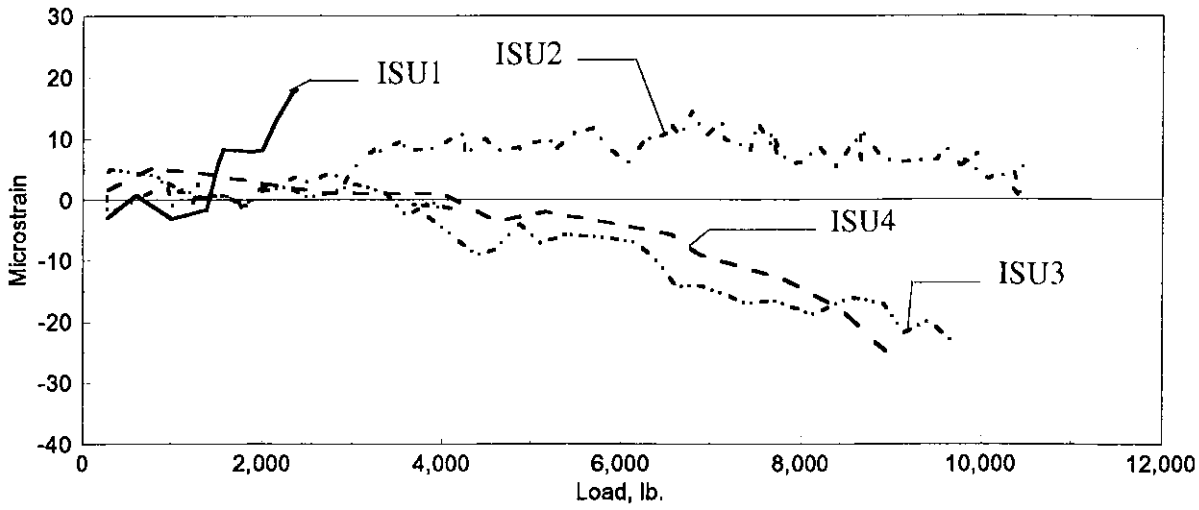


b. Springline

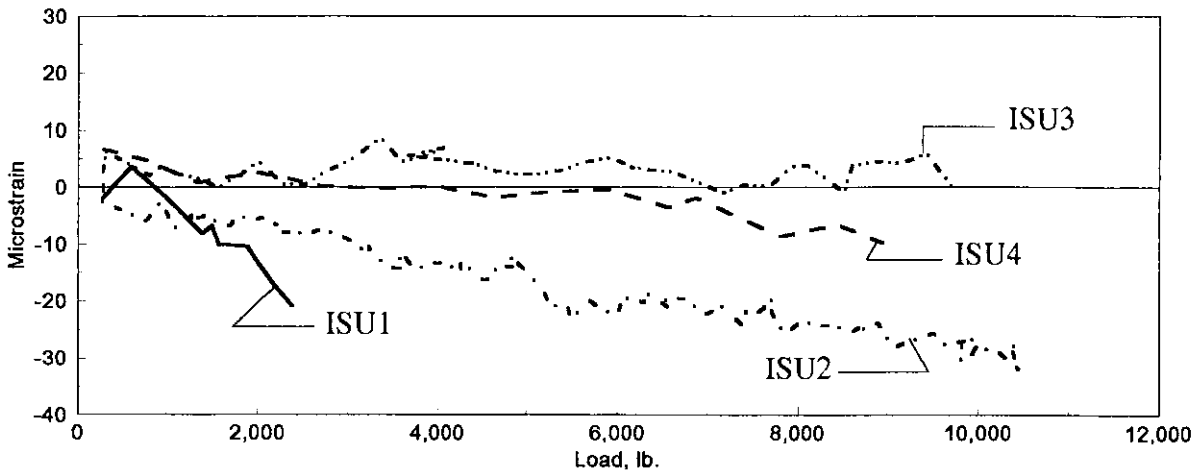


c. Invert

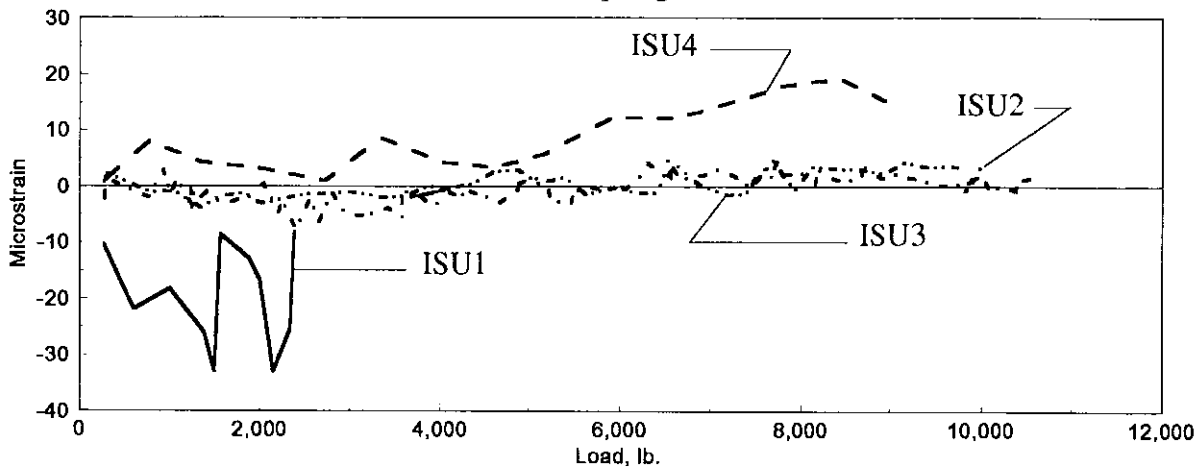
Figure 4.36. Longitudinal strain at Section 6: service load test; load at center.



a. Crown



b. Springline



c. Invert

Figure 4.37. Longitudinal strain at Section 7: service load test; load at center.

be attributed to the bottom of the pipe being fully supported by the foundation or cradle soil, which restrains the pipe from bending longitudinally. The strains decrease rapidly at the sections farther away from the load point. At Sections 3 and 5 (Figs. 4.33 and 4.35) the crown and springline strains show a change in sign from the center section (Fig. 4.34). However, strains on the invert of the pipe show no reversal of sign at either Sections 3 or 5 due to the continuous supporting foundation or cradle. In general, strains at Sections 3 and 5, which are symmetrical about the longitudinal centerline, differ by less than 5%, indicating symmetry about the center of the specimen. Sections 2 and 6 show significantly lower strains at the crown and invert than do the same positions at Sections 3, 4, and 5. This indicates that concentrated loads have little effect on the crown or invert at a distance of 5-ft from the load point. However, strains at the springline cannot be generalized for all the specimens tested. That generalization is valid for ISU2, ISU3, and ISU4 which had some type of compacted backfill. However in the case of ISU1, which had the "dumped" backfill, there was actually an increase in springline strain magnitudes when going from Sections 3 and 5 to Sections 2 and 4 respectively. This indicates that the effects of load were dissipated over a larger distance with decreasing soil envelope quality. Loading at Section 4 (centerline) had no noticeable effect at Sections 1 and 7, which were 7 1/2-ft from the load point.

A comparison of the longitudinal strains at Section 4 for a load of 2000 lb reveals that the strain at the springline in ISU1 is approximately 7 times larger than the strains in

ISU2, ISU3, and ISU4 which are all extremely small. This suggests that the effectiveness of the backfill at restraining the in situ pipe under live load is not so much dependent on the type of backfill material as the level of compaction of the material.

As was previously noted the magnitude of strain decreases rapidly with increasing distance from the load point. This is clearly shown in Fig. 4.38 which shows the strain at 1% deflection during the service tests. Also shown on this figure is the theoretical vertical stress distribution predicted by the Boussineq theory of stresses in a "homogeneous, elastic, and isotropic medium" (Das 1994) caused by a point load. As is clearly evident the curves are very similar in shape showing that the strain response is a direct function of distance from load. Shown in Fig. 4.39 is the theoretical horizontal stress distribution at the springline for various values of Poisson's ratio. The figure indicates that soils with lower Poisson's ratio distribute the load over a greater distance. Das (1994) indicates that looser soils generally have lower values of Poisson's ratio. This, coupled with the fact that ISU1 had a much lower density than ISU2, ISU3, and ISU4, indicates that the response would be dissipated over a greater distance in ISU1. This is clearly shown in Fig. 4.39.

Strain modulus is defined as the slope of the linear portion of the load-strain curve and indicates the strain rate during loading. Figures 4.40 through 4.42 show the variation in longitudinal strain modulus versus the distance from applied load. The data presented in these figures show several things: (1) symmetrical behavior of the specimen with respect to the specimen centerline, (2) the relative magnitudes of the rate of change of longitudinal

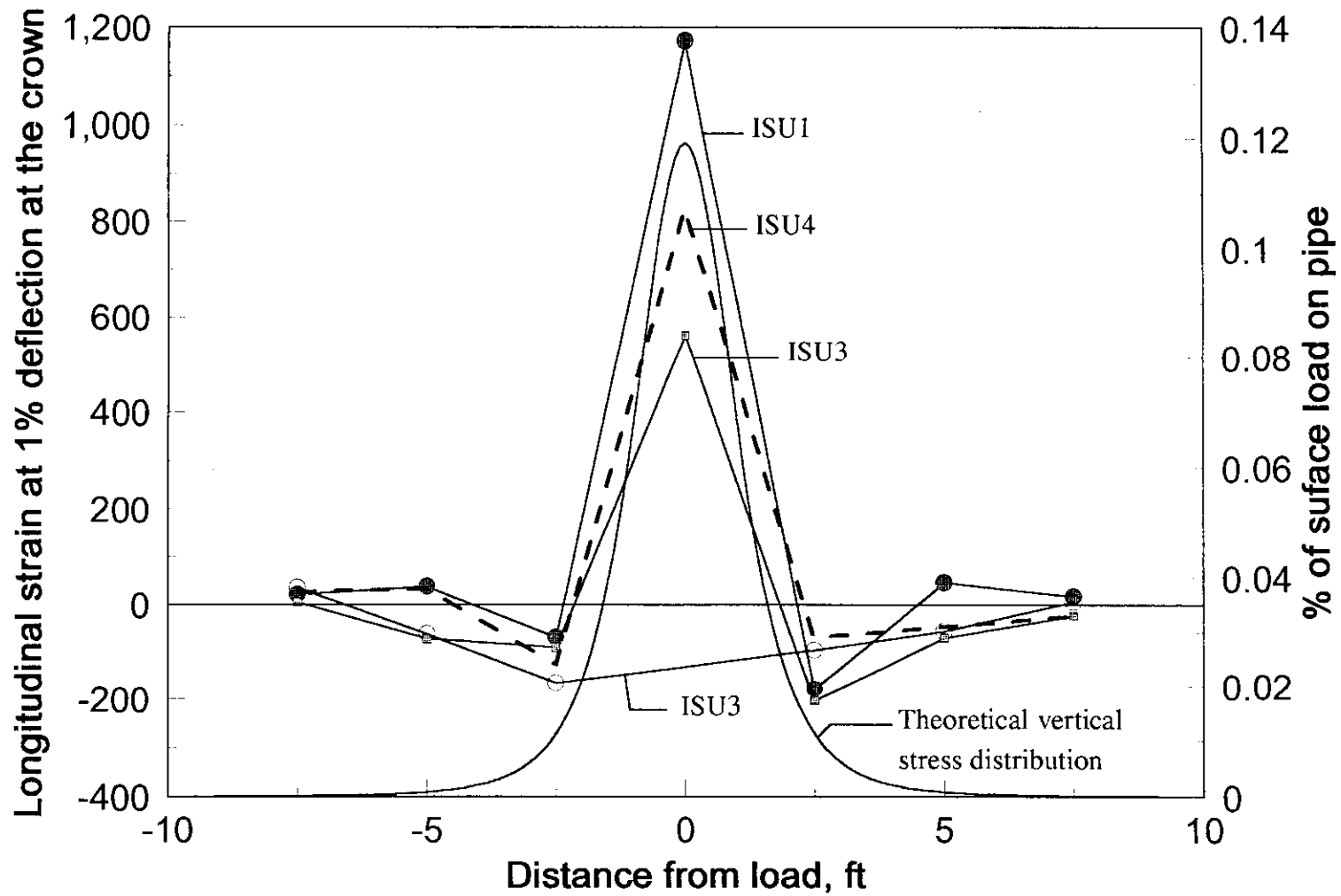


Figure 4.38. Comparison of theoretical vertical stress distribution and experimental strain at the crown.

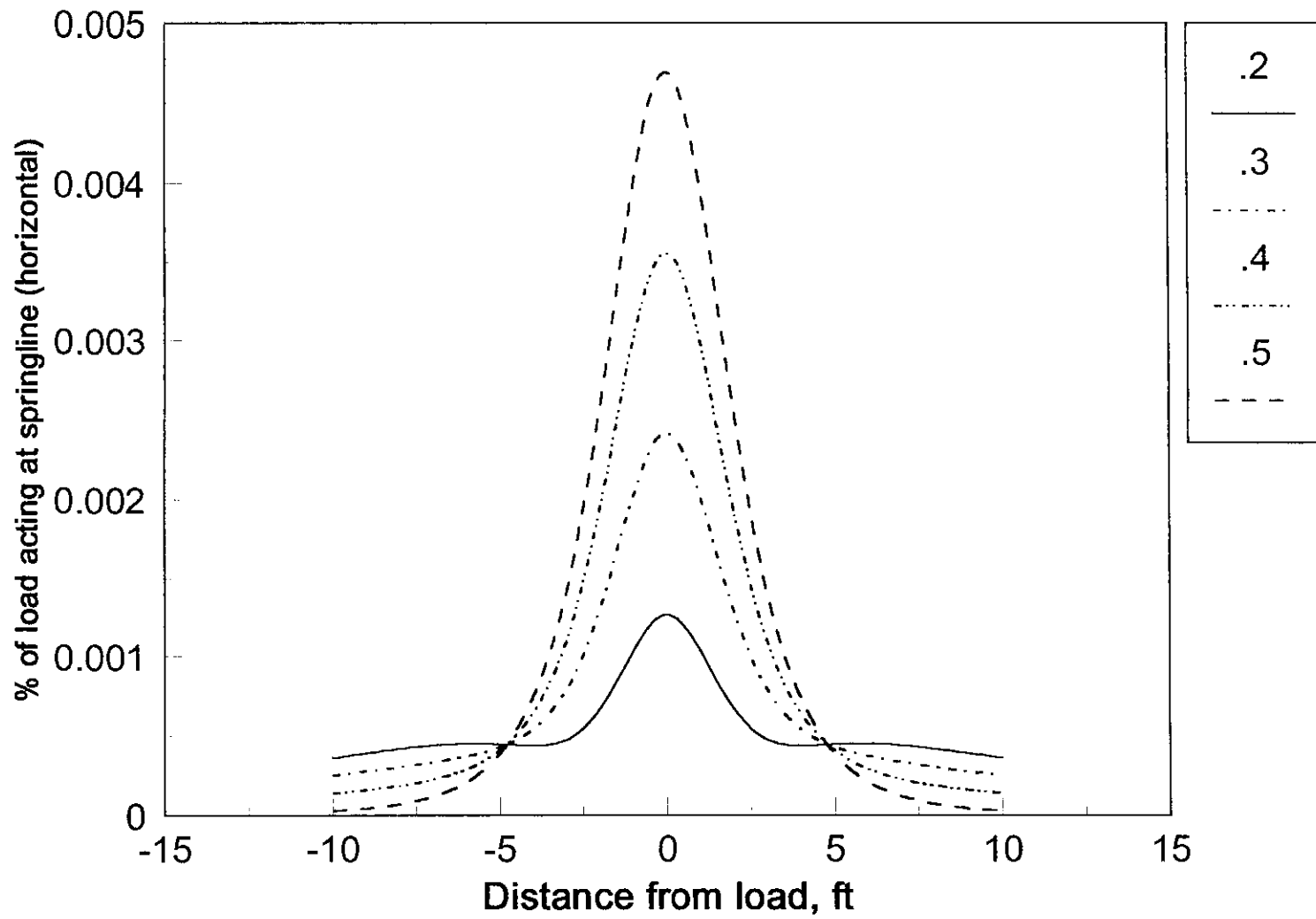


Figure 4.39. Theoretical horizontal stress distribution with varying poisson's ratio.

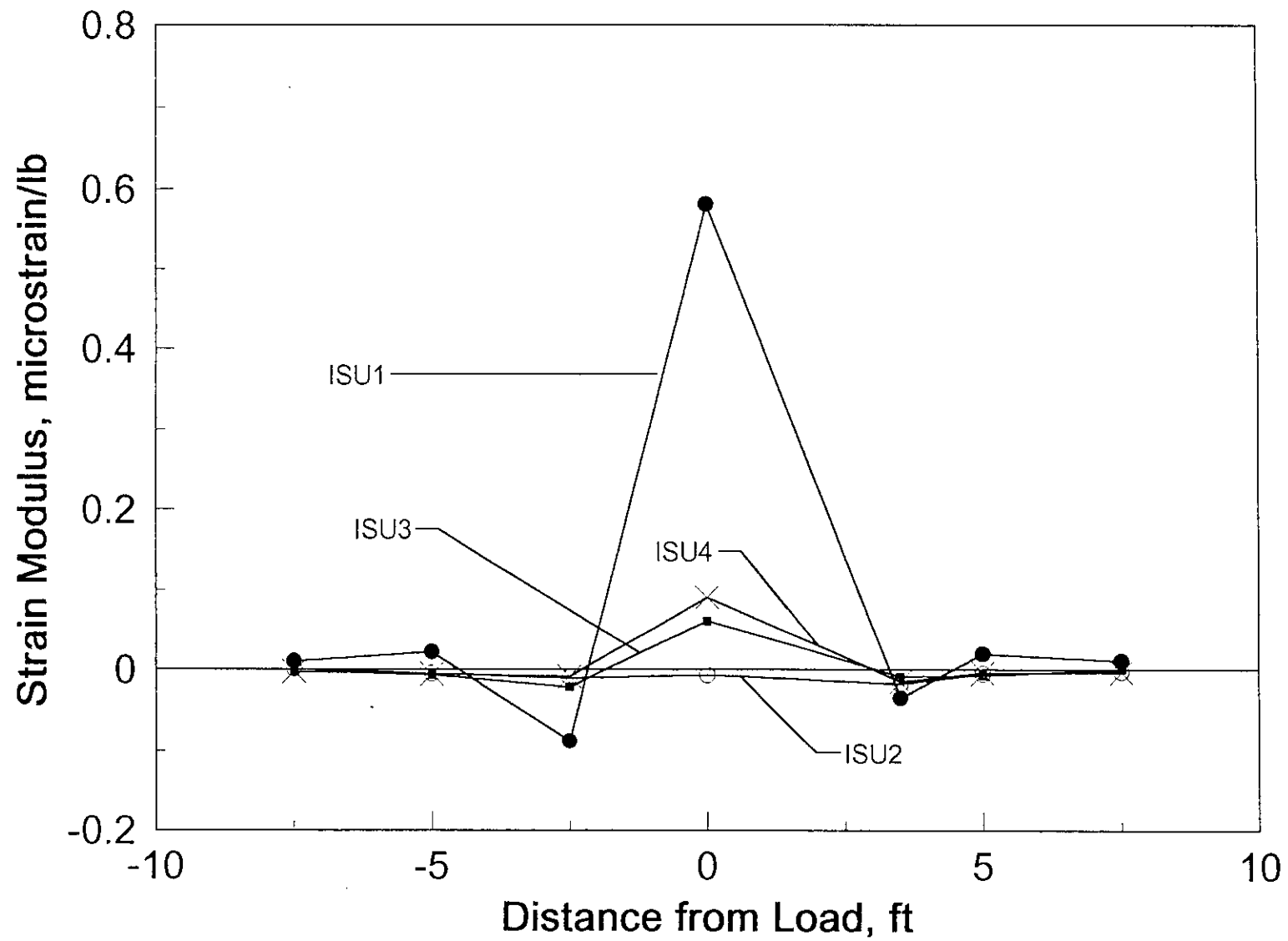


Figure 4.40. Longitudinal strain modulus at the crown versus distance from load.

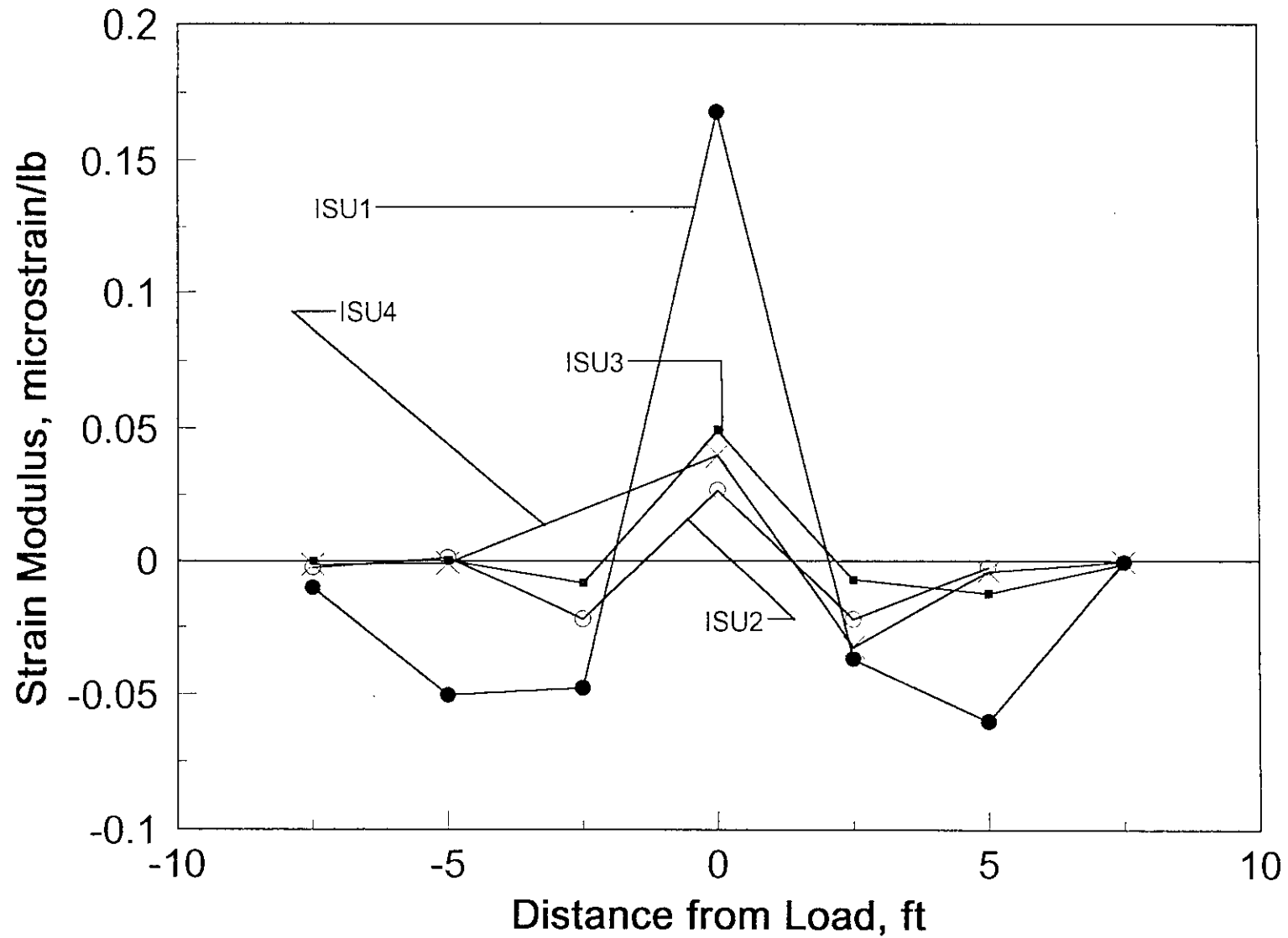


Figure 4.41. Longitudinal strain modulus at the springline versus distance from load.

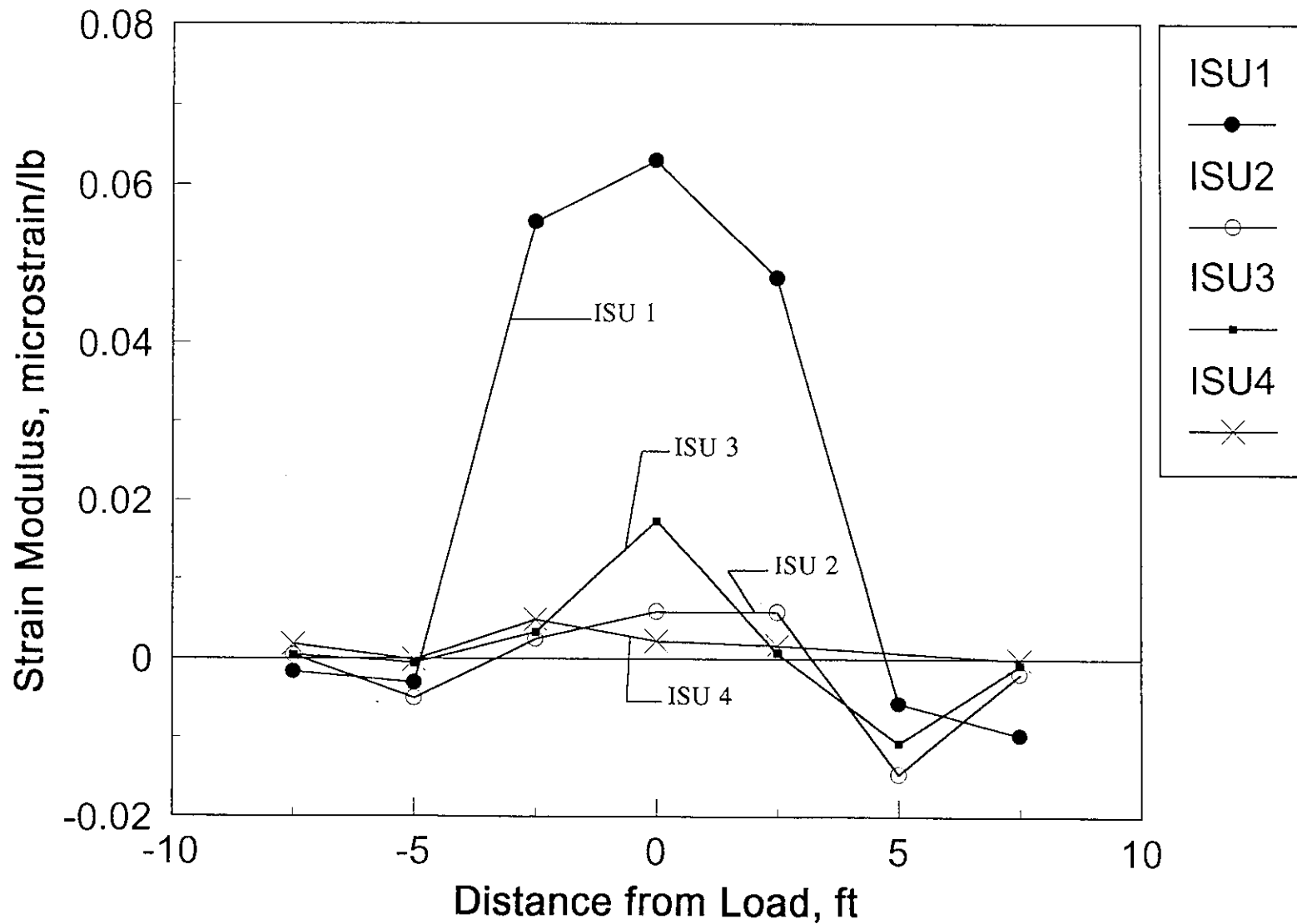
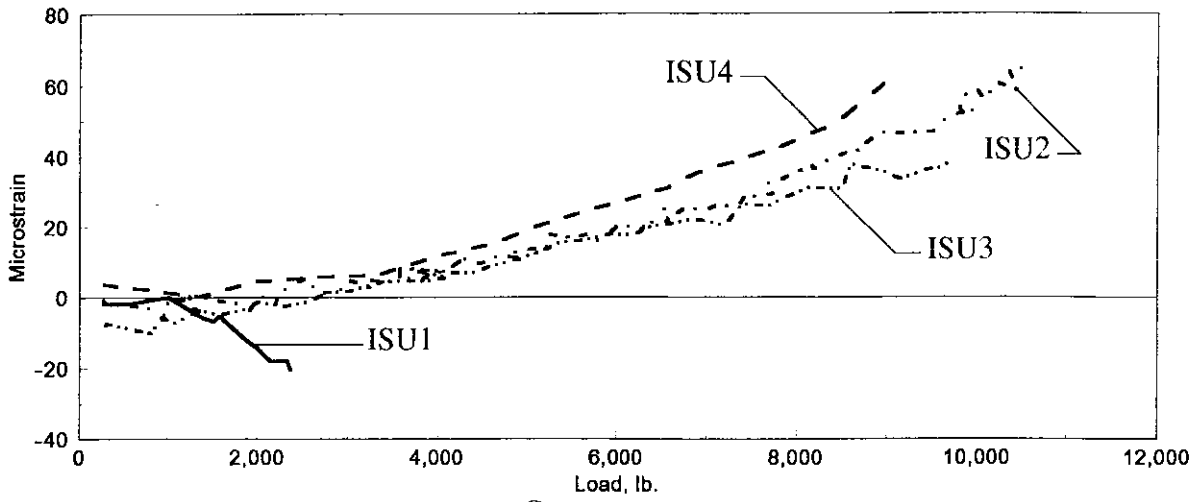


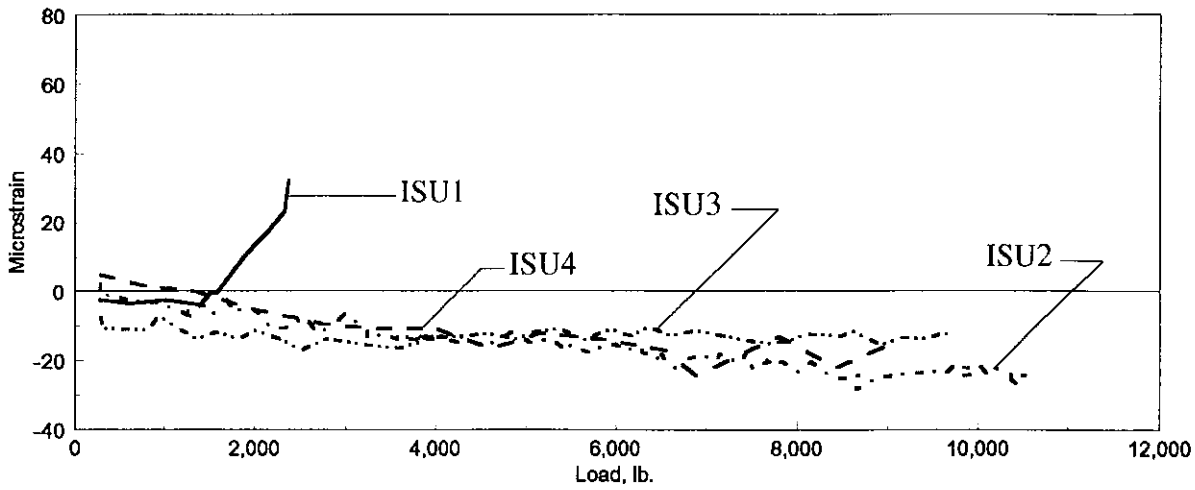
Figure 4.42. Longitudinal strain modulus at the invert versus distance from load.

strain for the different backfill conditions, and (3) the magnitude of strain modulus values at each location for each backfill condition. Negative distances indicate the sections are to the south of the load point whereas positive distances indicate sections to the north of the load point (see Fig. 3.12).

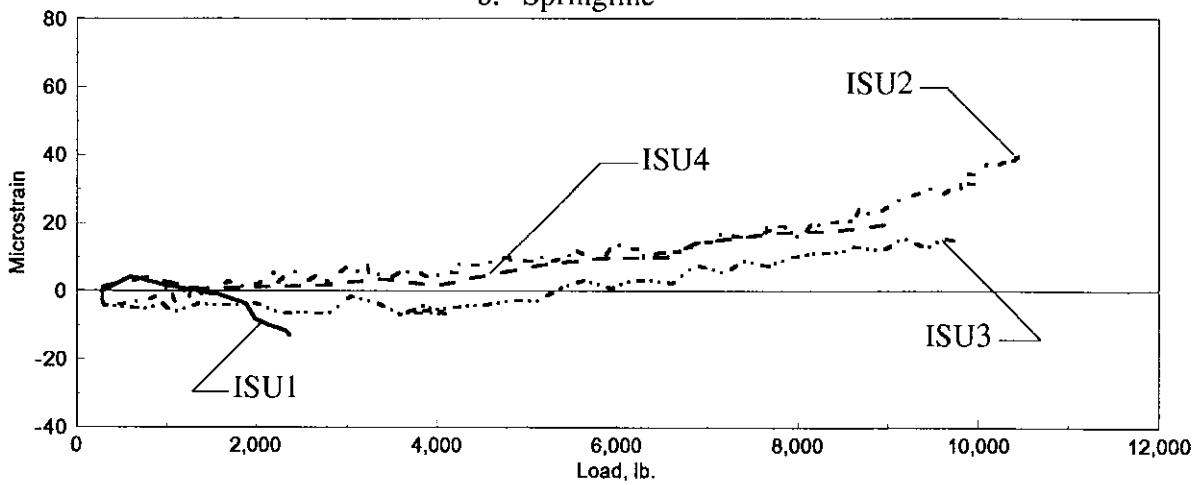
The circumferential strain data collected during the same service tests as described above are shown in Figs. 4.43 through 4.45. Each figure shows three graphs representing the strains at the crown, the springline, and the invert. The section numbers are the same as for longitudinal strains (see Fig. 3.12). At Section 4 (directly under the load), the largest strains occur at the springline. Vertical load on the soil above the pipe is transferred to the pipe, causing significant deformations and strain at the springline. Also of importance is the fact that the circumferential strains at the invert at Section 4 (Fig. 4.44c) are smaller than the strains at the springline or crown in all specimens. The strains at the invert of Sections 2 and 6 are nearly the same magnitude as the strains at the springline. These strains are small because the specimens were all placed on a continuous supporting base that provided significant restraint against bending deformations. The difference in sign of the strains between ISU1 and the other tests is attributed to the lack of compacted fill in the haunch area. This causes the invert to flatten under applied load and induces tension (positive) strains. This change in sign of the strain is not as pronounced at Sections 2 or 4 because the effect of the load is reduced significantly 5 ft from the load point. Circumferential strains at the crown of each specimen at Section 4 generally are



a. Crown

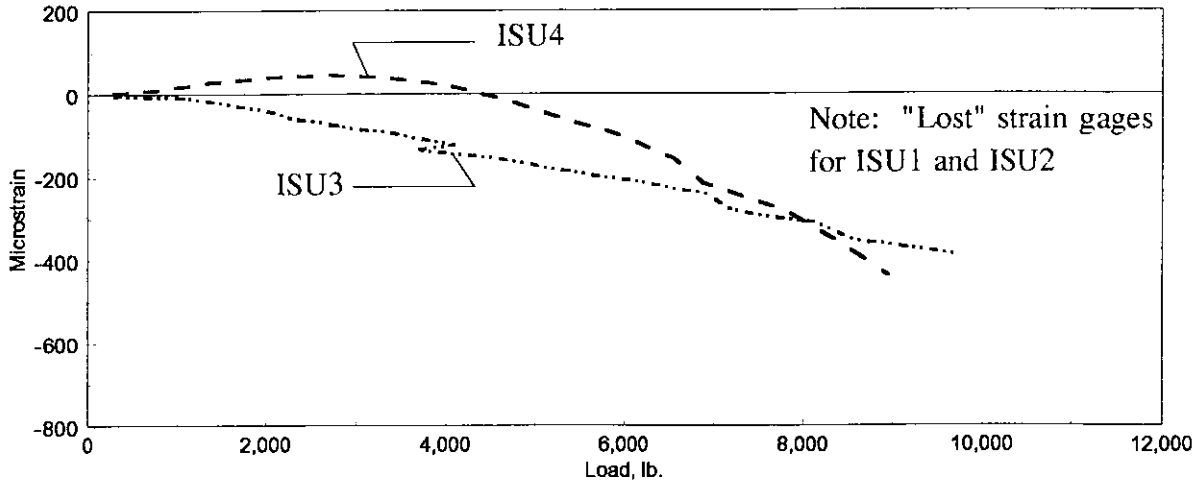


b. Springline

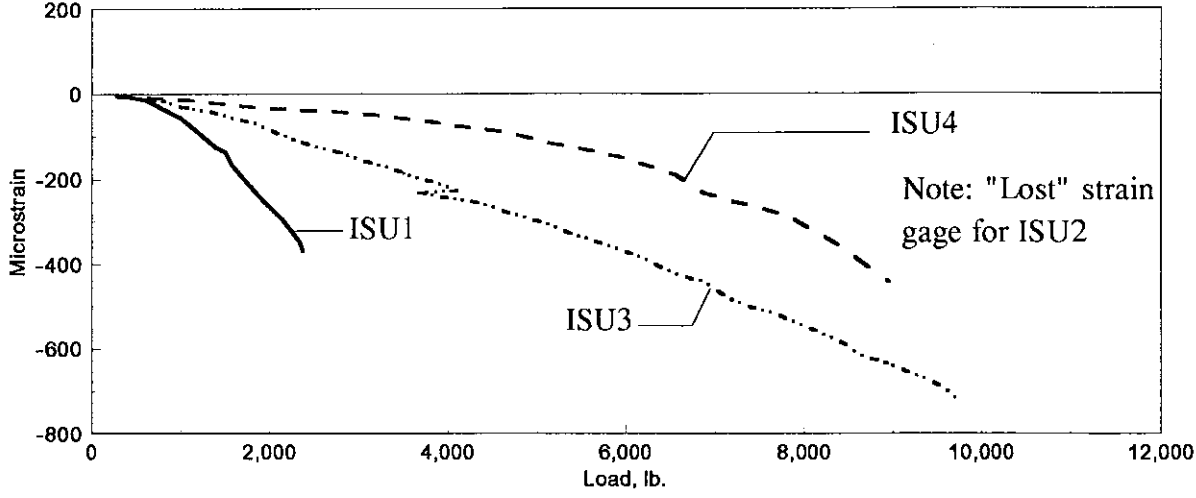


c. Invert

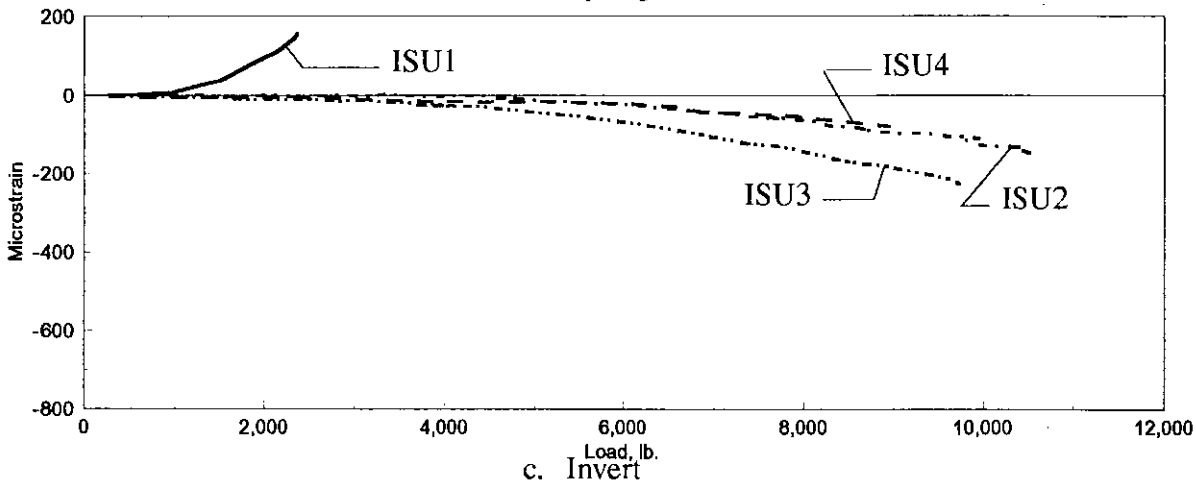
Figure 4.43. Circumferential strain at Section 2: service load test; load at center.



a. Crown

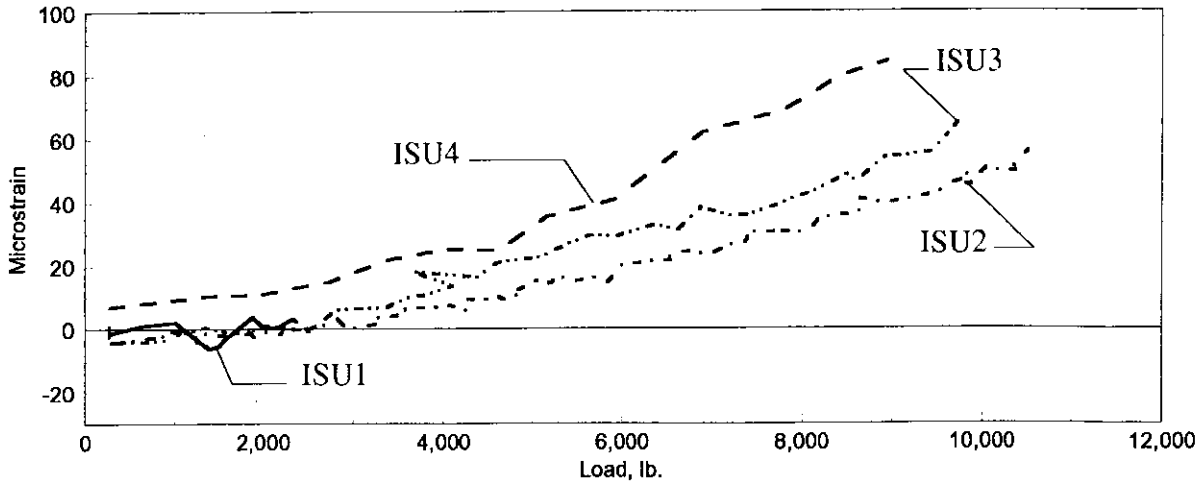


b. Springline

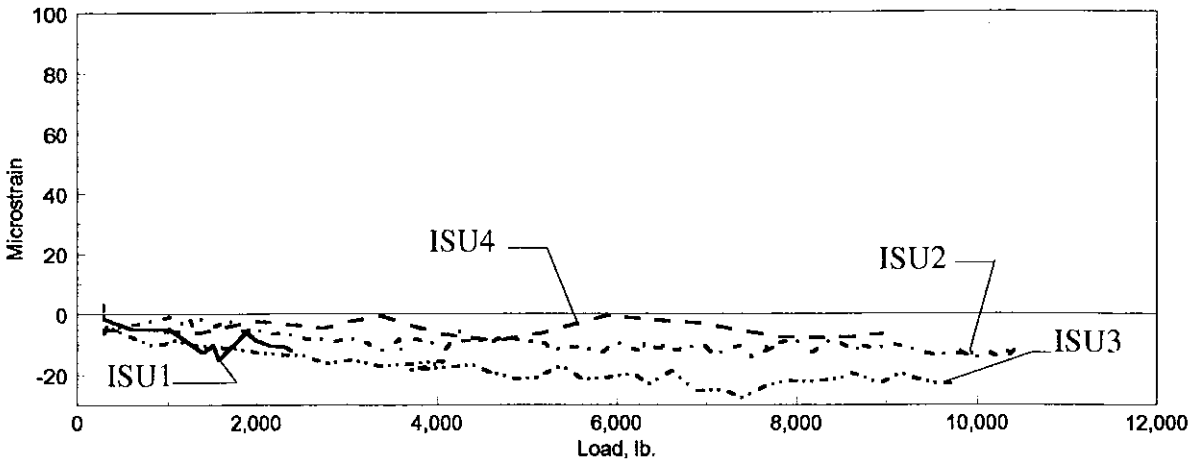


c. Invert

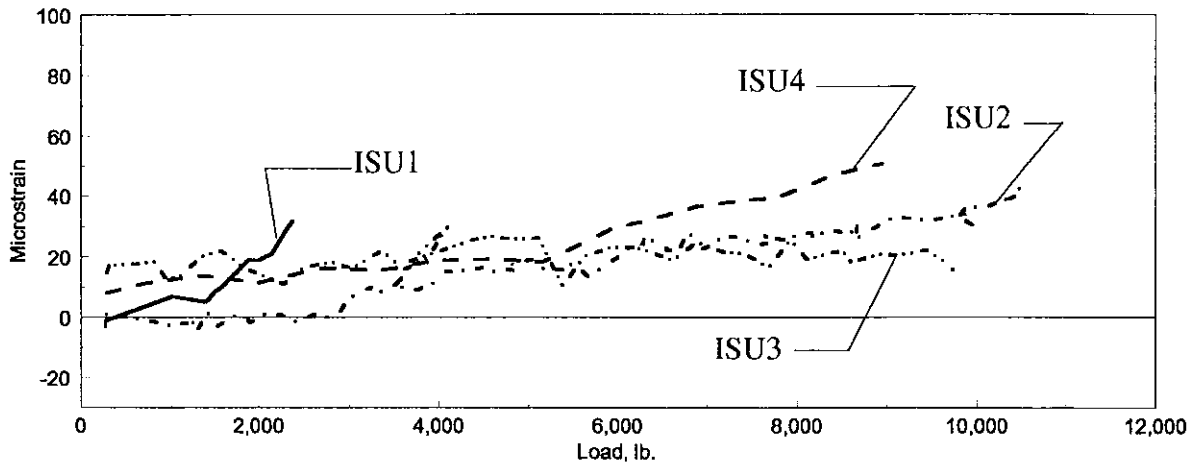
Figure 4.44. Circumferential strain at Section 4: service load test; load at center.



a. Crown



b. Springline



c. Invert

Figure 4.45. Circumferential strain at Section 6: service load test; load at center.

compressive (negative) for service tests but this trend was reversed during ultimate load testing after the pipe had buckled under the applied load.

Circumferential strains at Sections 2 and 6 were largest at the crown and smaller and nearly equal in magnitude at the springline and invert. The concentrated load at the center caused the ends of the pipe to try to deflect upward which caused the crown of the pipe to bear against the cover soil causing the higher strains. The tensile (positive) strains at the crown in ISU2, ISU3, and ISU4 occurred because the pipe was bearing against the soil which tended to flatten the crown, whereas in ISU1 the pipe was more likely to densify the backfill because it was not compacted causing an increased resistance thereby inducing compressive strains in a manner similar to the backfill process of ISU2, ISU3, and ISU4.

Longitudinal strains were generally larger than the circumferential strains at locations where strains were measured in both directions. This suggests that the longitudinal properties of the pipe may be more important in assessing the overall pipe performance in situ when it is subjected to concentrated vehicle loads.

Graphs of the variation of circumferential strain modulus versus distance from load are shown in Figs. 4.46 through 4.48. It should be noted that only three sections were instrumented with circumferential strain gages (see Fig. 3.12). As the graphs show, nearly all circumferential strain takes place at the center section (Section 4) and the only other position with noticeable circumferential strain is at the springline of Sections 2 and 6 of ISU1. As previously noted for the other graphs there is excellent symmetry relative to the

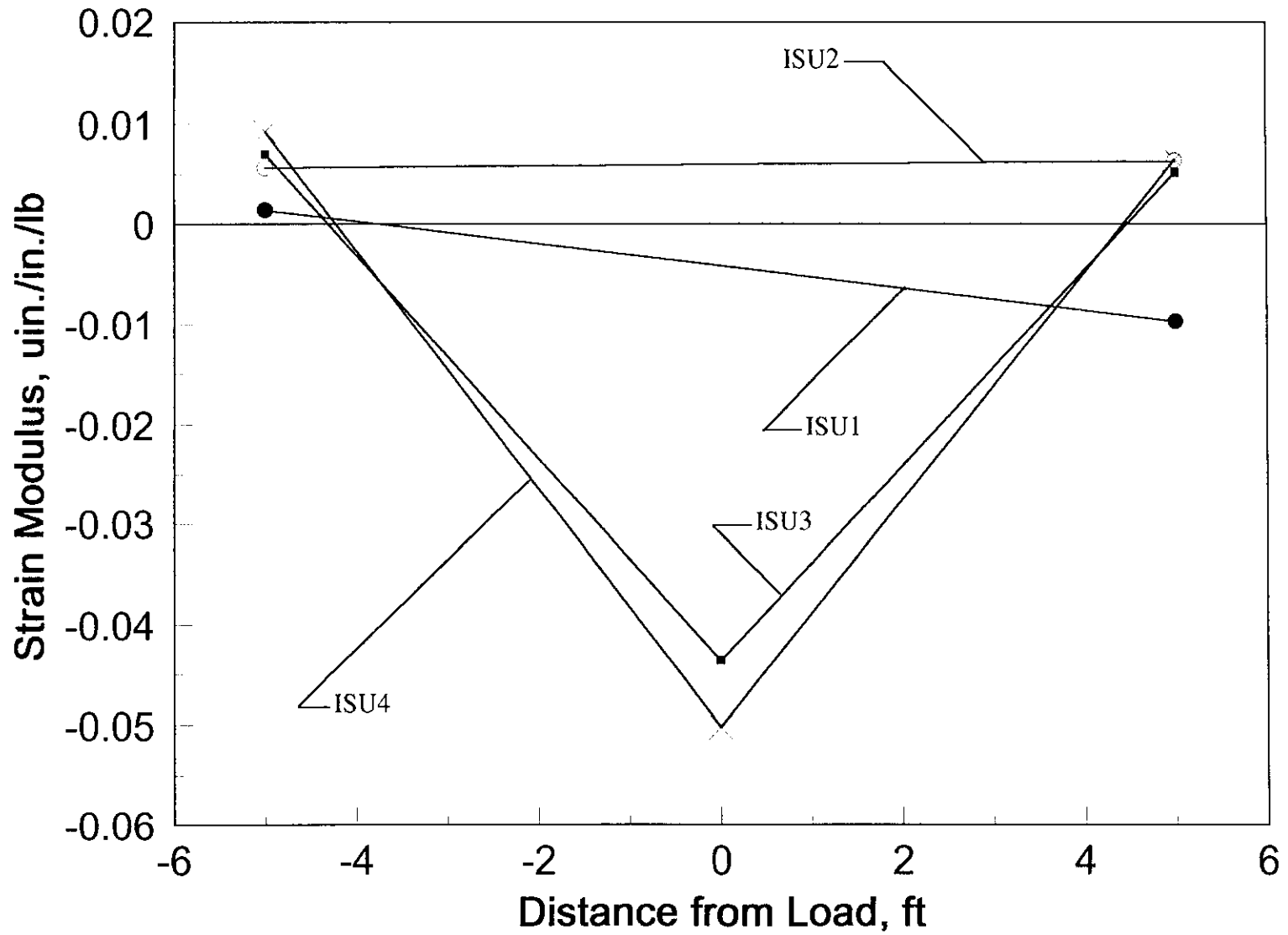


Figure 4.46. Circumferential strain modulus at the crown versus distance from load.

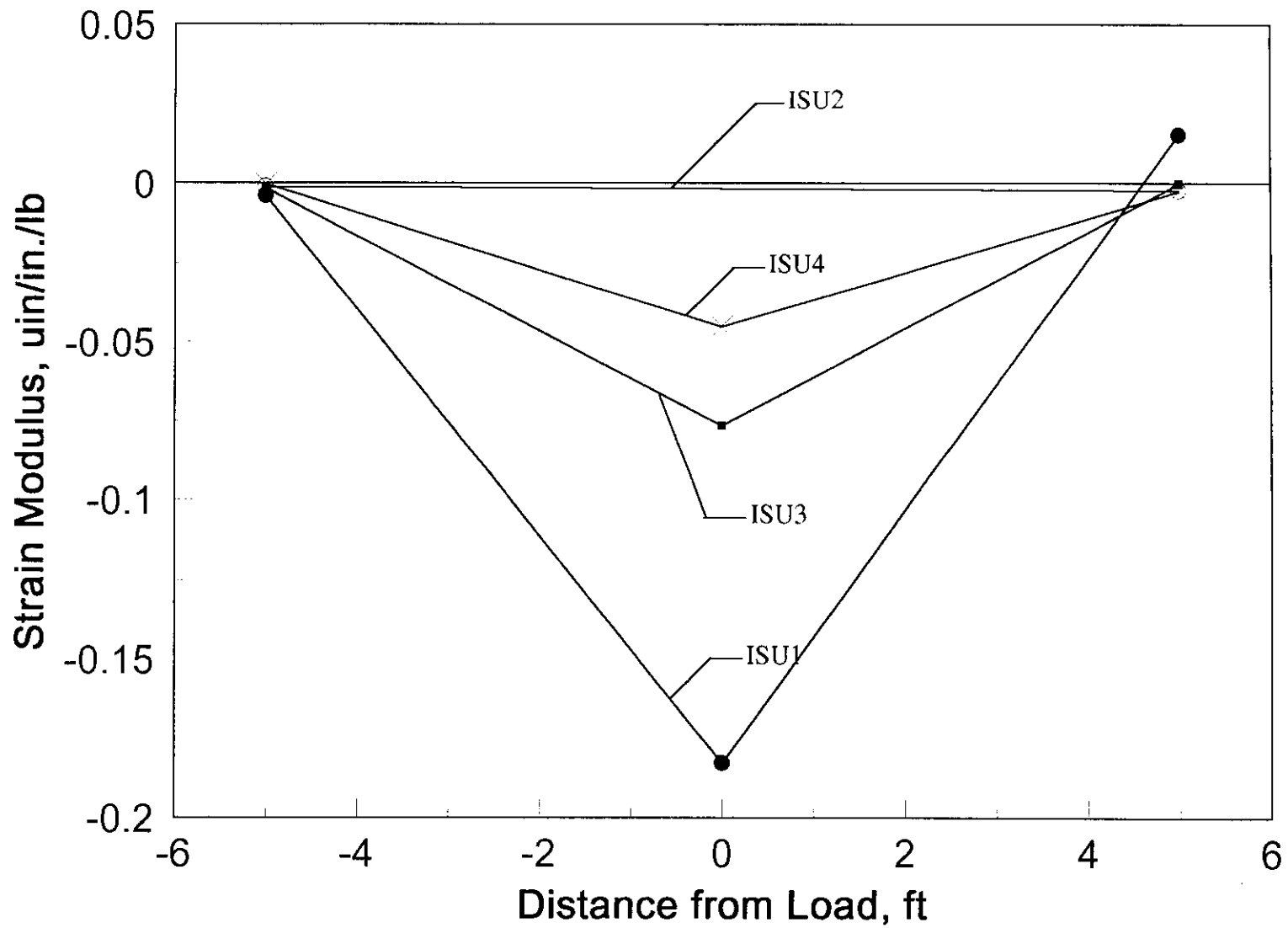


Figure 4.47. Cicumferential strain modulus at the springline versus distance from load.

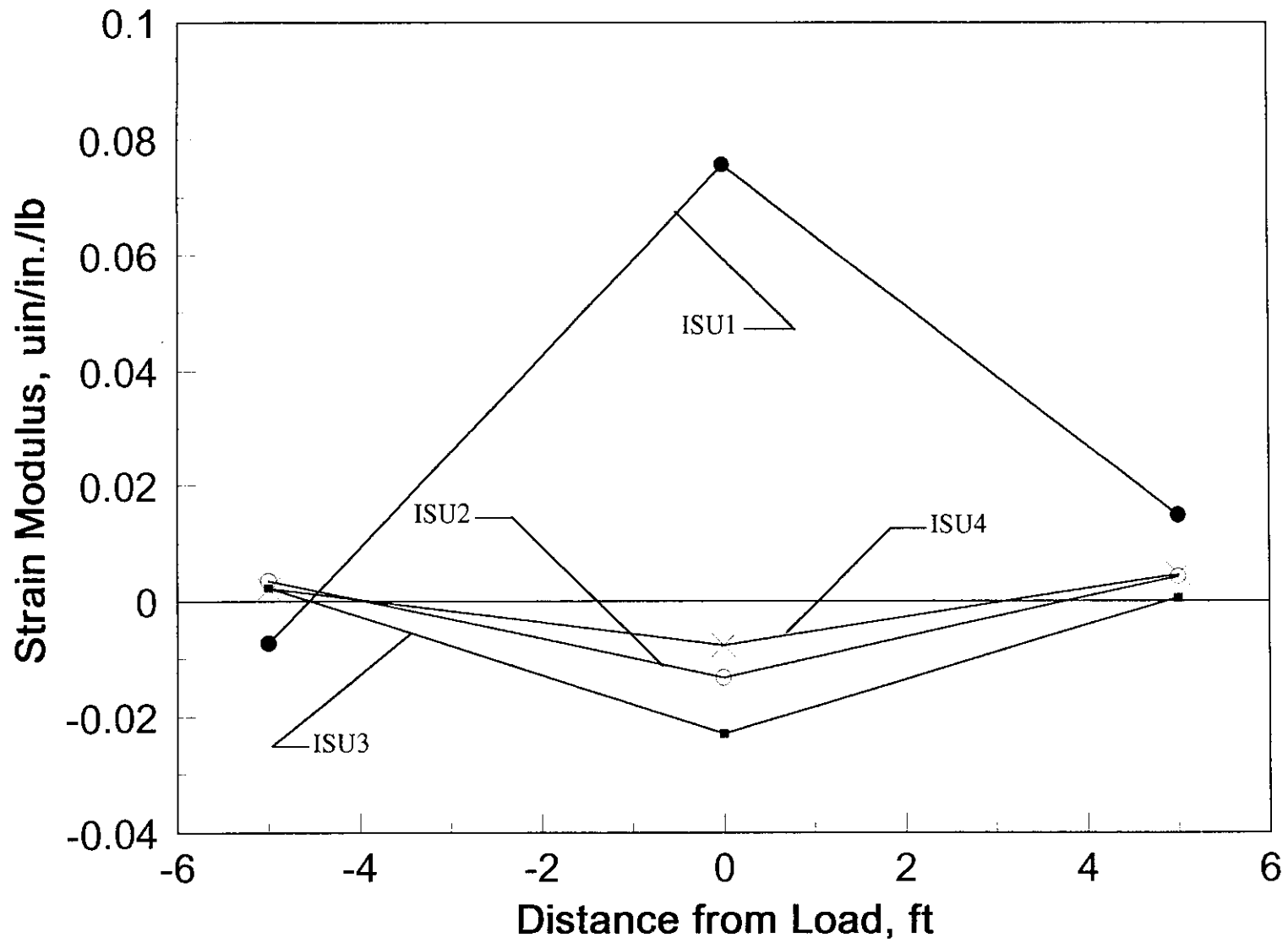


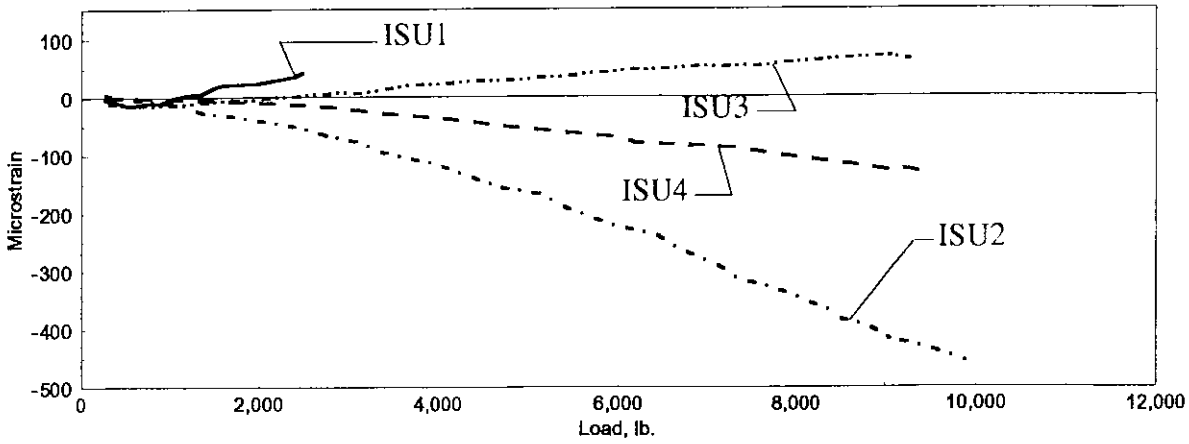
Figure 4.48. Cicumferential strain modulus at the invert versus distance from load.

centerline of the specimen. It is also interesting to note that strains at the springline were generally four times greater than those at the crown and approximately twenty times those on the invert with the exception of ISU1 for reasons previously noted.

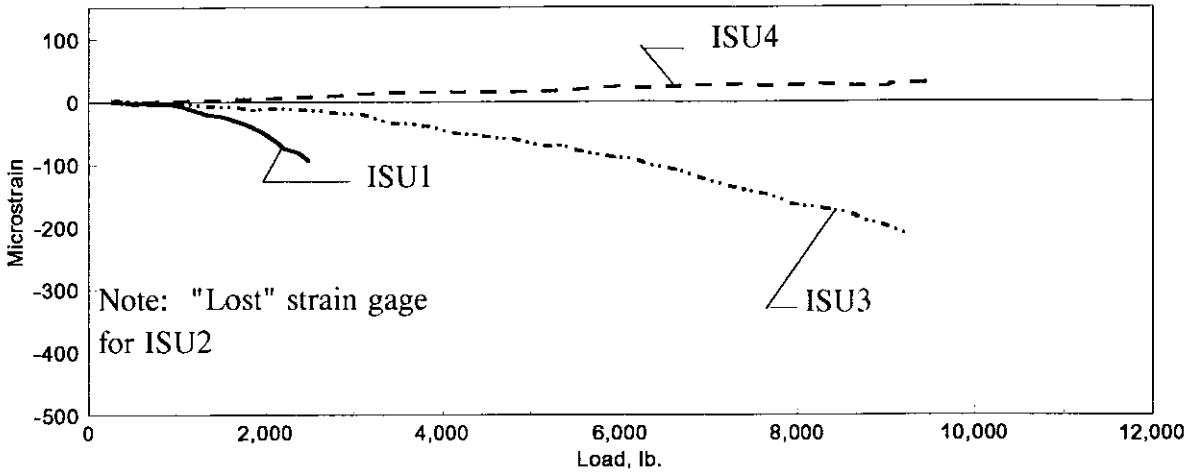
As noted in Chapter 3, deflections of the crown of the pipe at Sections 1, 3, 5, and 7 were also measured. Deflections measured during the four field tests were very small; the largest value measured was 0.05 in. Thus, deflection data have not been included in this report.

4.3.4.2 Load at Section 2

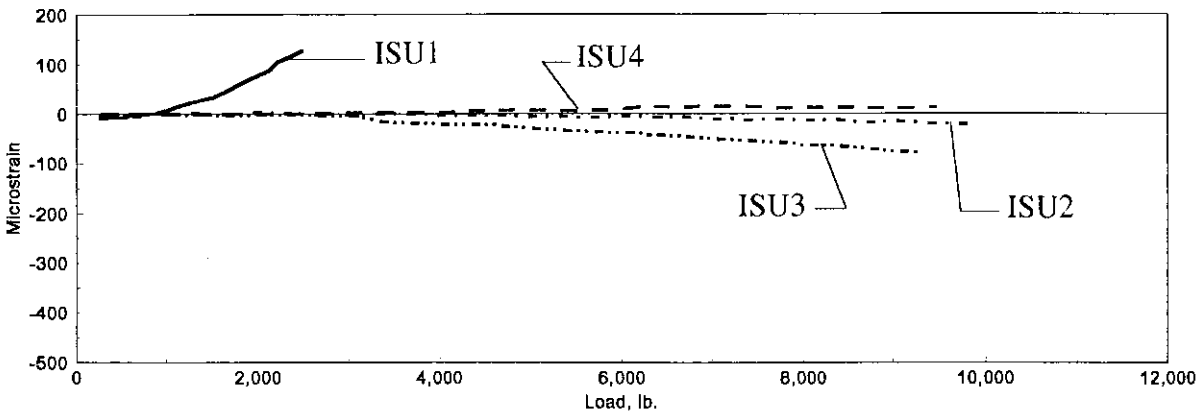
Load-strain data from service load tests with the load at Section 2 (see Fig. 3.12) are presented here. As before each figure contains graphs of strains at three locations (crown, springline, and invert). Shown in Fig 4.49 through 4.55 are the recorded longitudinal strains. As expected the largest magnitude of strains occurred directly under the load point with the maximum strains occurring at the crown. As in the tests with the load at the center, ISU1 had significantly higher strains than ISU2, ISU3, and ISU4. Additionally, as previously mentioned the strain response of ISU2, ISU3, and ISU4 did not vary significantly; indicating that the behavior of the "full" granular backfill and 70% granular backfill does not vary under the applied load. At Sections 1 and 3, the strain data show very little symmetry about the load point. This indicates that the end restraint of the pipe affects the response in those areas. It is clear that both sections undergo significantly



a. Crown

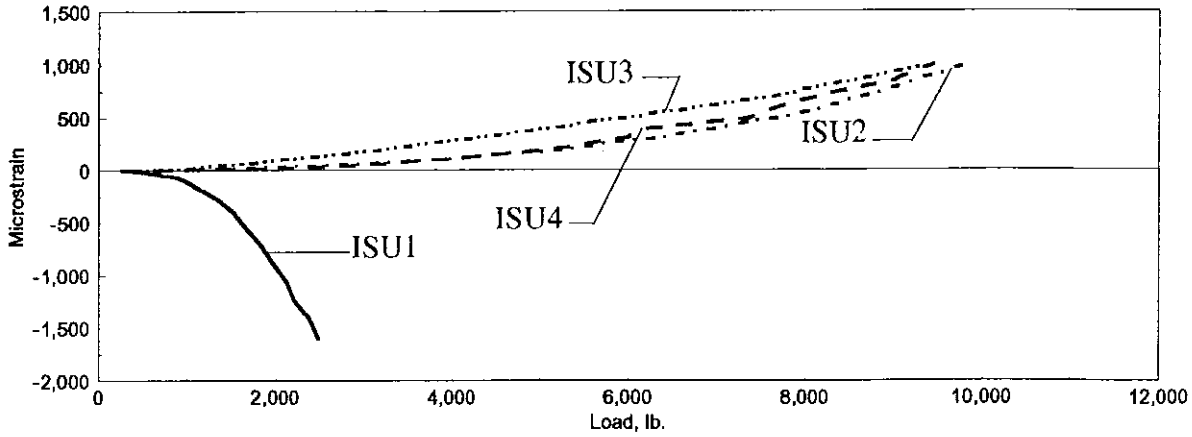


b. Springline

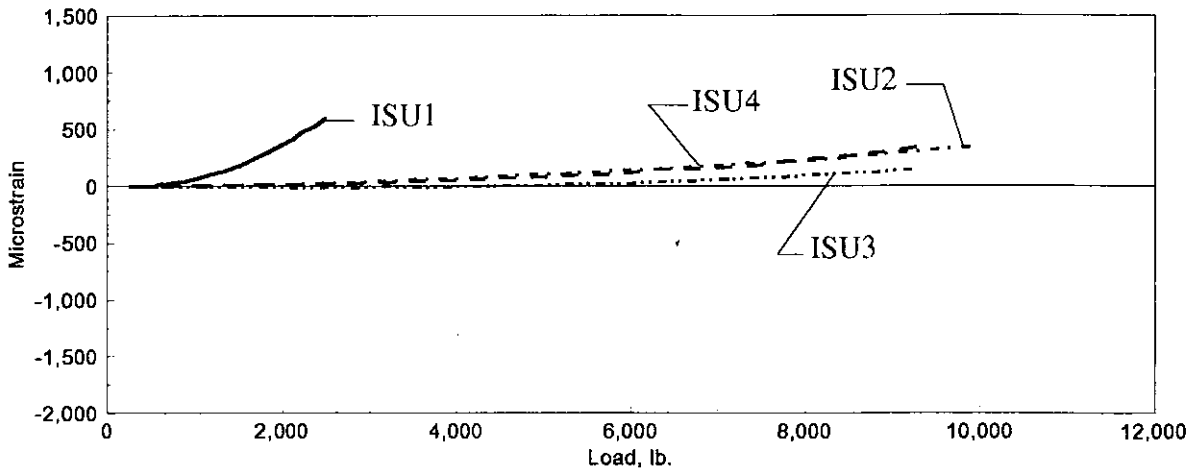


c. Invert

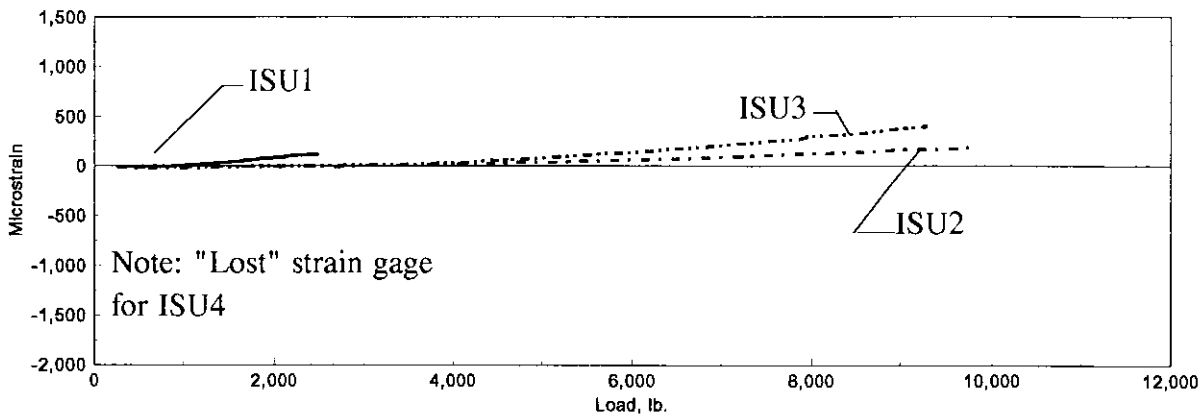
Figure 4.49. Longitudinal strain at Section 1: service load test; load at Section 2.



a. Crown

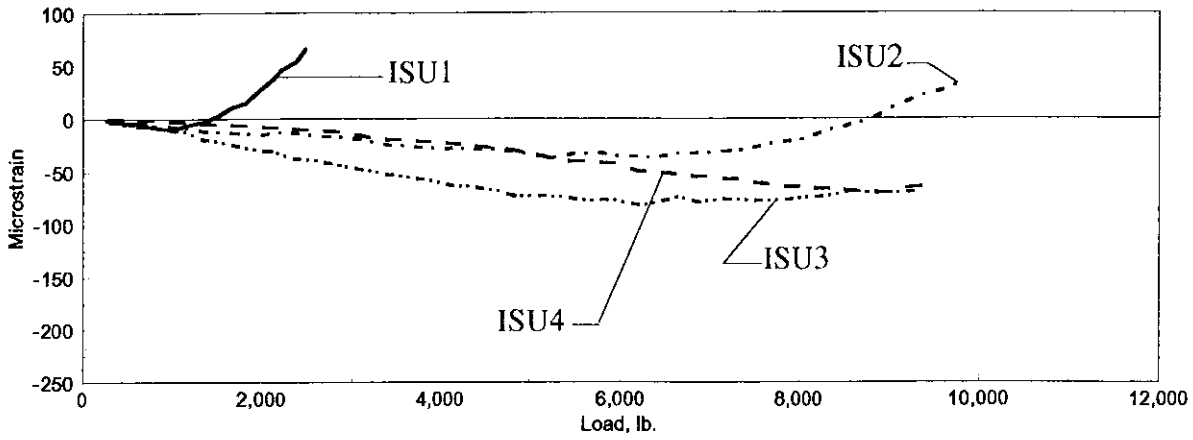


b. Springline

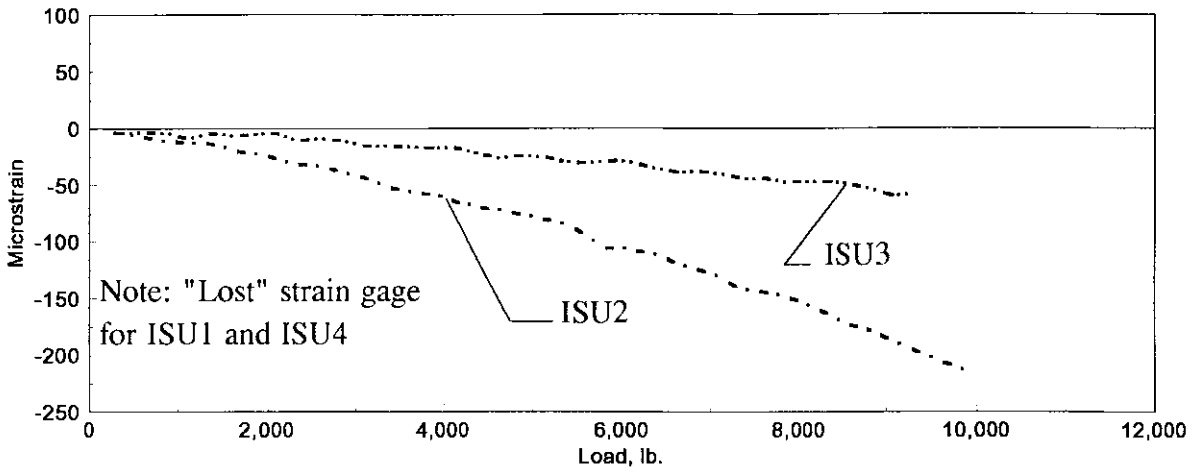


c. Invert

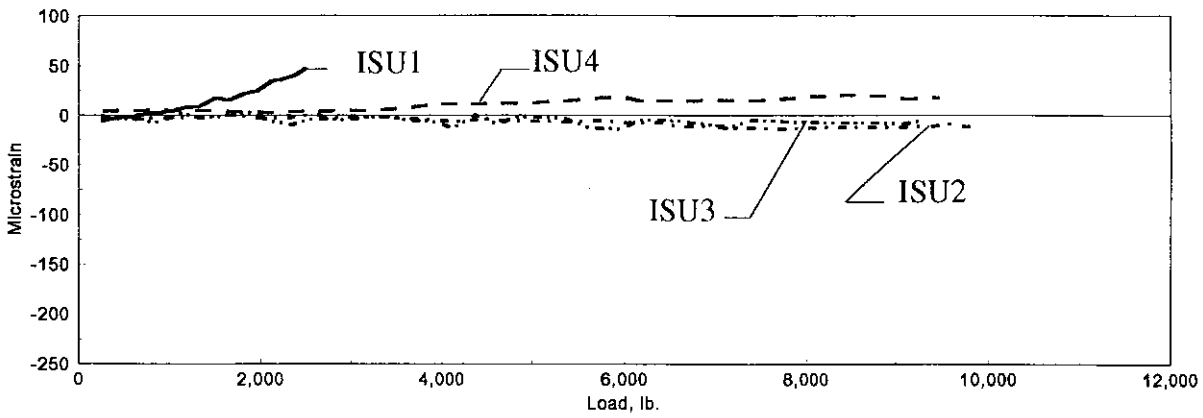
Figure 4.50. Longitudinal strain at Section 2: service load test; load at Section 2.



a. Crown

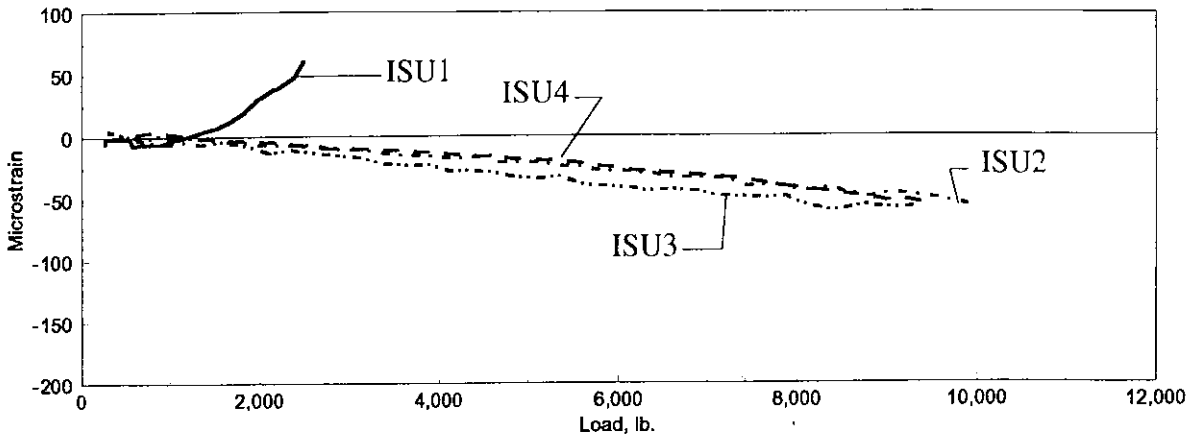


b. Springline

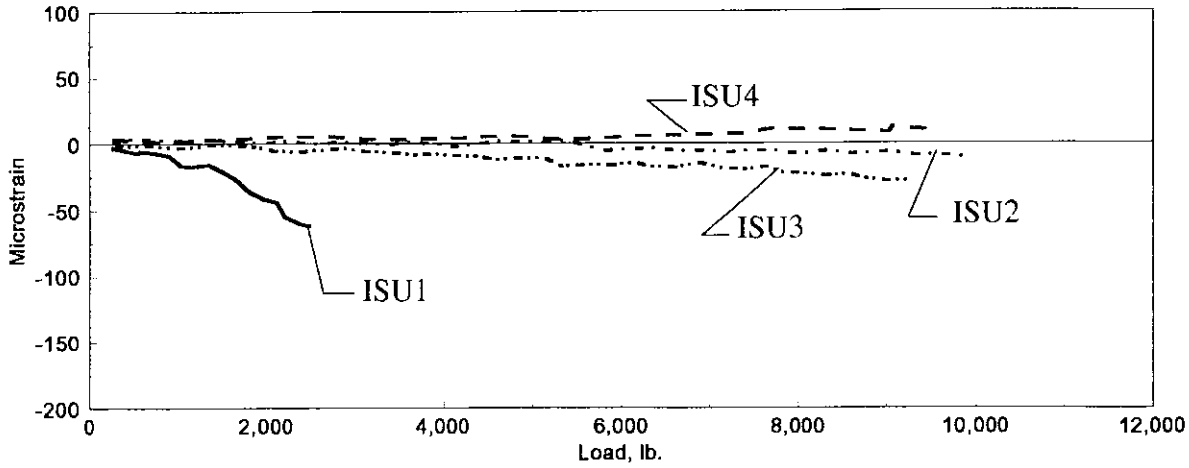


c. Invert

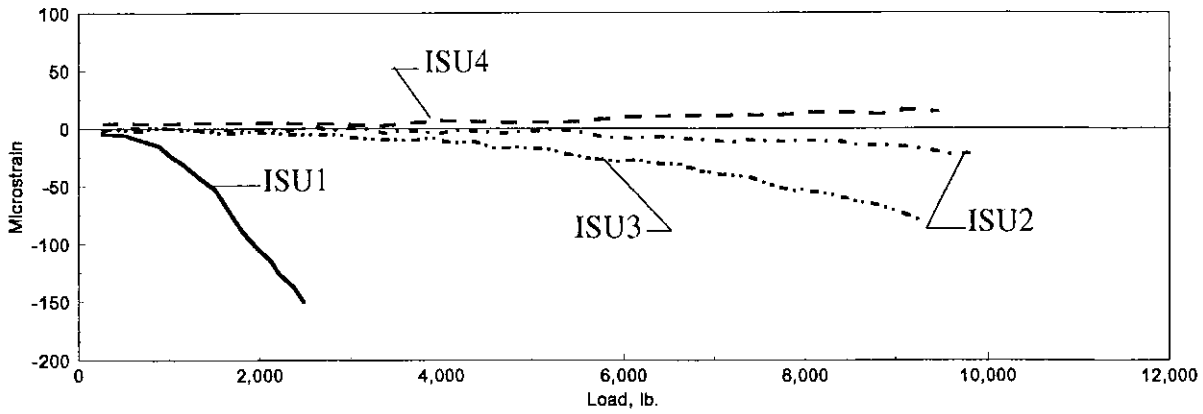
Figure 4.51. Longitudinal strain at Section 3: service load test; load at Section 2.



a. Crown

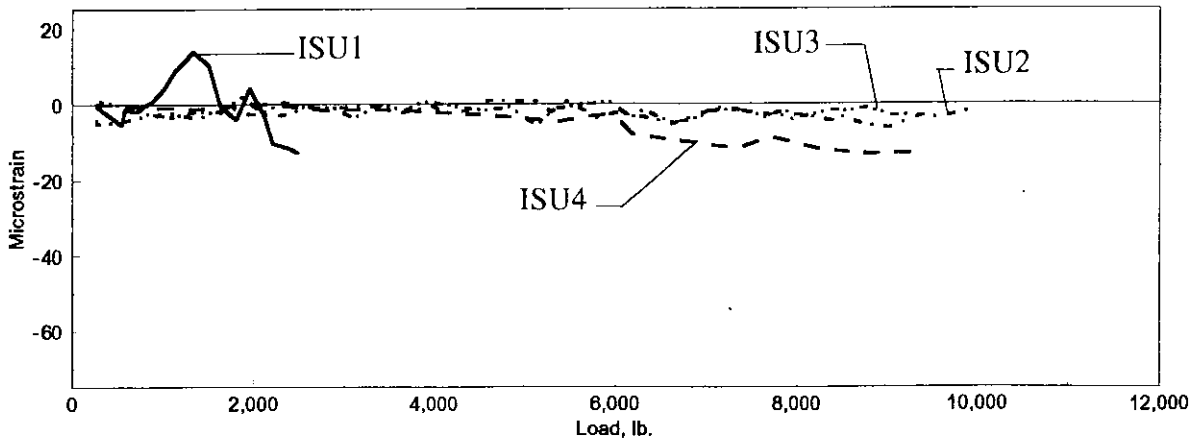


b. Springline

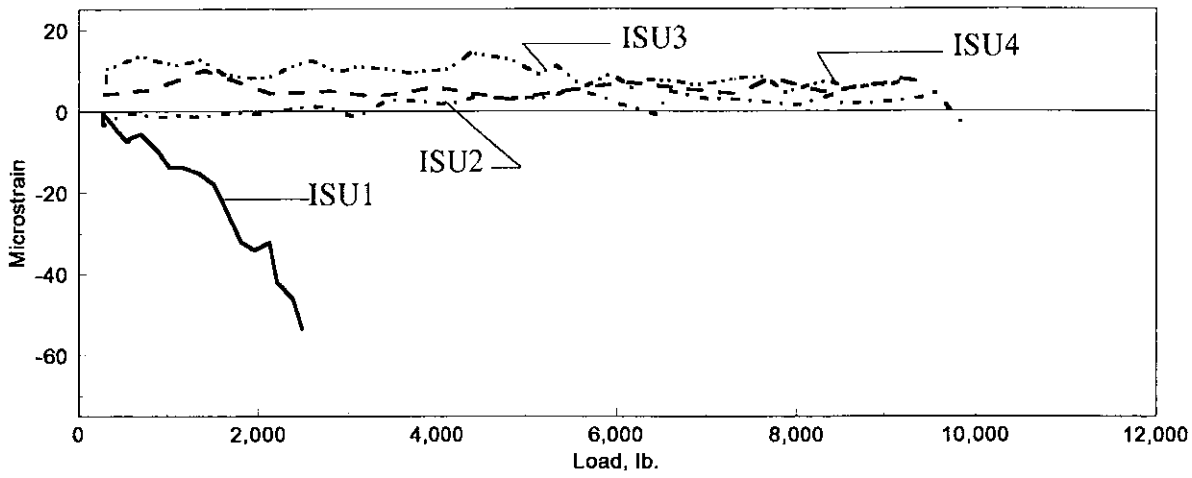


c. Invert

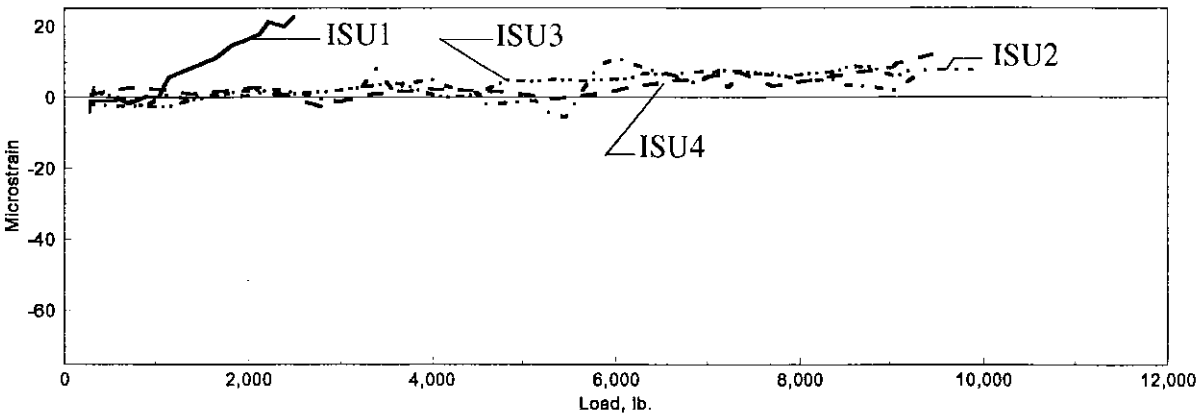
Figure 4.52. Longitudinal strain at Section 4: service load test; load at Section 2.



a. Crown

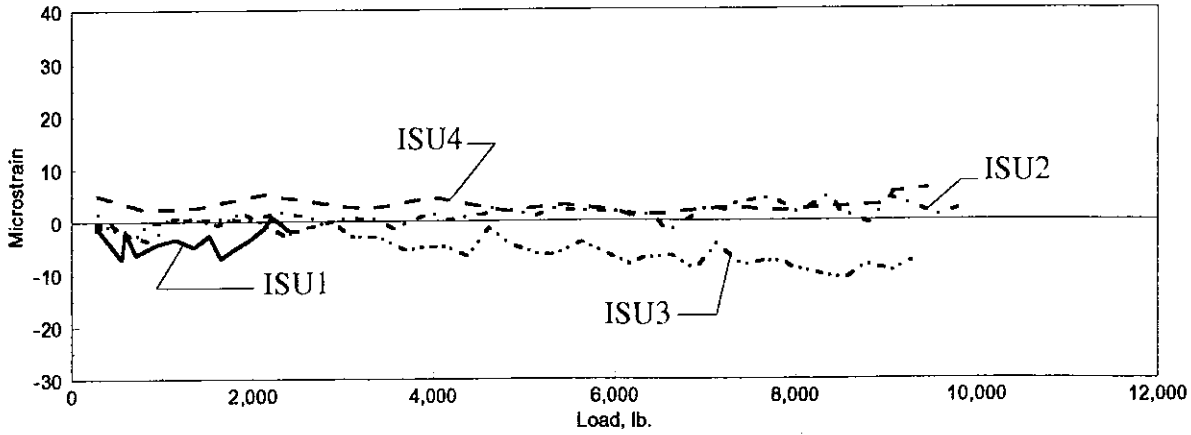


b. Springline

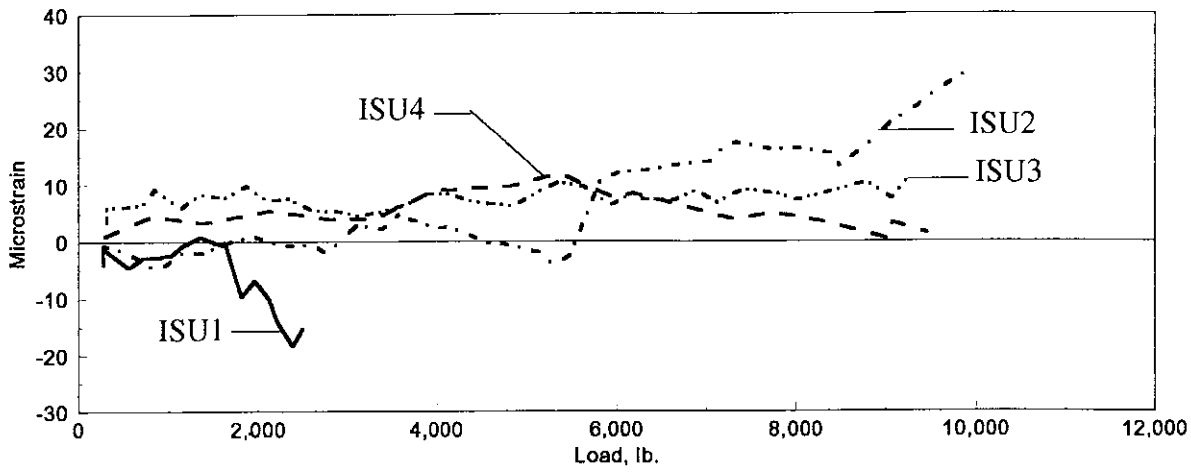


c. Invert

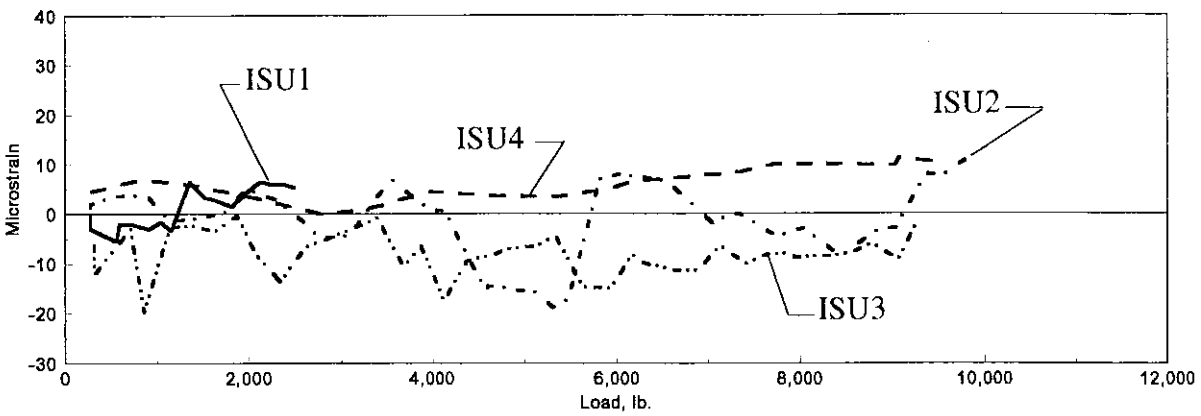
Figure 4.53. Longitudinal strain at Section 5: service load test; load at Section 2.



a. Crown

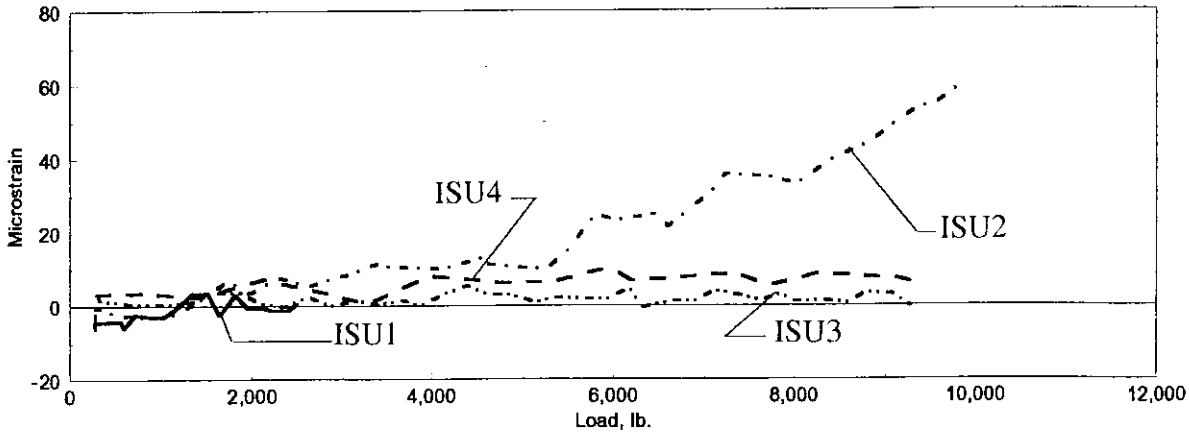


b. Springline

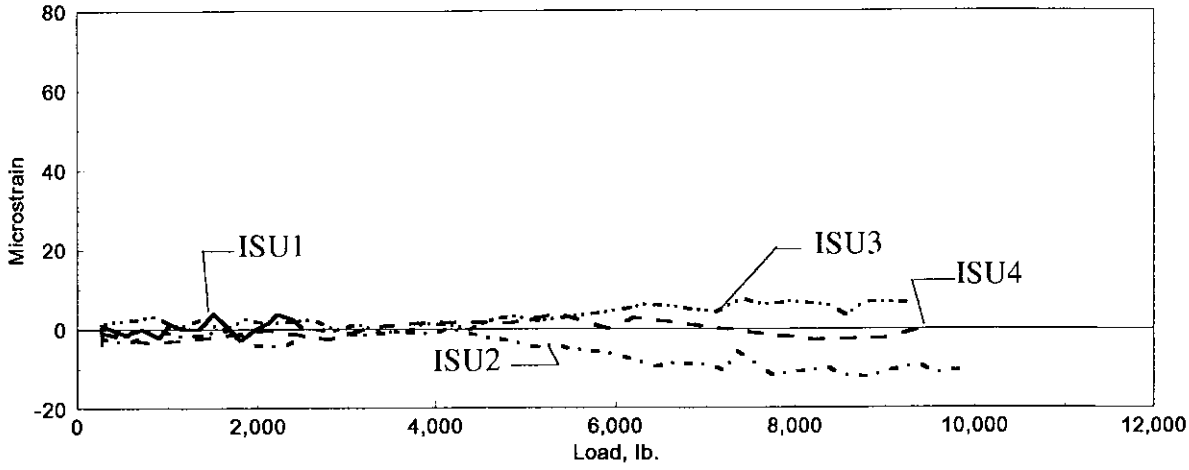


c. Invert

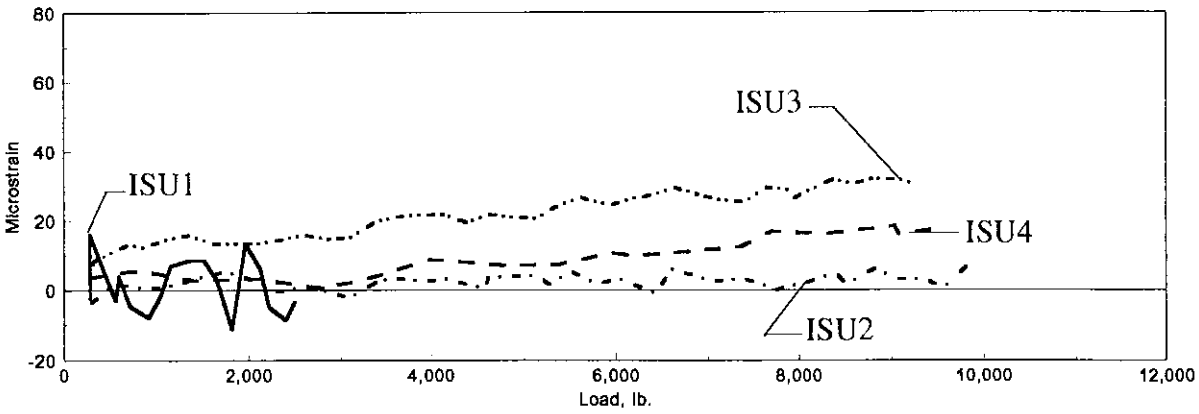
Figure 4.54. Longitudinal strain at Section 6: service load test; load at Section 2.



a. Crown



b. Springline



c. Invert

Figure 4.55. Longitudinal strain at Section 7: service load test; load at Section 2.

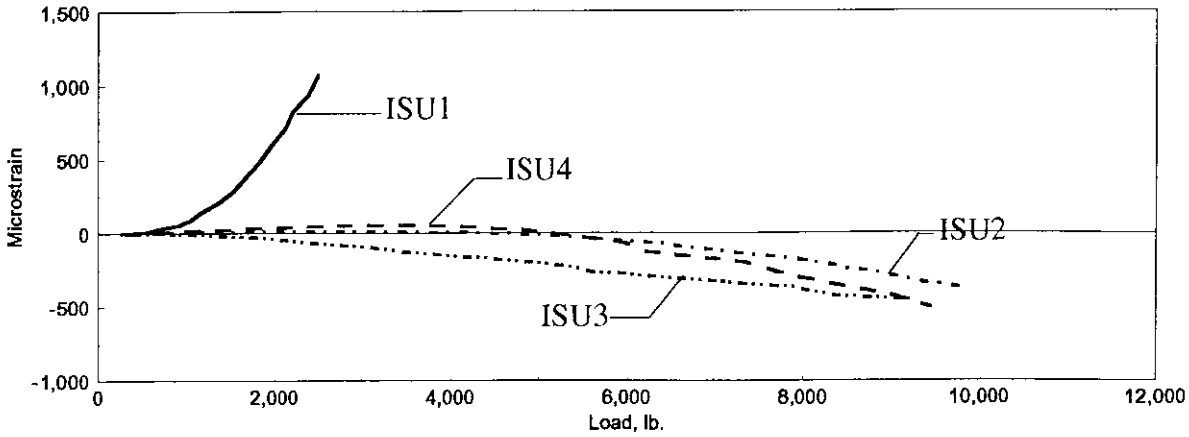
lower strain than locations directly under the load. The magnitude of the strains in Sections 4 through 7 (Figs. 4.52 through 4.55) show a steady decrease in strain as the distance from load increases for all specimens except ISU2. ISU2 shows this decrease in strain up to Section 7 where the crown has higher strains than at Section 6.

Figures 6.56 through 6.58 show the circumferential strains during the same service load test. Once again the largest strains occur at the section under the load. However, the strains are nearly equal at the crown and springline. Indicating that significant bending occurred at both sections. As before, the strains at the invert are significantly lower than at the springline or invert. Deformation of the pipe away from the load is reduced significantly 5 ft from the load point and there is little to no strain response 10 ft from the load.

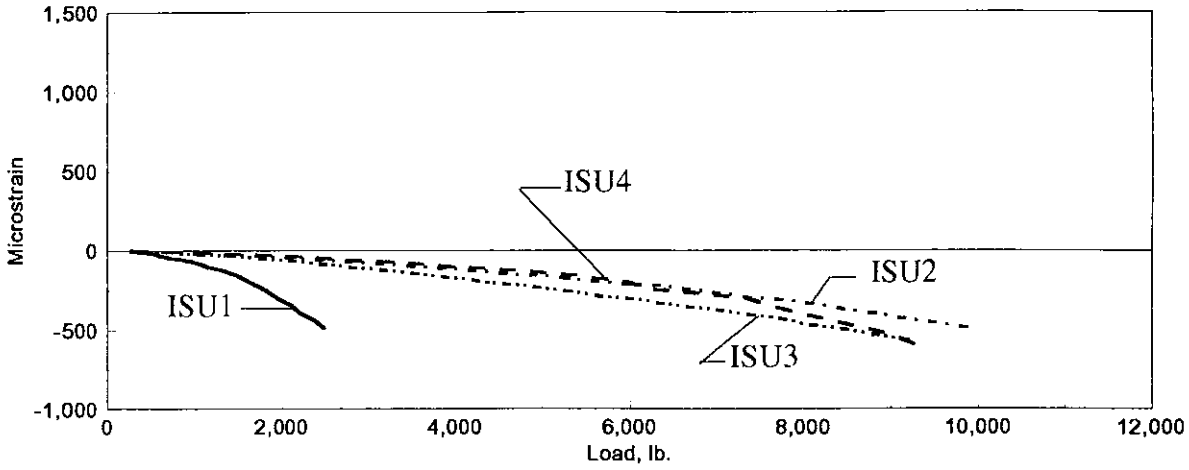
4.3.4.3 Load at Section 6

Results of the service load tests at Section 6 (see Fig. 3.12) are presented here. As for other service load tests, the maximum strains are directly under the load point. The longitudinal strains are shown in Figs. 4.59 through 4.65 and the circumferential strain data is presented in Figs. 4.66 through 4.68.

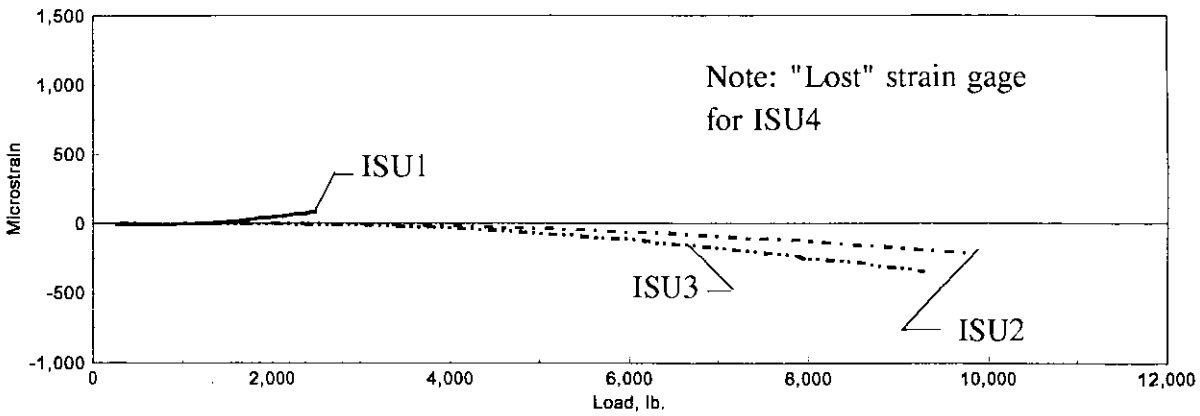
Note that symmetry between the tests at Section 2 and Section 6 is not realized. Sections in the same position relative to load are 1 and 7, 2 and 6, 3 and 5, and 4 and 4. Comparison of these sections for the respective tests shows that the response when the load



a. Crown

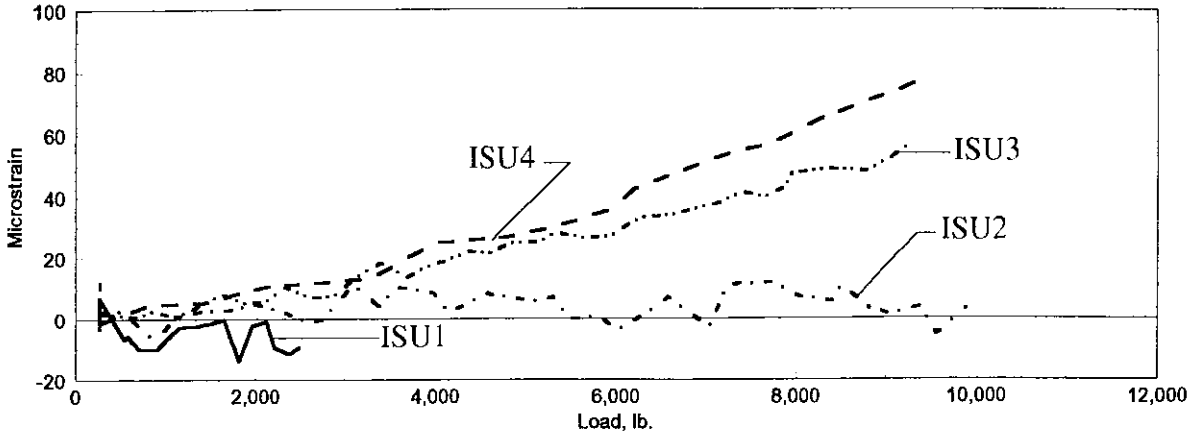


b. Springline

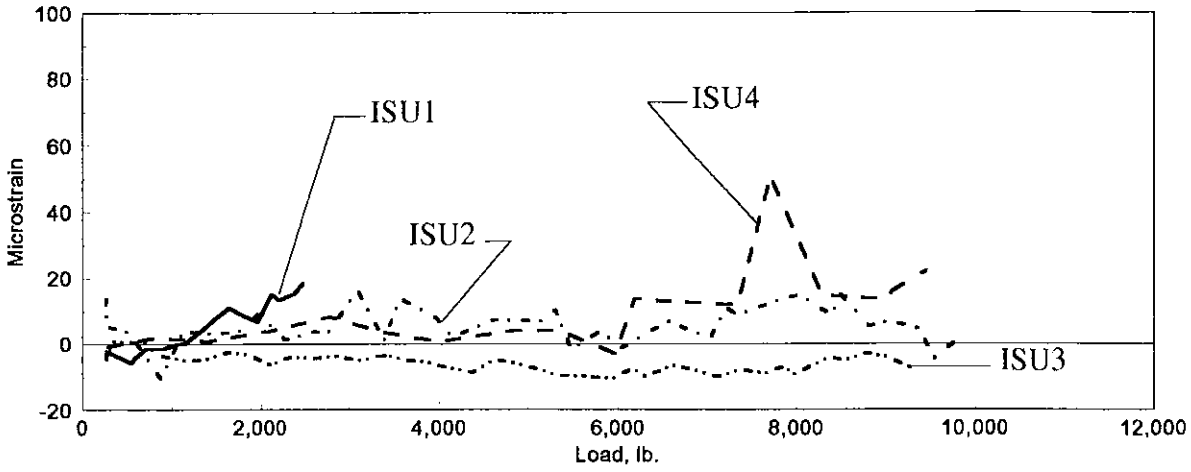


c. Invert

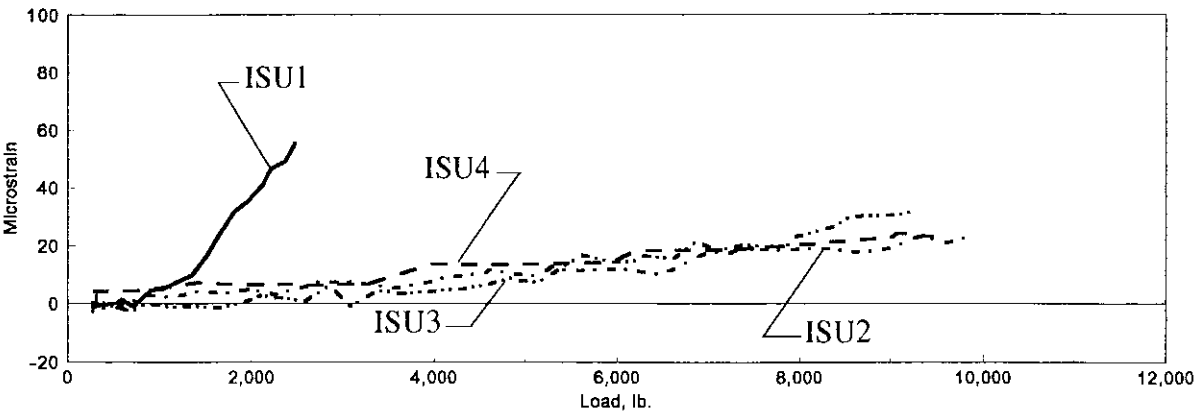
Figure 4.56. Circumferential strain at Section 2: service load test; load at Section 2.



a. Crown

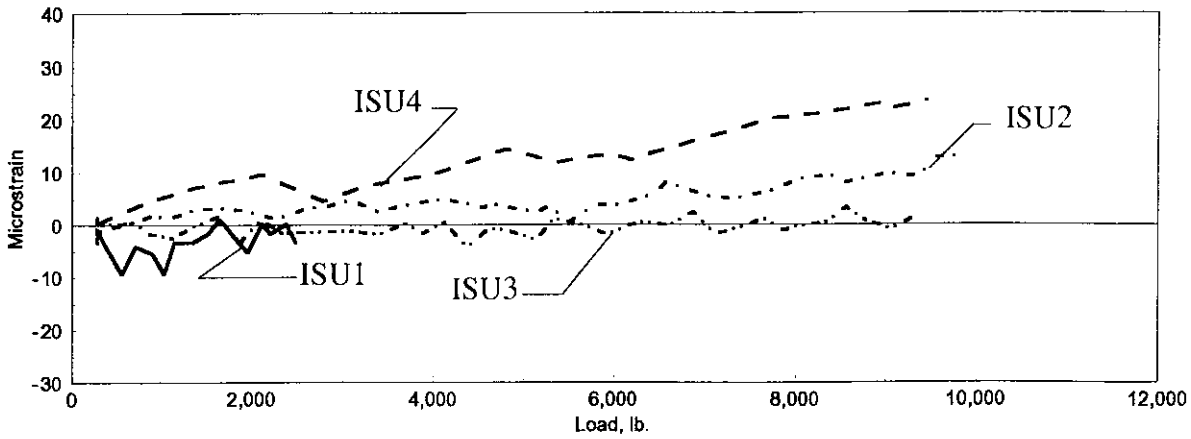


b. Springline

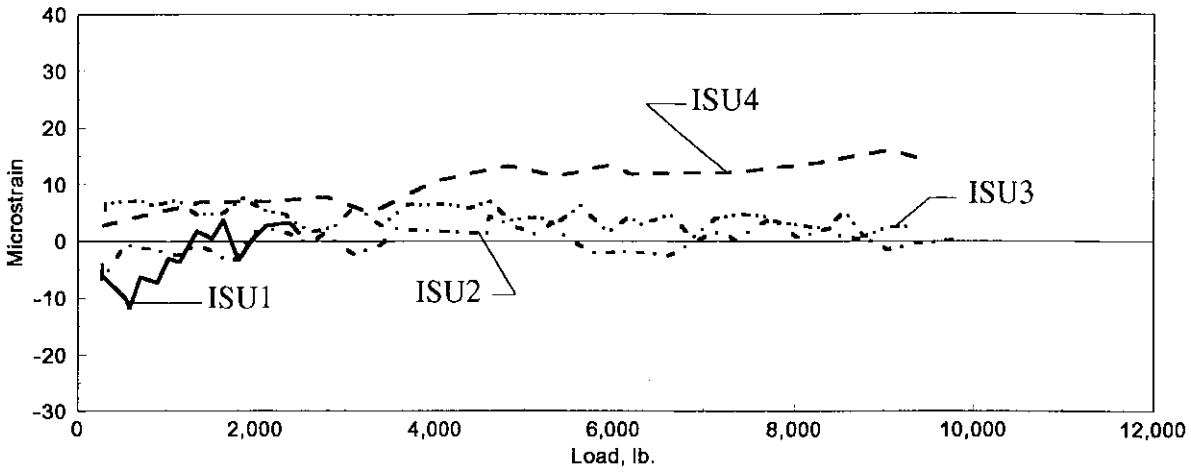


c. Invert

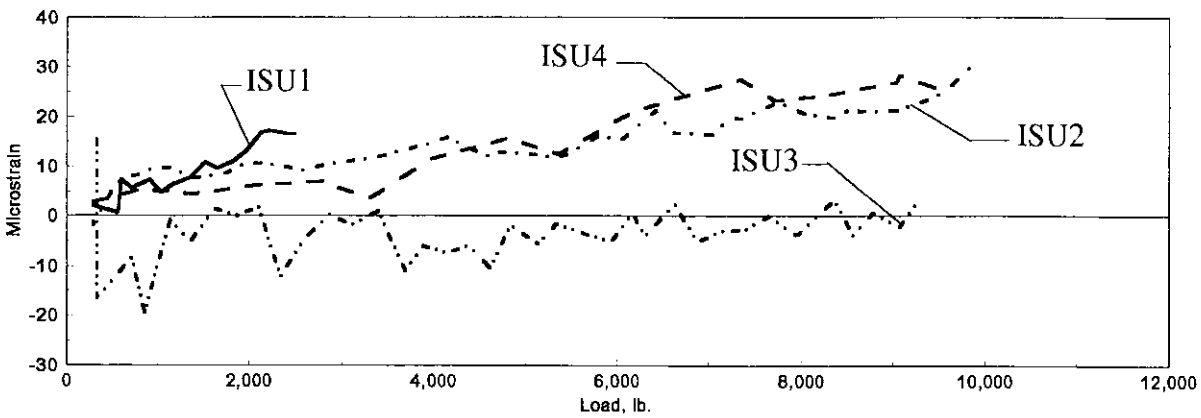
Figure 4.57. Circumferential strain at Section 4: service load test; load at Section 2.



a. Crown

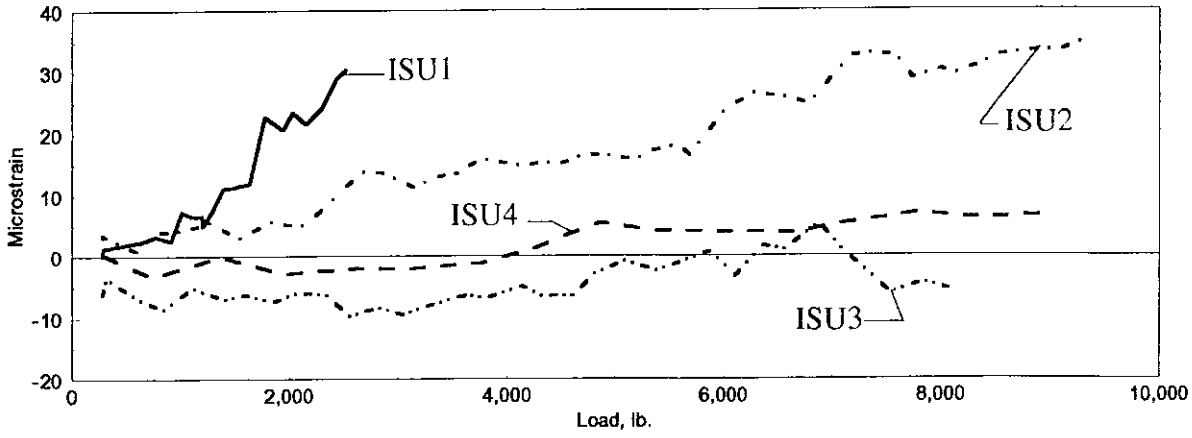


b. Springline

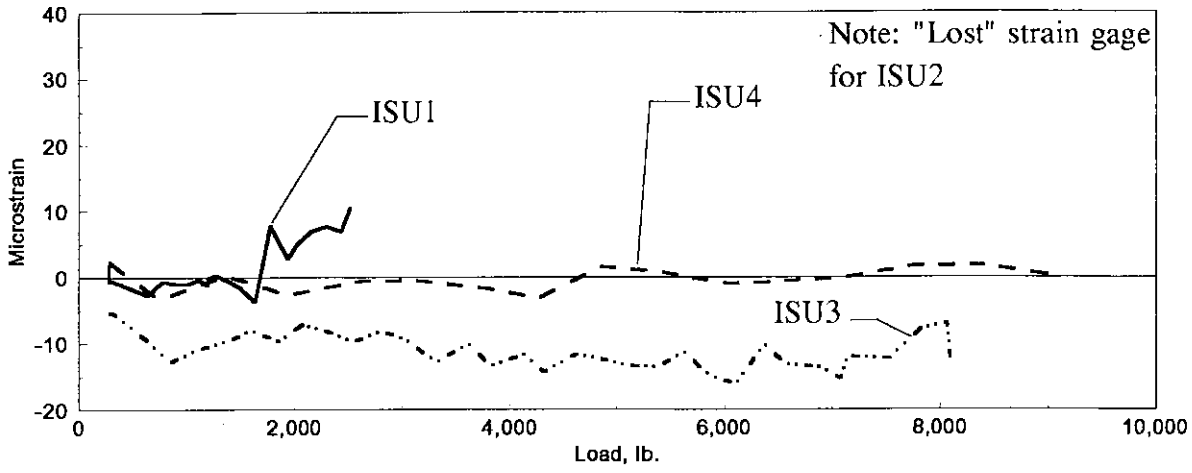


c. Invert

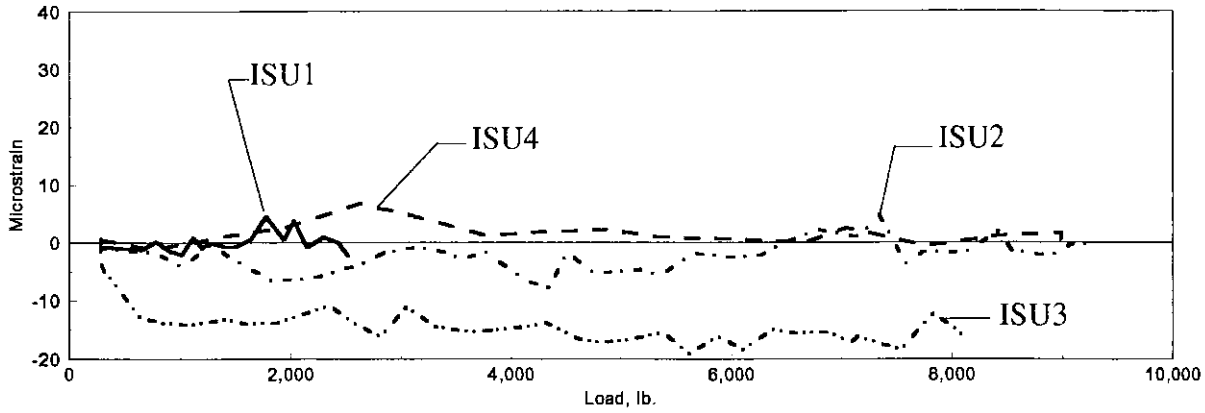
Figure 4.58. Circumferential strain at Section 6: service load test; load at Section 2.



a. Crown

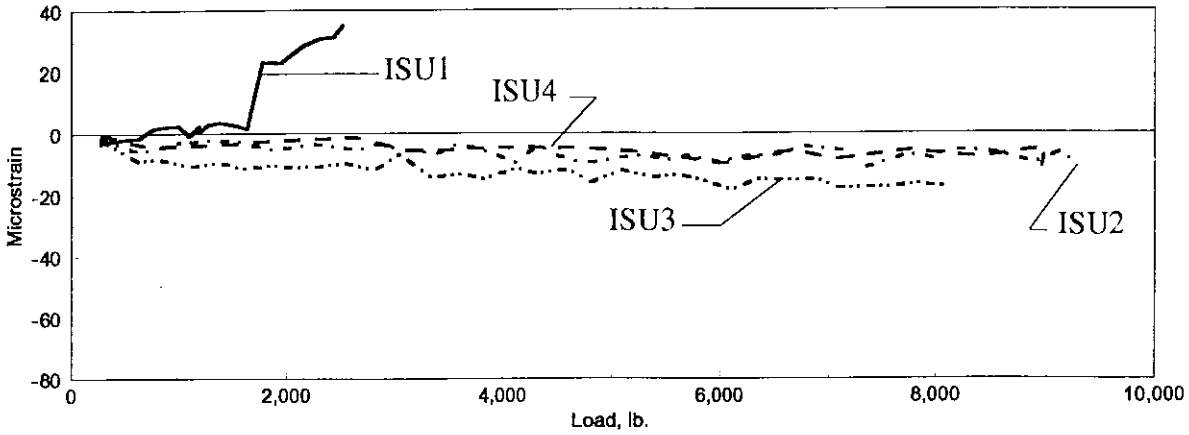


b. Springline

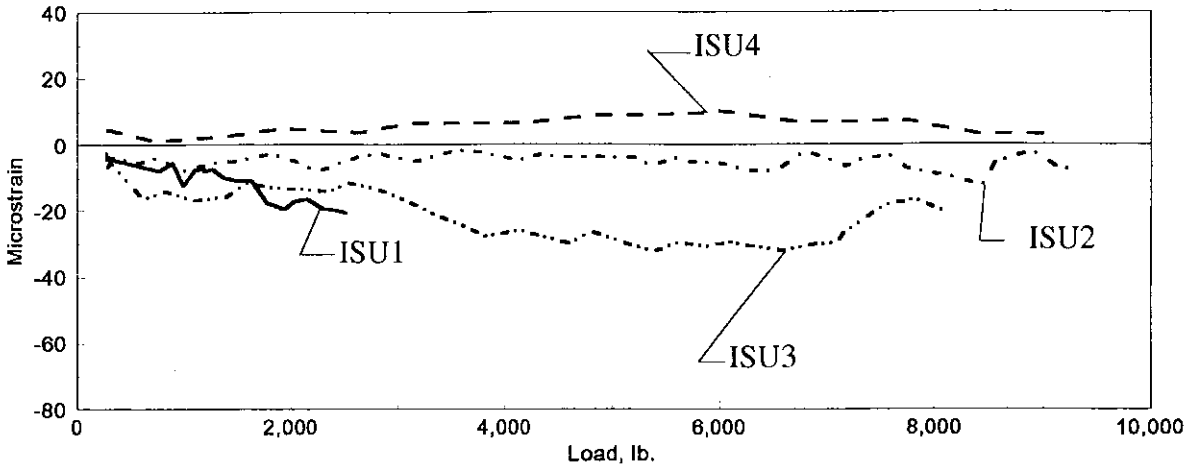


c. Invert

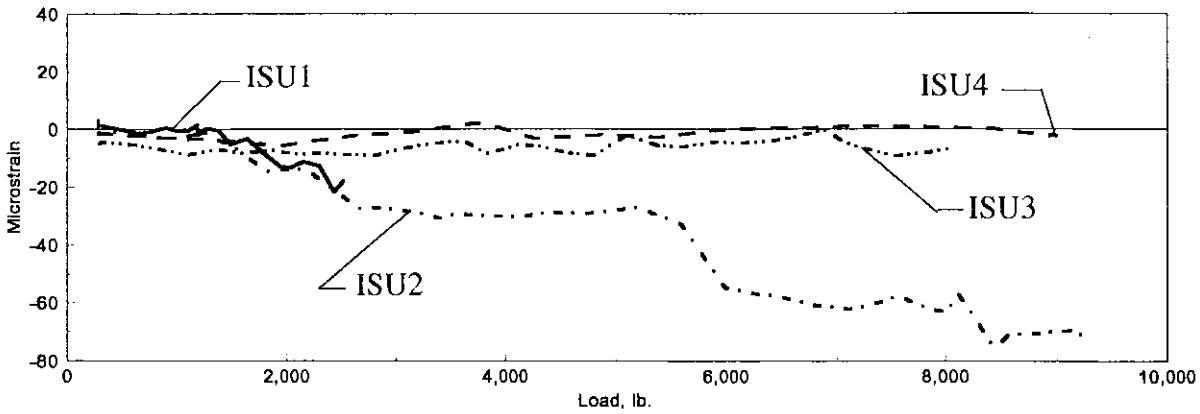
Figure 4.59. Longitudinal strain at Section 1: service load test; load at Section 6.



a. Crown

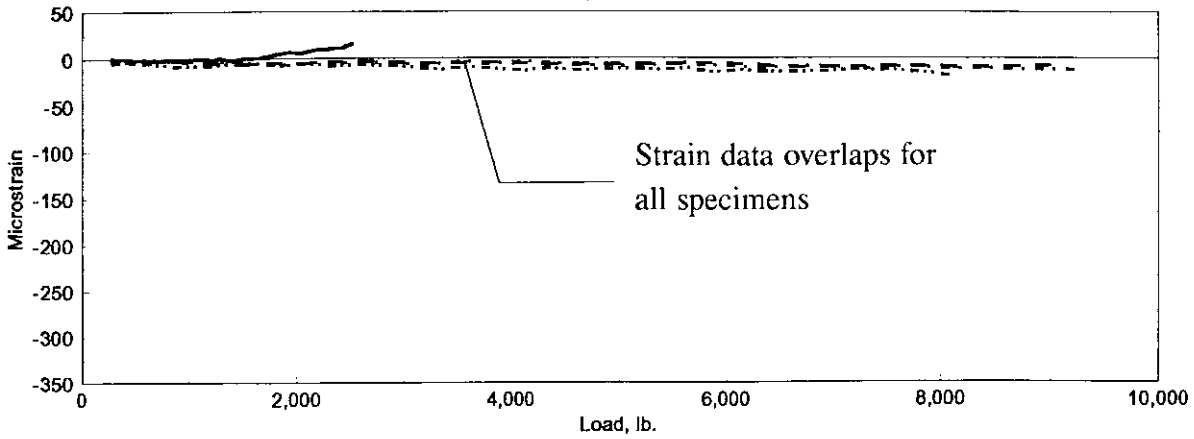


b. Springline

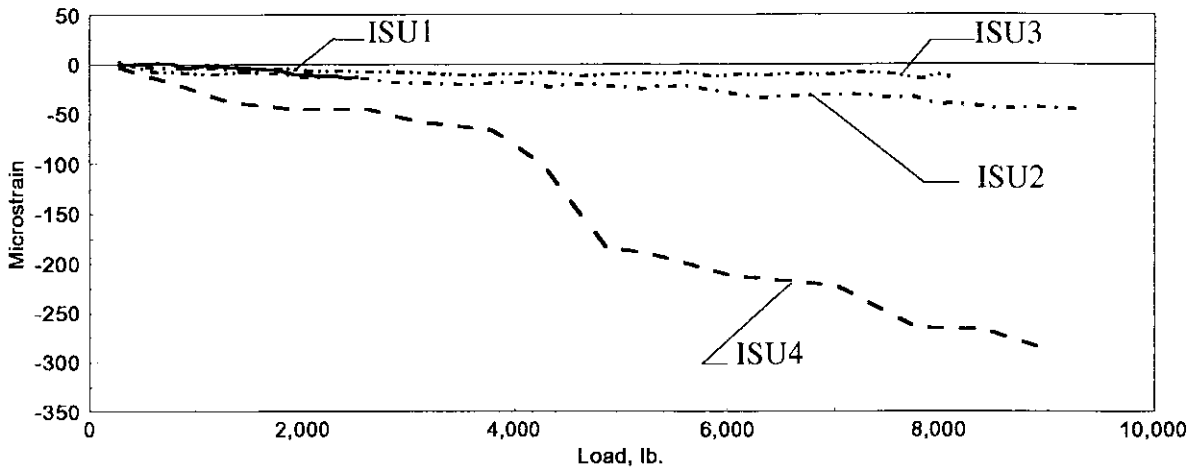


c. Invert

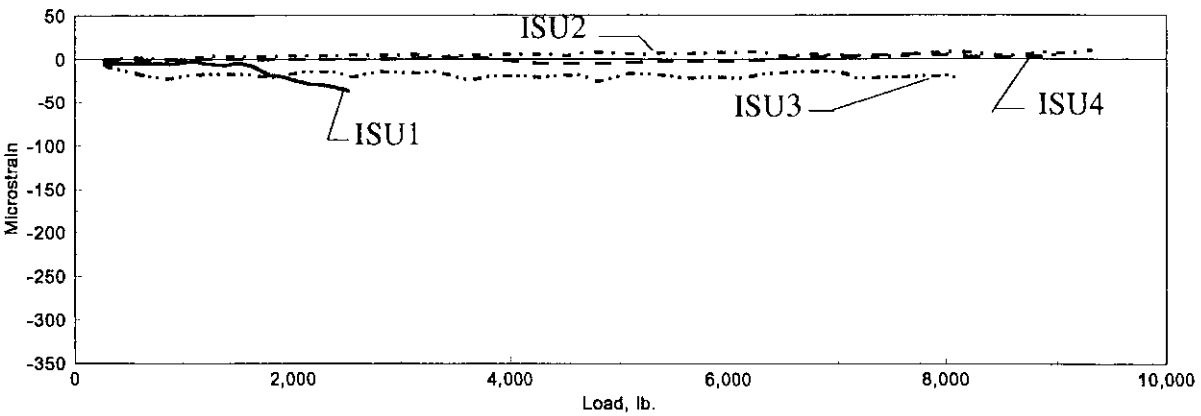
Figure 4.60. Longitudinal strain at Section 2: service load test; load at Section 6.



a. Crown

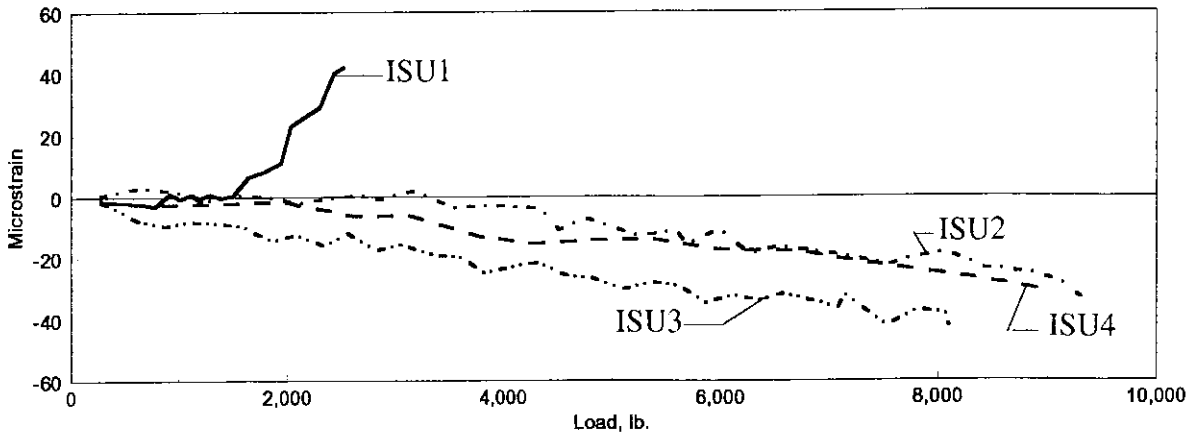


b. Springline

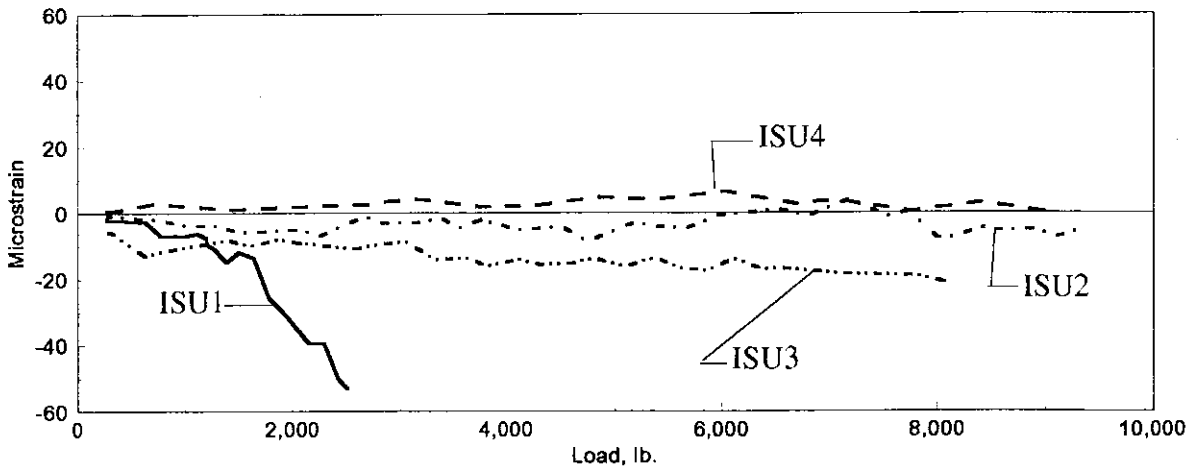


c. Invert

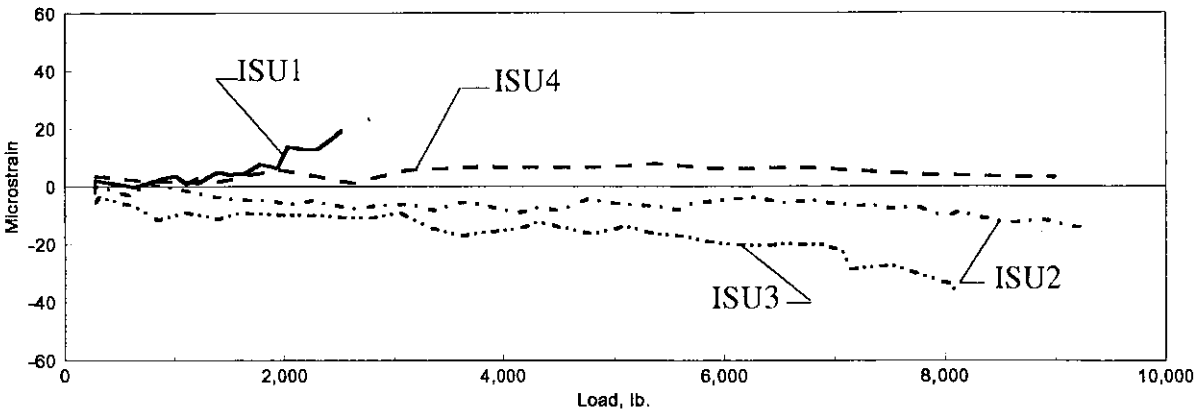
Figure 4.61 Longitudinal strain at Section 3: service load test; load at Section 6.



a. Crown

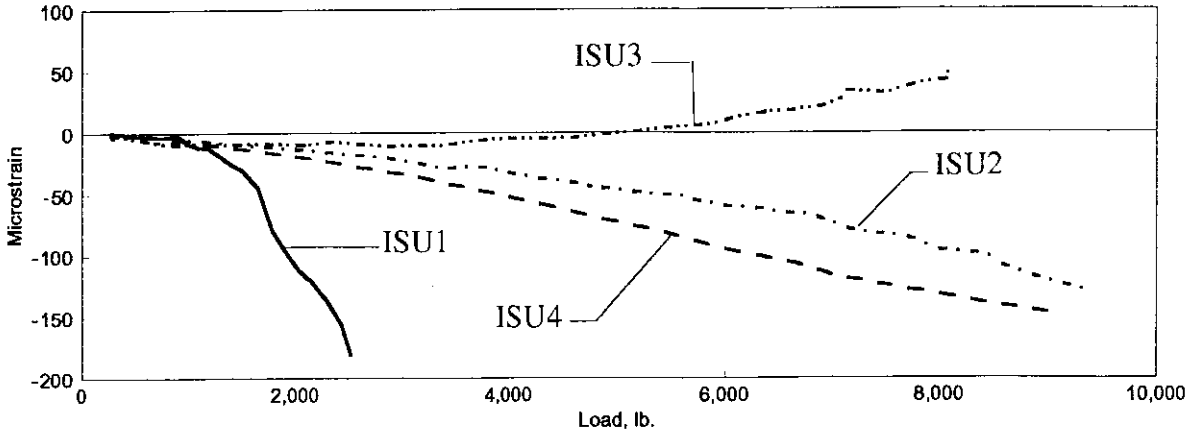


b. Springline

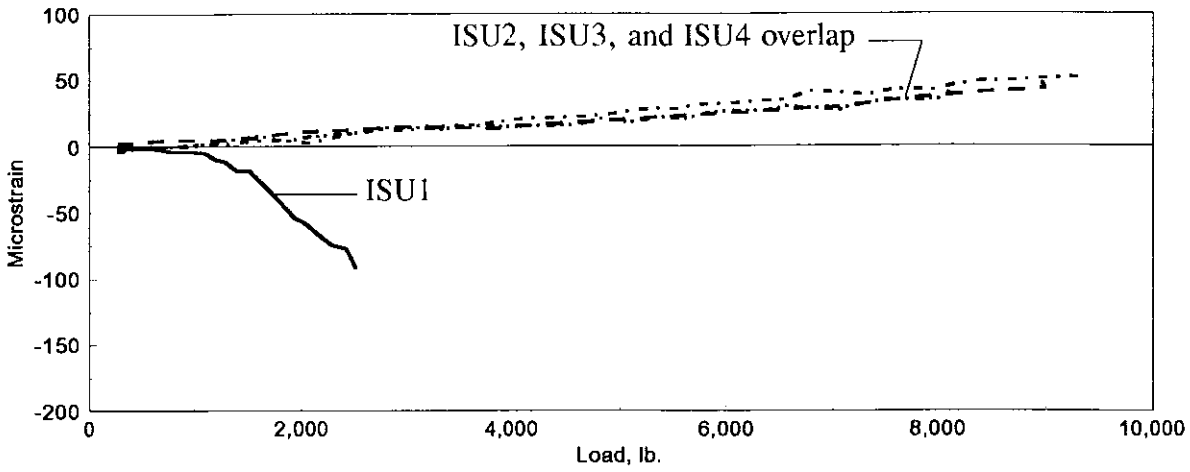


c. Invert

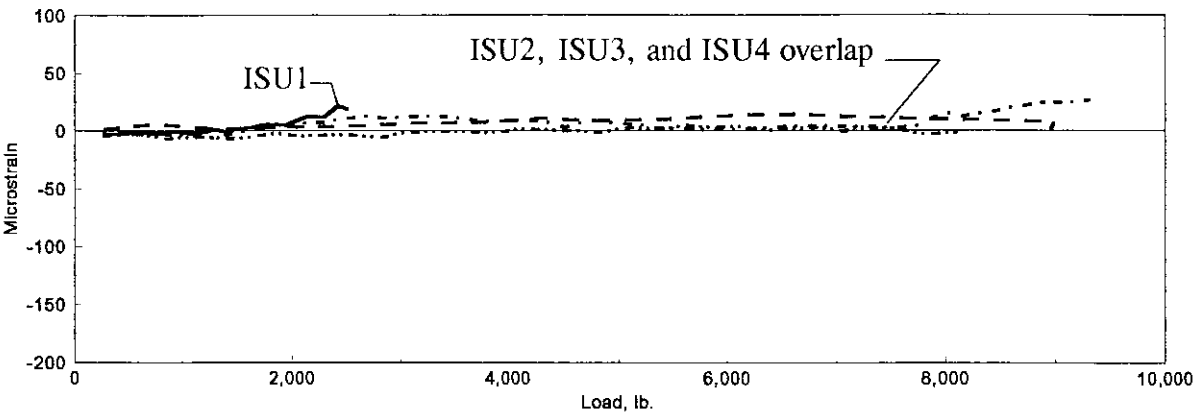
Figure 4.62. Longitudinal strain at Section 4: service load test; load at Section 6.



a. Crown

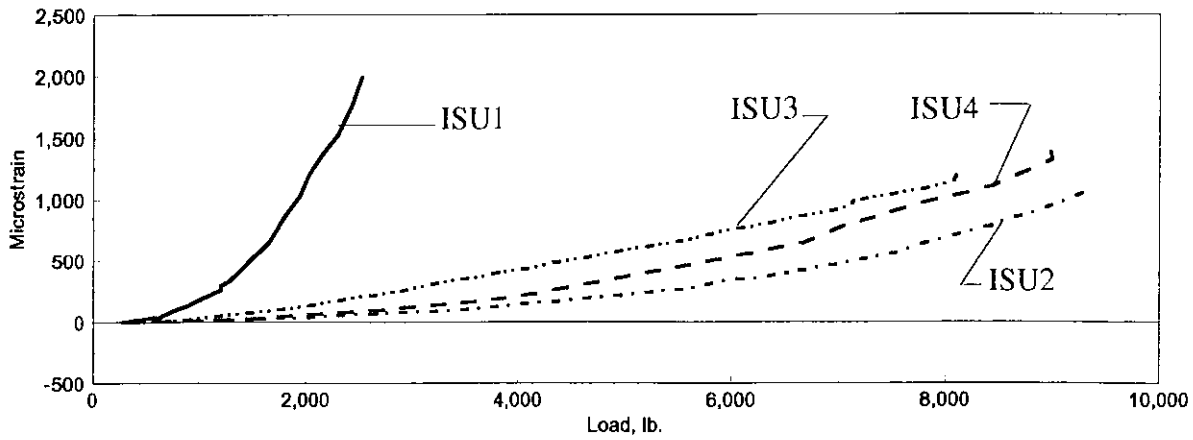


b. Springline

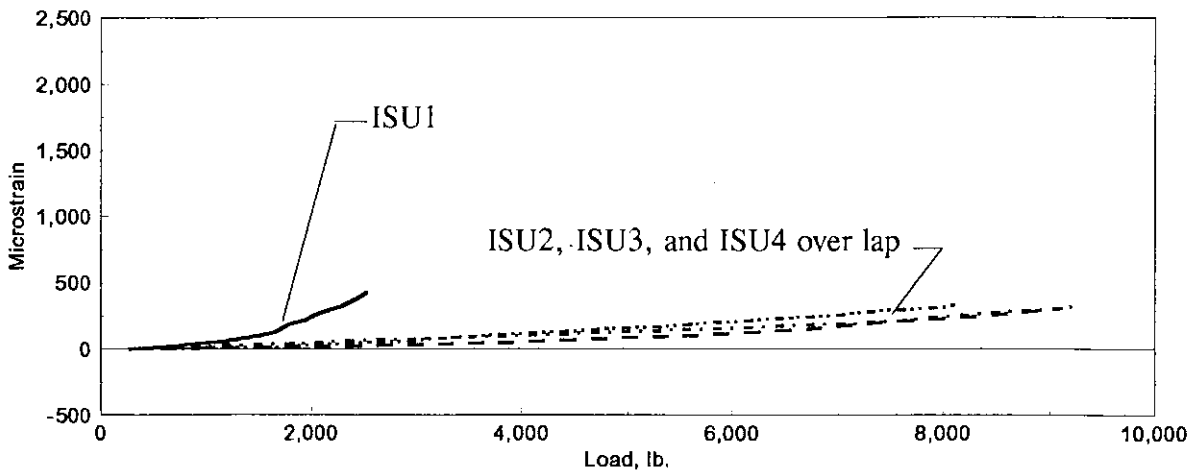


c. Invert

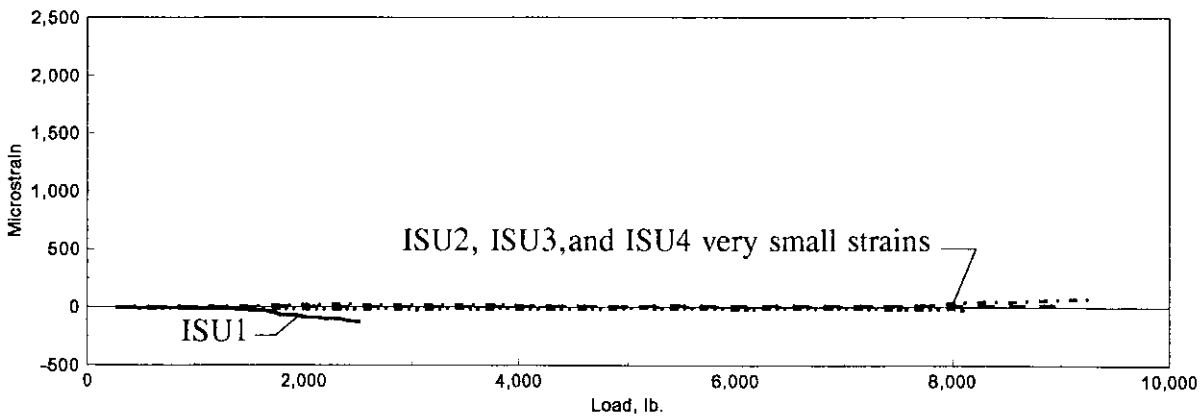
Figure 4.63. Longitudinal strain at Section 5: service load test; load at Section 6.



a. Crown

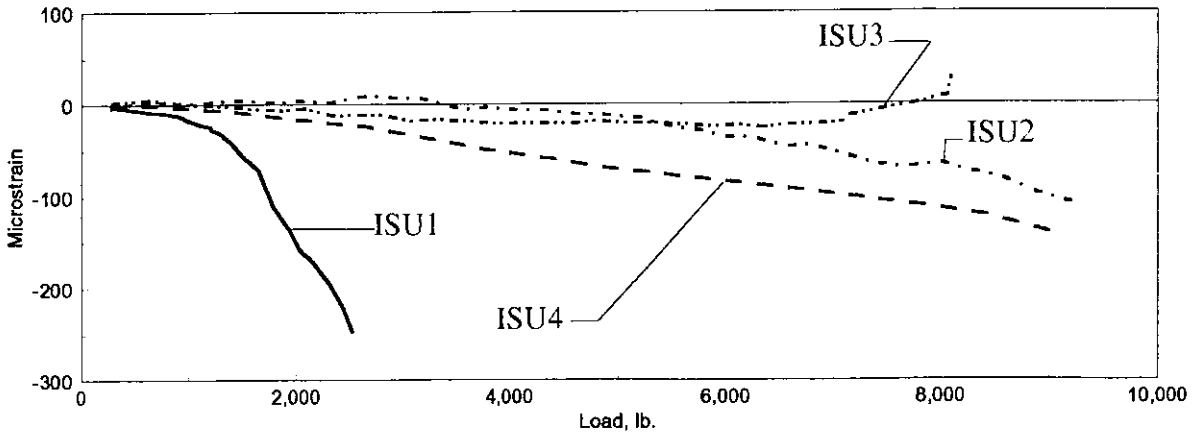


b. Springline

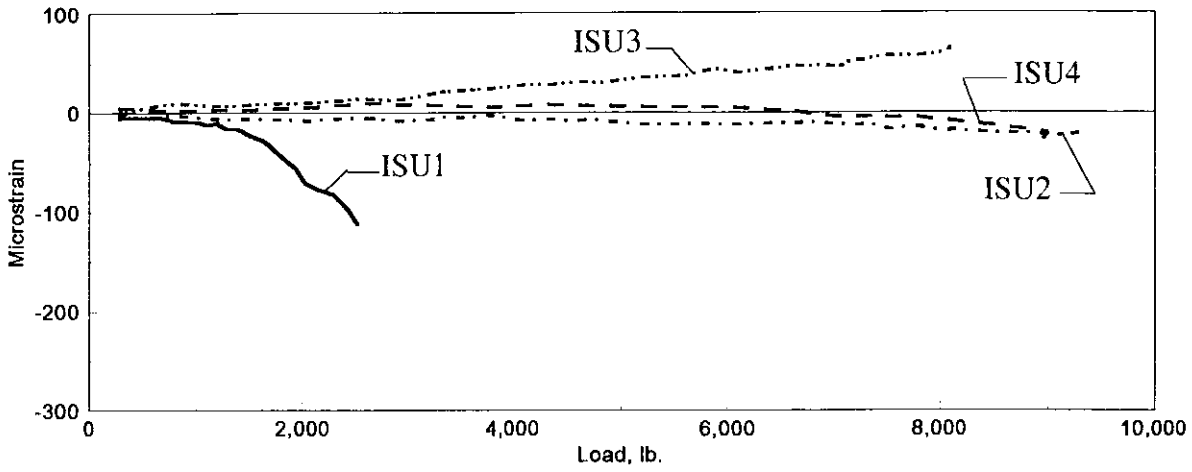


c. Invert

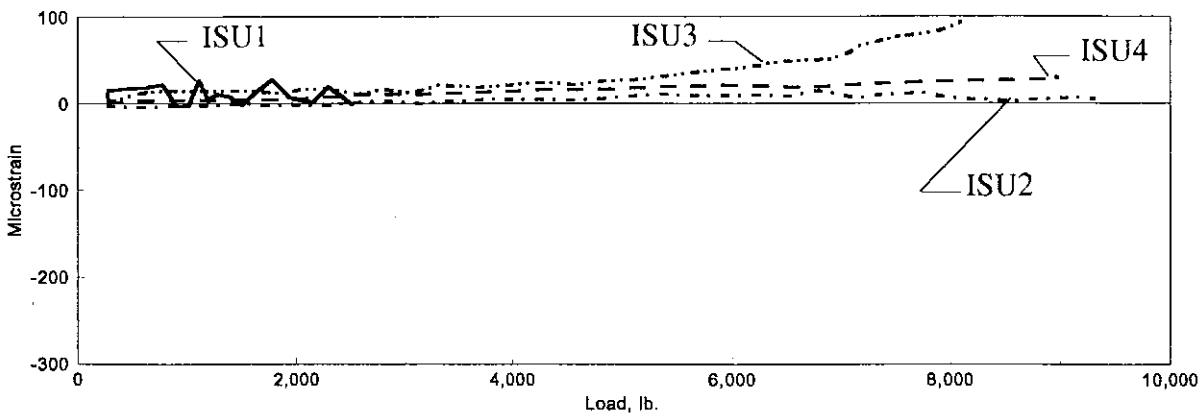
Figure 4.64. Longitudinal strain at Section 6: service load test; load at Section 6.



a. Crown

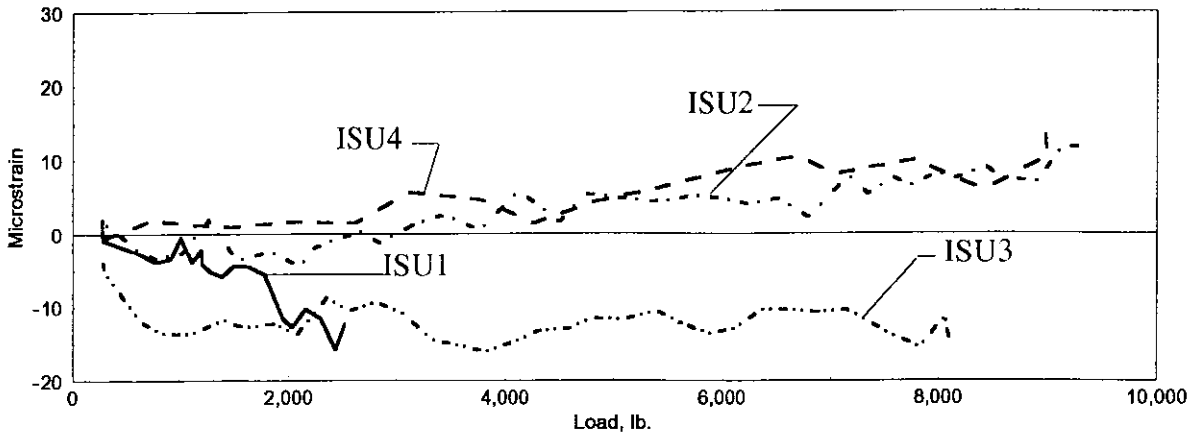


b. Springline

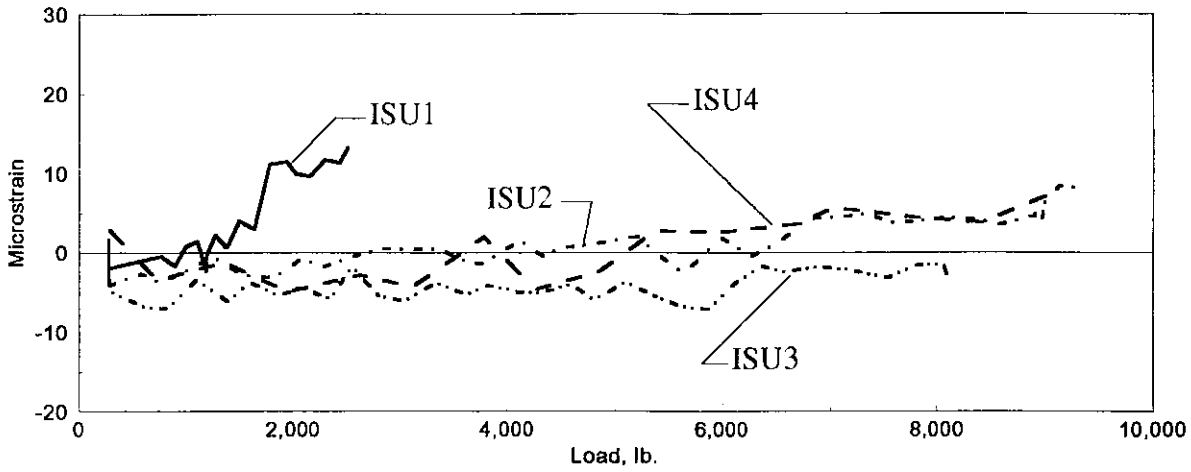


c. Invert

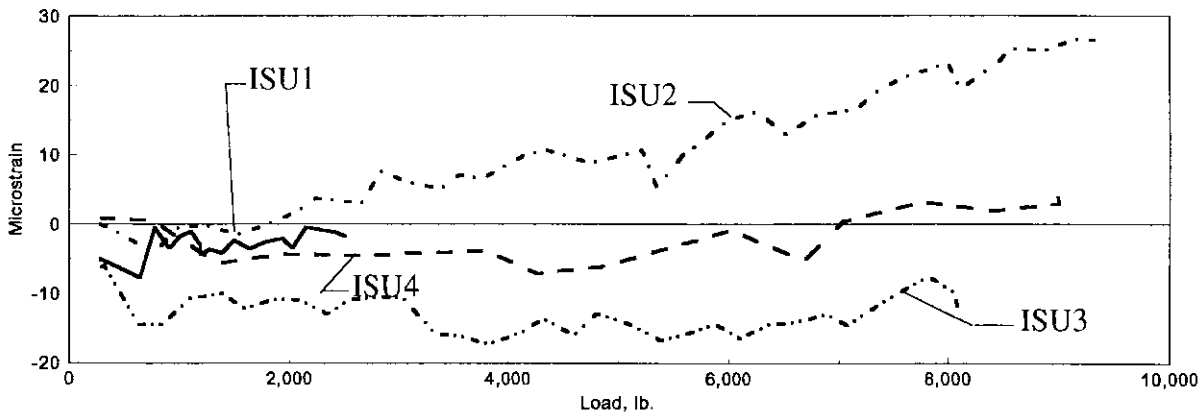
Figure 4.65. Longitudinal strain at Section 7: service load test; load at Section 6.



a. Crown

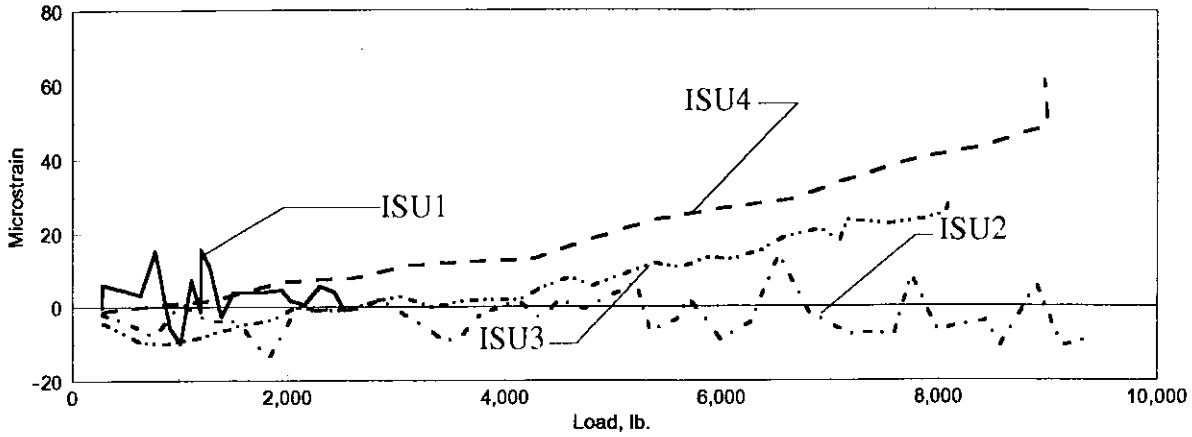


b. Springline

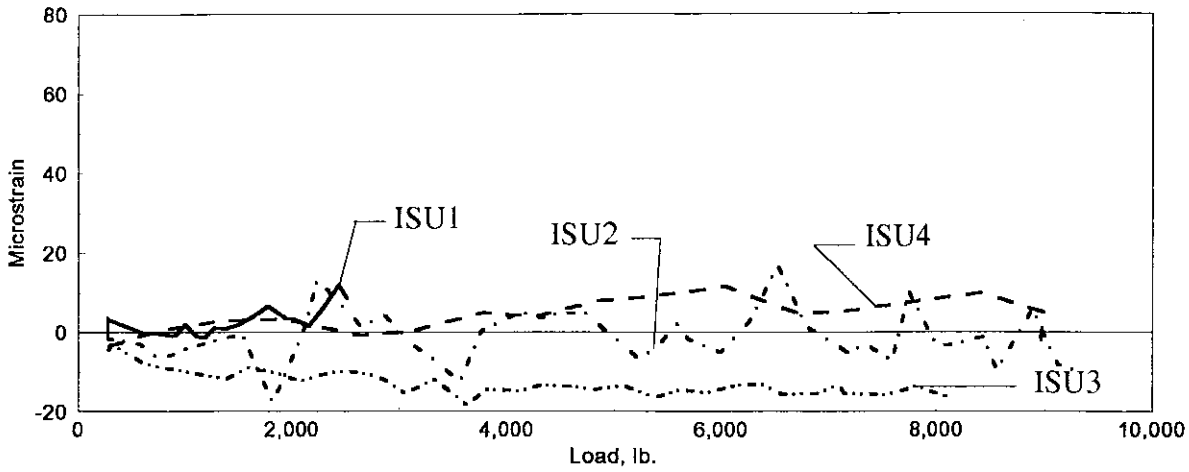


c. Invert

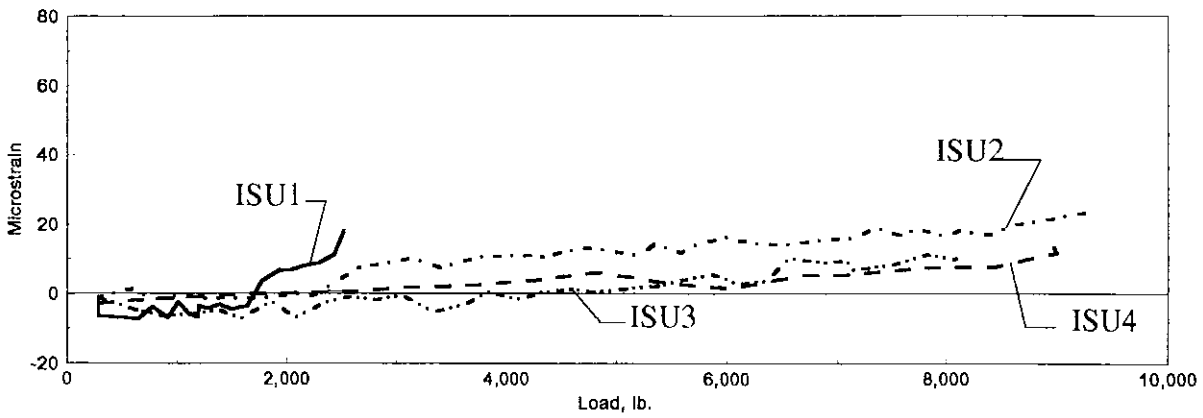
Figure 4.66. Circumferential strain at Section 2: service load test; load at Section 6.



a. Crown

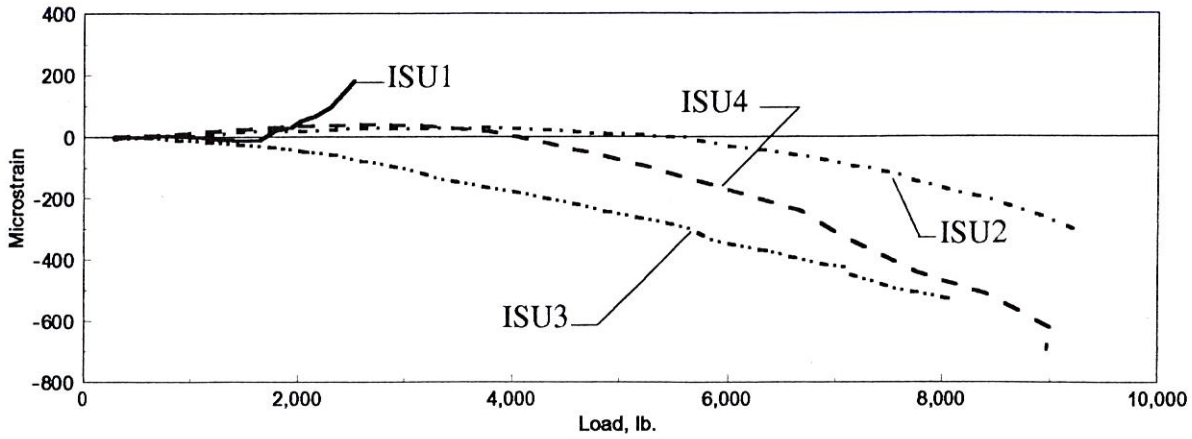


b. Springline

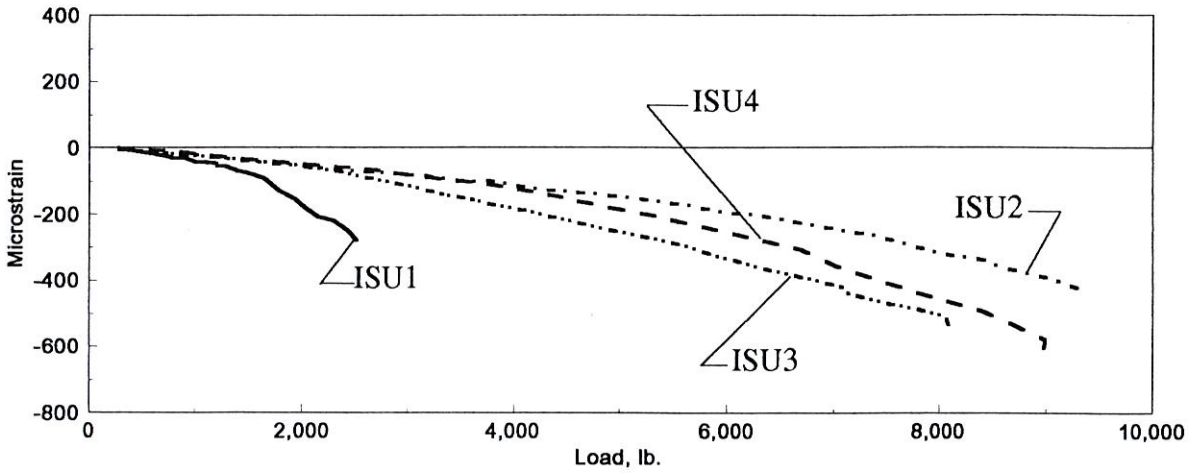


c. Invert

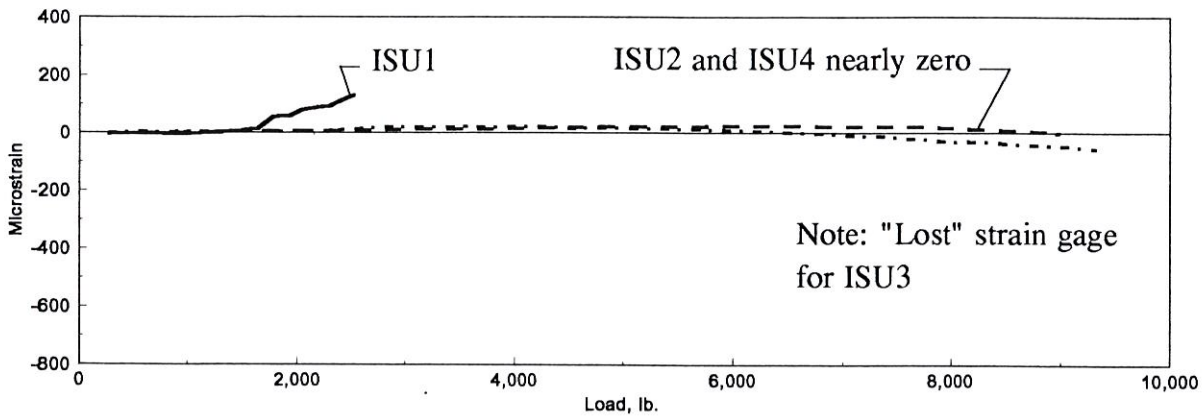
Figure 4.67. Circumferential strain at Section 4: service load test; load at Section 6.



a. Crown



b. Springline



c. Invert

Figure 4.68. Circumferential strain at Section 6: service load test; load at Section 6.

is near the ends is not predictable. This difference in behavior can be attributed to the combination of two facts. First, the response of the pipe is very sensitive to the restraint of the soil near the ends. Secondly, the fact that the north end was tested prior to testing the south end. This may have caused enough change in the backfill envelope to cause different behaviors.

4.3.4.4 Ultimate Load Tests

Ultimate loads from these tests are of interest and are presented in Table 4.5.

Position of load is as described in Fig 3.12 Two observations are apparent from the data. First, there is very little difference in failure values when load is applied at the three locations; in other words, the boundary conditions have minimal effect on the failure loads. Secondly, failure loads for ISU2, ISU3, and ISU4 are essentially the same even though the backfill conditions for ISU3 was different from those for ISU2 and ISU4, which had the same backfill condition.

Table 4.5. Ultimate loads for all field tests.

Specimen	Position of Load		
	Section 4	Section 2	Section 6
ISU1	8,200 lb.	6,900 lb.	8,100 lb.
ISU2	16,300 lb.	16,800 lb.	17,300 lb.
ISU3	18,200 lb.	11,800 lb. ^a	8,500 lb. ^b
ISU4	15,600 lb.	17,000 lb.	15,400

^aShear failure of soil due to boundary effect

^bPipe accidentally loaded to failure prior to testing

4.3.5 In Situ Backfill Pressure

The importance of the backfill envelope has long been known, however the importance of the type of backfill has been a major point of discussion. In this study, three separate backfill envelopes were tested. The results of these tests indicated that the only envelope to show significantly different results was the poorly compacted one (ISU1). The backfills with compacted backfill (i.e., ISU2, ISU3, and ISU4) showed little difference in the response and the strains induced in the pipe were shown to be basically the same even though the backfill envelopes were different. In Fig. 4.69, longitudinal strains at the springline for ISU1 through ISU4 for a 2000 lb load as a function of vertical soil pressure are presented. This figure implies the type of backfill material may not be as important as the proper compaction of the material. Vertical soil pressure was calculated using by multiplying the density measurement at the completion of each lift multiplied by the lift depth and summed up to give the pressure at the springline depth.

4.4 Comparison of Strain for Failure Tests

As was stated previously, the longitudinal properties of the pipe may have a greater impact on the in situ performance of HDPE pipe under live loads with minimal cover than was previously thought. An indicator of this is the magnitude of the longitudinal and circumferential strains at the failure load in each of the tests. The two types of laboratory tests tested the strength of the pipe in two directions (i.e., longitudinally and

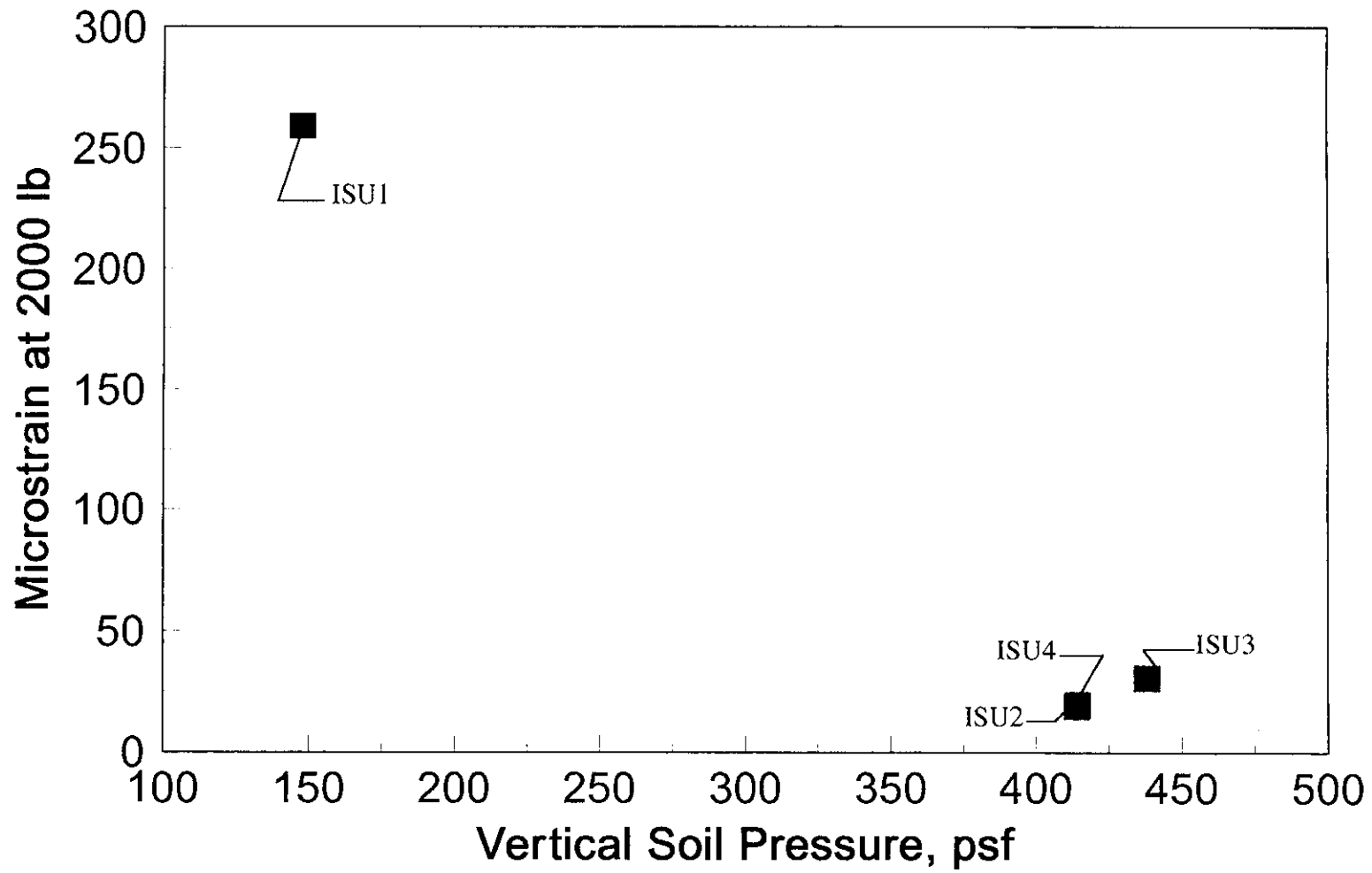


Figure 4.69. Longitudinal strain at 2000 lb of applied load versus vertical soil pressure.

circumferentially). The parallel plate tests tested the strength of pipe specimens in the circumferential direction and the flexural gave the longitudinal strength. Shown in Table 4.6 is a comparison of the maximum strain values for each type of test. Note that the longitudinal strains in the parallel plate tests and the circumferential strains in the flexural tests were negligible and have not been reported.

Table 4.6. Comparison of failure strain during failure tests.

Type of strain	Parallel plate	Flexural	ISU1	ISU2	ISU3	ISU4
Longitudinal	negligible	2950	3000	3100	3300	3200
Circumferential	12,800	negligible	N/A	N/A	1350	1840

N/A--"Lost" strain gage for this test

From these data, it is clear that the in situ pipes never achieved a level of strain associated with a circumferential failure as found in the parallel plate tests. On the other hand, it is clear that the level of longitudinal strain at the failure load in all types of backfill conditions are of the same magnitude as those associated with failure in the flexural tests. The type of backfill had little affect on the magnitude of the strain when the failure load was applied, indicating that the pipe (manufacturer C, 36 in. diameter) always failed at a level of longitudinal strain of approximately 3000 microstrain. Recall that the failure load for ISU1 was significantly less than that of ISU2, ISU2, and ISU3. This coupled with the data presented in Table 4.5 reinforces the widely known fact that the quality of backfill has

a marked effect on the pipe performance. However, it is clear that the failure of the pipe in situ is controlled by the pipe wall reaching a longitudinal strain of approximately 3000 microstrain rather than being controlled by the circumferential strength. This fact is contrary to the current belief that the circumferential properties are of greater importance. As Watkins (1985) stated, it is assumed that the longitudinal strength of pipes is adequate to resist applied loads. The reason that ISU1 (poor backfill envelope) failed at a circumferential strain of the same magnitude as ISU2, ISU3, and ISU4 (good backfill envelope) is due to the fact that as load was applied to the loose soil it was continually compacted to a state similar to the good backfill. The results of this testing indicates that for HDPE pipes this is not the case due to the fact that the pipes consistently failed due to excessive strain in the longitudinal direction. In fact, the circumferential strength has a factor of safety of 7 to 9.5 against a level of failure strain associated with a circumferential failure whereas the longitudinal strength is consistently at a factor of safety of 1 against a level of strain associated with a longitudinal failure.

5. SUMMARY AND CONCLUSIONS

In this phase of the investigation, the following tasks were completed: a literature review, a survey of Iowa counties on the usage of HDPE pipe, a review of data collected in a Tennessee DOT survey of state DOT's usage of HDPE pipe, 18 parallel plate tests, 6 flexural beam tests, and 4 in situ live load tests.

The following conclusions were formulated from the literature review, questionnaires, and results of the laboratory and field tests. It should be noted that these observations are based on a limited number of field tests (i.e., one depth of cover, three types of soil envelopes, one HDPE manufacturer, etc.). Generalizations of these conclusions for other situations may not, in some conditions, be valid.

1. A full investigation of the use of HDPE by Iowa county engineers was completed; only 17 counties reported the use of HDPE. Most installations used small diameter pipe (24 in. and smaller) and were generally used in non-essential situations.
2. A total of 18 parallel plate tests was conducted on HDPE pipe from 3 manufactures; the results of these tests indicate all specimens satisfied pipe stiffness by ASTM D2412 requirements. Additionally, the results did not vary significantly from test results determined by the individual manufacturers and by the Iowa DOT materials testing personnel.

3. Pipe response to parallel plate testing is predictable from the pipe wall geometry. A simple model was developed and when combined with approximate pipe wall properties, gave results consistent with the experimental investigation.
4. Six HDPE pipe specimens were loaded to failure in flexural beam type tests to determine experimental values for flexural EI factors and maximum moment capacity. The results indicate a wide variance in the flexural performance of pipes of different diameters and different manufacturers pipes.
5. A wide variation in recommended backfill soil envelope exists and ranges from the non-specific to the very specific.
6. Changes in the pipe's cross-sectional shape occur during backfilling as the backfilling proceeds to the top of the pipe. Most deformation takes place during backfilling of the region up to the springline of the pipe diameter. Additionally, strains induced in the pipe during backfilling are generally higher than strains experienced in the pipe during service loading but less than those at ultimate loads.
7. Circumferential strains are predictable during backfilling whereas the somewhat arbitrary longitudinal compaction of the soil along the length of the pipe induces more random variation in longitudinal strains.

8. The circumferential strains developed at the crown of the pipe during backfilling are greater than those at the invert since the invert is restrained in the very early stages of backfilling.
9. The soil envelope does have an effect on the performance of the HDPE pipes under static applied loads. However, the difference between the performances of 70% granular and "full" granular backfill is minimal. Additionally, even with a very poor soil envelope, the circumferential strains are considerably less than the strains occurring in a parallel plate test because of the additional restraint offered by the soil envelope. However, the failure load was much too low to withstand highway loadings with the poor soil envelope.
10. Under applied concentrated loading with 2-ft of cover, longitudinal strains at the springline are smaller than those at the crown because of the increased active soil resistance. Longitudinal strains at the crown and springline at sections 5-ft on either side of the loaded section reverse sign because excessive bending in the crown and springline change the backfill restraint in those areas.
11. Soil-structure interaction is imperative to a successful installation of HDPE pipe.
12. Boussinesq theory predicts a vertical stress distribution for a point load that

matches the experimental strain distribution for all soil envelopes. The horizontal stress distribution predicted by Boussinesq for variable Poisson's ratio indicates that looser soils distribute the load over a greater distance. This is obviously the case because ISU1 had a much greater response away from the load point than ISU2, ISU3, and ISU4.

13. Circumferential strain during parallel plate testing are 7.5 to 10 times greater than the circumferential strain at failure for the in situ tests. Longitudinal strain at failure in the flexural tests were approximately 3000 microstrain and the longitudinal strain at failure for all soil envelopes was approximately 3000 microstrain. This indicates that the pipes failed in the longitudinal direction. Currently, the only requirement for pipe strength is by parallel plate test which obviously does not test the failure direction of in situ pipes under concentrated loads with minimum cover. Based on this, it is apparent that in minimum cover applications, it should be required that HDPE pipes have a minimum longitudinal strength as tested by flexural beam tests.
14. There is evidence to believe that some of the pipe strains during backfilling in this investigation were influenced by the temperature variations in the specimens. The effect of temperature on HDPE pipes is not widely known and should be investigated to determine the effect temperature change has

on inducing pipe strains prior to loading.

The findings from the laboratory and field tests in this phase of the investigation along with the findings of the second phase of the investigation will provide engineers with significantly more information than currently exists on the use of HDPE pipe in highway applications. With this information, it will be possible to make the Iowa DOT specifications on the use of HDPE pipe more complete.

6. RECOMMENDED RESEARCH

Additional testing needs to be done concerning static live loading for different pipe manufacturers, pipe diameters, and varying soil envelopes. Additionally, testing on the couplers needs to be completed to ensure that the coupler is not the weak link in a pipe system. The effects of dynamic live loads on the soil-structure system also needs to be investigated.

As with other large diameter culvert pipes, hydrostatic uplift failure is a major concern. This aspect becomes more important as the diameter of HDPE pipes increase. To understand the type and amount of restraint required to resist this type of loading, uplift tests must be performed.

A finite element model should be developed and validated using the data from this research. Finite element models will allow more variables to be considered than can be done in an experimental study so that design standards can be developed.

REFERENCES

- Adams, D.N. T. Muindi, and E.T. Selig. "Polyethylene Pipe Under High Fill." Transportation Research Record 1231, Washington D.C.: Transportation Research Board, pp88-95, 1989.
- American Association of State and Highway Transportation Officials. AASHTO LRFD Bridge Design Specifications, Customary U.S. Units First Edition. Washington D.C.: American Association of State and Highway Transportation Officials, 1994.
- American Association of State and Transportation Officials. Standard Specifications for Highway Bridges 15th Edition. Washington D.C.: American Association of State Highway and Transportation Officials, 1992.
- Casner, D., N. Cochrane, and H. Bryan. "Polyethylene Maintenance Culvert Field Review." Columbus, Ohio: Maintenance Report by Pennsylvania Department of Transportation and Advanced Drainage Systems, Inc., Columbus OH: Advanced Drainage Systems, Inc., 1986.
- Culley, R.W. "Structural Tests on Large Diameter Polyethylene Culvert Pipe." Research Report 31, Feb. 31, Regina, Saskatchewan, Canada: Saskatchewan Department of Highways and Transportation, 1982.
- Drake, William B. Sr. "Performance Inspection of 26-inch Corrugated Polyethylene Pipe Storm Sewer." Lexington, KY: William B. Drake Sr., 1991.
- Fleckstein, L. John and David L. Allen. "Field Performance Report on Corrugated Polyethylene Pipe." Structural Performance of Pipes. Rotterdam, Netherlands: Center for Geotechnical and Environmental Research, pp. 67-77, 1993.
- Gabriel, L.H. "Checking the Premise-Deflections of Flexible Pipe are Predictable." Structural Performance of Pipes. Rotterdam, Netherlands: Center for Geotechnical and Environmental Research, 1993.
- Greenwood, Mark E. and Dennis C. Lang. "Vertical Deflection of Buried Flexible Pipes." Buried Plastic Pipe Technology. Philadelphia, PA: ASTM, 1990.
- Goddard, J.B. "Tech Report 4.103: Plastic Pipe Design." Plastic Pipe Design and Application Technical Seminar. Columbus, OH: Advanced Drainage Systems, Inc., 1992.

- Hancor. "High Density Polyethylene Drainage Handbook." Oelwien, IA: Hancor, Inc., 1991.
- Howard, Amster. "Earthwork for Pipeline Construction: Notes for 'Buried Pipe Installation Seminar' Sponsored by Hancor, Inc." Lakewood, CO: Amster Howard, 1995.
- Hurd, J.O. "Field Performance of Corrugated Polyethylene Pipe Culverts in Ohio.", Transportation Research Record 1087, Washington D.C.: Transportation Research Board, National Research Council, pp 1-6, 1986.
- Iowa Department of Transportation. Standard Specifications for Highway and Bridge Construction. Ames, IA: Iowa Department of Transportation, 1992.
- Kessler, R.J. and R.G. Powers. "High Density Polyethylene Pipe Fire Risk Evaluation." Report No. 94-74, Gainesville, FL: Florida Department of Transportation, 1994.
- Leonhardt, G., Belastungsannahmen bei erdvelegten GFK -Rohren, AVK, Freudenstadt 4 Okt. 1978.
- "Memorandum: Usage of Corrugated Polyethylene Pipe." , Memorandum from D.W Bailey of State of North Carolina Department of Transportation to Joe Warrenfells of Advanced Drainage Systems, Raleigh, NC: Office of the State of North Carolina Department of Transportation, October, 1991.
- McDaniel, P. "Field Performance of Corrugated Polyethylene Pipe Culverts in Missouri.", Field Investigation by the Missouri Highway and Transportation Department, Office of the State of Missouri Department of Transportation: MO, 1991.
- Moser, A.P. Buried Pipe Design. New York: McGraw-Hill, 1990.
- Moser, A.P. "The Structural Performance of Buried 48 inch Diameter N-12HC[®] Polyethylene Pipes.", Research Report submitted Sept., 1994 to Advanced Drainage Systems, Inc., Logan, UT: Utah State University, 1994.
- Moser, A.P. "Research Problem Statement, Title: Thermoplastic Pipe Design Procedure.", A research problem statement submitted to members of TRB committee A2C06 'Culverts and Hydraulic Structures' on Feb. 9, 1995, Logan, UT: Utah State University, 1995.

- Moser, A.P. and K.G. Kellogg. The Structural Performance of Buried 48 in Diameter Hi-Q[®] Polyethylene Pipes. Research Report submitted to Hancor, Inc., Logan, UT: Utah State University, 1993.
- Nazar, S. "Performance of Plastic Drainage Pipe" , ORF Contract No. 68-10830, Mississauga, Ontario, Canada: Plastics Technology Center, Ontario Research Foundation, 1988.
- "Performance Evaluation of AASHTO M294 Type 'S' Polyethylene Pipes." Raleigh, NC: Materials and Tests Unit of North Carolina Department of Transportation, Aug. 1991.
- Selig, E.T., L.C. DiFrancesco, and T.J. McGrath. "Laboratory Test of Buried Pipe in Hoop Compression." Buried Plastic Pipe Technology: 2nd Volume, ASTM STP1222, D. Eckstein, Ed., Philadelphia: ASTM, pp 1-14, 1994.
- Schrock, B. Jay. "Technical Work on Flexible Pipe/Soil Interaction Overview -1990." Presented at the International Pipeline Design and Installation Conference, 1990.
- "Southern California 'Green Book' Standard Specifications for Public Works Construction." Joint Cooperative Committee of the American Public Works Association and the Associated General Contractors, Currently in print.
- Spangler, M.G. "The Structural Design of Flexible Pipe Culverts." Engineering Experiment Station, Ames, IA: Iowa State University, Bulletin 153, 1941.
- Todres, H.A. and M. McClinton. "Stress and Strain Responses of a Soil-Pipe System to Vehicular Traffic." Advances in Underground Pipeline Engineering. Proceedings of the International Conference sponsored by the Pipeline Division of the American Society of Civil Engineers, Ed. Jey K. Jeyapalan, pp 428-437, 1985.
- Watkins, Reynold K. "Longitudinal Stresses in Buried Pipes." Advances in Underground Pipeline Engineering. Proceedings of the International Conference sponsored by the Pipeline Division of the American Society of Civil Engineers, Ed. Jey K. Jeyapalan, pp 408-416, 1985.
- Watkins, R.K. and R.C. Reeve. "Effect of Heavy Loads on Buried Corrugated Polyethylene Pipe." Columbus, OH: Advanced Drainage Systems, 1982.

Watkins, R.K, R.C. Reeve, and J.G. Goddard. "Effect of Heavy Loads on Buried Corrugated Polyethylene Pipe." Transportation Research Record 903, Washington D.C.: Transportation Research Board, pp 99-108, 1983.

Zicaro, Joseph P. "Flexible Pipe Design." Presented at the International Conference on Pipeline Design and Installation sponsored by the Pipeline Division of ASCE, March 25-27, 1990, Las Vegas, NV, 1990.

ACKNOWLEDGMENTS

The study presented herein (HR-373) was conducted in conjunction with the Engineering Research Institute of Iowa State University. The research was sponsored by the Project Development Division of the Iowa Department of Transportation and the Iowa Highway Research Board.

The author wishes to thank the various Iowa DOT and county engineers who helped with the project and provided their input and encouragement. In particular, I would like to thank Kurtis Younkin and Brad C. Barrett for assistance in various aspects of the investigation.

Appreciation is also extended to I. Perez of Advanced Drainage Systems Inc., R.L. Baldwin of Hancor Inc., and G.O. Soderlind of Prinsco Inc. for their donation of the numerous sections of high-density polyethylene pipe used in the investigation. The assistance of Construct, Inc., (Ames, Iowa) in excavating the trench for the numerous field tests and the delivery of the granular backfill and of Hallet Materials, Inc. (Ames, Iowa) for donating the granular backfill used in the field tests is also gratefully acknowledged.

I would like to thank my major professors F. Wayne Klaiber, Terry Wipf, and Robert Lohnes for their guidance and input during the course of this project. I would also like to thank Dan Adams for serving on my program of study committee.

Special thanks are accorded to the following undergraduate civil engineering and construction engineering students for their assistance in various aspects of the project:

Matthew E. Fagen, David D. Oxenford, Scott McMahon, Matthew Helmers, Trevor D.

Brown, Cara Hoadley, Troy D. Hodap, Chad Devor, and Andrea R. Heller.

APPENDIX A

**EI FACTORS FOR FLEXURAL SPECIMENS AT ALL LOAD INCREMENTS FOR
ONE SERVICE TEST**

Table A.1. Flexural EI factors for service test #1 for specimen A36.

Moment, (ft-lb)	EI (center), (kip-in ² *10 ⁴)	EI (west quarter pt.) (kip-in ² *10 ⁴)	EI (east quarter point) (kip-in ² *10 ⁴)
85.03	4.64	4.96	4.72
178.49	5.83	5.99	5.71
254.26	6.02	6.15	5.93
330.73	6.06	6.13	6.00
413.39	6.17	6.17	6.08
490.94	6.15	6.14	6.08
577.17	6.08	6.07	6.04
651.77	6.07	6.01	5.99
732.88	6.11	6.03	6.02
789.79		5.88	5.87
Average ^a	5.91	5.96	5.85
Calm Average ^b	5.91	5.96	5.85

^a Average is the average of all EI factors

^b Calm average is the average based on the deflections that were of sufficient magnitude to eliminate significant digit errors.

Table A.2. Flexural EI factors for service test #1 for specimen A48.

Moment, (ft-lb)	EI (center), (kip-in ² *10 ⁴)	EI (west quarter pt.), (kip-in ² *10 ⁴)	EI (east quarter pt.), (kip-in ² *10 ⁴)
167.15	37.39	32.17	32.21
330.94	29.65	27.48	27.52
444.80	26.52	26.31	24.33
591.61	24.45	23.82	22.34
754.12	24.23	24.35	22.28
919.56	24.01	24.40	22.02
1080.03	23.75	24.16	22.15
1216.93	23.34	23.70	21.70
1337.60	22.71	23.25	21.12
1504.29	22.24	23.06	20.65
1645.01	21.37	22.03	19.76
Average	25.43	24.98	23.28
Calm Average	23.63	23.90	21.82

Table A.3. Flexural EI factor for service test #1 for specimen C36.

Moment, (ft-lb)	EI (center), (kip-in ² *10 ⁴)	EI (west quarter pt.), (kip-in ² *10 ⁴)	EI (east quarter pt.), (kip-in ² *10 ⁴)
266.82	140.62	498.63	190.92
303.39	126.74	320.46	189.26
379.66	113.09	180.85	200.79
498.39	88.91	116.42	100.21
651.35	71.05	80.73	71.06
813.99	63.08	71.39	66.90
994.44	58.33	61.00	61.24
1150.31	55.73	61.69	56.19
1326.34	48.38	52.73	48.89
1466.08	48.50	51.39	49.46
1653.93	47.21	50.10	48.36
1814.17	45.09	48.01	45.78
1984.81	44.70	47.55	45.85
2140.44	44.57	46.80	46.04
2298.74	44.18	46.34	45.13
2473.92	43.66	46.26	44.51
2629.65	43.20	45.53	44.03
2795.58	41.40	43.42	41.87
2963.03	41.17	43.31	41.42
3122.05	41.07	43.04	41.41
3322.77	40.98	42.57	41.26
3442.92	40.19	42.07	40.81
3634.69	38.19	40.17	39.09
3802.24	38.14	39.81	38.86
3957.93	37.78	39.27	38.30
4122.19	37.59	39.39	38.17
4285.78	34.26	36.09	34.42
4449.05	34.29	36.13	35.00
4620.22	33.71	35.62	34.49
Average	58.72	85.44	67.42
Calm Average	45.68	48.19	46.51

Table A.4. Flexural EI factors for service test #1 for Specimen C48.

Moment, (ft-lb)	EI (center), (kip-in ² *10 ⁴)	EI (west quarter pt.), (kip-in ² *10 ⁴)	EI (east quarter pt.), (kip-in ² *10 ⁴)
416.94	1405.50	250.12	N/A
453.57	836.61	208.07	709.79
605.47	672.61	188.87	308.97
747.04	575.04	160.35	216.49
954.88	496.53	147.95	175.11
1041.30	440.67	134.60	162.95
1210.04	409.31	128.68	141.10
1317.13	393.76	123.26	138.64
1475.24	363.27	115.82	126.38
1638.59	360.78	116.52	128.21
1776.35	349.40	116.74	122.28
1955.75	345.73	1121.5	122.10
2075.84	339.15	110.38	117.70
2230.34	334.40	111.74	115.32
2392.13	331.23	110.39	115.78
2518.69	323.98	106.95	111.97
2669.58	325.00	107.50	112.91
2808.94	325.00	107.03	109.35
2990.78	319.88	105.86	110.04
3098.16	317.81	103.99	107.90
3269.79	309.74	103.66	106.60
3387.96	306.67	103.21	103.15
3521.90	302.54	101.73	105.85
3667.17	297.01	100.82	103.71
3883.29	295.89	99.83	101.96
Average	431.11	127.05	157.27
Calm Average	341.87	109.96	119.81

APPENDIX B
QUESTIONNAIRES

EXHIBIT B-1
IOWA COUNTY ENGINEERS QUESTIONNAIRE

**Investigation of
Plastic Pipes for
Highway Applications
HR-373**

**Research
Sponsored by the
Iowa Highway Research Board
and the Iowa Department of
Transportation Highway Division**

Please answer all of the questions. If you wish to comment on any question(s) or qualify your answer, please use the margins or a separate sheet of paper.

Return the completed questionnaire by **Dec. 1, 1994** using the enclosed envelope or fax to:

Prof. F. Wayne Klaiber
Dept. of Civil & Construction Engineering
Iowa State University
Town Engineering Building
Ames, IA 50011
(Fax No.: 515-194-8763)

Questionnaire Completed by: _____

Position/Title: _____

Address: _____

City: _____ State: IA County: _____

Phone No.: _____ Fax No.: _____

GENERAL INFORMATION:

1. Do you use any large diameter plastic pipes (2 ft or greater) in new construction?
Yes _____ No _____

2. If yes, approximately how many have been installed in the base few years?
1-2 _____ 3-4 _____ 5-6 _____ more than 6 _____

3. Do you use any large diameter plastic pipes in the remediation of deteriorating culvert pipes?
Yes _____ No _____

4. If yes, approximately how many have been used?
1-2 _____ 3-4 _____ 5-6 _____ more than 6 _____

5. Have you used any unusual installation techniques? Yes____ No____
If yes, briefly describe:

6. Have you experienced any problems with the installations: Yes____ No____
If yes, what problems? Collapse____ Chemical Deterioration____
Uplift failure____ Clogging____ Excessive Deformations____ Other____

EXHIBIT B-2
TENNESSEE DOT QUESTIONNAIRE

POLYETHYLENE PIPE QUESTIONNAIRE

STATE: _____

CONTACT PERSON: _____

TELEPHONE NUMBER: _____

1. Does your state presently use Polyethylene Pipe on roadway projects?

YES _____ NO _____

If the above answer is YES, please go to Question Number 4; if the answer is NO, please continue with Question Number 2.

2. Has your state ever used Polyethylene Pipe in the past?

3. When did your state stop using Polyethylene Pipe?

4. What year did your state begin using Polyethylene Pipe on roadway projects?

5. When your state started using Polyethylene Pipe, was the usage on a limited or test basis? If so, please explain.

6. Check the types of usage that Polyethylene Pipe is used for presently.

<u>Locations</u>	<u>Length used last year</u>	<u>Cost</u>
Underdrains _____	_____ft	\$
Sidedrains _____	_____ft	\$
Crossdrains _____	_____ft	\$
Sliplining _____	_____ft	\$

7. Does your state allow the use of Polyethylene Pipe on all projects?

8. Is Polyethylene Pipe let as alternates with concrete or metal pipe for all locations on all projects?

9. Please provide any cost comparison information your state has available for polyethylene, metal, and concrete pipe in highway construction.

10. Does your state have any problems with fires in Polyethylene Pipe? If yes, please explain.

11. Are any special end treatments required on Polyethylene Pipe?

12. Please provide a copy of the current Specifications for Polyethylene Pipe and any Special Provisions that would apply to its use.

13. Please provide a copy of any pertinent research your state may have done on the use of Polyethylene Pipe.

Please return to: Harris N. Scott, III
Civil Engineering Manager 2
TN Dept. of Transportation
Special Design and Estimates Office
Suite 1000 James K. Polk Bldg.
Nashville, Tennessee 37243-0350

Telephone No.: (615) 741-2806
Fax No.: (615) 741-2508

APPENDIX C

STATE RESPONSES TO HDPE PIPE SURVEY

Note: 11 states gave no additional comments on their use of HDPE pipes.

Alabama

- diameter, up to 36 in
- AASHTO M294
- AASHTO M252 (underdrains)
- 12 minimum cover
- no problems stated

Alaska

- AASHTO M294, type S, double wall
- AASHTO M252 (underdrains)
- no problems stated

Arizona

- AASHTO M294
- pipe sizes 12 in.-24 in., > 24 in. by approval of the engineer
- no problems stated

Arkansas

- AASHTO M252 (underdrains)
- AASHTO M294, type S (culverts)
- no problems stated

California

- AASHTO M294 ~ Corrugated HDPE pipe
- ASTM F894 ~ Ribbed HDPE pipe
- no problems stated

Colorado

- 1st installation in 1988
- one culvert burned for about 10 ft into one end as a result of the ignition of sawdust that had collected in it from a nearby sawmill
- AASHTO M294

Connecticut

- PE pipe shall conform to AASHTO M252 or M294
- no problems stated

Delaware

- PE pipes conform to AASHTO M294
- no problems stated

Indiana

- AASHTO M294 for specified sizes
- no problems stated

Iowa

- AASHTO M294
- 24 in. maximum diameter
- minimum compaction of 85%
- no problems stated

Kansas

- Corrugated HDPE tubing for entrances
- Corrugated HDPE pipe for underdrains
- no problems stated

Kentucky

- PE pipe for culverts or storm drains will be permitted only on projects with \leq 4000 ADT
- Follow AASHTO M294, type S specification (size ~ 12 in. to 36 in.)
- Backfill - coarse aggregate ~ no. 8, 9M, 11, or 57
- Field performance report done on corrugated HDPE pipe on KY 17 in Kenton County

~ This report documented the installation and performance of corrugated smooth lined HDPE pipe during construction of KY 17 in Kenton County.

Sags in grade, misalignment, poor coupling, and vertical deformation were observed during visual inspections and do not appear to be a material related problem but are largely due to poor construction techniques.

The pipes appeared to be functioning satisfactorily even with sagging, misalignments, and vertical deformation. Pipes that have vertical deformation over 10 % should be monitored for any additional movement.

It is recommended that HDPE pipe should be used under the following limitations:

1. Granular backfill should be used to a height of one foot above the crown of the pipe.
2. An ASTM Class I or Class II type backfill should be used for HDPE pipe.
3. Entrance pipe should have a minimum of one foot cover.
4. More aggressive inspection of all pipe installations should be implemented.

5. Continued long-term inspections of selected installations using various materials are suggested.

Maine

- Use corrugated HDPE drainage tubing for underdrains
- AASHTO M294 for diameters 12 in. to 24 in.
- all pipe and tubing shall be smooth lined
- no problems stated

Maryland

- High density PE pipe
- size limits: 15 in. to 36 in.
- use pipe meeting the requirements of AASHTO M294, type S only
- to be used outside the pavement template only, unless prior approval obtained through Highway Design Division
- must use gravel backfill around pipe
- minimum cover of two ft
- no problems stated

Michigan

- PE pipe used as Class A and B culverts and Class A and B storm sewers
- Backfill material shall be Granular Material Class III or IIIA except no stones larger than one inch in diameter shall be placed within six inches of the pipe.
- minimum 24 in. cover over pipe
- no problems stated

Minnesota

- usage of HDPE pipe is limited to 12 in. - 24 in. for culverts under all side roads adjacent to trunk highways
- usage of HDPE pipe is limited to 12 in.-24 in. for storm sewer under all roadways
- All pipes must be dual wall
- PE pipe conform to AASHTO M294
- two ft of cover for public roads, do not exceed 10 ft
- have not had any problems with fire associated with HDPE pipe, use galvanized steel aprons on all open ends of storm sewer and both ends of culvert

Mississippi

- HDPE pipe conform to the requirements of AASHTO M294, type S
- 12 in.-24 in. diameter pipe, side drains only
- no problems stated

Missouri

- conform to AASHTO M294 standard
- no problems stated

Montana

- use HDPE pipe for approach pipes up to 18 in.
- no HDPE pipe is allowed under mainline roadways
- no AASHTO standard stated
- no problems stated

Nebraska

- corrugated HDPE pipe for driveway culverts, underdrains, and storm sewers shall conform to the requirements of AASHTO M294
- sizes: 12 in. to 24 in.
- no problems stated

New Jersey

- conform to AASHTO M294, type S
- backfill to a height of two ft above top of pipes and culverts
- use coarse aggregate no. 8 as backfill
- Construction personnel have reported some difficulties properly installing polyethylene pipe.
- Extreme care must be exercised to fully and evenly support the pipe and some joints do not always align evenly and/or do not seal water tight, allowing infiltration of fines and eventual pavement deflection.
- In general, it was found that installation of HDPE pipe can be problematic and inspection intensive without a clear cost benefit or performance advantage.

New Mexico

- conform to AASHTO M294 and ASTM D 1248
- no problems stated

New York

- AASHTO M294, type C
- maximum height of cover is 15 ft
- minimum height of cover is 12 in.
- used in open and closed drainage systems
- PE pipe has the potential to burn. However, the risk of burning has been determined to be very low. The designer should consider less flammable materials at locations where the risk is expected to be high.
- Density of HDPE pipe is less than water, therefore when wet conditions are expected and dewatering may be a problem, polyethylene pipe will float and should

not be specified.

- end sections should be galvanized steel

North Carolina

- AASHTO M294, type S
- The AASHTO specifications note that soil provides support for this pipe's flexible walls and it is therefore sensitive to installation procedures and the quality of backfill material.
- 18 month evaluation ~ The evaluation confirmed that if corrugated HDPE pipe is placed utilizing controlled installation procedures, it will perform acceptably.
- this type of HDPE pipe is therefore limited to: temporary installations, such as detours, and permanent slope drain installations.

Ohio

- AASHTO M294, type S or SP
- aware of the flammability of HDPE pipe but do not believe the risks outweigh the advantages of using this material.

Oklahoma

- Conducted research on 3 sites
- Results:
 - HDPE pipe was found in excellent condition
 - only one small section had slight deflection
 - no corrosion or abrasion was observed
 - all installations inspected were performing as intended
 - construction phase seems to be the most critical time period for this pipe
 - its flexibility allows it to be placed over and/or around obstacles

Oregon

- corrugated HDPE drain pipe ~ AASHTO M252
- corrugated HDPE culvert pipe ~ AASHTO M294, type S
- nominal inside diameter of culvert pipe is 12 in. to 24 in.
- no problems stated

Pennsylvania

- no specification found on the material available
- filled out the Tennessee survey:
 - presently using HDPE pipe
 - no problems with fires
 - selective use of HDPE pipe
 - no special end treatments required

South Carolina

- AASHTO M294, type S only
- minimum compaction of 95%
- secondary roads only, low volume < 1000 ADT
- "C" projects only
- pipe sizes: 12 in. to 36 in.
- conducted inspections on three projects that used HDPE pipe
 - Results:
 - At one site the pipe was deflected and out of round. It was felt that the damage to the pipe had probably been done during construction when lack of protective cover and heavy equipment caused the pipe to loose shape. Despite the deflection in the one pipe, in all the projects the pipes were working as intended.

Tennessee

- HDPE corrugated pipe, fittings, and couplings shall meet the requirements of AASHTO M294, type S
- bedding material ~ Class "A" Grade D or Class "B" Grade D
- pipe sizes: 12 in.-36 in.
- conducted a flammability test on HDPE pipe, it did catch on fire and burned one ft into the pipe until extinguished

Texas

- AASHTO M294
- from the information available, as of March 30, 1994, TXDOT has discontinued use of HDPE pipe ~ information on reasons are not present

Vermont

- AASHTO M294
- no problems stated

Virginia

- HDPE corrugated underdrain pipe ~ AASHTO M252
- HDPE corrugated culvert pipe ~ AASHTO M294, type S for storm drains and entrances, type C for other applications
- sizes: 12 in.-36 in.
- backfill shall meet the requirements for Class III Granular material, no stones larger than one inch diameter shall be placed within six inches of the pipe
- no problems stated

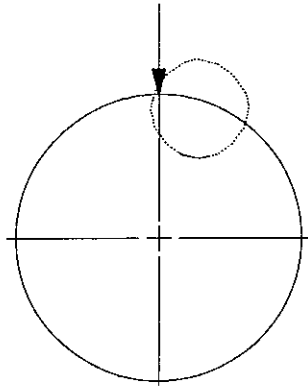
Wisconsin

- AASHTO M294, type S, 12 in.-36 in. sizes
- AASHTO M252, type S, 8 in.-10 in. sizes
- minimum cover is 12 in., maximum cover is 15 ft

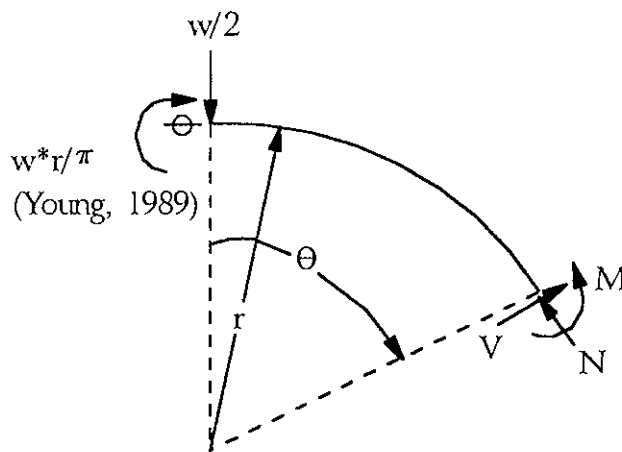
APPENDIX D

DERIVATION OF STRAIN RESPONSE TO PARALLEL PLATE TESTING

The freebody diagram shown in Fig. D.1 is the basis for the calculations presented here.



a. Schematic of parallel plate set up with location of free body diagram.



b. Free body diagram.

Figure D.1. Parallel plate test setup and free body diagram.

Summing forces in the direction of the normal force, N , gives the following:

$$N = \frac{w}{2} * \sin(90 - \theta) \quad (D.1)$$

Summing moments at the point of the cut (i.e., at the angle Θ) gives the following moment at the cut:

$$M = \frac{w}{2} * r * \sin(\theta) - \frac{w * r}{\pi} \quad (\text{D.2})$$

The stress at the inner surface is then calculated as the following:

$$\sigma = - \frac{N}{\text{area}} + \frac{M * y}{I} \quad (\text{D.3})$$

with

- I = Moment of inertia of the cross section.
- area = Area of the cross section.
- y = Distance from inner surface to centroid of the cross section.

With the formulae for N and M inserted:

$$\sigma = - \frac{w * \cos(90 - \theta)}{2 * \text{area}} + \frac{\left[\frac{w * r}{\pi} - \frac{w * r * \sin(\theta)}{2} \right] * y}{I} \quad (\text{19})$$

The state of stress on the system is shown in Fig. D.2.

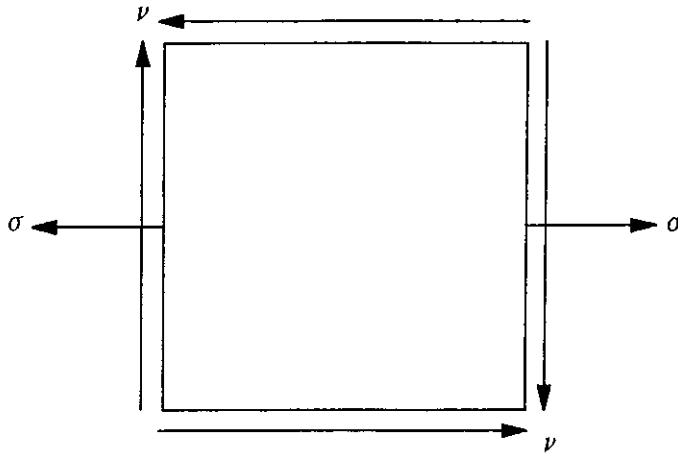


Figure D.2. State of stress at an element on the inside of the pipe wall.

From this figure it is apparent that a uniaxial state of stress exists and therefore the strain is:

$$\varepsilon = \frac{\sigma}{E} \quad (D.5)$$

with

ε = Strain in the direction of the load.

APPENDIX E

**APPROXIMATION OF SECTION PROPERTIES FOR PARALLEL PLATE TEST
ANALYSIS**

Shown in Fig. E.1 is the approximate shape used for calculation of section properties used in the parallel plate test analysis.

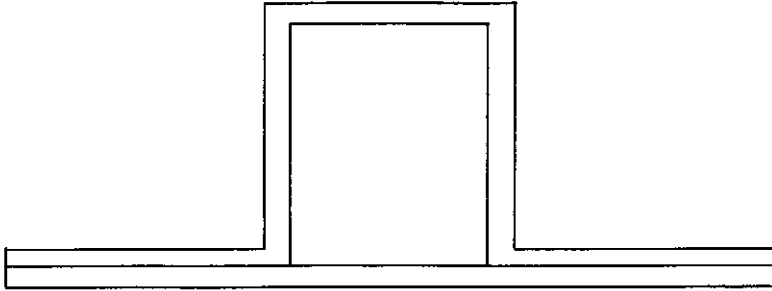


Figure E.1. Approximate shape used for section properties.